

HUMAN HEALTH

ENVIRONMENTAL HEALTH

# POLYMER ANALYSIS SOLUTIONS



## POLYMER ANALYSIS SOLUTIONS

### The solutions and expertise you need to succeed in today's industrial arena.

Today's plastics are some of the most used materials on a global volume basis. Broadly integrated into today's industrial and commercial lifestyles, they make a major, irreplaceable contribution to virtually every product category.

The Polymer Market consists of a huge diversity of industrial manufacturers who run many different processes and face the same overall challenge - to achieve high product quality and reduce costs in order to stay one step ahead of the competition.

PerkinElmer's comprehensive portfolio and polymer expertise can help you save money, ensure effective quality control and streamline your processes for outstanding operational efficiency. Additionally, they can implement cost effective solutions by reverse engineering and even ensure your products meet European and other national standard requirements.

### Multiple techniques, multiple expertise from one company!

Material Science is becoming increasingly important, consequentially, new technologies and applications are making it easier to meet your daily challenges and regulations in a more cost efficient way. PerkinElmer solutions focus on providing more insight into product performance and process optimization. Our 65 years of experience and comprehensive portfolio of thermal analysis, molecular spectroscopy, chromatography, atomic spectroscopy and hyphenated techniques is the ideal choice for ensuring the quality and reliability of polymers.

### Discover all our advanced solutions for...

- Packaging
- Building and construction
- Automotive, aviation, space and defense
- Electronics
- Tire and rubbers
- Plastic goods and components
- Paints and resins

In this compendium you will find a wide range of applications for polymers, plastics, rubbers and advanced materials. Discover how to put these applications to work for you simply and efficiently.

## TABLE OF CONTENTS

### CONTROL OF RAW MATERIAL AND FINISHED PRODUCTS

Polymer Identification Using Mid Infrared Spectroscopy.....	3
Quantitative Analysis of Polyethylene and Polypropylene in Their Blending Utilizing Infrared Spectrometer .....	8
Characterizing Polymer Laminates Using IR Microscopy.....	12
ATR Imaging Laminates .....	17
Plasticizer Characterization by TG-IR .....	23
Characterization of Polymers Using TGA.....	26
How to Optimize OIT Test?.....	30
Measurement of Tg of Polypropylene Using the Double-Furnace DSC.....	34
Isothermal Crystallization Study for Quality Assurance.....	38
Mechanical Properties of Films and Coatings .....	42
Tg and Cure of a Composite Material.....	45
Characterization of LDPE Over a Large Frequency Range.....	47
Color Analysis on LAMBDA PDA UV / Visible Spectrophotometer.....	49

### SIMULATION OF PROCESSES

HyperDSC – A Breakthrough Method For Materials Characterization.....	52
Characterization of Polyketone Copolymer by High Speed DSC.....	56
Crystallization Temperature vs. Cooling Rate: the Link with "Real-Life" Polymer Processes .....	62
Double-DSC Isothermal Crystallization Studies for Improved Injection Molding of Polymers .....	65
Importance of DSC Rapid Cooling for the Analysis of Plastic Microwave Food Trays .....	69
Preparation of Poly (Glycidyl Methacrylate) Polymers With Multiple Pendant Azide Functionalities .....	74
Effect of Processing Temperature on the Analysis of PVC Samples For Gelation Using The DSC 4000 .....	77

### FAILURE ANALYSIS AND REVERSED ENGINEERING

Rapid Characterization of Multiple Regions of Interest in a Sample Using Automated IR Microscopy .....	80
Detecting Weak Glass Transition (Tg) in Polymers by HyperDSC .....	84
Study Rigid Amorphous Fraction in Polymer Nano-Composites StepScan and HyperDSC .....	87
The Analysis of PVC with Different Phthalate Content by TG-MS and TG-GC/MS .....	91
Better Characterization of Polymer Blends Using StepScan DSC.....	94
Improved HyperDSC Method to Determine Specific Heat Capacity of Nanocomposites and Probe for High-Temperature Devitrification .....	97
Measuring Absorptance (k) and Refractive Index (n) Thin Films with the PerkinElmer LAMBDA 950/1050 High Performance UV/Vis/NIR .....	100
Determination of Monomers in Polymers by Multiple Headspace Extraction – GC/MS.....	109

### ANALYSIS OF CONTAMINANTS AND POLLUTANTS - ENVIRONMENTAL ANALYSIS

Detection and Identification of Contaminations in the Manufacturing Process Using an IR Microscope .....	112
Detection and Identification of Microplastic Particles in Cosmetic Formulations Using IR Microscopy .....	115
Lead and Other Toxic Metals in Toys Using XRF Screening and ICP-OES Quantitative Analysis .....	119
Determination of Formaldehyde Content in Toys and Fabrics Using UV/Vis Spectrometry .....	124
Confirmation of Presence of Styrene Butadiene Resin (SBR) Polymer in Drywall Primer Applications .....	128
Increasing Sensitivity in the Determination of Volatile Organics in Toys with Headspace Trap-GC/MS .....	134
Measuring Alkylphenols in Textiles with Gas Chromatography/ Mass Spectrometry .....	139
The Analysis of Ethylene Vinyl Acetate by TG-MS .....	143

### RECYCLING

Polymer Recycling Pack .....	145
Analyzing Recycled Polyethylene Resin for Polypropylene Contamination Using FT-IR .....	147
The Advantages of Mid-IR Spectroscopy for Polymer Recycling .....	150
Rapid and Reliable PVC Screening in Packaging Material .....	155



## Polymer Identification Using Mid Infrared Spectroscopy

### Introduction

Synthetic polymers are very widely used today, with diverse applications in various industries such as food, automotive, and packaging. The quality of plastic products depends on the quality of the polymers or polymer blends used during manufacturing,

so identity verification and quality testing of those materials during every stage of manufacturing is necessary to ensure that only high-quality material is used.

Infrared (IR) spectroscopy is ideally suited to qualitative analysis of polymer starting materials and finished products as well as to quantification of components in polymer mixtures and to analysis of in-process samples. IR spectroscopy is reliable, fast and cost-effective. This application note describes several approaches to the measurement and analysis of IR spectra of typical polymer samples, and applies the techniques to the identification of some industrial polymer samples. The compact and rugged Spectrum Two™ FT-IR spectrometer supports a range of reflectance and transmission sampling accessories that are suitable for polymer analysis, and is now available with a Polymer Resource Pack that provides information and advice to help generate good quality spectra and extract meaningful information as simply as possible.

## Mid Infrared Spectroscopy

The IR spectrum derives from absorption of light exciting molecular vibrations. The positions of absorption bands in the spectrum give information about the presence or absence of specific functional groups in a molecule and as a whole the spectrum constitutes a "fingerprint" that can be used to determine the identity of the sample. A difference between two spectra indicates that the two samples are made up of different components.

Figure 1 shows the IR spectra of several common polymers: polyethylene (PE), polypropylene (PP), polystyrene (PS), and polytetrafluoroethylene (PTFE), measured using the PerkinElmer Spectrum Two FT-IR with UATR sampling accessory, as shown in Figure 2. The clear differences between the spectra allow a ready discrimination between the materials by visual inspection. Additional interpretation of the spectra can yield information about the structure: for example, looking at the C–H stretch region around  $2950\text{ cm}^{-1}$ , differences can be seen between PE and PP due to the differing ratios of  $\text{CH}_2$  and  $\text{CH}_3$  groups. PS has bands above  $3000\text{ cm}^{-1}$ , indicating the presence of aromatic groups. PTFE has no C–H groups at all, so the very weak bands present must be due to impurities or surface contamination.

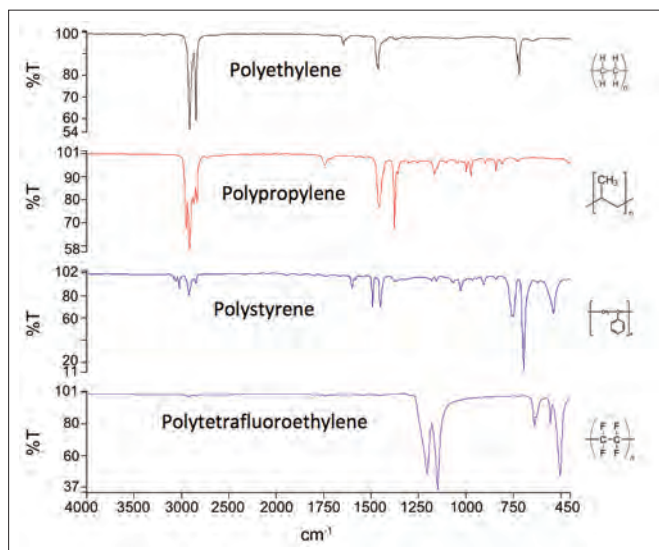


Figure 1. Mid-IR spectra of common polymers.



Figure 2. Spectrum Two FT-IR with UATR.

## Sampling methods

Selection of the appropriate sampling method and sample preparation is critical to achieving good results. Which method is appropriate depends on the type, form, and amount of sample to be analyzed. Polymer samples can take a number of forms, as shown in Table 1. Transmission measurements require a short pathlength, and this can be obtained by pressing the sample into a thin film or, for soluble samples, obtaining a film through solvent casting. However, the most popular method today for measuring polymer spectra is attenuated total reflectance (ATR), in which the sample is pressed against a diamond, zinc selenide or germanium crystal and the absorption of the evanescent wave is measured. This technique requires little to no sample preparation and very reliably produces high quality spectra.

Diffuse reflectance (DRIFT) has been widely used in the past for polymers, and remains a useful technique where the sample is physically too large to measure with ATR and a sample can be taken by abrasion.

**Table 1. Sampling techniques for FT-IR spectroscopy of polymers.**

Sample Form	Suitable Techniques
Thin films (<25 $\mu\text{m}$ )	Transmission
Fine powders (<2 $\mu\text{m}$ )	Transmission (KBr), ATR, DRIFT
Large items	DRIFT (abrasive sampling)
Irregular shapes, pellets	ATR, DRIFT (abrasive sampling)
Polymers soluble in volatile solvents	Transmission (cast film)
Flat, reflective surfaces	Specular reflectance, ATR, DRIFT (abrasive sampling)
Single fibers	Diamond ATR or IR microscope

The PerkinElmer Polymer Resource Pack provides step by step instructions in order to obtain a good quality sample spectrum for a variety of sample types using both ATR and transmission. The Polymer ATR library included with the Pack can be used to determine sample identity.

Several of these sampling techniques are illustrated below, using polystyrene as an example material.

### ATR

The sample was directly placed on the UATR top plate mounted in the sample beam of the spectrometer. The measurements were completed within 30 seconds and ATR spectrum was obtained as shown in Figure 3.

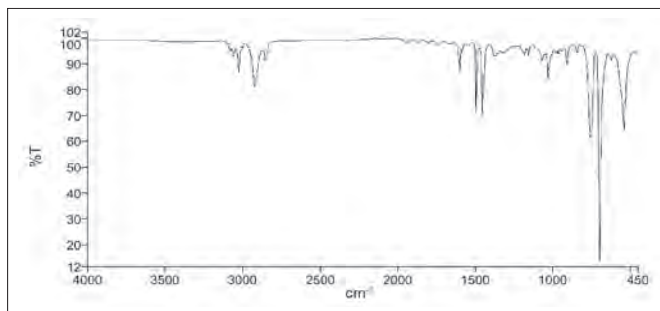


Figure 3. ATR spectrum of plastic sample.

While the short pathlength afforded by ATR makes it easy to measure good quality spectra, it is important to remember that, because of this factor, ATR is effectively a surface technique. If the surface of the sample is not representative of the bulk – for example, due to migration of plasticizer to the surface – some sample preparation is necessary. Additionally, if the sample is very hard but not flat, it may be difficult to get sufficient contact with the crystal. Accordingly the following general approach can be used:

1. If the sample is soft, cut a bulk sample with a sharp knife or scalpel to prepare a flat piece of polymer with a fresh surface and press this against the ATR crystal.
2. For hard and round-shaped samples like granulates that are more difficult to cut, use a pair of clean flat-nose pliers to flatten the sample.
3. In all other cases, use the sample as it is.

ATR spectra exhibit some differences from transmission spectra, the most obvious of which is that, since the effective path-length varies inversely with wavelength, the bands at high wavenumber are relatively weaker than in transmission. This can affect library searching, so it is recommended either to use an ATR library or to apply an ATR correction (such as that built into Spectrum software) to the spectrum prior to searching.

### Film casting

The sample was found to dissolve in xylene, so a thin film of the sample was prepared by the following procedure:

1. Dissolve 2 g of the sample in 10 mL xylene.
2. Place an IR crystal (such as KBr) window on top of a paper towel on a hot plate set at 40 °C.
3. Deposit 2–3 drops of the sample solution on the crystal window.
4. Allow the solvent to evaporate, leaving behind the thin film of the sample.

The thin film so obtained was placed in the IR beam and the IR spectrum obtained (Figure 4).

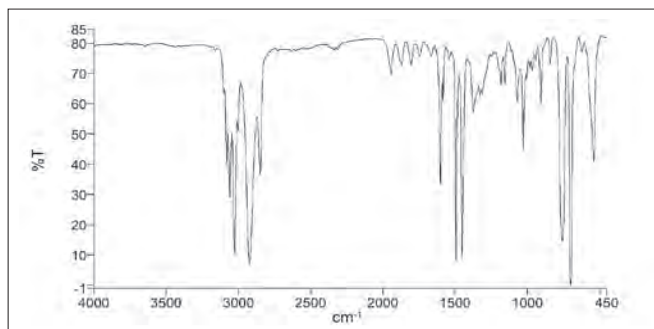


Figure 4. Transmission spectrum of plastic sample prepared as thin cast film.

The film casting technique is simple and cost effective and can produce a good quality spectrum. However, it is only applicable to soluble polymers and is rather time-consuming.

### DRIFT

DRIFT measurements of the same sample were carried out using DRIFT accessory and an abrasive stick. The background was acquired with a clean abrasive stick in place. The stick was then rubbed against the sample and placed in the DRIFT accessory. Figure 5 shows the resulting spectrum.

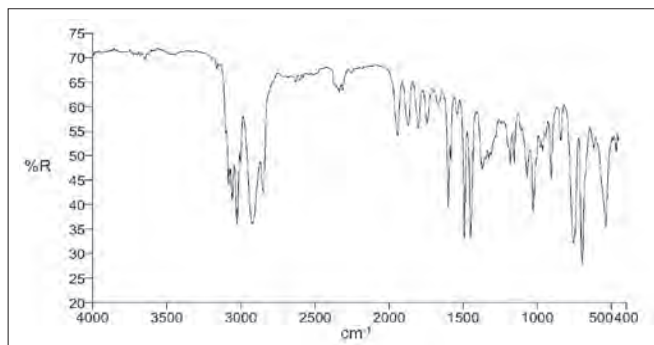


Figure 5. DRIFT spectrum of plastic sample.

DRIFT measurements with abrasive sticks provide a convenient sampling option for large samples, but it is sensitive to the amount of sample used so a greater degree of skill is required than for ATR sampling.

### Identification of Industrial Samples

Three samples were provided by an automotive parts manufacturer: one plastic headlight cover and two black interior trim pieces (Figure 6). The aim of the infrared analysis is to identify these materials.



Figure 6. Automotive plastic samples. Left: headlight glass, right: interior trim parts.

Spectra were obtained with the UATR accessory as described above. The headlight cover was found to have a coating, so this was removed prior to analysis. The spectrum was compared against the PerkinElmer ATR polymers library (included with the Polymers QA/QC FT-IR Reference Pack) using the Search function in Spectrum 10 (Figure 7). The results indicate that the sample is polycarbonate.

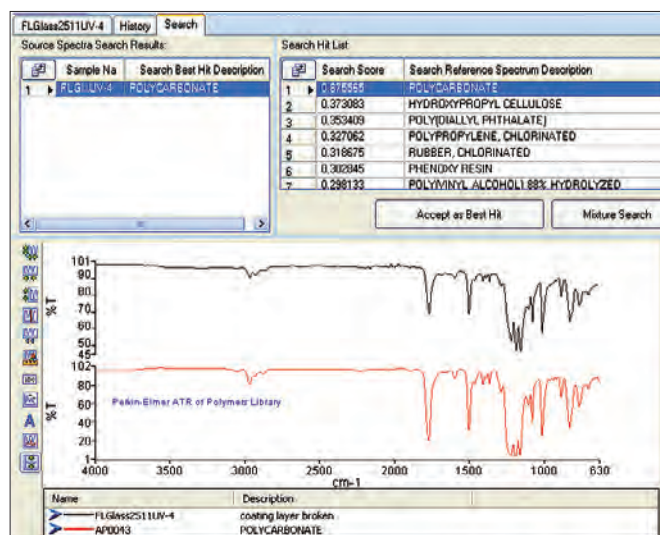


Figure 7. Search results for the headlight cover, showing a good match against the Polycarbonate reference.

Spectra of the black trim materials were also measured with the UATR accessory. Often, black materials require an even shorter pathlength than diamond ATR provides, and benefit from a germanium crystal. In this case, however, satisfactory spectra were obtained with diamond (Figure 8).

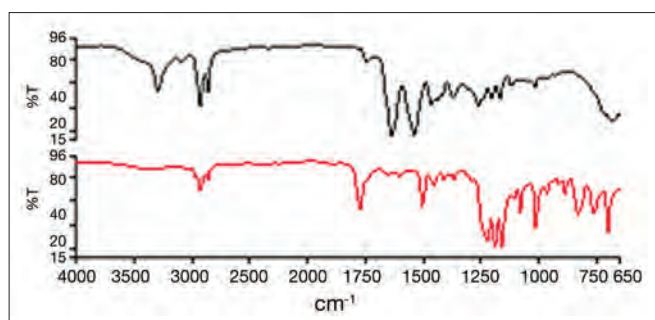


Figure 8. Mid IR spectra of auto-components. Top: sample 1, bottom: sample 2.

Using the Search function of Spectrum software and the ATR Polymers library, the materials were identified as nylon (sample 1) and polycarbonate (sample 2).



Figure 9. Sample 1 identified as Nylon base material.

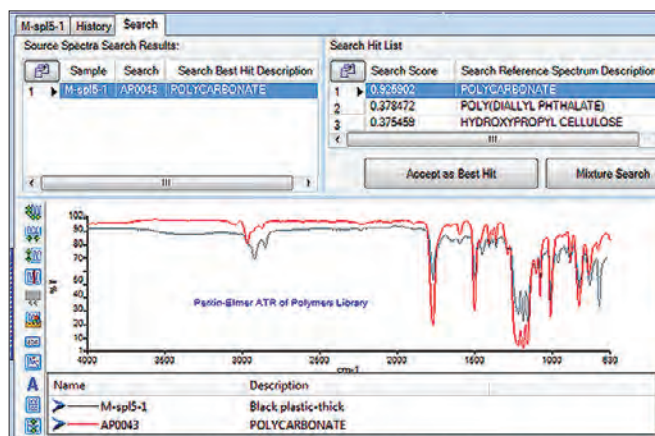


Figure 10. Sample 2 identified as Polycarbonate base material.

## Conclusions

FT-IR spectroscopy is a powerful tool for polymer analysis, and a range of sampling methods are available with varying degrees of sample compatibility and time requirements.

The Spectrum Two FT-IR spectrometer with the UATR sampling accessory and the Polymers QA/QC FT-IR Resource Pack is the ideal system for routine analysis and identification of polymer samples. With ATR sampling, good-quality spectra were obtained from industrial samples in seconds, and the materials were identified by searching against the library supplied with the system.

## Ordering Information

FT-IR Polymer Resource Pack:	L1608013
PerkinElmer Spectrum Two Polymer QA/QC Analysis System:	L160000V
Rectangular semi-demountable Potassium Bromide cell windows	L1271192
Metal-coated Abrasive Sticks	L1275105
Diamond Abrasive Sticks	L1275102
Silicon Carbide Abrasive disks	L1272348
Diamond Abrasive disks	L1272349

PerkinElmer, Inc.  
940 Winter Street  
Waltham, MA 02451 USA  
P: (800) 762-4000 or  
(+1) 203-925-4602  
[www.perkinelmer.com](http://www.perkinelmer.com)



For a complete listing of our global offices, visit [www.perkinelmer.com/ContactUs](http://www.perkinelmer.com/ContactUs)

Copyright ©2011, PerkinElmer, Inc. All rights reserved. PerkinElmer® is a registered trademark of PerkinElmer, Inc. All other trademarks are the property of their respective owners.

## Authors

Chunhong Xiao

PerkinElmer, Inc.  
940 Winter Street  
Waltham, MA 02451

Chris Ernst

Advanced Blending  
Technologies  
531 W Williamsburg Dr.  
Tiffin, OH 44883



## Quantitative Analysis of Polyethylene and Polypropylene in their Blending Utilizing Infrared Spectrometer

The use of post-consumer recycled high density polyethylene (HDPE) in products has been steadily growing. According to the Association of Postconsumer Plastic Recyclers latest report 974,000,000 pounds of HDPE were recycled in 2011.

There are generally two grades offered to converters, natural and pigmented. The natural material comes from dairy bottles while the pigmented is made from all the

other colored polyethylene bottles typically found in the home identified by the recycling code. Most of the pigmented bottles have polypropylene (PP) caps and pour spouts, some quite large in comparison to the bottle, like liquid laundry detergent and softener bottles.

When recyclers process/convert the bottles into usable resin they first grind the bottles into a small flake, then wash the flake in large water filled tanks to remove residue, paper labels and allow heavier than water materials (PVC, PET, PS etc.) to sink out of the lighter HDPE and PP materials, because both HDPE and PP have densities lower than water they both emerge from the wash system together, finally the material is dried, extruded, pelletized and packaged ready for shipment/sale.

These recycled materials can then be used in a variety of finished products to include but not limited to sheet, pipe, bottles, electrical conduit, parking blocks, decking, and nursery containers.

The PP content (from caps and pour spouts) in recycled HDPE resin has been found to vary from 2 - 26% percent, but commonly ranges from 5 - 12% percent. PP negatively affects many physical properties of the resin and finished products; two of the more important affected properties are impact strength and Environmental Stress Crack Resistance (ESCR). Impact strength can be significantly reduced causing products to be considerably more brittle or likely to crack during handling or use. ESCR has a longer cracking failure mode; the short definition of ESCR is the formation of cracks over time caused by stresses in the product and exposure to some environmental condition.

Small amounts of PP have been found to be acceptable in many products while larger percentages can be detrimental to functionality and quality. The PerkinElmer Spectrum Two provides a quick and accurate method for determining the PP percent in pelletized recycled HDPE. With the PP content and other key physical properties known to the manufacturer, they are able to adjust the amount of recycled resin used in a blend to limit the PP to an acceptable level. Blend optimization software like Advanced Blending Technologies' OptiMISER™ can be used for this purpose.

## Experimental

Standards were provided and prepared by Advanced Blending Technologies (Table 1). Samples of virgin HDPE pellets were first dry blended with virgin homopolymer PP pellets at the percentages shown in Table 1, then hot melt compounded through a ¾ inch single screw laboratory extruder. To ensure a homogenous mix the samples were dry blended and re-extruded two additional times for a total of three passes through the extruder.

Table 1. Standards at 4 Different Blends of Polyethylene (PE) and Polypropylene (PP)

Name	Polypropylene (%)	Polyethylene (%)
12% PP 4	12	88
9% PP 4	9	91
6% PP 4	6	94
3% PP 4	3	97

PerkinElmer Spectrum Two was used to collect spectra of the standards at 4 cm<sup>-1</sup> and 4 co-adds. PPPE pellets were placed/pressed on the diamond crystal and measured directly without any further sample preparation. Each standard was tested 5-6 times using different pellets. PerkinElmer Spectrum Quant software was used to build a calibration method with the standards data. Spectrum Quant is a software package using Beer's Law, which allows area, peak or maximum peak or peak ratio with baseline options. Besides linear regression fit type, there are also quadric, cubic and user defined options.

PE has a lot CH<sub>2</sub> compared with PP and PP has a lot CH<sub>3</sub> compared with PE. Peak at 719 cm<sup>-1</sup> is from CH<sub>2</sub> rocking, peak at 1376 cm<sup>-1</sup> is from CH<sub>3</sub> symmetric bending (Fig 1.), therefore, a peak ratio of CH<sub>3</sub> at 1376 cm<sup>-1</sup> to CH<sub>2</sub> at 719 cm<sup>-1</sup> was used to monitor the PP and PE composition in the blends. For PP, peak height ratio was used with linear fit type; for PE, peak area ratio was used with Quadric fit type. The reason to use different parameter is discussed in the last session.

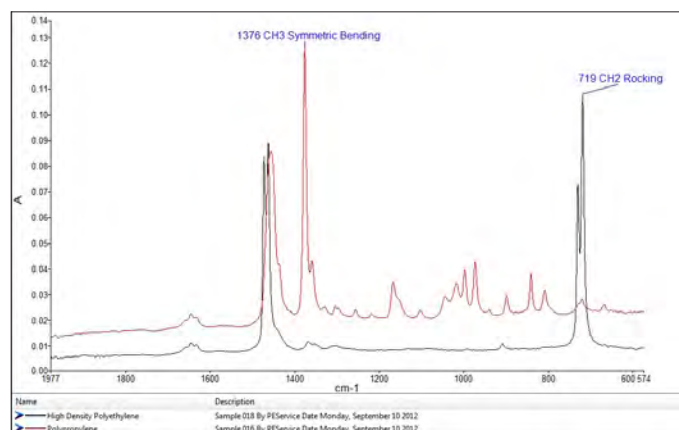


Figure 1. Spectral Comparison of High Density Polyethylene and Polypropylene.

## Results

Calibration model was built for PP and PE respectively. The correlation score for PP is 0.999 with 0.19 standard error of prediction (SEP) (Fig. 2). With the same standards data, the correlation score for PE is 0.976 with 0.51 % SEP (Fig. 3).

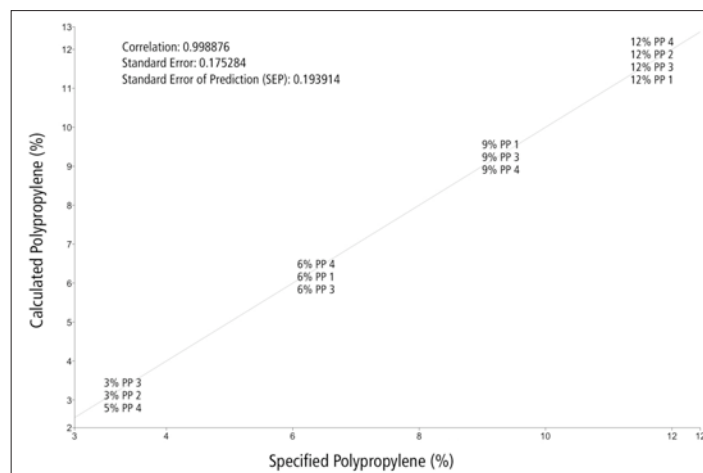


Figure 2. Calibration Model for PP

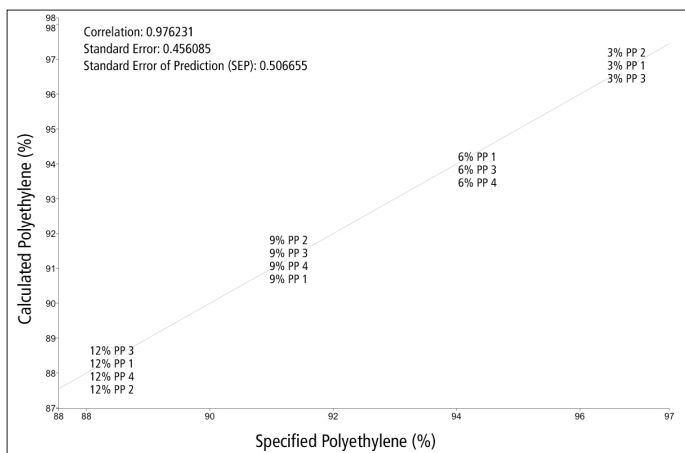


Figure 3. Calibration Model for PE

In any quantitative analysis, one critic step is validation. Independent validation was done within Spectrum Quant. Table 2 and Table 3 show the validation results for PP and PE respectively.

Table 2. Validation Results for PP

Validation Samples Specified	Calculated	Residual
12% PP validation 12	11.7817	0.218282
9% PP validation 9	9.30215	-0.302153
6% PP validation 1 6	5.60739	0.392614
6% PP validation 2 6	5.70573	0.294273
3% PP validation 3	3.17936	-0.179363

Table 3. Validation Results for PE

Validation Samples Specified	Calculated	Residual
12% PP validation 88	87.6553	0.344686
9% PP validation 91	90.4717	0.528268
6% PP validation 1 94	93.9556	0.044399
6% PP validation 2 94	93.6588	0.34121
3% PP validation 97	96.7416	0.258392

## Discussion and Conclusion

The calibration method was built for PP in the range of 3% to 12% and PE in the range of 88% to 97%. Due to the less content of PP in these standards and not much difference on the intensity at 719  $\text{cm}^{-1}$  from virgin PE and the intensity at 1376  $\text{cm}^{-1}$  from virgin PP, the signal for PP at 1376  $\text{cm}^{-1}$  is much weaker than the signal at 719  $\text{cm}^{-1}$  from PE in these standards. The PP calibration model had 0.18% SEP by the peak ratio of 1376  $\text{cm}^{-1}$  to 719  $\text{cm}^{-1}$ . However, when we used the peak ratio of 719  $\text{cm}^{-1}$  to 1376  $\text{cm}^{-1}$  for the PE calibration model, the standard prediction error increased to 1.55% (Fig. 4). The big SEP for PE was due to the weak signal at 1376  $\text{cm}^{-1}$ . Thus, we changed to peak area ratio. For peak area ratio, the SEP was 1% with linear regression fit type, and it was improved to be 0.51% by using quadratic regression fit type (Fig. 5).

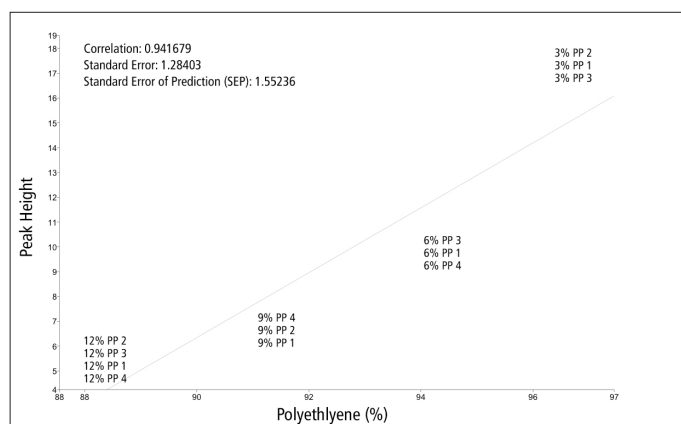


Figure 4. PE Calibration Plot of Peak Height vs Specified Concentration with Peak Ratio and Linear Regression Fit Type

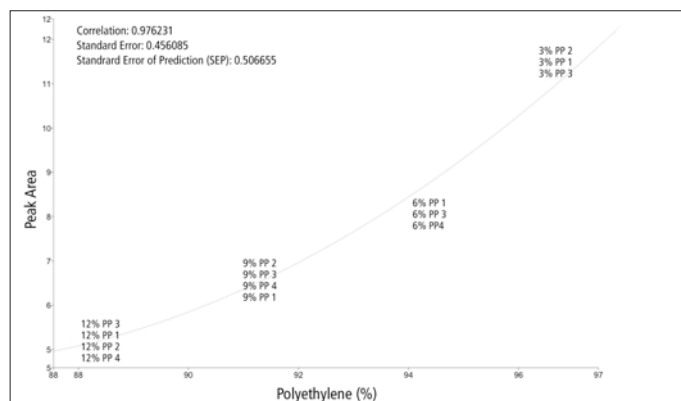


Figure 5. PE Calibration Plot of Peak Area vs Specified Concentration with Peak Area Ratio and Quadratic Regression Fit Type

With the new and more powerful Spectrum Quant software, we were able to develop one quantitative method for both PP and PE. With both components quantified at the same time, the results can be double checked and confirmed. This method was built to quantify low level of PP (3-12%), for high level of PP, a separate Quant method can be built in the same way for a better accuracy.

**PerkinElmer, Inc.**  
940 Winter Street  
Waltham, MA 02451 USA  
P: (800) 762-4000 or  
(+1) 203-925-4602  
[www.perkinelmer.com](http://www.perkinelmer.com)



---

For a complete listing of our global offices, visit [www.perkinelmer.com/ContactUs](http://www.perkinelmer.com/ContactUs)

Copyright ©2013 PerkinElmer, Inc. All rights reserved. PerkinElmer® is a registered trademark of PerkinElmer, Inc. All other trademarks are the property of their respective owners.

011092\_01

## Infrared, IR Microscopy

Author:

Ian Robertson

PerkinElmer, Inc.

Seer Green, UK

## Characterizing Polymer Laminates Using IR Microscopy

### Introduction

Multilayer polymer films, or laminates, are used in a wide variety of industries. A major use of these materials is for packaging of foods and consumer products. The composition of multilayer films can often

be quite complex as they may have to satisfy a variety of requirements to preserve the contents. A package must collate and contain the product, requiring strength and the ability to seal the packaging. It must be machineable at a reasonable cost. In the case of food products, it must be able to preserve the contents and protect it from external influences that would affect the product quality or safety, ultimately leading to increased shelf-life. Each of the layers in the laminate will perform a different barrier function, protecting the product from different external factors, such as moisture, light, oxygen, microbial materials and other chemicals or flavors.

Generally, traditional polymer materials, such as polyethylene terephthalate (PET), polyethylene (PE), polystyrene (PS), and polypropylene (PP), have been used for packaging materials. These packaging materials account for a significant proportion of materials ending up at landfill sites or recycling plants. Some of these materials biodegrade slowly or do not biodegrade at all and are environmentally unfriendly. Consequently, there is increasing focus on the use of biodegradable or compostable polymers that can be used as packaging materials. Bio-based materials are partly or entirely made of renewable raw materials, such as cellulose, starch or polylactic acid (PLA). These bio-based plastics can be biodegradable, but are not always. Compostable plastics can be completely biodegraded by microorganisms leaving only water, carbon dioxide, and biomass. These materials are more environmentally friendly and are expected to be used increasingly in the future.

Infrared microscopy has long been the most important technique for characterizing multilayer polymer films. Infrared spectroscopy has the ability to identify materials and the addition of an infrared microscope allows for small samples (down to <10 microns) to be analyzed, including the determination of the identities of the different layers of laminates. This Application Note describes the use of infrared microscopy applied to “traditional” multilayer polymer films as well as the newer compostable materials.

## Infrared Microscopy of Multilayer Polymers

Infrared microscopy of polymer films can be performed using transmission or Attenuated Total Reflectance (ATR) techniques. Infrared transmission measurements require the sample to be optically thin, generally not thicker than 20 to 30 microns. This requires the sample to be prepared as a thin film by the use of a microtome. The sample can then be placed on an infrared-transmitting window material, such as potassium bromide (KBr), for measurement of transmission spectra. ATR measurements can be performed on optically thick materials as ATR is a surface technique. The sample needs to be physically supported, either in an embedding resin or in a sample clamp specially designed for use in infrared microscopes. ATR measurements have the additional benefit of generating spectra at a significantly better spatial resolution than transmission measurements.<sup>1</sup>

## Transmission of Laminate

A polymer laminate sample was cut to a thickness of 25 microns using a microtome and taped flat onto a 7 mm diameter KBr window. This sample was then placed in a standard microscope sample holder on the microscope stage of the PerkinElmer Spotlight™ 200i. A visible image of the sample is shown as Figure 1. The laminate is approximately 350 micrometers across (top to bottom).

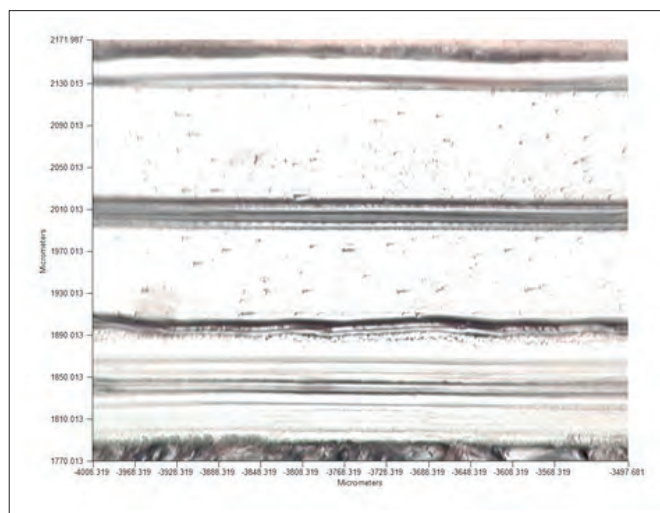


Figure 1: Visible image of polymer laminate measured in transmission.

If detailed information is required about all of the layers in the laminate then it is possible to setup a linescan, collecting spectra at very small intervals across the laminate. Such an experiment was set up to collect spectra at 3 micrometer steps across the laminate, using an aperture size of 5 micrometers with a total of 140 spectra collected. The linescan data is shown as Figure 2.

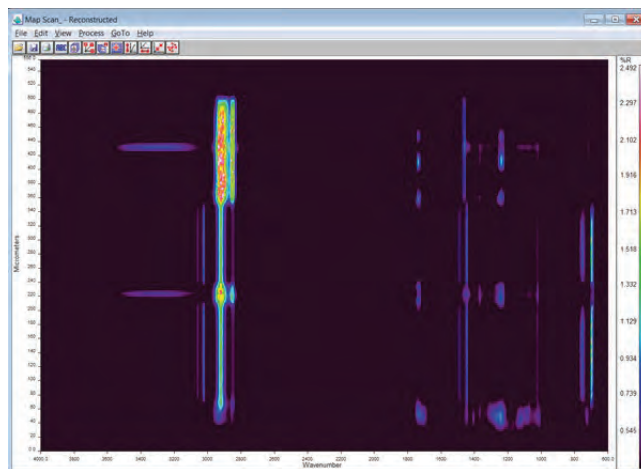


Figure 2: Linescan data for polymer laminate transmission measurements.

The results indicated that several different polymer types were present in the sample as shown in Figure 3. These were identified using Search libraries as; PET, modified PS, PE, ethylene-vinyl acetate (EVA), and ethylene-vinyl alcohol (EVOH).

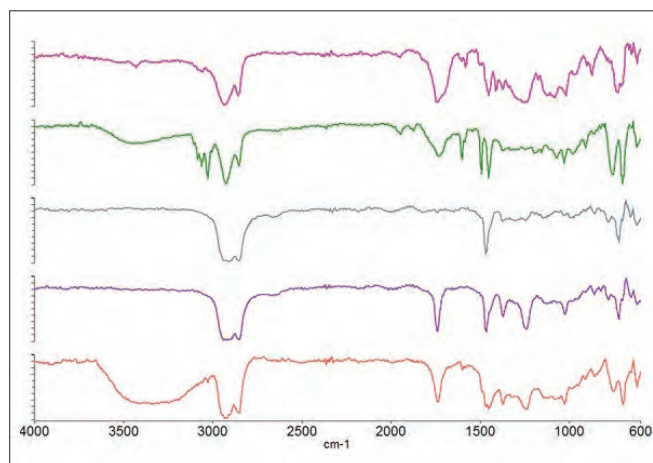


Figure 3: Spectra of the polymers present in the different laminate layers.

Profiles can be generated to show the distribution of the different polymer types throughout the laminate giving significant structural information. The profiles for polystyrene (1600  $\text{cm}^{-1}$ ), polyethylene (1450  $\text{cm}^{-1}$ ), ethylene-vinyl acetate copolymer (1746  $\text{cm}^{-1}$ ), and ethylene-vinyl alcohol copolymer (3334  $\text{cm}^{-1}$ ) are shown as Figure 4.

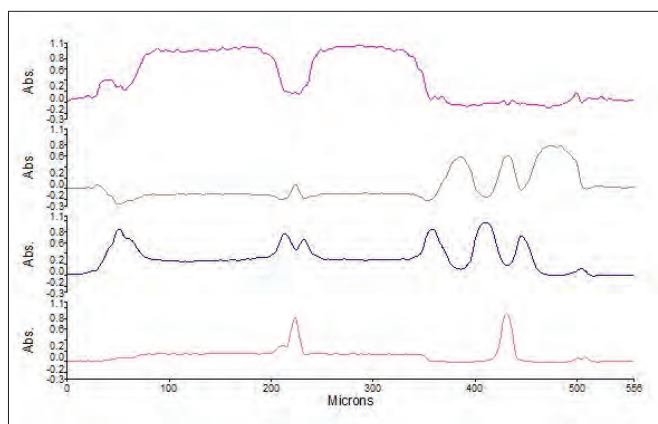


Figure 4: Distribution profiles for polymer types in laminate. From top to bottom: polystyrene, polyethylene, ethylene-vinyl acetate co-polymer and ethylene-vinyl alcohol co-polymer.

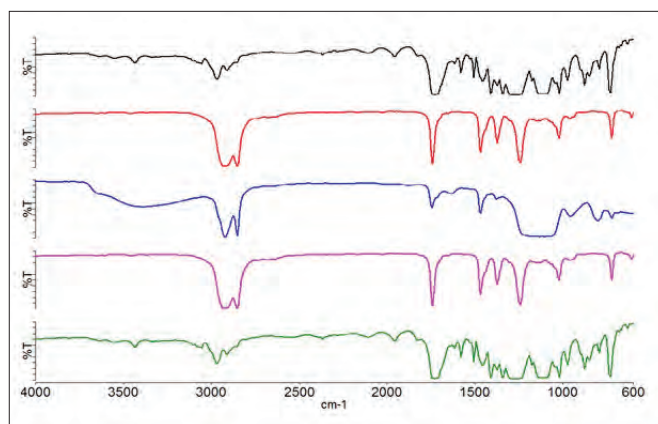


Figure 6: Spectra of layers 1 are shown (top) to 5 (bottom) in polymer laminate.

If the only requirement for the analysis is to detect and identify the layers in the laminate, then the Analyze Image function within the Spectrum 10 software can be used. This function will analyze the visible image of the sample, detect the layers present, and maximize the measurement area for each layer, all completed automatically. In the case of a multilayer sample, it will collect a single spectrum for each layer, giving the maximum signal-to-noise and significantly reduce the analysis time compared to mapping or measuring a linescan on the same sample. Figure 5 shows an example of a five-layer laminate.

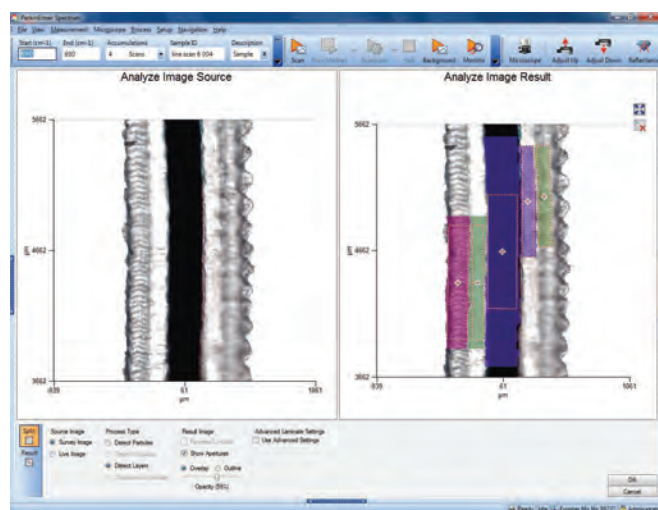


Figure 5: Automatic detection of layers in a laminate shows five layers.

After detection of the laminate layers, spectra were automatically recorded at the marker positions, shown in Figure 6. An automatic library search identified each of the layers as polyethylene terephthalate (layers 1 and 5), ethylene-vinyl acetate copolymer (layers 2 and 4), and silica-loaded polyethylene (layer 3).

### ATR Measurements of Polymer Laminates

ATR provides a fast and easy way of measuring an infrared spectrum of a material. ATR on an infrared microscope is capable of measuring spectra of very small materials down to just a few micrometers in size. A macro ATR crystal/accessory for the microscope has been utilized to collect data on food packaging laminates. This ATR accessory can generate spectra at a significantly better spatial resolution than transmission measurements<sup>1</sup>. For the ATR measurements the samples were embedded in a resin and polished to give a flat, clean surface for the ATR measurement. Embedding the sample generates a stronger multilayer surface than simply clamping the sample and prevents deformation or compression of the sample under ATR pressure.

A sample of a multilayer food package manufactured using "traditional" polymers was prepared for ATR measurement in the Spotlight 200i. The visible image of this sample was measured and is shown as Figure 7. The width of the laminate is seen to be approximately 200 micrometers and consists of several polymer layers.

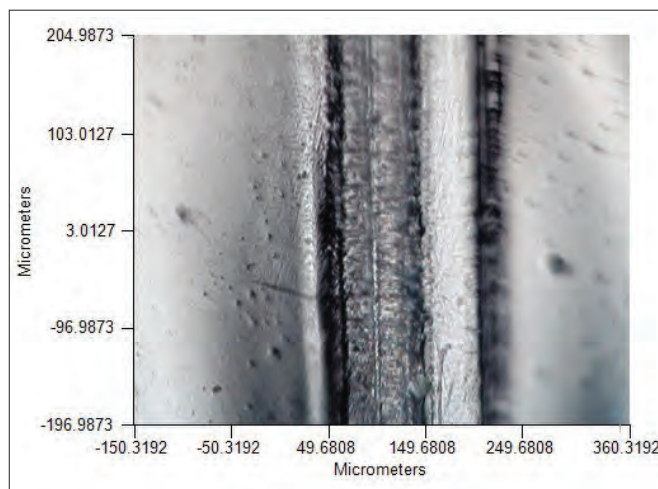


Figure 7: Visible image for multilayer food packaging material.

The macro ATR crystal for the IR microscope was placed in contact across the entire width of the sample. Spectra were collected across the laminate with an effective aperture size of 5 x 5 micrometers at a step size of 5 micrometers. The linescan data collected is shown as Figure 8.

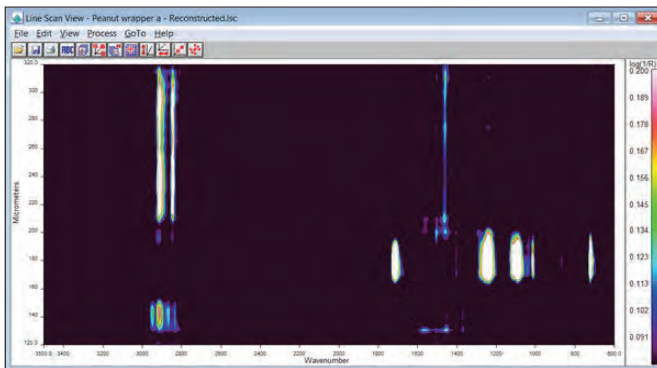


Figure 8: Linescan data for food packaging material.

Several different polymer types seem to be present in the sample. The spectra obtained from the major layers are shown in Figure 9. A search against polymer databases identifies the layers as polypropylene, polyethylene terephthalate, polyethylene, and modified polyethylene.

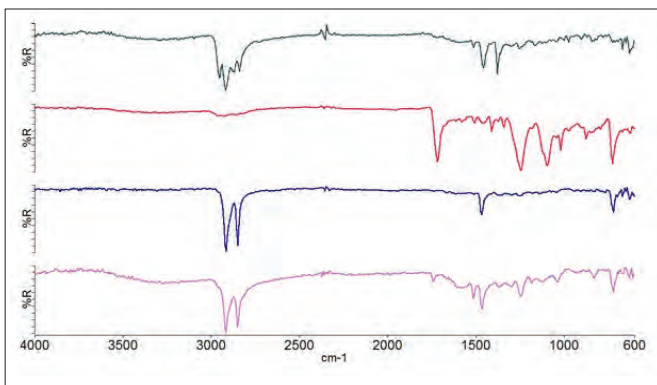


Figure 9: Spectra of major layers are identified as PP, PET, PE and modified PE.

In addition, several other minor layers were detected and their infrared spectra shown as Figure 10. A region of the data (around 160 micrometers in the display) gave no spectral details at all, as it was a thin foil layer.

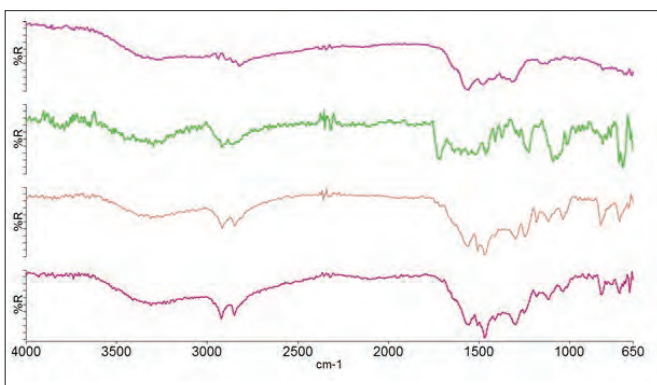


Figure 10: Spectra of minor layers in multilayer food packaging material.

A new generation of biodegradable polymer materials has been developed as a replacement for the "traditional" polymer packaging material. A compostable food packaging material has been analyzed on the Spotlight 200i. The sample was prepared for IR-ATR microscopy in the same way as the "traditional" packaging material that was shown previously.

The visible image of the embedded sample appears as Figure 11. The laminate is seen to be approximately 80 micrometers wide, consisting of a small number of visible layers.

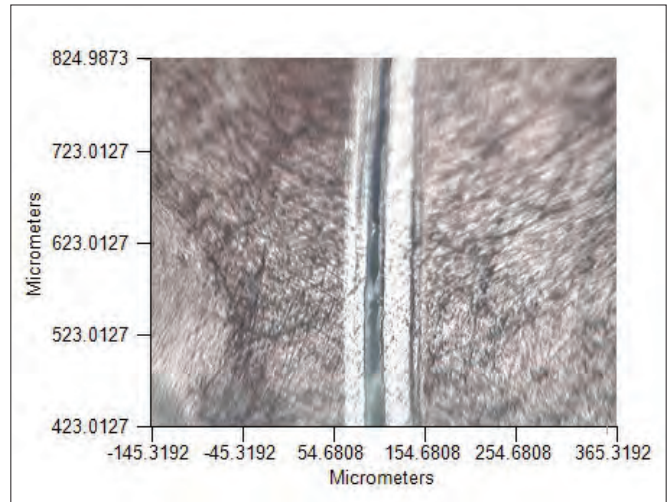


Figure 11: Visible image of a compostable food packaging laminate.

The infrared data collected on the sample is shown as Figure 12. The sample consists of three major layers each of approximately 25 micrometers width.

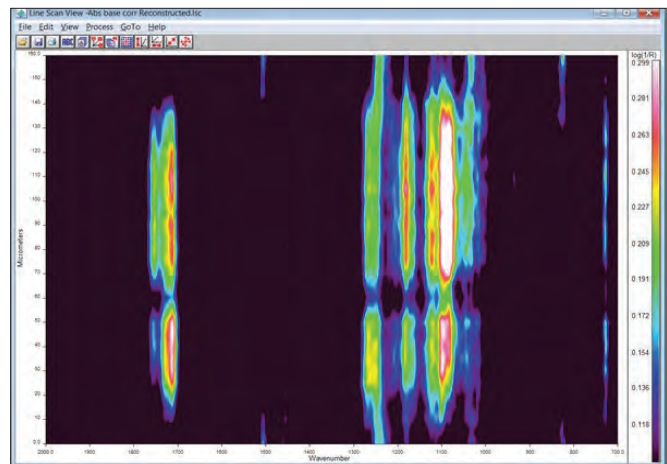


Figure 12: Linescan data for compostable laminate sample.

The spectra are shown as Figure 13. The spectra of the layers all look similar, however, they exhibit spectral differences in the C=O region between 1700-1760  $\text{cm}^{-1}$ . The materials are known to be polylactic acid (PLA)-based copolymers. The region at approximately 60 micrometers in the display does not exhibit spectral features, as there is a thin layer of foil present in the sample.

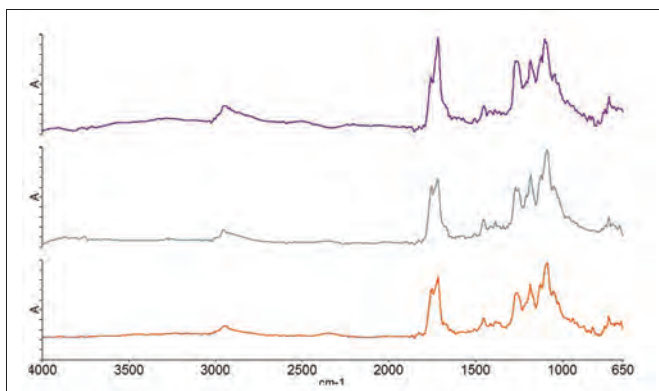


Figure 13: Shown here are spectra of the three different layers in the compostable polymer laminate.

## Summary

Packaging materials, especially food packaging, are complex materials in order to satisfy the numerous requirements for the product contained within. Multilayer laminates are a means of fulfilling these requirements. However, disposal of food packaging materials is a significant environmental problem. Biodegradable packaging materials are a possible solution.

IR microscopy has been shown to be an excellent technique for the characterisation of these “traditional” and newer multilayer materials. Transmission or ATR measurements can easily be deployed depending on the sample preparation that is available.

## Reference

1. PerkinElmer Technical Note 007641A\_03, Spatial Resolution in ATR Imaging

## FT-IR Imaging

## Author

Jerry Sellors, Ph.D.

PerkinElmer, Inc.  
Shelton, CT 06484 USA

## ATR Imaging of Laminates

### Introduction

The use of polymer laminates is widespread in many industries, and their structure and composition vary greatly. Individual layer thicknesses can range from less than 4 microns to many tens of microns or more. Transmission infrared microscopy is an excellent tool for the study of these materials and widely employed, along with other micro-spectroscopy techniques such as Raman.<sup>1</sup>

ATR imaging is a relatively new technique offering additional advantages compared with other FT-IR imaging methods, and is poised to become highly useful for laminates studies. For successful FT-IR microscopy, it is necessary to avoid too strong FT-IR infrared absorption by cutting the samples into thin sections (~10 micron thickness). Presenting samples in this manner is quite challenging from a practical viewpoint, and maintaining integrity of the sample can be difficult. In addition, the presence of the sample of finite thickness in a highly converging FT-IR beam can lead to issues that can limit the spatial resolution achievable<sup>2</sup> regardless of microscope used.

## Introduction

The use of polymer laminates is widespread in many industries, and their structure and composition vary greatly. Individual layer thicknesses can range from less than 4 microns to many tens of microns or more. Transmission infrared microscopy is an excellent tool for the study of these materials and widely employed, along with other micro-spectroscopy techniques such as Raman.<sup>1</sup>

ATR imaging is a relatively new technique offering additional advantages

compared with other FT-IR imaging methods, and is poised to become highly useful for laminates studies. For successful FT-IR microscopy, it is necessary to avoid too strong FT-IR infrared absorption by cutting the samples into thin sections (~10 micron thickness). Presenting samples in this manner is quite challenging from a practical viewpoint, and maintaining integrity of the sample can be difficult. In addition, the presence of the sample of finite thickness in a highly converging FT-IR beam can lead to issues that can limit the spatial resolution achievable<sup>2</sup> regardless of microscope used.

ATR imaging can overcome some of these limitations and resolve detail which is difficult, if not impossible, to observe using conventional FT-IR microscopes. First, as a reflectance

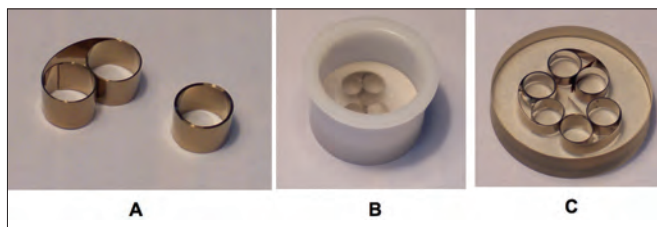


Figure 1. Fixing and embedding laminate samples.

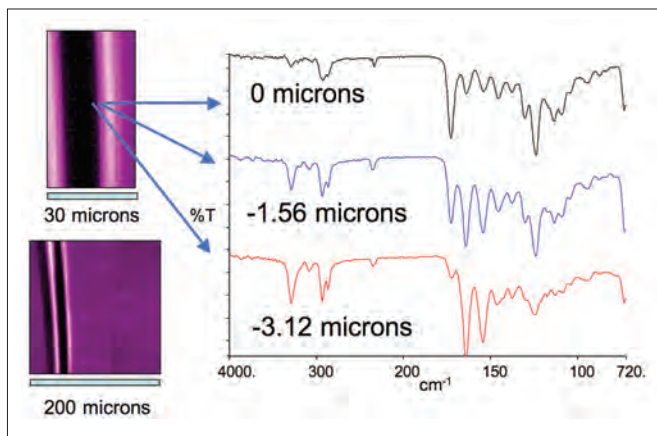


Figure 2. Spectra across layer boundary.

technique, the samples need not be cut into such thin cross sections, making it easier to conserve the integrity of the samples. Typically, samples are mounted in an embedding resin or between blocks and polished to a flat surface. Second, the amount of sample interrogated by the FT-IR beam is relatively low – of the order 1-2 microns using germanium ATR crystals. Images tend to be sharper and spectra show fewer artifact problems since they do not suffer the same beam divergence issues as in transmission through the samples in air.<sup>2</sup> Another potential problem with transmission work is when samples are presented as thin films. Multiple reflections within the sample can lead to interference fringe artifacts or ‘channel spectra’ superimposed on the measured spectra. This problem is not evident with ATR work. Another major advantage with ATR imaging is the ability to measure with higher spatial resolution than transmission imaging.<sup>3</sup> The description and measurement of spatial resolution is described in another technical note<sup>4</sup> where it is shown that a resolution of less than 4 microns is achievable with ATR, whereas the physical diffraction limit for transmission work is typically 3-4 times this figure in the mid-infrared fingerprint region – and that is assuming the sample limitations described above can be overcome.

An ATR imaging accessory has been developed for the PerkinElmer® Spotlight™ FT-IR imaging system which can deliver these advantages.<sup>3</sup> The device uses a germanium cone which is pressed against the cross section of the laminate. One important feature of this accessory is the relatively large tip area. The standard tip diameter of ca. 500 microns means that many more samples can be scanned over the entire laminate structure using a single contact with the sample. In addition, a larger diameter of ca 1200 microns diameter is available. With other devices using much smaller active areas, multiple impressions into the sample would be needed to cover the entire thickness of the sample.

This note describes use of the ATR imaging accessory to measure polymer laminate samples, to show the level of detail that can be revealed routinely, and to provide some practical considerations for laminate measurements using the ATR technique.

## Experimental

**Sample Presentation:** To obtain good ATR images, the sample must be brought into close, uniform contact with the ATR crystal across the entire area to be imaged. This requirement is particularly important and becomes increasingly so for measurements at shorter FT-IR wavelengths (e.g., the C-H stretching fundamental region at ca. 3 microns). This is because the evanescent wave at the crystal/sample interface decays more rapidly at higher frequencies.<sup>3</sup> To achieve this,

the laminate needs to have a flat surface at the point of contact, and be adequately supported to avoid distortion as the sample is pressed against the crystal.

A number of techniques have been explored and, presently, the preferred techniques involve (a) embedding the sample in an appropriate resin and polishing the surface and (b) clamping the sample between two blocks and polishing. We have found in general that method (a) provides slightly superior consistency of sample quality and is ultimately easier from a practical perspective despite initial impressions to the contrary. The sample is clamped vertically in a spring clip (Figure 1A), placed in a mold (Figure 1B), and set in an epoxy or other resin to a depth of ca. 1-2 mm above the clip and below the edge of the sample. After curing, the top surface is cut and polished to a flat surface. Polishing typically involves use of lapping paper with distilled water at grit sizes of ca. 30 microns down to ca. 1 micron to produce a smooth, highly polished surface (Figure 1C). The thickness of the polished block is ca. 5-8 mm. This is placed directly on an anvil on the ATR accessory and the anvil is raised to bring the sample into firm contact with the crystal. Using the embedding technique, there is of course some risk of spectral interference from the resin in the images, but in practice (provided the materials are chemically distinct) this does not create a problem in the subsequent data analysis. Samples of this nature usually have a clearly defined edge and the data analysis software 'Hyperview' incorporates a feature to readily mask out pixels due to the embedding material from the image analysis.

The Spotlight system typically runs with scan conditions between 1-16 scans per pixel with a spectral resolution of 4-16  $\text{cm}^{-1}$  for these samples. The data collection software allows rectangular image areas of various aspect ratios to be defined – a useful advantage of using small linear detector arrays. This is very useful for laminates where a long, thin image shape is often more efficient for scanning across a laminate sample. Image collection times are usually of the

order of minutes to tens of minutes depending on the conditions selected.

## Results

### Example 1: High Image Contrast

It is possible to obtain an idea of the contrast achievable by examining the spectral mixing between component spectra as one scans across a sharp boundary between two layers in the sample. Part of the instrument factory test for spatial resolution involves imaging across a special polymer material with a 'rooftop' cross section to provide a very distinct edge. The steepness of change of the FT-IR signal across the boundary is used to estimate spatial resolution.<sup>4</sup> Laminate samples often provide sharp boundaries between materials. Figure 2 shows spectra of a polyamide layer at such a boundary, measured in steps of 1.56 microns across the boundary. One can see that at a distance of 3.12 microns, the degree of spectral mixing between the polyamide and neighboring layer is sufficiently low to allow excellent discrimination at these distances. In the FT-IR fingerprint region, materials a distance of ca. 3 microns apart can be clearly distinguished provided their spectra are sufficiently different.

### Example 2: Packaging Material

Figure 3A shows the visible image of a packaging material section embedded in epoxy resin. In this example, the quality of finish due to polishing was relatively poor as seen by the surface scratches in the image. Despite this relatively poor surface finish, it was possible to generate good ATR images because (a) the sample was slightly compliant, allowing the crystal tip to be pushed into the sample, and (b) by appropriate data analysis to minimize the effects of the slightly varying contact across the image. Figure 3B shows the FT-IR-reconstructed image where the scratches are no longer apparent.

To obtain the reconstructed image, and with no prior knowledge of the sample composition, the image spectra

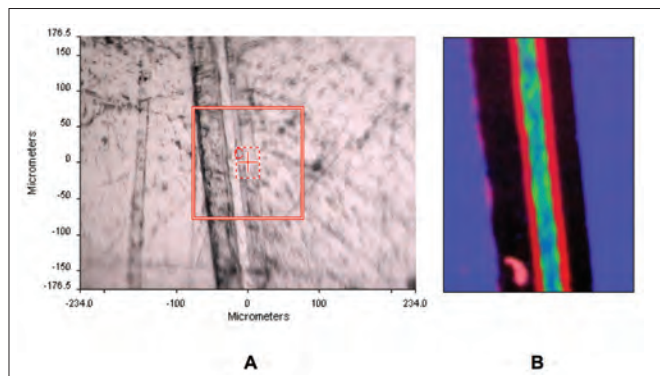


Figure 3. Visible and IR-reconstructed images from embedded laminate.

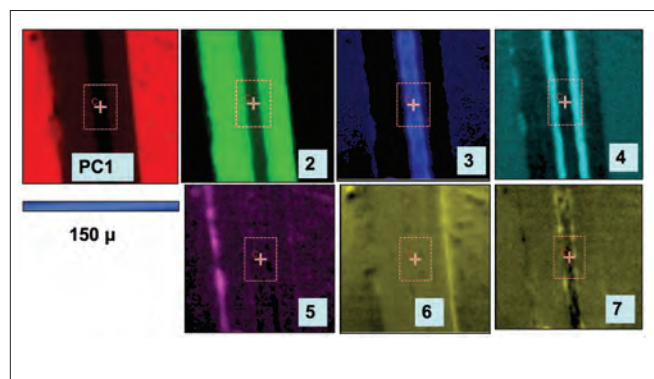


Figure 4. Principal component score images.

were derivatized, offset-corrected, and subject to principal components analysis (PCA). This technique effectively sorts the image spectra into an independent set of sub-spectra (principal components, or factors) from which the image spectra can be reconstructed. Ideally, if there are, for example, five layers present in an image of, say, 1000 spectra, then five sub-spectra would be sufficient to describe all the 1000 image spectra. In practice, more than five spectra are usually required due to the presence of impurities and other spectral contribution, such as baseline variations, and other artifacts, such as variable amounts of atmospheric absorption. This technique does filter out much of the random noise in spectra very effectively without broadening the spectral features due to the sheer numbers of spectra contained in the image; hence, it is a very useful tool for assisting exploratory studies where survey images are required in the shortest time possible. The amounts of the principal components in the original image spectra, or scores, are calculated at each pixel, and the resulting score images are extremely useful in enhancing the FT-IR image contrast. For this sample, the first seven PC score images are shown in Figure 4. Here, the major layers are all accentuated using PCA, along with some minor, more subtle features which will be described. The first score

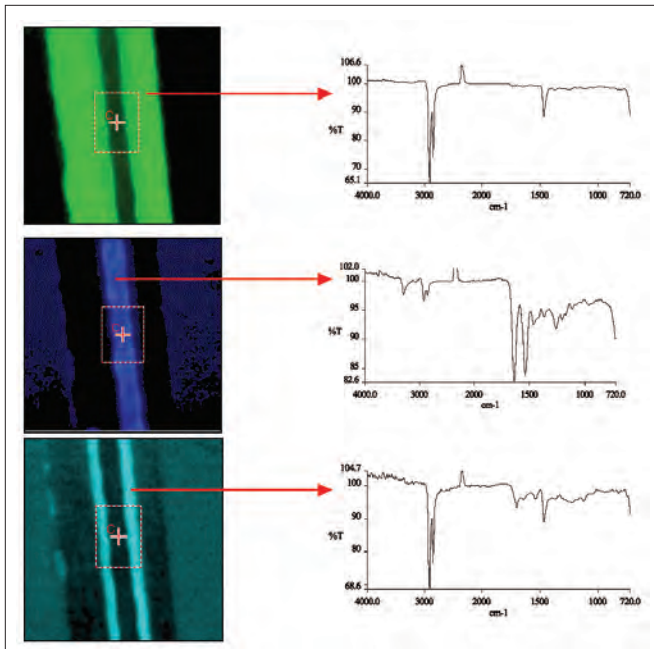


Figure 5. Score images for PCs 2, 3, and 4.

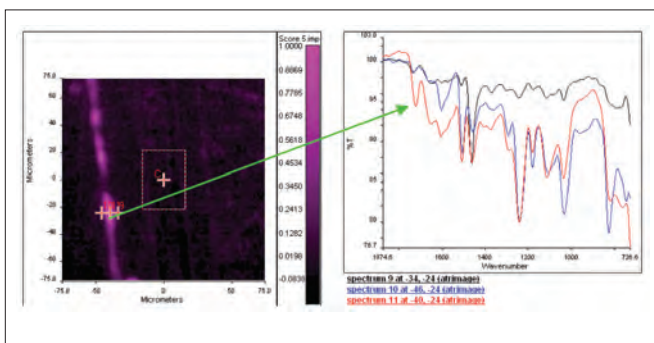


Figure 6. Score image for PC5.

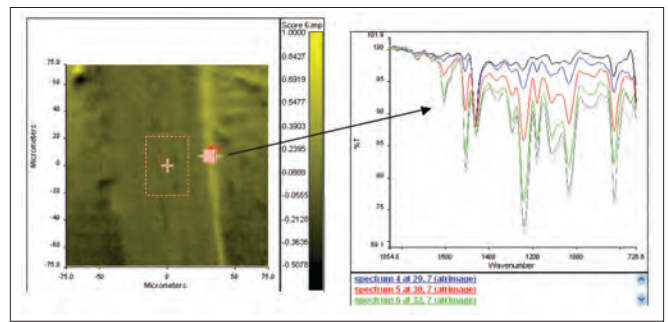


Figure 7. Score image for PC6.

image, PC1, is due to the embedding medium.

The second and third PC score images in Figure 5 show the major laminate layers, a polyethylene and polyamide with intermediate layers ca. 6 microns in thickness, sandwiched by the PE and PA, as revealed in the PC4 image. Here, the layers are readily identified by examination of the underlying raw image pixel spectra. In addition, the features due to the minor variance are shown in the PC5 and PC6 score images in Figure 6. The PC5 image shows a feature of 3-4 microns thick, close to the outer edge of the sample. Using the Spotlight Overlay Manager software, it is possible to view the raw spectra underlying these features, tracking through the feature at steps of 1.56 microns. In the layer itself, there are unique carbonyl features in the spectra which are not present on either side of the layer, thus confirming the distinct chemical composition of the layer. This can be compared with the situation in Figure 7. Here, the PC score image also reveals a 'layer'; however, no distinct chemical

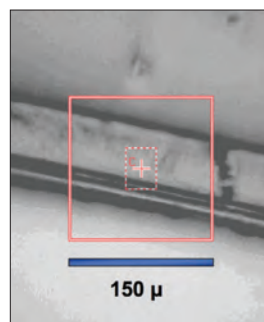


Figure 8. Visible image of laminate with thin adhesive layer.

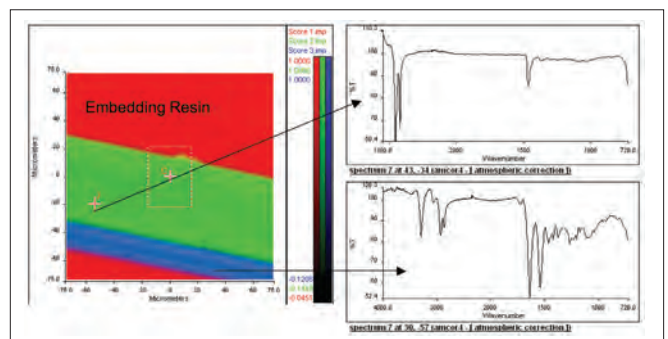


Figure 9. 1st three principal component score images overlaid.

feature appears on examination of the spectra throughout the layer, rather a relatively smooth gradation in spectral intensity from one material to the next. The inference here is the presence of a physical boundary such as a ridge in the sample itself rather than a distinct chemical constituent.

### Example 3: Revealing Fine Detail

This example shows a laminated film with common components but with intermediate layers of less than 5 microns in thickness. As with the previous samples, the material was embedded in resin and polished. The ATR image was collected over a 150x150 micron area using a spectral resolution of 8 cm<sup>-1</sup>. Figure 8 shows the visible image of the sample with the ATR image area highlighted by the red boundary. The image was analyzed using principal components analysis in the 'Show Structure' function in Spotlight and peak height/ratio methods. The overlaid PC score image (Figure 9) shows the embedding material readily differentiated and the major layer (polyethylene) shown in green. Of interest in this example was the layer structure immediately below the thick PE layer. Here, there are more than three chemical constituents present in the image. With three or less components, using a simple red/green/blue (RGB) representation to view the combined image works well with the human eye. But attempting to show more than three components/colors in such an overlaid image can lead to problems when there

is overlap between constituents. The overlapped pixels could be represented as the average of the contributing pixels: white, black, or other ways. This invariably confuses image interpretation. The Overlay Manager function in Spotlight has the ability to change the rules for displaying pixels where overlap occurs, for example, giving priority to the highest intensity color and thereby changing the image contrast. Used in conjunction with examination of the underlying spectra, this feature can be very useful in enhancing contrast. Figure 10 shows the resulting score composite image where, first, the image is shown with colors averaged in regions of overlap and, second, where the pixel colors are set by the most intense component in overlap regions. The improvement is quite striking, and overlaying the color-enhanced image with the raw data confirms that real chemical differences are observed within the different colored regions (Figure 11). Once one is satisfied that all the layers are revealed, it can be helpful to overlay the individual images and adjust the brightness and contrast of the individual layers to generate the most appropriate display for reporting purposes. Figure 12 shows such a composite created from the individual PC score images after exporting to the ImageJ public domain software package.<sup>5</sup>

### Discussion

These examples demonstrate the measurement capability of the ATR imaging accessory with polymer laminate materials.

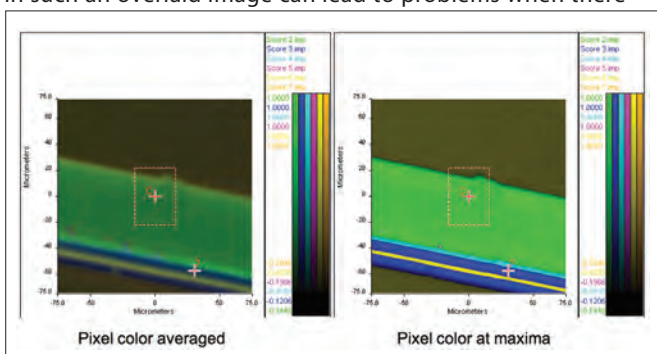


Figure 10. Use of color overlay options to enhance detail.

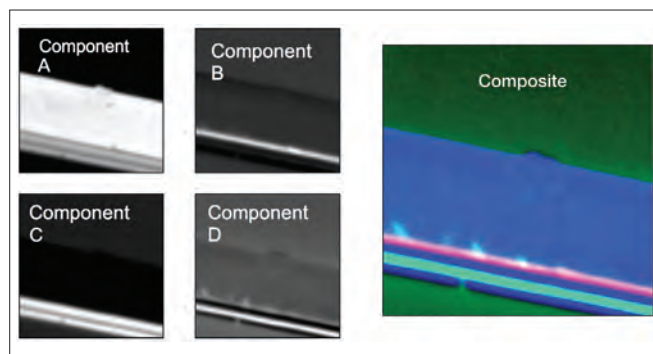


Figure 12. Composite image.

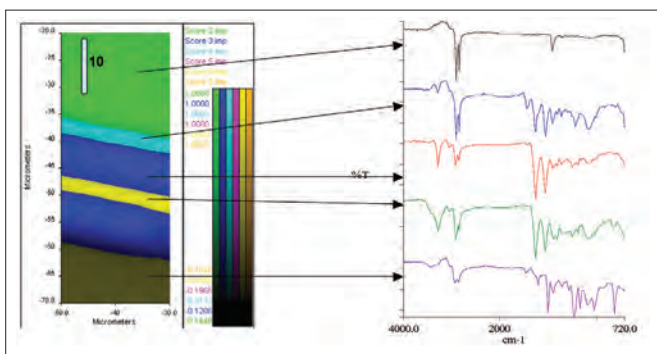


Figure 11. Spectra from individual layers.

With these examples, the sample embedding technique works well with little or no sample degradation. When information on the film constituents is not available, principal components analysis can be useful (compared with peak height/ratio methods) for analyzing survey images and helps reveal fine structure. It is, however, advisable to view the derived score images in conjunction with the raw data to verify the basis for the calculated image structure, as the PCA can effectively 'find' physical and morphological structure in the sample, which can be confused with chemical differences. For presentation of calculated images, it is worthwhile to consider alternative mechanisms for displaying pixels in overlap regions, provided again that the results are checked with the raw data to confirm the contrast revealed.

The data quality obtained with this system is generally good enough to be used directly with commercial spectral search libraries to assist interpretation, which has been performed successfully with a number of samples not reported here. When using standard libraries containing spectra scanned in transmission, search results can potentially be improved by applying ATR correction software to correct for the wavelength dependence of ATR absorption prior to spectral searching.

## Conclusion

Using the Spotlight imaging system, the ATR imaging technique adds a number of benefits compared with the tried and tested method of transmission FT-IR imaging for polymer laminate samples. In addition to somewhat simpler sample presentation and lower risk of spectral artifacts, such as interference fringes, ATR imaging can provide improved spatial resolution. Individual layers of 4 microns or less can be identified. This is particularly important for a number of laminate materials where adhesives and other components may have thicknesses less than 5 microns. As such, use of the technique is likely to grow significantly in laminate studies in the coming years.

## References

1. See, for example, 'Raman Microscopy,' P. Dhamelincourt, in Handbook of Vibrational Spectroscopy, Vol. 2, 1419, Wiley (2002).
2. 'Mid-Infrared Transmission Microspectroscopy,' A.J. Sommer, in Handbook of Vibrational Spectroscopy, Vol. 2, 1369, Wiley (2002).
3. A. Canas, R. Carter, R. Hoult, J. Sellors, and S. Williams, Spatial Resolution in Mid-IR ATR Imaging: Measurement and Meaning, FACCS Conference (2006).
4. 'Spatial Resolution in FT-IR ATR Imaging,' PerkinElmer Technical Note No. 007641\_03 (2006).
5. W.S. Rasband and J. Image, U.S. National Institutes of Health, Bethesda, Maryland, USA, <http://rsb.info.nih.gov/ij/> (1997-2006).

## Thermogravimetric- Infrared Analysis

### Authors

Maria Grazia Garavaglia

Peng Ye

PerkinElmer, Inc.  
Shelton, CT 06484 USA

## Plasticizer Characterization by TG-IR

### Introduction

Plasticizers are additives that are added to polymeric material to increase flexibility. For example, phthalates are usually added to hard PVC plastics to make it soft. Many properties of the polymer will be changed by the addition of a plasticizer, such as the glass transition temperature (T<sub>g</sub>) which will be reduced dramatically; the hardness which will be reduced; the strength which will decrease and the processability which will be improved. Since

plasticizer is often made up of small molecules, it will migrate to the surface and evaporate from the polymer matrix over time or upon heating. One common example is the smell of a new car which is caused by the plasticizer evaporating from the car's interior polymer parts. Because the plasticizer may be toxic and be harmful to human health, restrictions often apply to some types of phthalates such as in children's toys in the United States and European Union. It may be important to know the plasticizer added to the polymer product and its content.

Thermogravimetric analysis (TGA) is a common technique that is used to study the weight loss during heating. It can tell you the percentage of weight loss quantitatively and accurately. But TGA alone will not tell you anything about the chemical components of the evolved off gas. The hyphenation between TGA and FT-IR is able to identify the off gas from TGA and give a more complete picture of material characterization.

In this note, the sample is a complex mixture of solvent, plasticizer and polymers from a paint and varnish producer who require data concerning the plasticizer and its percentage.

## Instrument

A PerkinElmer TGA 8000 and Frontier FT-IR system connected by the state-of-the-art TL 8000 transfer line was used for this analysis (Figure 1)



Figure 1. The TL 8000 transfer line couples a Frontier FT-IR to a TGA 8000.

The advantages of this system include:

- Insulated heated transfer line with replaceable SilcoSteel® liner.
- Heated zero-gravity-effect 'ZGCell' gas cell for the Spectrum instrument incorporating automatic accessory identification, low volume, and efficient sample area purging.
- Control unit incorporating a mass flow controller, particle filters, flow smoothing system, independent transfer line and gas cell temperature controllers, and vacuum pump with exhaust line.
- Automatic triggering of IR data collection from the Pyris software.
- Spectrum Timebase software for time resolved experiments.

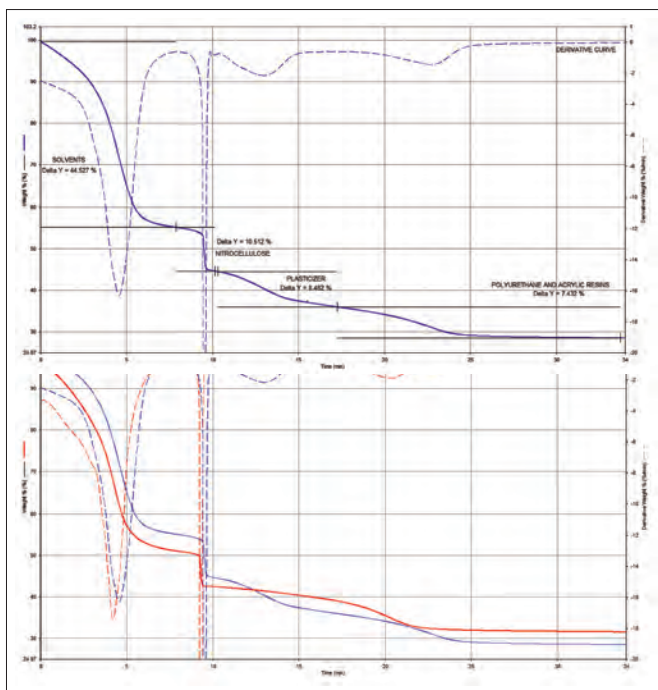


Figure 2. TGA and its derivative curve. Red curve: sample without plasticizer; Blue curve: sample with about 8% plasticizer.

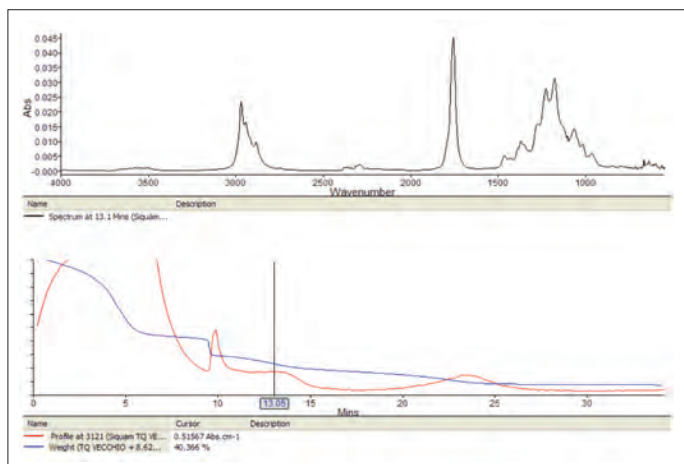


Figure 3. The IR spectrum at 13 minutes.

## Result

Two samples were analyzed by TG-IR. The red TGA curve is the sample without plasticizer; the blue TGA curve is the same sample with the addition of approximately 8% of plasticizer in Figure 2. The derivative of weight loss is also shown in order to help identify the weight loss event.

For the red curve, the first loss of weight is due to the solvents; the second loss is attributed to nitrocellulose polymer and the third loss is due to polyurethane + polyacrylate polymers. For the blue curve, the first loss is from solvents; the second loss is again from nitrocellulose polymer; the third loss is supposed to be from the added plasticizer and the fourth loss is from polyurethane + polyacrylate polymers. All components were identified from gaseous fragments in TG-IR. So by comparing the red curve with the blue curve, it can be seen that the only difference is the weight loss due to plasticizer from the blue curve. The content of plasticizer is determined to be 8.48%.

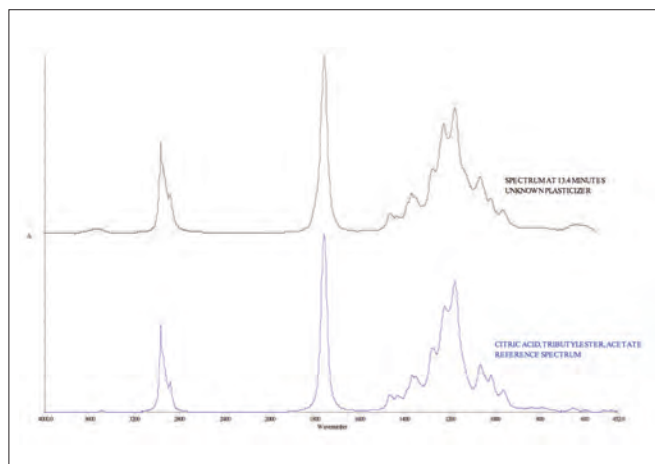
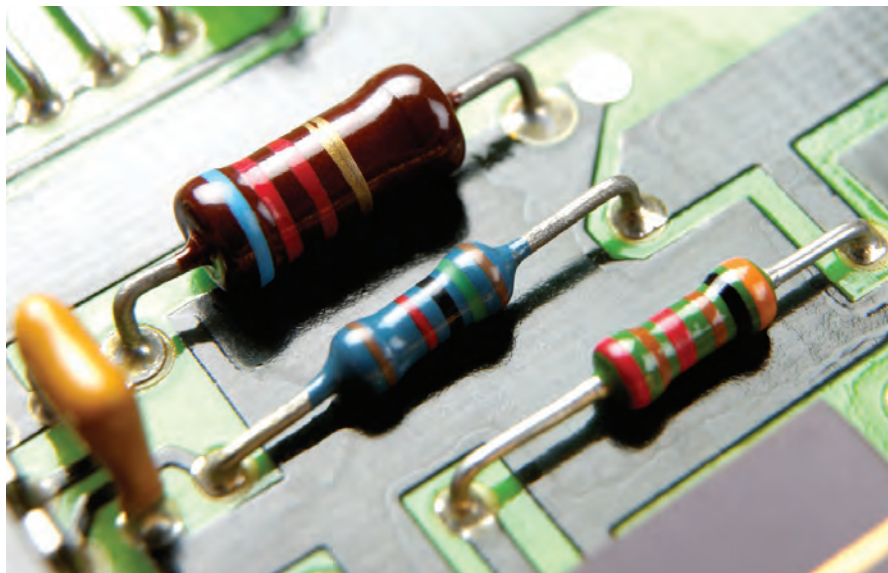


Figure 4. Unknown plasticizer spectrum vs. reference spectrum.

In order to identify the plasticizer, the IR spectrum is used in Figure 3. The IR spectrum at 13 minutes is used because from TGA curve it can be seen that the evolved gas at this point is from the plasticizer. By looking at this IR spectrum and comparing it to reference spectrum (Figure 4), it can be shown that the plasticizer used here is citric acid, tributylester, acetate.

## Conclusion

The TG-IR hyphenation technique has been widely used for the polymer industry, in this case the identification of plasticizer in paint. It combines the strength of TGA and FT-IR analysis and offers a more comprehensive material characterization. The PerkinElmer TG-IR system with the TL 8000 transfer line has proven to be the ideal solution for this analysis. It is easy to use and its design features guarantee the highest quality and most reliable results.



## Characterization of Polymers Using TGA

### Introduction

Thermogravimetric analysis (TGA) is one of the members of the family of thermal analysis techniques used to characterize a wide variety of materials. TGA provides complimentary and supplementary characterization information to the most commonly used thermal technique, DSC.

TGA measures the amount and rate (velocity) of change in the mass of a sample as a function of temperature or time in a controlled atmosphere. The measurements are used primarily to determine the thermal and/or oxidative stabilities of materials as well as their compositional properties. The technique can analyze materials that exhibit either mass loss or gain due to decomposition, oxidation or loss of volatiles (such as moisture). It is especially useful for the study of polymeric materials, including thermoplastics, thermosets, elastomers, composites, films, fibers, coatings and paints.

TGA measurements provide valuable information that can be used to select materials for certain end-use applications, predict product performance and improve product quality. The technique is particularly useful for the following types of measurements:

- Compositional analysis of multi-component materials or blends
- Thermal stabilities
- Oxidative stabilities
- Estimation of product lifetimes
- Decomposition kinetics
- Effects of reactive atmospheres on materials
- Filler content of materials
- Moisture and volatiles content

PerkinElmer offers a variety of high performance TGA instruments encompassing a wide range of application needs and operational requirements. All of the TGA instruments feature an optional, state-of-the-art autosampler for reliable, unattended operation. In addition, all PerkinElmer TGA can be adapted for evolved gas analysis with either FT-IR, MS, or GC/MS.

The extended capabilities of the PerkinElmer TGA, as a valuable tool for polymeric characterization and quality assurance are demonstrated by these applications.

### Thermal Stabilities and Moisture Content

Figure 1 shows the TGA results generated on nylon 6,6 toothbrush bristles. The plot shows the percent mass as a function of sample temperature for the nylon 6,6 bristles under a nitrogen purge. Approximately 10 mg of sample was heated at a rate of 20 °C/min with the PerkinElmer TGA.

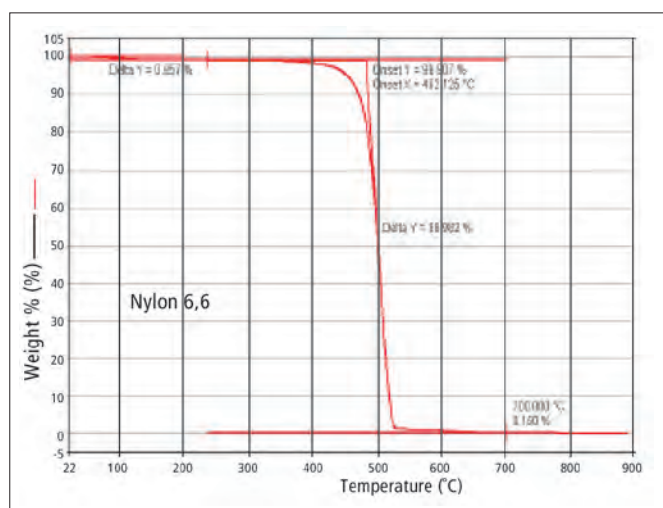


Figure 1. TGA results obtained for nylon 6,6 bristles showing thermal degradation.

The TGA results show that the nylon 6,6 polymer undergoes thermal degradation beginning at 482 °C and with a total mass loss of 99.0%. There is a small amount of inert residue remaining (0.15%).

Nylon polymers absorb a small amount of ambient moisture and TGA can be used to determine this level of water. This may be seen in Figure 2 for the nylon 6,6 sample, which is an enlarged view of the TGA results in the temperature region below the onset of degradation. At about 56 °C, the nylon polymer starts to evolve the small amount of moisture, which is found to be 0.86% by TGA. A high performance TGA instrument is required to detect this small level of moisture content. Knowing this moisture content is important as it has a major bearing on the end use properties and processing performance of nylon.

### Filler Content in Polymers

One major application of TGA is the assessment of the filler content in polymers and composites. The level of fillers can have a significant impact on the end use properties (thermal expansion, stiffness, damping) of the final product. This is particularly important for electronics applications where the level of filler affects the coefficient of thermal expansion (CTE) as measured using the TMA. It is important for the components in a printed circuit board to have very similar expansivities or else built-in stresses over time can occur. Because the amount of filler is one of the possible causes to changes in the thermal expansion, TGA is used to determine the amount of filler present. Displayed in Figure 3 are the TGA results generated on a glass filled epoxy resin used for electronic applications.

The epoxy resin undergoes thermal degradation beginning at 440 °C with a mass loss of 57.4%. At 650 °C, the purge gas flowing over the sample was automatically switched to oxygen and the carbon residue was burned off at 655 °C with a mass loss of 10.5%. [The PerkinElmer TGA instruments all feature the option of an automated gas flow and gas switching accessory for ease of conducting TGA thermo-oxidative experiments]. The material remaining behind after exposing the sample to oxygen is the inert glass filler, which the TGA shows comprises 31.8% of the mass of the epoxy resin.

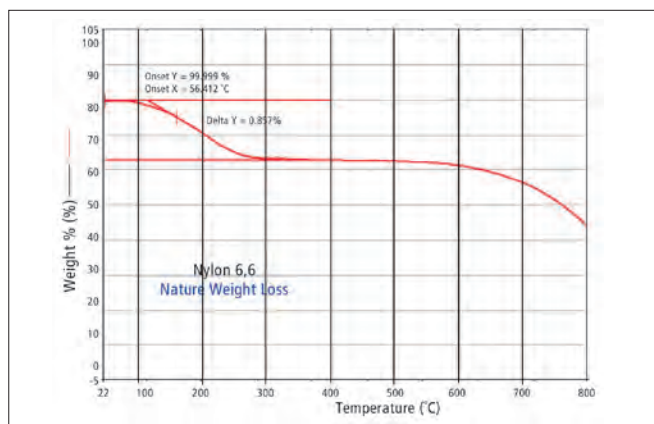


Figure 2. TGA results water weight loss for nylon 6,6.

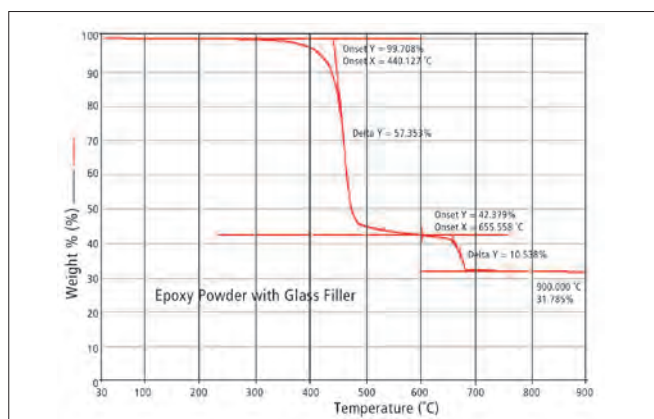


Figure 3. TGA results for epoxy-glass powder.

## Characterization of the Differences in Polymers

A high performance TGA, such as the ones available from PerkinElmer, allow for the detection of subtle, but potentially important, differences between polymers. Shown in Figure 4 are the TGA results obtained on two different high density polyethylene (HDPE) containers. One is an opaque soap container while the other is a semitransparent water bottle. The soap bottle HDPE resin has a slightly, but significantly, higher level of filler (2.1% versus 0.65%). This information is important for the production of the containers.

## Compositional Analysis of Multi-component Polymers

One of the most important applications of TGA is the assessment of the compositional analysis of polymeric blends. The compositional characterization information can be enhanced through the use of Auto Stepwise TGA, where the TGA instrument automatically heats the sample and then holds it under isothermal conditions when the instrument detects a significant weight loss. This provides the highest possible separation of overlapping decomposition events and provides for the most accurate compositional analysis of polymers.

An example of the ability of the Auto Stepwise approach to provide useful compositional information is in the characterization of ABS. This is a polymer alloy comprised of a SAN matrix (styrene acrylonitrile copolymer) with butadiene. The butadiene is a rubbery component and provides the desired impact and toughness properties to the ABS blend. ABS is typically used for housings for personal computers and other electronic equipment and the material's impact resistance is important for its long term durability. The weight loss transition of the butadiene rubber component occurs extremely close to the decomposition of the SAN copolymer. Standard TGA cannot separate out the two events.

However, Auto Stepwise TGA does provide the ability to resolve the two weight loss events and makes the quantitative compositional analysis of the ABS possible. This may be seen in the Auto Stepwise TGA results obtained on ABS displayed in Figure 5. The butadiene, rubber component is nicely separated from the SAN decomposition and this provides excellent characterization information.

Another example of the ability of the Auto Stepwise approach to provide outstanding separation of overlapping weight loss events is for tire elastomers. These elastomers consist of a blend of polymer, oil extender, carbon black and fillers. It is difficult to separate out the oil from the polymer using standard TGA since the two events severely overlap. However, with the Auto Stepwise approach, all of the components in a tire elastomer can be clearly identified as is shown in Figure 6. This information is valuable for the production of an automotive tire with the desired end use and long term properties.

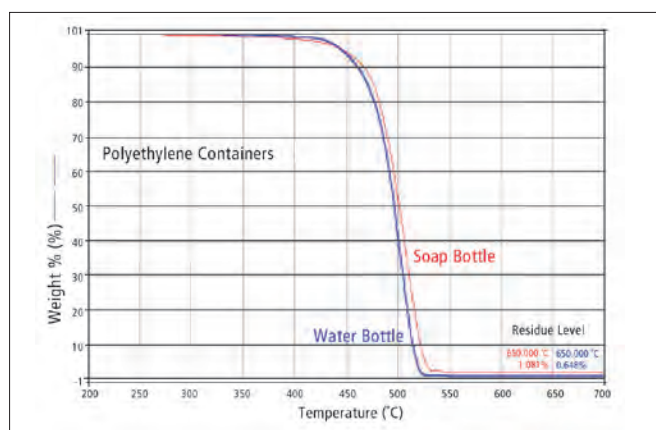


Figure 4. TGA degradation for two different HDPE bottles.

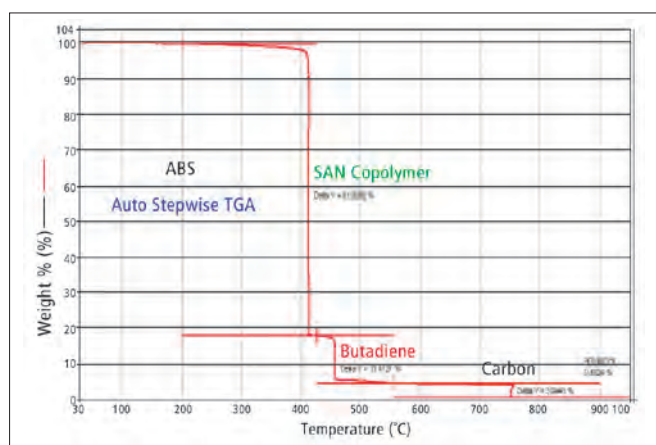


Figure 5. Auto Stepwise TGA results for ABS showing separation of SAN and butadiene components.

## Measurement of Low Level of Volatiles

Many polymer applications are sensitive to the occurrence of low level volatilization. On a large production basis, even a small level of volatiles (e.g., less than 1%) can have a major impact on the processing of the polymer. It is known that low levels of volatiles can affect the injection molding or blow molding processing of polymers. Shown in Figure 7 is the low level of volatilization obtained for a single pellet of PET resin. This measurement was performed holding the sample under gentle isothermal conditions at 130 °C. The mass loss observed at 10 hours was 0.219% for the PET pellet. This is an important aspect for PET resins used to make beverage containers as low levels of soluble volatile components can affect the taste of the beverage. The high performance TGA instruments from PerkinElmer provide the high degree of sensitivity and stability to make these long term measurements possible.

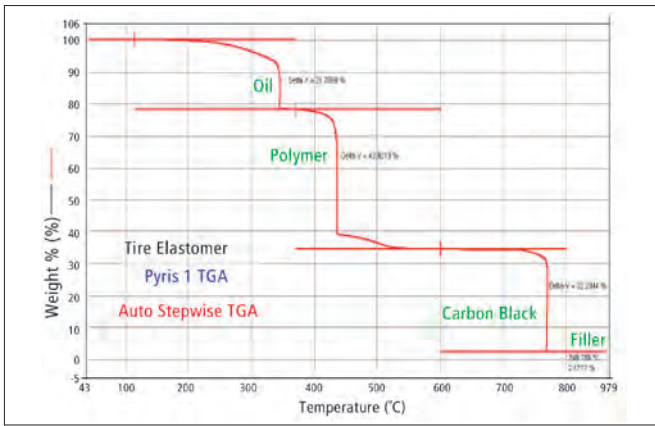


Figure 6. Auto Stepwise TGA compositional results for tire elastomer showing separation of oil, polymer, carbon black and filler.

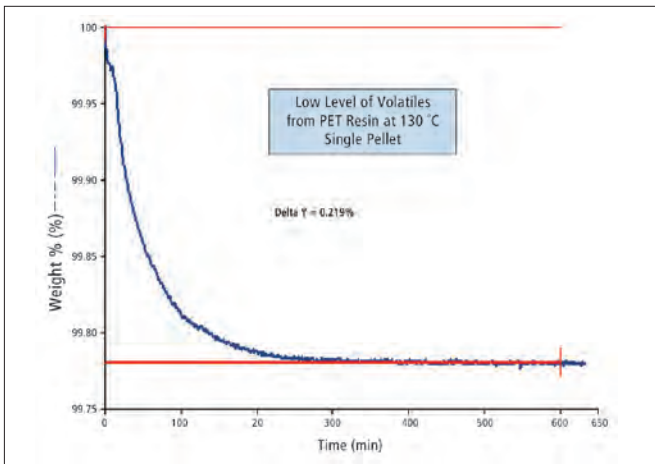


Figure 7. Low level emission of volatiles from single PET chip under gentle isothermal conditions at 130 °C.

### TGA Decomposition Kinetics for Lifetime Predictions

TGA decomposition information can be used to predict the useful product lifetimes of some polymeric materials, such as the coatings for electrical or telecommunication cables. The sample is heated at three or more different heating rates. The use of the different heating changes the time scale of the decomposition event. The faster the applied heating rate, the higher the given decomposition temperature becomes. This approach establishes a link between time and temperature for the polymer decomposition and this information can be used to model the decomposition kinetics.

Shown in Figure 8 are the TGA results generated on a sample of polyethylene at heating rates ranging from 1 to 40 °C/min. As the heating rate is increased, the onset of decomposition is moved to higher temperatures. This data can then be analyzed using the PerkinElmer TGA Decomposition Kinetics Software. The kinetics analysis provided by the software provides valuable predictive information on polymeric materials, including lifetime estimations. Displayed in Figure 9 are the isoconversion curves, which presents the time to achieve a particular level of conversion as a function of temperature. These are particularly useful for product lifetime assessments. If the desired level of critical conversion is known, then the time to achieve this critical level at a particular operating or end use temperature can be predicted.

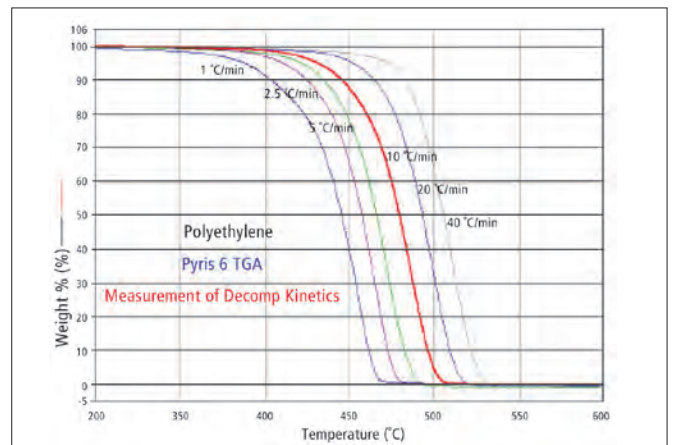


Figure 8. Effect of heating rate on the thermal decomposition of polyethylene.

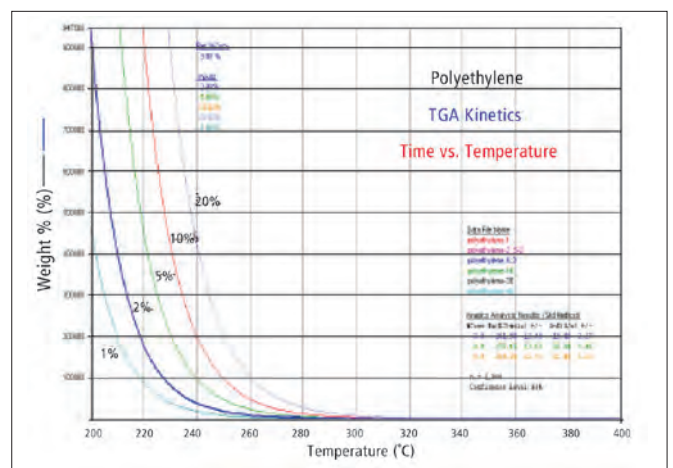


Figure 9. Isoconversion curves for polyethylene thermal degradation based on kinetics modeling.

## Thermal Analysis

## Authors

Peng Ye

Boon-Chun Tan

PerkinElmer, Inc.  
Shelton, CT USA

## How to Optimize OIT Tests?

### Introduction

OIT is the abbreviation for oxidative induction time. It provides information about the oxidative stability of mainly polymer materials. This information is important because plastic parts age throughout their lifetime due to exposure to environmental elements such as heat, oxygen, light and radiation. Aging causes the degradation of the physical properties of the polymers and will lead to their failure. Antioxidants are often added during the plastics formulation to hinder the aging caused by oxygen and to increase their lifetime. Because the reaction between polymers and oxygen (O<sub>2</sub>) is exothermic, OIT determination using Differential Scanning Calorimetry (DSC) is an ideal solution to study this process.

In the OIT test method, the test specimen is heated to a specific temperature in an open pan under an inert atmosphere. After a short period of time, at the isothermal temperature, the gas is switched from inert purge to O<sub>2</sub>, or air purge. The time taken from the O<sub>2</sub> gas switching to the onset of oxidation reaction is defined as OIT. OIT is an accelerated test used as a qualitative evaluation of the oxidative stability of a material. This time can be used as criteria of the thermal stability of polyolefins in an oxidative atmosphere. The OIT method is standardized in ASTM® D 3895 and DIN EN 728 for polyolefins. The OIT test is of great interest to companies who produce or utilize polyolefins, which are used at elevated temperatures under an oxygen atmosphere such as tubes or pipelines, cable or wire insulation, geomembranes or vapor-barrier-films. It can be used to compare the aging resistance of different plastics, to detect the impact of antioxidant concentration and to assess the effectiveness of antioxidants.

In this application note, we will review several influential factors for the OIT method. They are:

- Isothermal measurement temperature
- Sample selection
- Sample geometry
- Pan material

The data was generated on the PerkinElmer® Jade DSC\*. The Jade DSC\* has been designed to be both rugged and reliable. The system utilizes a precisely-machined disc of hardened nickel chromium and a low-mass aluminum coated furnace to give the instrument high resistance against contamination or aggressive gases, and to provide accurate, reproducible results. The integrated gas flow control and switching device assures high stability and best control over purge gases.



Figure 1. DSC 4000.

## Experiments and discussions

### Isothermal temperature

The crucial parameter in OIT determination is the isothermal temperature. This temperature is usually above the melting temperature for crystalline polymers. Low temperature will make the experiment too long and may not be acceptable economically, while high temperature can cause fast oxidation and lead to poor reproducibility and resolution. As shown in Figure 2, increasing the isothermal temperature from 205 °C to 215 °C resulted in decreased OIT. Usually an OIT between 5 and 60 minutes is desired. So in this case, isothermal measurements at 205 °C are the preferred choice.

### Sample selection

For sample selection, the storage time (the time interval between when the part is made and when the actual OIT measurement takes place) should be taken into consideration because the oxidation starts as soon as the plastic part is manufactured. The antioxidant additive may be consumed during processing and storage, which can lead to a lower OIT compared with a virgin part. The sampling

location on the part also has an impact on the OIT result because various locations of the sample may have different concentrations of antioxidant additives. For example, in the case of a water pipe, the sample taken from the outside of the pipe may have a lower OIT than the sample taken from the center of the pipe because the antioxidant additive at the surface can be extracted by water.

### Sample geometry

Sample geometry is another important influential factor in OIT measurements. Since oxidation happens between sample and oxygen, the surface area relative to the sample volume is important. Different sample geometries have different surface-to-volume ratios. Figure 3 illustrates the effect of sample geometry on the onset time and rate of oxidation. In this example, the standard sample was a compact disk.

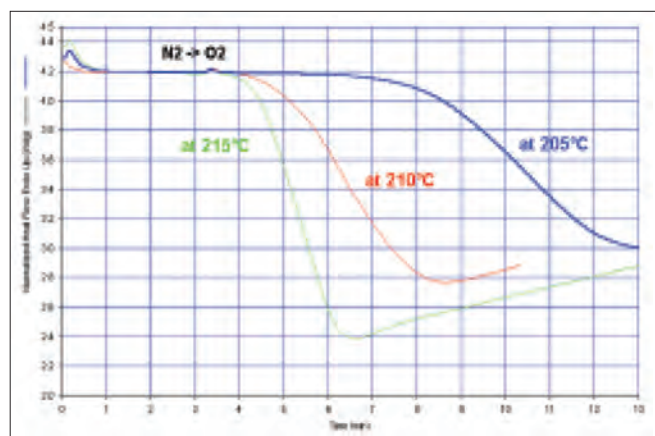


Figure 2. Influence of isothermal temperature on OIT for LLDPE.

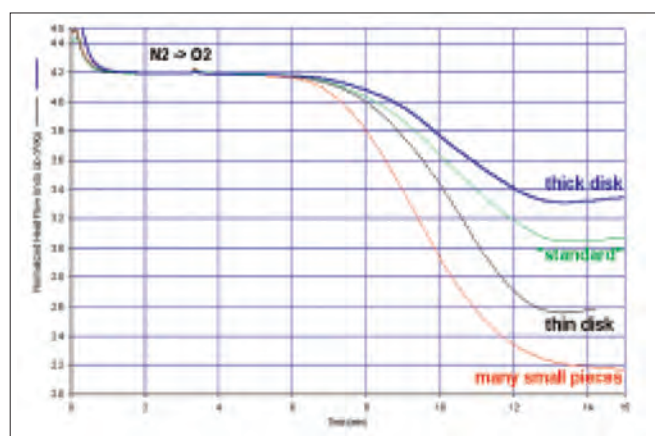


Figure 3. The effect of sample geometry on OIT measurement of LLDPE at 205 °C.

\*Jade DSC instrument is superseded. It has been replaced by DSC 4000.

The thin disk and small pieces had the same mass as the standard sample. The thick disk mass was about 3 times that of the standard sample. To ensure a good measurement of onset oxidation time, the thin disk is preferred because of its good contact with the sample pan and its large surface area relative to the volume. The thick disk has a smaller surface-to-volume ratio and less sharp onset than a thin disk. The small pieces sample has a very large surface-to-volume ratio, however the thermal contact with the pan and the heat transfer within the sample is poor. In addition, the surface-to-volume ratio of small pieces is very irreproducible. In order to get highly reproducible results for OIT tests, a constant and thin disk sample geometry is favorable.

### Pan material

The curves in Figure 4 show a big difference in the stability of the sample with respect to the pan material. The sample with the copper pan has a significantly lower OIT than the sample with the aluminum pan. The reason for this is because copper catalyzes the oxidation reaction. In some application areas this must be taken into account. When products come in contact with copper during their usage it is obvious that their lifetime decreases. This is very important for the cable industry.

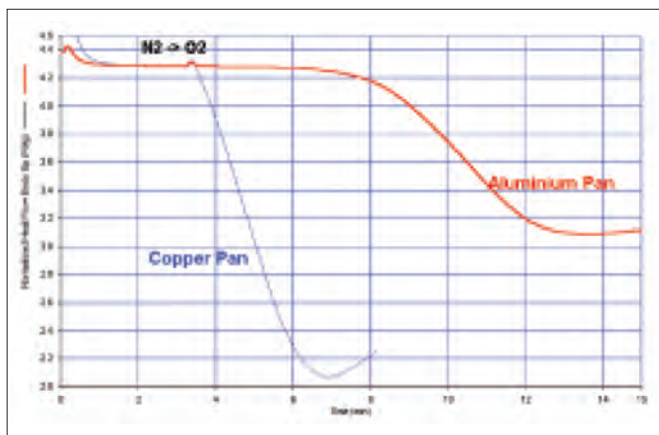


Figure 4. The influence of sample pan material.

### Data analysis

The OIT determination with Pyris™ software is easy and offers many beneficial features. The user can select criteria in the method set-up for the OIT measurement that, for example, stops the measurement after the start of the oxidation, but before the sample completely decomposes.

In the calculation window you can find the analysis for OIT (Figure 5). The standard package of the PerkinElmer Pyris software also includes the Pyris Player. The Player software is useful in many cases. It allows you to automate the work routine. Not only can this software be used with an autosampler, this package offers the user to option to set up a sequence that will automatically calculate the OIT at the end of a single sample run.

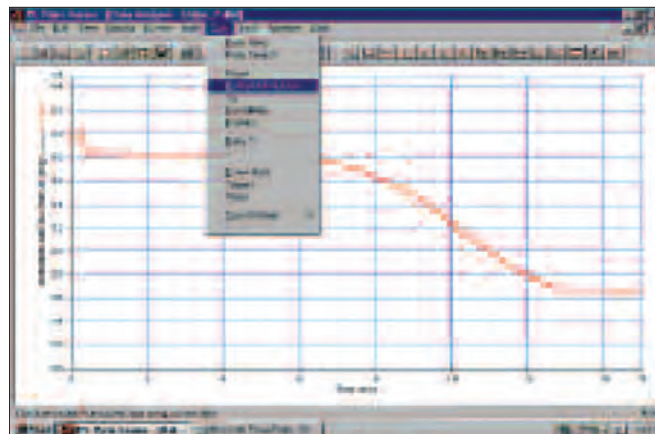


Figure 5. The OIT calculation window in the Pyris software.

Another valuable feature is the tolerance test. The customer determines the criteria for pass or failure of the test. The OIT criterion can be within a range, greater than or less than a defined value. When using an autosampler the customer can specify the action upon failure. The action can be to either stop, continue, skip to the next sample or block the sequence.

One final example of OIT application is given in Figure 6. It is the measurement of a HDPE pipe piece. The temperature was ramped from 30 °C to 200 °C at 20 °C/minute and held isothermally. The gas switched from N<sub>2</sub> to O<sub>2</sub> at 2 minutes on the isothermal hold. The onset, at about 95 minutes, defines the time interval from time zero (switch to O<sub>2</sub>) to the onset of the oxidation reaction. The tolerance test feature confirms that this material passed the test.

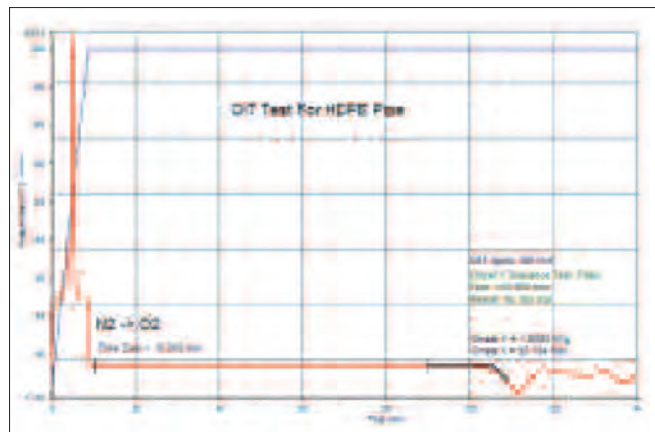


Figure 6. OIT test for HDPE pipe.

## Summary

In order to get good, reproducible OIT data, you need to assure a:

- Stable isothermal temperature
- Constant sample morphology, geometry and weight
- Reliable and consistent purge gas flow rate
- Similar pan material is used

The Jade DSC\* with integrated mass flow controller and Pyris software is a great combination to perform OIT tests. It is an ideal, cost-effective solution for reliable tests in QA/QC labs or as part of product development.

## Reference

Gottfried W. Ehrenstein, Gabriela Riedel and Pia Trawiel, Thermal Analysis of Plastics, 2004.

\*Jade DSC instrument is superseded. It has been replaced by DSC 4000.

PerkinElmer, Inc.  
940 Winter Street  
Waltham, MA 02451 USA  
P: (800) 762-4000 or  
(+1) 203-925-4602  
[www.perkinelmer.com](http://www.perkinelmer.com)



---

For a complete listing of our global offices, visit [www.perkinelmer.com/ContactUs](http://www.perkinelmer.com/ContactUs)

Copyright ©2007-2016, PerkinElmer, Inc. All rights reserved. PerkinElmer® is a registered trademark of PerkinElmer, Inc. All other trademarks are the property of their respective owners.

Differential Scanning  
Calorimetry

## Measurement of T<sub>g</sub> of Polypropylene Using the Double-Furnace DSC



DSC 8500

### Introduction

One of the more commonly used thermoplastics is polypropylene because of its versatility. The polymer exhibits excellent chemical resistance, low density, high tensile strength and relatively high melting point, especially in comparison to its counterpart, polyethylene. Polypropylene finds widespread use for a variety of applications including fibers, packaging and capacitor films, food containers, home appliances, automotive components, telecommunication cables and injection molded products.

As with all thermoplastics, it is important to characterize the thermophysical properties of polypropylene, including melting temperature, percent crystallinity, crystallization when cooling from the melt, and the glass transition temperature, T<sub>g</sub>. Different grades of the polypropylene will result in different physical properties and for process control and optimization, it is important to characterize the polypropylene material. Additionally, it is essential to analyze the thermophysical properties of the end product for quality assurance purposes.

Thermal analysis provides an ideal means of characterizing the properties of polymers, including polypropylene. Differential Scanning Calorimetry (DSC) is a particularly useful technique for the characterization of polypropylene.

The measurement of the glass transition event, T<sub>g</sub>, of polypropylene is generally considered difficult by DSC given that the transition is weak. However, a DSC with high sensitivity and flat and reproducible baseline is able to detect the weak T<sub>g</sub> associated with polypropylene. The high performance DSC from PerkinElmer® can readily detect the T<sub>g</sub> of polypropylene.

### Power Compensation DSC

The double-furnace DSC uses the exclusive Power Compensation approach which applies or removes power (or energy) to two independently controlled furnaces (sample and reference). While other, more conventional DSC instruments, employ the heat flux DSC approach (single, high mass furnace), the Power Compensation DSC uses two very lightweight furnaces with a mass of only 1 g. This provides exceptionally nimble performance in terms of rapid equilibration and the ability to heat and cool at ultra fast rates (up to 500 °C/min).

In contrast, some of the heat flux DSC devices employ a large, high mass silver block (150 g), which then yields a sluggish response by virtue of its high thermal inertia. The physical difference in masses between the heat flux and Power Compensation DSC furnaces is displayed in the following figure.



The Power Compensation DSC uses new technology which combines ultra fast responsiveness with high stability.

This provides the highest performance of any DSC on the market.

In this study, the physical properties of polypropylene were studied using the Power Compensation DSC.

### Experimental

The following conditions were utilized to characterize a sample of polypropylene (high density, isotactic polypropylene film).

Experimental Conditions	
Instrument	PYRIS Power Compensation DSC
Heating rate	20 °C/min
Sample mass	Approximately 10 mg
Sample pan	Crimped standard aluminum pan
Purge gas	Nitrogen
Cooling system	Intracooler II
Temperature range	-50 to 200 C

The DSC was calibrated for temperature and enthalpic responses using high purity indium metal.

The baseline response of the Power Compensation DSC was highly linear, such that no baseline subtractions were necessary.

### Results

Displayed in Figure 1, are the DSC results generated on the as-received polypropylene film sample. The polymer exhibits a number of melting transitions (due to processing and thermal history factors). The main melting peak is observed at 168 °C with other processing-induced peaks occurring at 163 and 78 °C. The heat of melting is found to be 107.0 J/g for the as-received film sample. The rate of heating is a very important characteristic of thermoplastics as it is related to the percent crystallinity of the material. The heat of melting can be used to determine the percent crystallinity using the following simple relationship.

$$\% \text{ Xtal} = (\Delta H_m / \Delta H_m^\circ) \cdot 100\%$$

In this expression, ΔH<sub>m</sub> is the measured heat of melting by DSC and ΔH<sub>m</sub><sup>°</sup> is the reference value for the heat of melting. For polypropylene, this reference value is 207 J/g. This yields an estimated percent crystallinity of 51.7% for the as-received polypropylene film.

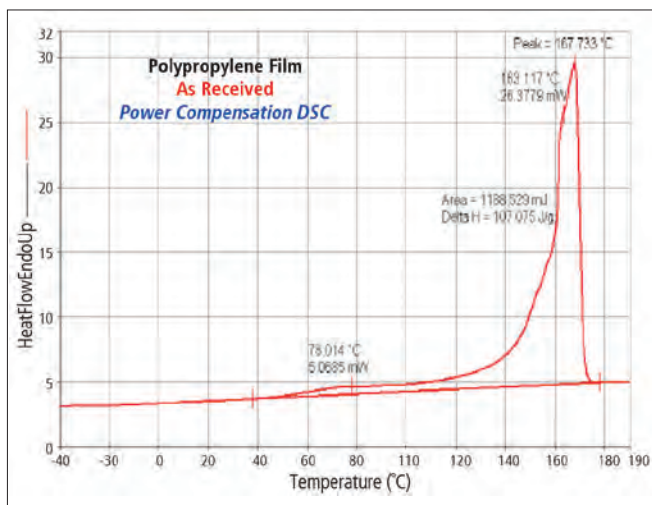


Figure 1. DSC results on as received polypropylene film sample showing multiple melting peaks.

The as-received polypropylene film also has a glass transition event, Tg. Although this is very weak, due to the highly crystalline and oriented nature of the film sample, the Power Compensation DSC has the necessary high degree of sensitivity to be able to detect the Tg. This may be seen in Figure 2, which is an enlarged view of the heat flow response in the regions below the main melting transition.

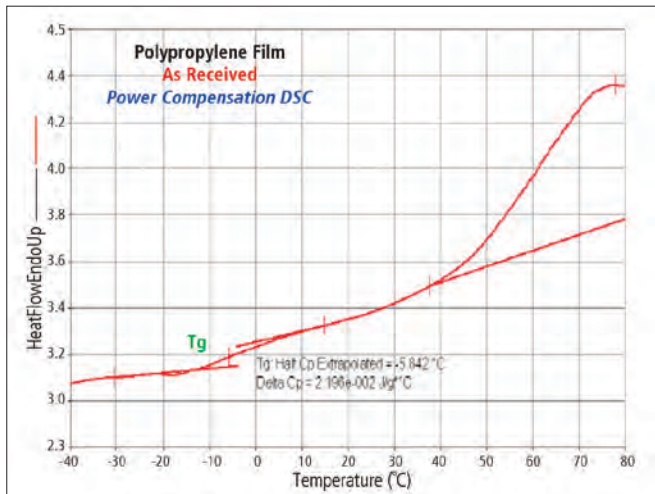


Figure 2. Enlarged view of Tg of as received polypropylene film sample.

The Tg of the as-received, oriented film is observed at  $-6^{\circ}\text{C}$  as a small, stepwise change in the heat flow response. Although this Tg is exceedingly weak, the Power Compensation DSC has the very high degree of sensitivity that permits its detection.

The polypropylene sample was cooled back to  $-50^{\circ}\text{C}$  and reheated at a rate of  $20^{\circ}\text{C}/\text{min}$  to demonstrate the effects of thermal history. Shown in Figure 3, is an overlay of the DSC results from four (4) reheat experiments performed on the polypropylene material over the complete temperature interval. These results demonstrate the outstanding reproducibility of the Power Compensation DSC instrument as the different data sets are virtually indistinguishable.

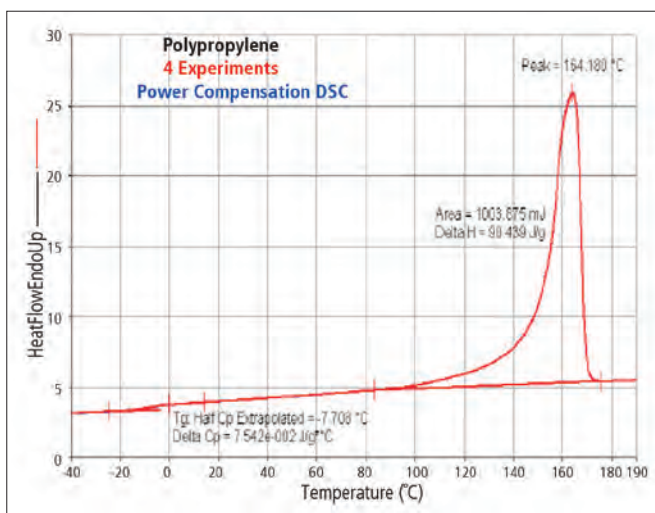


Figure 3. Overlay of four (4) reheat experiments performed on polypropylene sample.

After the polypropylene film specimen is melted, cooled and reheated, only a single melting peak is obtained at  $164.2^{\circ}\text{C}$ . The heating of melting is  $90.5\text{ J/g}$ , which yields a percent crystallinity of  $43.7\%$ . This is significantly less than the crystallinity value of the as-received film sample, which is attributable to the differences in thermal histories. The Tg of the reheat polypropylene sample is observed at  $-7.7^{\circ}\text{C}$  and is more readily observable as compared to the original, as-received film sample.

The high quality results obtained for the Tg of the polypropylene sample may be seen in Figure 4. The figure shows an overlay of the Tg results generated for the four separate experiments on the reheat polypropylene sample. The data is all the more remarkable considering that it was generated *without* the need for baseline subtraction. This demonstrates the very high performance level of the Power Compensation DSC. Although the detection of the Tg of polypropylene by DSC is normally considered difficult, the Power Compensation DSC is readily able to handle this particular measurement.

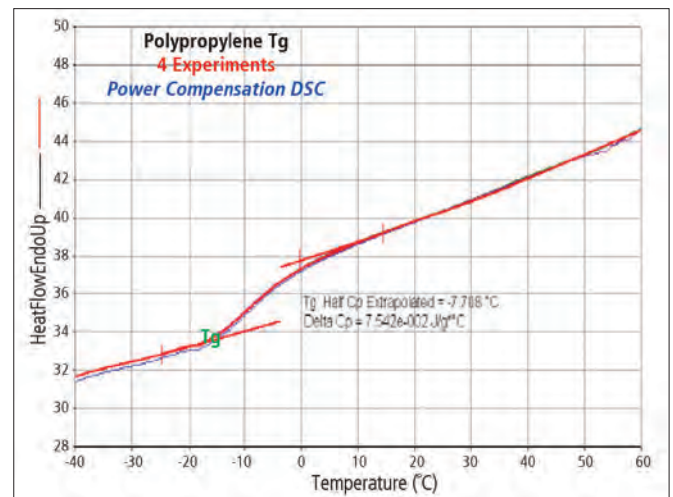


Figure 4. Reproducibility of Tg of reheat polypropylene sample showing overlay of four (4) DSC experiments.

The differences in the thermophysical properties between the as-received and reheat polypropylene samples may be seen in Figure 5. These results are a direct overlay of the two different sets of DSC data. These overlay type of data presentations are highly useful for comparative purposes. It may be seen that the given thermal history has a major effect upon the thermal characteristics of the polypropylene material. The high resolution response of the Power Compensation DSC makes these differences evident.

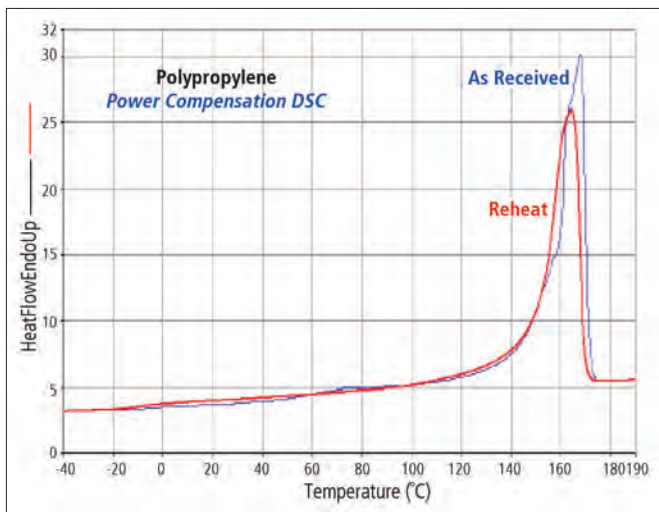


Figure 5. Overlay of DSC results for as received polypropylene film and melt-cool-reheat sample.

## Summary

The Power Compensation DSC provides an ultra high level of performance. This is exemplified by the results generated on a polypropylene film sample. The Power Compensation DSC is able to detect the weak T<sub>g</sub> of the melt-cooled resin as well as the very weak T<sub>g</sub> of the highly crystalline and oriented film sample. The outstanding calorimetric response of the Power Compensation DSC yields outstanding reproducibility for both the melting as well as the T<sub>g</sub> of the polypropylene material. The Power Compensation DSC provides the highest research-grade performance of any DSC on the market.

## Thermal Analysis

**Authors**

Tiffany Kang

PerkinElmer, Inc.  
Kaohsiung, Taiwan R.O.C.

Peng Ye

PerkinElmer, Inc.  
Shelton, CT USA

## Isothermal Crystallization Study for Quality Assurance

### Introduction

The crystallization behavior of polymer resin is important to know. For polymer processors, it helps to optimize the processing conditions like mold temperature and holding time. DSC is traditionally used to study the thermophysical properties of polymers. The isothermal crystallization

experiment is very useful to determine the crystallization kinetic parameters. In an isothermal crystallization experiment, the polymer sample is first heated to above its melting temperature and held for some time to fully melt out any existing crystals. Next, the sample is quench-cooled quickly to the desired isothermal temperature which is usually between its melting temperature and its glass transition temperature. The sample is left crystallized under this temperature and the heat generated during this crystallization process is recorded by the DSC instrument. The experiment may stop when the crystallization finishes and heat flow signal reaches the baseline. The isothermal crystallization experiment can be conducted at a series of temperatures and the result curves can be processed by the software to get kinetic parameters like reaction order and activation energy.

The isothermal crystallization result is very sensitive to the sample properties. It can be influenced by many factors, including average molecular weight, molecular weight distribution, type and concentration of nucleating agent, and its concentration, presence of plasticizers or presence of regrind. Therefore, it is a sensitive test and can be used to show the difference between various batches of material, which may show little difference under a conventional heating experiment. Batches with different crystallization behavior will lead to variation in the quality of the final processed product. For polymer resin manufacture, it can be used for quality assurance purposes, the optimization of resin formula or the evaluation of a competitor's resin.

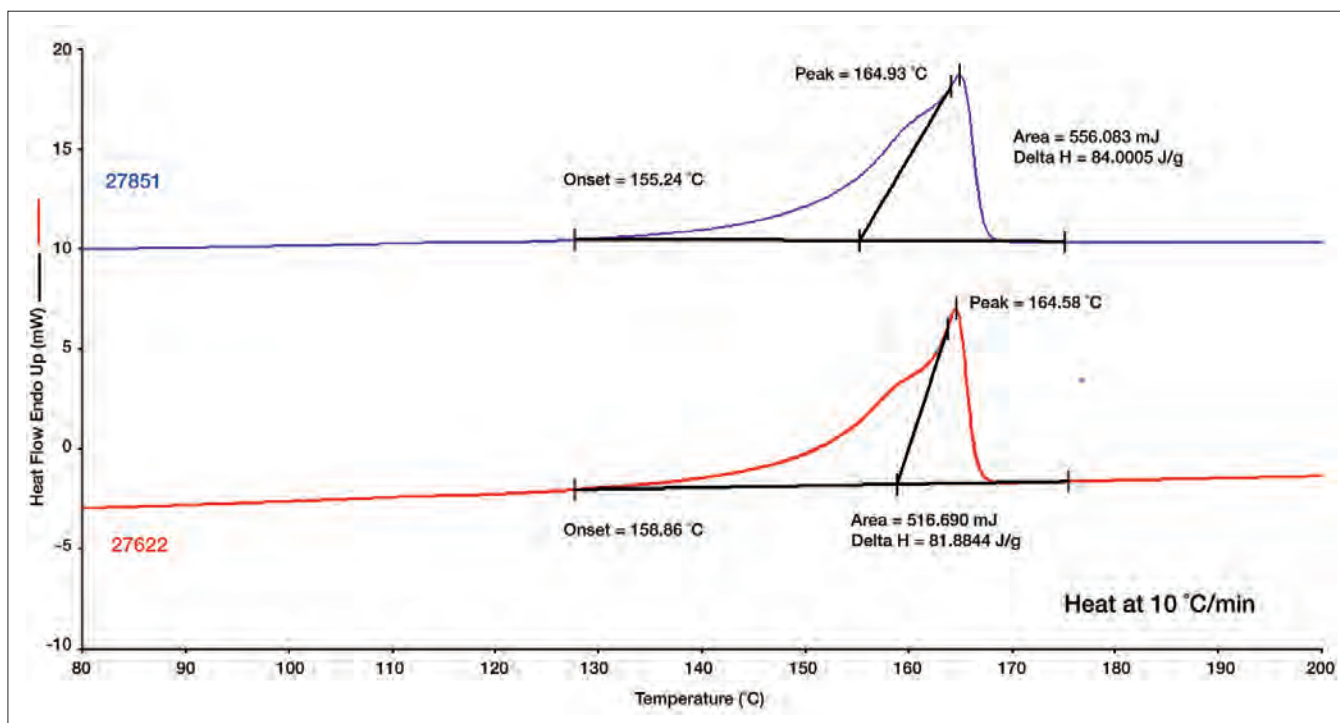


Figure 1. Conventional heating scan on batch A and B.

Power compensation DSC has been preferred for this application. A true isothermal crystallization experiment can only be performed on power compensation DSC due to its null principle and power compensation scheme. In heat flux DSC, the sample temperature can actually increase during the isothermal crystallization experiment because of the exothermal reaction of crystallization. Fast cooling is also very critical for the accurate determination of kinetic data. Fast cooling is critical for the accurate determination of kinetic data and in this case, a high rate of cooling is needed to prevent the resin from crystallization before it reaches the isothermal temperature. This is especially true for some polymers with high rates of crystallization. Conventional heat flux DSC has a big furnace and cannot achieve the fast cooling rate needed for an isothermal crystallization experiment. On the contrary, power compensation DSC has a much smaller furnace and can achieve a controlled cooling rate up to 500 °C/min. So, improved isothermal crystallization data can be obtained from power compensation DSC.

### The Challenge

In this case, a polypropylene resin manufacturer had made two batches of product resin. They were suspected to be of different quality. Conventional heating experiments were conducted, but failed to show any difference. The isothermal crystallization test was tried and was able to show the difference clearly between the two batches.

### The Result

The variation of crystallization behavior of resin will affect the final product's crystallinity after injection molding, and thus the physical properties of the molded part. It is important to make sure the polymer crystallizes reproducibly and that any variations in the crystallization are detected. Conventional heating and cooling experiments were first performed on these two batches and the results are shown in Figures 1 and 2.

The heating was done at typical 10 °C/min and cooling at 20 °C/min. The melting profiles upon heating look similar with some difference in melting enthalpy. The crystallization peaks during cooling are almost the same. The heating and cooling method was not effective at detecting the difference between batch A and B.

Since the isothermal crystallization test is very sensitive to resin property, it was tried on these two batches. The resin was first heated above its melting temperature to 220 °C, and held for 2 minutes to melt any crystalline structure. Next, it was rapidly cooled to the isothermal crystallization temperature, which was 140 °C in this case. The sample was left to sit at 140 °C for 5 minutes to complete the crystallization process.

The successful isothermal crystallization experiment depends on the quick cooling to the isothermal temperature so that no significant crystallization will happen before it reaches the isothermal temperature. Power compensation DSC is

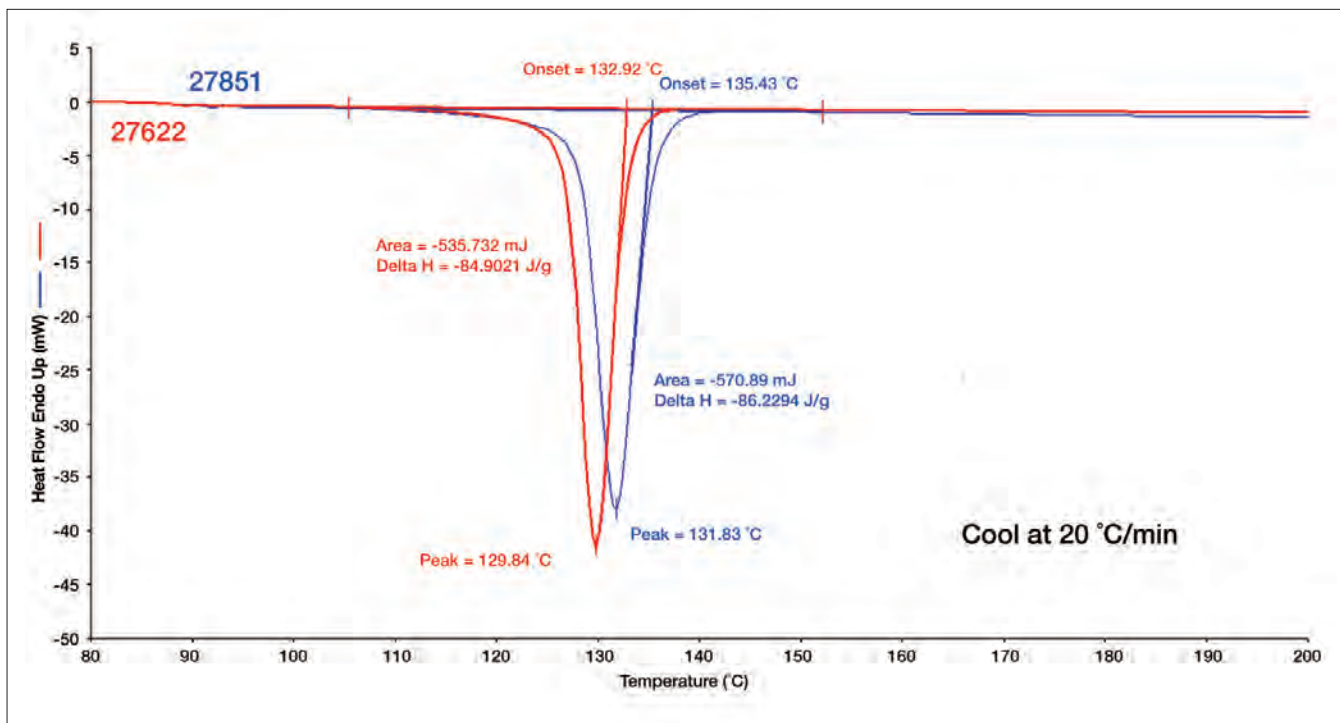


Figure 2. Conventional cooling scan on batch A and B.

known for the fastest cooling rate in DSC. In this case, 200 °C/min cooling rate was used and the sample temperature vs. time was plotted in Figure 3. As shown in Figure 3, the controlled cooling was realized over this temperature range. Note, in this experiment setup, only a water circulator was used as a cooling accessory with helium purge. Intracooler or liquid nitrogen cooling accessory will allow even faster cooling rate. The PerkinElmer® DSC 8000 can achieve a cooling rate up to 500 °C/min.

The isothermal crystallization experiment results for batches A and B are shown in Figure 4. For batch A resin, the crystallization at 140 °C finished at around 3 minutes and the peak position is at 1.333 minutes. However, for batch B, the crystallization completed within 2 minutes and

crystallization peak appeared at 0.867 minute. The difference is clearly demonstrated. Batch B crystallizes more quickly than batch A at this temperature. For resin quality assurance, the source of variance needs to be identified.

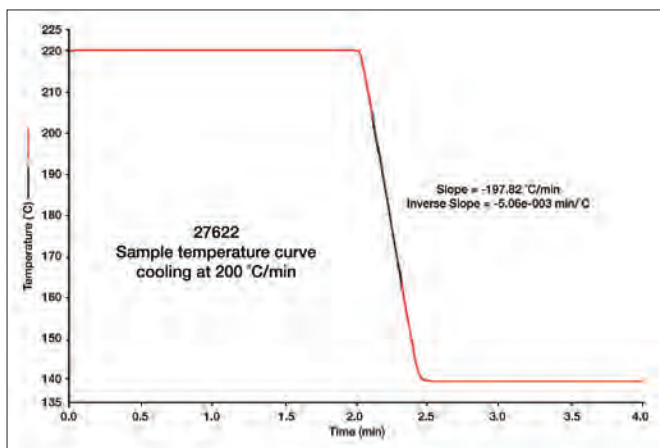


Figure 3. Sample temperature vs. time profile of the isothermal crystallization experiment.

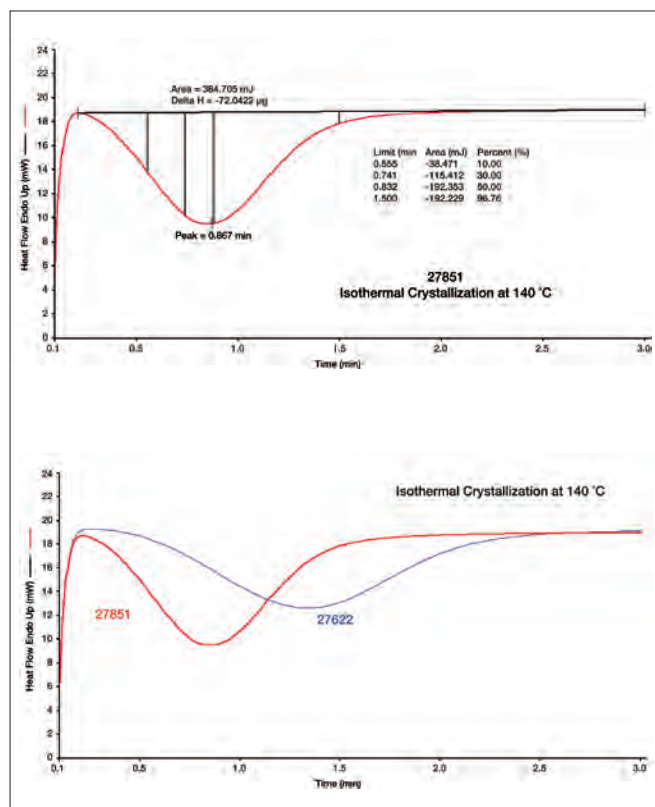


Figure 4. Overlay of the isothermal crystallization results of batch A and B.

## Summary

The isothermal crystallization test has been shown to be able to detect the difference between two batches of polypropylene resin, which is otherwise not seen by conventional heating and cooling experiment. This information is useful to resin manufacturers for quality assurance purposes. The DSC 8000 with power compensation is the ideal tool for isothermal crystallization experiment. The fast cooling rate and true isothermal operation give superior results.

PerkinElmer, Inc.  
940 Winter Street  
Waltham, MA 02451 USA  
P: (800) 762-4000 or  
(+1) 203-925-4602  
[www.perkinelmer.com](http://www.perkinelmer.com)



---

For a complete listing of our global offices, visit [www.perkinelmer.com/ContactUs](http://www.perkinelmer.com/ContactUs)

Copyright ©2009-2011, PerkinElmer, Inc. All rights reserved. PerkinElmer® is a registered trademark of PerkinElmer, Inc. All other trademarks are the property of their respective owners.

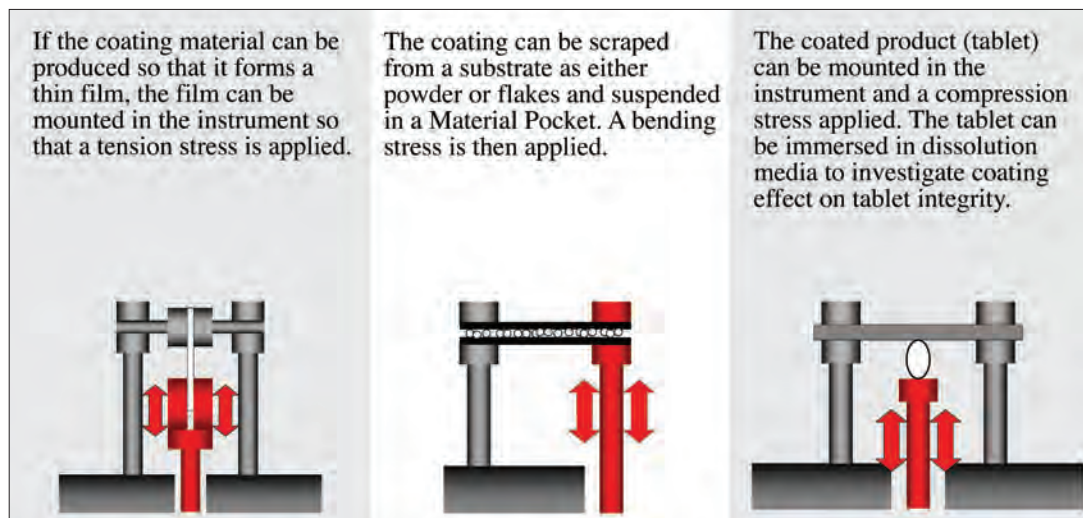
008497A\_01



## Mechanical Properties of Films and Coatings

Dynamic Mechanical Analysis (DMA) is a technique used to investigate the stiffness of materials as a function of temperature, humidity, dissolution media or frequency. A mechanical stress is applied to the sample and the resultant strain is measured by the instrument. These parameters are used to evaluate glass transitions, degree of crystallinity and stiffness behavior of the sample.

There are three options when dealing with films and coatings:



A DMA is essentially a relaxation detection instrument. It is many times more sensitive than other techniques (e.g. DSC) at identifying relaxation events, such as a glass transition (T<sub>g</sub>).

Data from two coating materials is shown in Figure 1. Each of the coatings had a slightly different pre-treatment prior to analysis. The glass transition temperature is shown as the peak value of the tan δ vs temperature and as the drop in the storage modulus. It is shown that the pre-treatment greatly affects the glass transition temperature. For this material, the glass transition temperature was critical for the performance of finished product.

It is possible to investigate the properties of the coating under the influence of a controlled relative humidity environment. Figure 2 shows the effect of moisture on the same coating material. It is clear that the glass transition temperature is lowered by the influence of water. A small beta relaxation is seen in the wet sample indicating that water dramatically affects the mechanical properties of the material.

The development of Material Pockets, which are used to hold a powder or film for use in a DMA, have opened the door for many different materials to be analyzed in the DMA 8000.

Figure 3 shows data from the testing of thin films made by curing a layer of adhesive in the material pocket. This method allows the testing of films that are not self-supporting and also the monitoring of their curing. In this case, two films were made and tested directly in the Material Pocket and reveal a significant difference in the T<sub>g</sub>.

Finally, the PerkinElmer Fluid Bath allows us to look at the dissolution of a coating from a capsule. Figure 4 shows a gelcap, a gelatin capsule containing a product, as it is tested in the DMA 8000 and Fluid Bath. In both samples, the modulus decreases with time after immersion reflecting the sample getting less stiff as it dissolves. Eventually, the sample disintegrates so much that the data is meaningless. This is the point where data collection was ceased. The sharp decrease in modulus indicates this point. It is worth noting that the rate of softening and the time taken to destroy the

sample were both faster at 38 °C than 25 °C. Also, the initial ingress of water into the gelatin to start the dissolution process was much faster at 38 °C, as shown by the short time between immersion and modulus decrease starting.

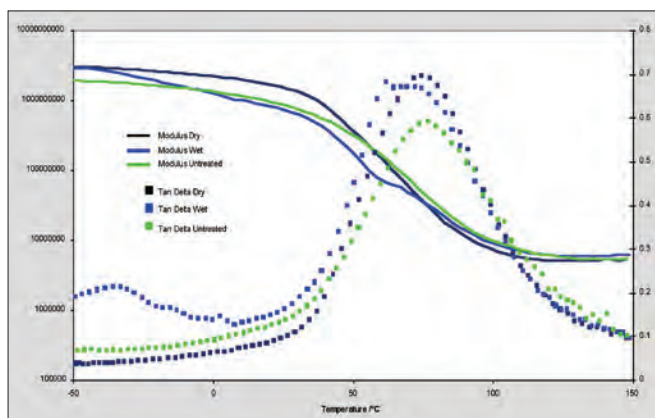


Figure 2. The effect of running the coating from Figure 1 in solution using the Fluid Bath.

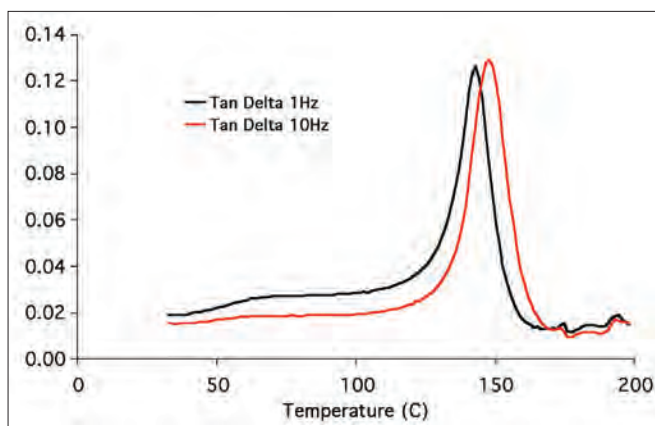


Figure 3. Measurement of thin adhesive films cured in a Material Pocket.

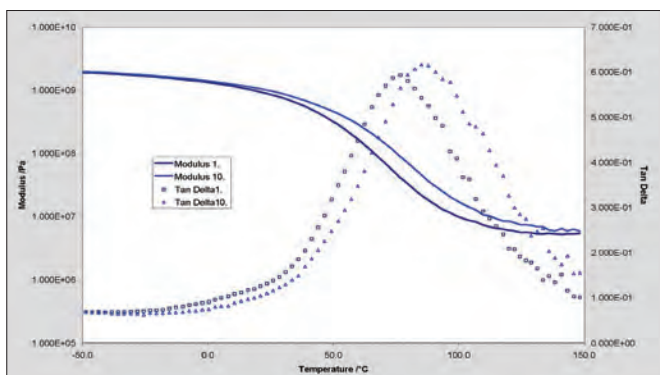


Figure 1. A comparison of pre-treated and untreated coatings run in tension.

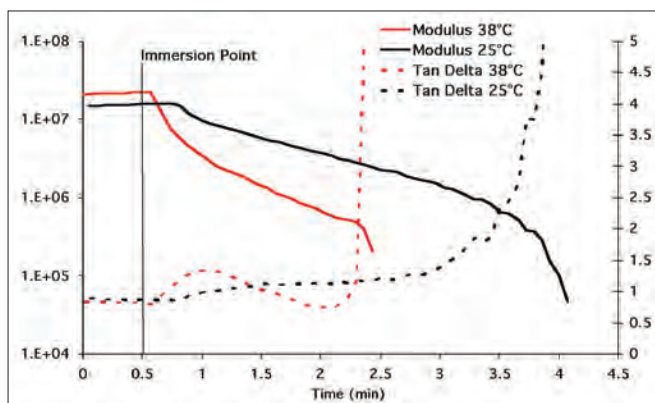


Figure 4. Two gelatine capsules tested in the Fluid Bath.

PerkinElmer, Inc.  
940 Winter Street  
Waltham, MA 02451 USA  
P: (800) 762-4000 or  
(+1) 203-925-4602  
[www.perkinelmer.com](http://www.perkinelmer.com)



---

For a complete listing of our global offices, visit [www.perkinelmer.com/ContactUs](http://www.perkinelmer.com/ContactUs)

Copyright ©2007-2011, PerkinElmer, Inc. All rights reserved. PerkinElmer® is a registered trademark of PerkinElmer, Inc. All other trademarks are the property of their respective owners.

007771B\_05

## Thermal Analysis



## T<sub>g</sub> and Cure of a Composite Material



### Summary

A powder-filled, epoxy-based composite material is investigated in this application note. A multi-frequency thermal scan will give information about the glass transition and cure of the material. An isothermal experiment, after raising the temperature above the cure temperature is also discussed. This latter experiment gives unusual frequency dependence information. The glass transition and the cure behavior of composite materials are of special importance due to the types of applications they are used for.

### Introduction

Dynamic Mechanical Analysis (DMA) is one of the most appropriate methods to investigate relaxation events. A composite, by definition, contains more than one component. There are multiple types of composite materials used for various applications from glass fiber reinforced concrete to sophisticated aeronautical polymer composites. In these experiments, a powder filled composite of epoxy polymer proposed for battery manufacture is used.

The PerkinElmer® DMA 8000 works by applying an oscillating force to the material and the resultant displacement of the sample is measured. From this, the stiffness can be determined and  $\tan \delta$  can be calculated.  $\tan \delta$  is the ratio of the loss component to the storage component. By measuring

the phase lag in the displacement compared to the applied force it is possible to determine the damping properties of the material.  $\tan \delta$  is plotted against temperature and glass transition is normally observed as a peak since the material will absorb energy as it passes through the glass transition.

Being an epoxy-based composite, the glass transition is not so simple in that there is also a cure process happening at the same time. An explanation of both the thermal scan and isothermal cure data is discussed.

## Experimental

### 1. Multi-frequency temperature scan of composite.

The sample was mounted in the single cantilever bending clamps and run through the temperature scan at multiple frequencies.

### 2. Isothermal frequency scan of composite. A fresh sample was mounted in the single cantilever bending clamps and heated quickly to 100 °C. Modulus and $\tan \delta$ data were collected for 3 hours.

Equipment	Experimental Conditions	
DMA 8000 1L Dewar	Sample:	Composite Material
	Geometry:	Single Cantilever Bending
	Dimensions:	9.7 (l) x 10.1 (w) x 1.7 (t) mm
	Temperature:	(1) 25 °C to 250 °C at 3 °C/min <sup>-1</sup> (2) Isothermal at 100 °C
	Frequency:	0.316, 1.0, 3.16, 10.0 and 31.6 Hz

## Results and conclusion

Figure 1 shows the thermal scan of the composite material. A clear frequency dependence is observed in both the modulus and the  $\tan \delta$  data indicating a relaxation event. As the material passes through the  $T_g$ , a cure reaction also takes place. The material gets less stiff (modulus decreases) as a result of the  $T_g$  and the increasing temperature despite the cure process going to completion. The frequency dependence is as expected with higher frequencies giving higher glass transition temperatures. The  $T_g$  at 1 Hz is approximately 92 °C.

The result from the isothermal experiment is graphed in Figure 2. 100 °C was chosen for the experiment as it was slightly higher than the  $T_g$  from the first experiment.

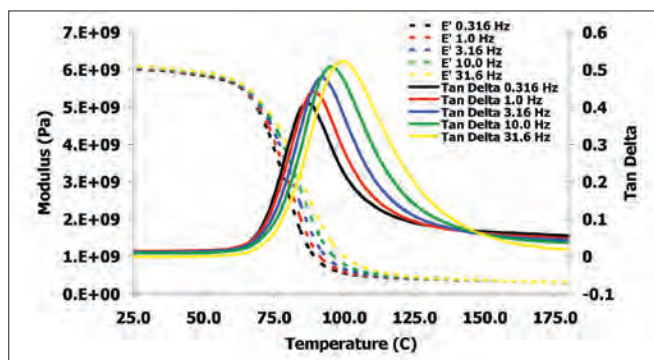


Figure 1. Thermal scan data of composite material.

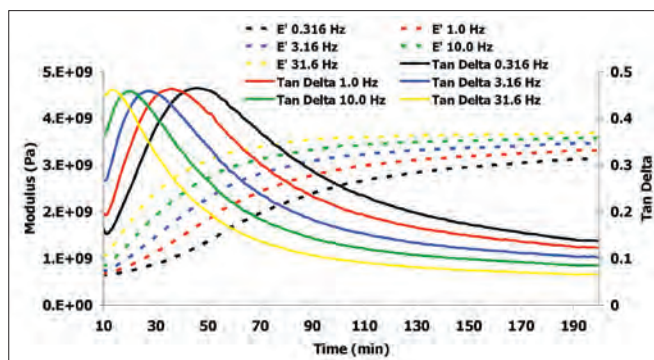


Figure 2. Isothermal experiment results.

The peak in the  $\tan \delta$  shows a combination of the glass transition and the cure process. It appears that the frequency dependence is the opposite to that observed in the first experiment, with the higher frequency peak occurring first.

The isothermal experiment results are a function of time, not temperature and are shown in Figure 2. The curing of the epoxy will be the dominant process observed in these data. As the cure progresses, the relaxation time will get longer. A maximum in  $\tan \delta$  will be observed when the relaxation time is approximately the same as the probing frequency. Hence, the high frequency event (shortest probing frequency) will occur first as the relaxation time will be the shortest. The lowest frequency peak occurs when sufficient cure has taken place to lengthen the relaxation time appropriately.

This application note has described the ability of DMA to investigate curing and glass transition events in composite materials. The isothermal cure experiment gave data that better describes the cure than the  $T_g$  event.

## Thermal Analysis



## Characterization of LDPE Over a Large Frequency Range



### Summary

LDPE (Low Density Poly Ethylene) is an important polymer used in the manufacture of plastic products. This application note details DMA experiments over a temperature and frequency range. The combination of frequency and temperature are important factors for the practical application of LDPE. Relaxations are frequency dependant, so they will occur at different temperatures depending on the distortion frequency the material is subjected to. A temperature scan of the material will be discussed, as will a frequency sweep at a series of discrete temperatures.

### Introduction

Dynamic Mechanical Analysis (DMA) is one of the most appropriate methods to investigate relaxation events. The PerkinElmer® DMA 8000 is capable of measuring data over a very large frequency range (up to 300 Hz in all geometries). When investigating the frequency dependant behavior of materials, this high frequency range is very useful. The temperature dependence of the material is also important so a temperature scan will also be displayed with these data. LDPE is semi-crystalline and it has been reported that the  $\delta$  relaxation event is associated with a crystalline phase relaxation.

DMA works by applying an oscillating force to the material and the resultant displacement of the sample is measured. From this, the stiffness can be determined and the modulus and  $\tan \delta$  can be calculated.  $\tan \delta$  is the ratio of the loss modulus to the storage modulus. By measuring the phase lag in the displacement compared to the applied force it is possible to determine the damping properties of the material.  $\tan \delta$  is plotted against temperature and glass transition is normally observed as a peak since the material will absorb energy as it passes through the glass transition.

## Experimental

### 1. Temperature scan of LDPE.

The LDPE sample was mounted in the Single Cantilever Bending clamps and run from ambient to melting temperature. Data was collected at three frequencies.

### 2. Frequency scan of LDPE at five temperatures.

The LDPE sample was mounted in the Single Cantilever Bending clamps. The temperature was stepped from 0 °C to 100 °C in 25 °C increments. A series of discrete frequencies were investigated at each temperature.

### 3. Isothermal frequency scan of LDPE (30 discrete frequencies).

The LDPE sample was mounted in the Single Cantilever Bending clamps and run at ambient temperature at multiple frequencies.

#### Equipment Experimental Conditions

DMA 8000		
1L Dewar	Sample:	LDPE
	Geometry:	Single Cantilever Bending
	Dimensions:	5.0 (l) x 3.6 (w) x 5.0 (t) mm
	Temperature:	0 °C to 100 °C in step isothermal mode
	Frequency:	0.1 to 300 Hz

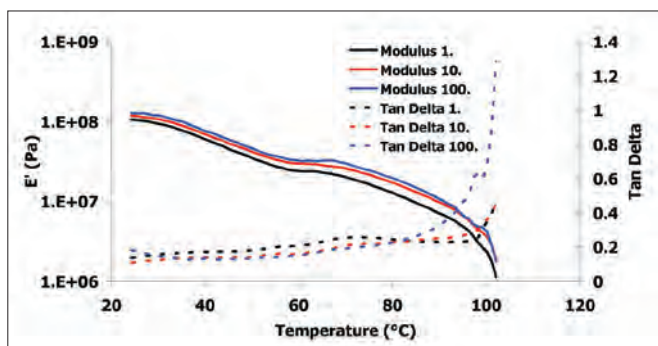


Figure 1. Temperature data at three frequencies.

## Results and conclusion

Figure 1 shows the temperature scan data at three frequencies for LDPE. The large increase in tan d and decrease in modulus at around 100 °C is the onset of melting. Note, just prior to the melting event, there is a frequency dependence. As melting

behavior is not frequency dependent, this event has to be a relaxation quite separate from melting. As mentioned in the introduction, it has been reported that there is an  $\delta$  relaxation associated with the crystalline phase in this temperature range. The data here confirms this.

Figure 2 shows a more comprehensive frequency sweep of LDPE run at 22.5 °C. There is a general trend of decreasing  $\tan \delta$  as frequency is increased and the modulus remains approximately constant.

Figure 3 shows frequency data at a range of temperatures. Fairly linear relationships are observed for  $\tan \delta$  and modulus which is to be expected if no relaxation event is present. At 100 °C this relationship changes and  $\tan \delta$  increases with frequency. This result further supports the theory of a relaxation event at around 100 °C.

Note, the distortion in the data at 250 Hz corresponds to the resonance frequency of the sample. The instrument was able to continue with the frequency sweep through resonance to collect the full range of data.

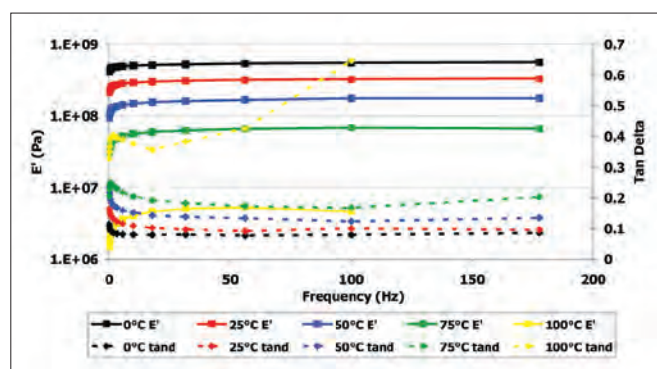


Figure 2. Frequency data at various temperatures.

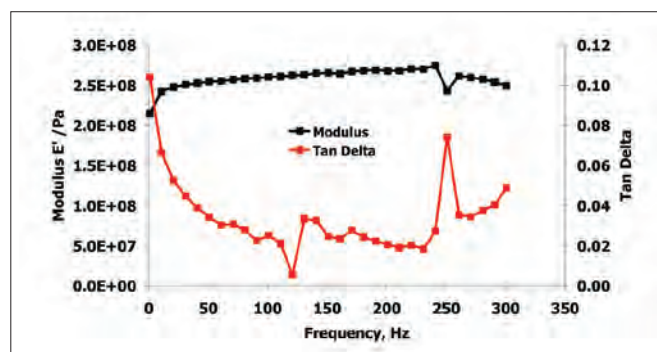


Figure 3. LDPE run at 22.5 °C.

## Color Analysis on the LAMBDA PDA UV/ Visible Spectrophotometers

### Introduction

Using the Color Analysis mode of the UV Lab™ software, CIE L\*,a\*,b\* values of liquid or solid color samples

can be obtained. It is very useful in the quality control process of the dye or beverage industry because it is easy to compare product color to color standards.

L\*, a\*, b\* color space(CIELAB) is the most general color space for measuring color within industry. L\* indicates the lightness and it may have values between 0 and 100. a\* and b\* may have values between around -80 and +80. Colors with no chroma always have the value a\*=b\*=0. Because the opponent color theory is used to develop the transformation, one of coordinates(a\*) shows the redness or the greenness of color and the other coordinate(b\*) shows the yellowness or the blueness. The greenness and blueness are given with negative sign whereas redness and yellowness are given with positive sign.

$L^*$ ,  $a^*$ ,  $b^*$  color space and color differences that result form this color space are described with the following equations.

$$\Delta E^*_{ab} = [(\Delta L^*)^2 + (\Delta a^*)^2 + (\Delta b^*)^2]^{1/2}$$

$$\Delta E^*_{ab} = [(\Delta L^*)^2 + (\Delta C^*_{ab})^2 + (\Delta H^*_{ab})^2]^{1/2}$$

Where,  $L^*$  = Lightness

$a^*$ ,  $b^*$  = chroma coordinates

$\Delta C^*_{ab}$  = chroma

$\Delta H^*_{ab}$  = chroma

$$L^* = 116 \left( \frac{Y}{Y_n} \right)^{1/3} - 16$$

$$a^* = 500 \left[ \left( \frac{X}{X_n} \right)^{1/3} - \left( \frac{Y}{Y_n} \right)^{1/3} \right]$$

$$b^* = 200 \left[ \left( \frac{Y}{Y_n} \right)^{1/3} - \left( \frac{Z}{Z_n} \right)^{1/3} \right]$$

Where,  $\frac{Z}{Z_n} > 0.008856$       $\frac{X}{X_n} > 0.008856$

$$\frac{Y}{Y_n} > 0.008856$$

## Reagents and Apparatus

1. LAMBDA™ 265/465 UV-Vis Spectrophotometer
2. Advanced Transmission Holder
3. UV Lab software Color Analysis Mode
4. Color Filter Samples

## Procedure

1. Open Color Analysis Mode.
2. Set parameters and click OK.
3. Measure Blank.
4. Measure Target.
5. Measure Samples.
6. Compare CIE color coordination.

## Instrument Parameters

Parameter Setting	OK
<b>Instrument Setup</b>	
Scan No.	10
Integration No.	1
Data Type	%T
<b>Color Measurement Setup</b>	
Illuminant	D65
Observer Angle	2 Deg

Figure 1. Parameter Setting of Color Analysis Mode.

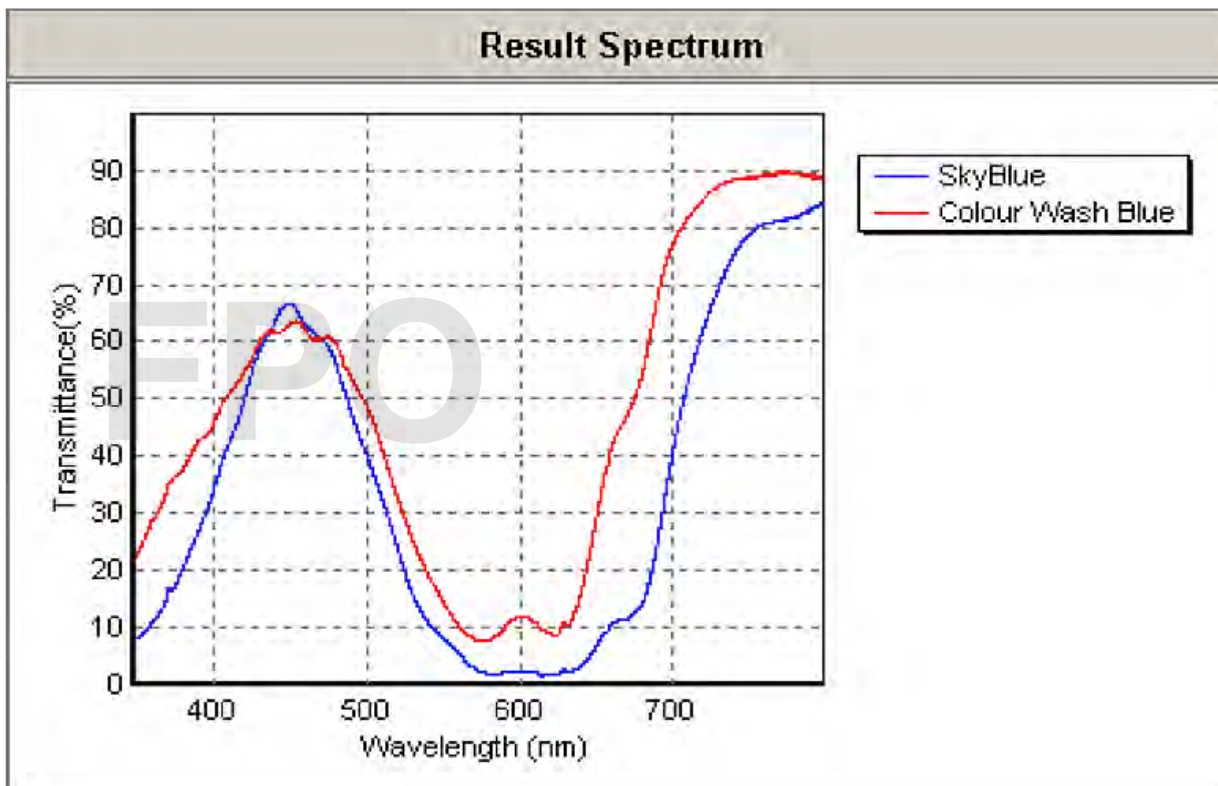


Figure 2. Transmittance spectrum of color filters.

The <Result Analysis Value> on the left side of Figure 3 shows the difference of color values between standard and sample and the <Result Colors> shows their colors.

<Result Analysis Values>										<Result Colors>	
Sample	dE*	dL*	da*	db*	dC*	dH*	L*	a*	b*	Standard	Sample
SkyBlue	None	None	None	None	None	None	42.5449	12.0727	-66.5604		
Carbana Blue	37.5163	-10.59	33.4914	-13.1777	24.1918	19.4641	31.9549	45.5641	-79.7381		
Mikkel Blue	55.1397	-17.1813	48.3416	-20.2059	38.081	24.5685	25.3636	60.4143	-86.7663		
Colour Wash t	19.6373	9.7823	-4.7071	16.3638	-16.9123	-1.9328	52.3272	7.3656	-50.1966		
Durham Daylig	58.7501	-6.5926	-11.9404	57.1449	-58.23	-9.4755	35.9523	0.1323	-9.4155		
Berry Blue	27.0417	-11.7009	23.2242	-7.4149	14.3183	15.2274	30.844	35.2969	-73.9753		
Old Steel Blue	52.654	37.062	-27.7214	42.231	-38.7189	-223.0297	79.6069	-15.6487	-24.3294		
Deeper blue	32.4328	-21.6154	23.9951	2.9828	5.4494	19.2859	20.9295	36.0678	-63.5776		
Cold blue	32.6388	2.3139	-3.3155	32.3673	-32.3693	4.0912	44.8588	8.7562	-34.1731		
J.winter blue	47.5898	-31.2792	35.1318	7.1821	8.209	26.2034	11.2657	47.2045	-59.3783		
Moonlight blue	39.6692	9.3355	-35.8266	14.2459	-10.1916	-214.7014	51.8804	-23.7539	-52.3145		

Figure 3. CIE system coordination values and difference values of color filters and Result Colors.

## Conclusion

Using the LAMBDA 265/465 and UV Lab software the color difference values of color samples were calculated. Rapid acquirement of spectra and good sensitivity were obtained using the LAMBDA instrument. The Color Analysis Mode of the UV Lab software was used effectively for this test and to process the data efficiently.

## Thermal Analysis

**Authors**

Svenja Goth  
PerkinElmer, Inc.  
Shelton, CT 06484 USA

Tim Mann  
Paul Gabbott  
PETA Solutions  
Beaconsfield, UK

## HyperDSC – A Breakthrough Method for Materials Characterization

**Abstract**

Increasing the sensitivity and throughput of Differential Scanning Calorimetry (DSC) analysis has always been a challenge for thermal analysts in research and development. A relatively fast temperature scanning rate (20 °C/min or 40 °C/min) using traditional DSC has been sufficient

for most applications. However, DSC analysis becomes difficult when a sample size is small due to the weak signal and the number of samples that have increased as a result of the demand for high throughput. Because of the slow heating rate, some materials may experience re-crystallization during the melting process or decompose immediately after melting. This may cause difficulty in obtaining a true analysis and may also generate some additional, unexpected thermal phenomena.

HyperDSC™ is a DSC analysis technique by PerkinElmer with fast scanning rates enabling increased sensitivity and high throughput. With very fast temperature scanning rates (100-500 °C/min) in heating as well as in cooling over a broad temperature range, sensitivity and throughput have dramatically increased by a factor of ten over most conventional DSC analyses. Due to the fast scanning rate, the re-crystallization during melting, decomposition after melting, and unknown thermal behavior are either completely eliminated or significantly reduced by this method. In this study, we will present the HyperDSC technique and demonstrate the benefits of this method for several applications in polymers and pharmaceuticals.

## Introduction

HyperDSC is a breakthrough method for materials characterization, providing extra sample information in seconds rather than minutes. HyperDSC can run samples as fast as 500 °C/min under control, measuring the real sample temperature,<sup>1</sup> whereas, for a conventional DSC method, the scan rate is normally 20 °C/min or 40 °C/min. As a result of these fast scanning rates, throughput is at least 10 times faster. To achieve these fast scanning rates, ultra low mass furnaces and small dimensions (Figure 1) are required to ensure the system is under control during the scans with rates up to 500 °C/min. This is significantly faster than any conventional heat flux DSC. The HyperDSC technique is only possible on power-compensation DSC, which measures heat flow directly and does not require complex mathematics to get premium results.

Because the DSC output is mW (J/sec), HyperDSC gives increased sensitivity with shorter scan times and smaller sample mass. The technique enhances DSC analysis and allows the measurement of small samples down to a few micrograms. Examples of small samples are very thin layers in multilayer films, coatings or very small amounts of materials for pharmaceutical development. Another major interest in the pharmaceutical industry is the study of polymorphism. The use of fast scanning rates can reveal the dependence of the polymorphic transitions and can allow better interpretation of related processes.<sup>2</sup>

In the past, the simulation of realistic conditions (like injection molding) that occur in the polymer production process represented a challenge for the polymer industry. The cooling rates in polymer processing strongly influence crystallization behavior.<sup>3,4</sup> HyperDSC provides fast cooling capability and new insights in material processes. In addition to fast controlled cooling rates, polymer production also expressed a great need for fast heating rates.<sup>1,5</sup> The analysis and the linking of melting behavior prior to crystallization is often a challenge. A product which is cooled down quickly and then gets analyzed with a conventional heating rate of 10 °C/min or 20 °C/min often raises questions since the results are not reflective of the material at room temperature due to re-organization processes during the slow heating. Such reorganization can be prevented by heating at a high rate so that the relationship between crystallization and the subsequent melting becomes more transparent.<sup>1</sup>

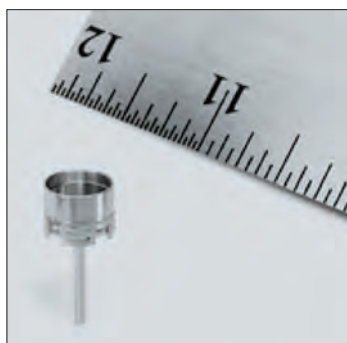


Figure 1. Sample furnace of a power-compensation DSC.

For all measurements it is important to ensure that the instrument is under control (program and sample temperature have the same slope) when using these fast scanning rates of HyperDSC.

## Experimental

Several examples of different material types will be shown in this study. A PerkinElmer Diamond DSC\* was used for these measurements. The DSC was calibrated for temperature and heat flow with reference materials having transitions in the range of interest. Depending on the required cooling rates, different cooling devices such as Intracooler or CryoFill (a liquid nitrogen device) were used. The CryoFill system requires Helium or a Helium/Neon mixture for sample purge which provides a temperature range from -180 °C to 585 °C with good thermal conductivity. The Intracooler configuration can also use nitrogen as purge gas.

## Results and discussions

Figure 2 depicts how the small transients in the Diamond DSC\* at the start of a measurement allow data to be obtained without going to extremely low temperatures. The power-compensation DSC technique provides a stable baseline in less than 20 seconds.

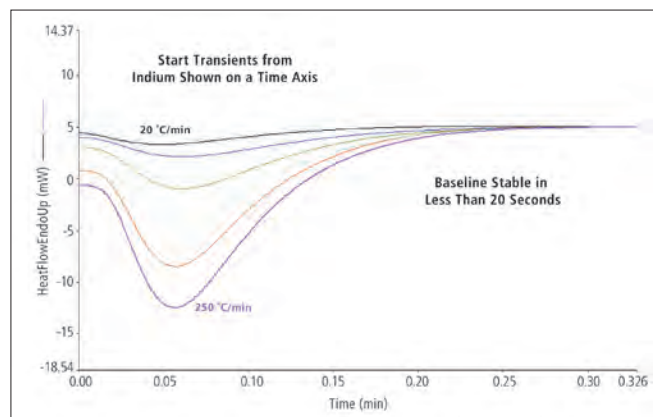


Figure 2. Start transients from indium with several different scanning rates.

With classical heating rates of 10 °C/min or 20 °C/min, it is often difficult to find small transitions or to identify them as seen on the DSC curve of polypropylene generated at 10 °C/min. Increasing the scan rate to 150 °C/min raises the sensitivity and allows the easy determination of the glass transition (T<sub>g</sub>) on this polypropylene sample as shown in Figure 3. This scan took less than two minutes compared to the 20 minutes that a classical DSC method requires. The results show that the onsets of the glass transitions line-up very nicely.

\*Diamond DSC instrument is superseded. It has been replaced by DSC 8500.

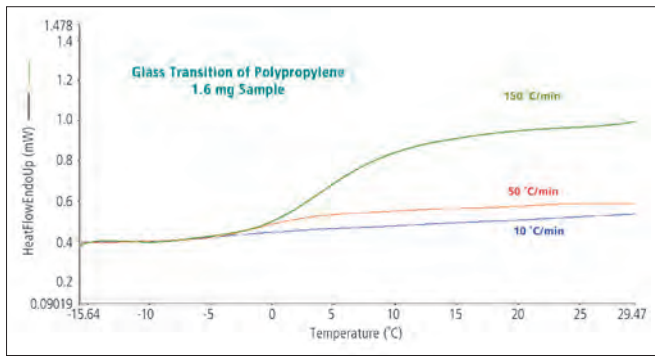


Figure 3. Polypropylene scans with 10 °C/min (blue), 50 °C/min (red) and 150 °C/min (green).

Often, to eliminate any thermal history, material is initially heated and then cooled down under control. This is a slow process using the conventional DSC approach.

Analysis is then performed on the second heat since the sample has a known thermal history. This material is no longer in the condition in which a production process delivers it. Figure 4 shows how cooling rates can impact crystallization behavior.

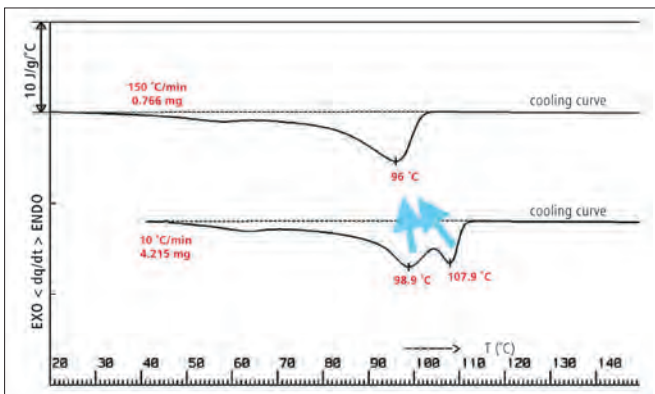


Figure 4. Polyethylene blend with different cooling rates.

Cooling a polyethylene blend at 10 °C/min shows two crystallization peaks. Increasing the rate to 150 °C/min changes the crystallization process and curve characteristic.

The next example shows the analysis of two polypropylene films. Depending on the required material properties, these films are stretched in one (regular) or two (biaxial) directions. Measuring these samples at a heating rate of 10 °C/min using traditional DSC analysis, results in very similar melting temperatures of 162 °C and 165 °C. However, if the experiment is conducted using HyperDSC, the differences are remarkable (Figure 5). The regular film shows a melting peak at 157 °C and the biaxial film at 166 °C. HyperDSC allows you to measure the real properties of the actual sample, unveiling the subtle differences which would be obscured and disappear as the sample is conditioned at low scan rates.

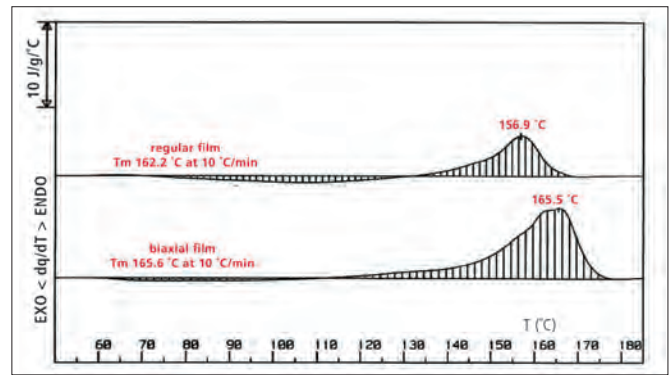


Figure 5. Polypropylene films.

Another polymorphic example where HyperDSC proves to be highly beneficial is Carbamazepine (Figure 6). In this particular case, two phase transitions are shown as the sample is heated. The first one is much smaller than the second and very difficult to see at slow scanning rates. The energy calculation of the small peak shows the same result independent of the heating rate. This indicates that the transition is not related to a polymorphic transition and was determined to be a dehydration process.

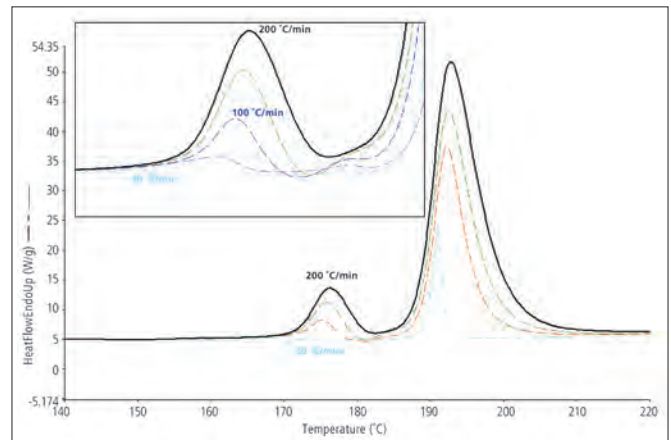


Figure 6. Carbamazepine at different scan rates.

The heat flow curve of Carbamazepine at 200 °C/min and the second derivative (Figure 7) show the transitions that are present. The second derivative at a very high scanning rate demonstrates that HyperDSC is able to pick up closely related events.

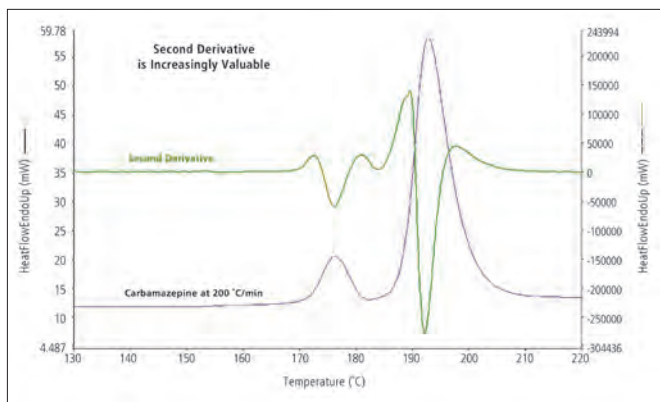


Figure 7. Carbamazepine heat flow and second derivative.

An unfounded concern using HyperDSC is the loss of resolution. Figure 8 shows the run of Dotriacontane at 250 °C/min and the second derivative. It is a very valuable tool for the use of HyperDSC since it clearly shows several transitions which are not resolved in the high scanning rate heat flow curve. The information can be generated in less than two minutes and helps in the selection of samples which may provide additional information at lower scan rates.

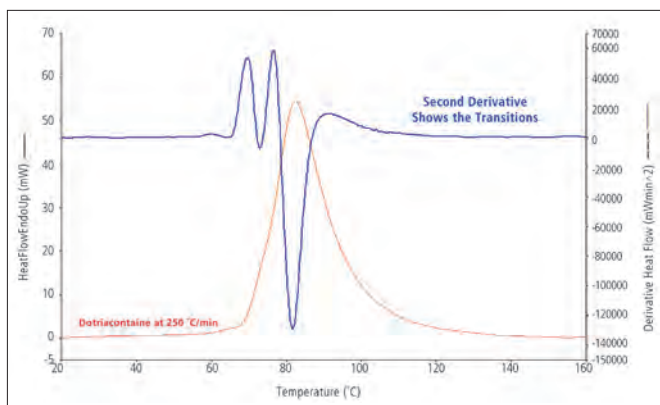


Figure 8. Heat flow of Dotriacontane, scanned with 250 °C/min.

## Conclusions

HyperDSC is a very important tool for the pharmaceutical and polymer industries. It meets the urgent needs for measurements performed under process conditions. HyperDSC can also provide true information of the sample without

introducing any additional interference, such as re-crystallization or decomposition. HyperDSC eliminates misinterpretation of material behavior and helps to improve product quality. The fast scanning rates allow users to increase sample throughput easily to 100 or more runs per day. HyperDSC can be a powerful tool for screening new materials.

The increased sensitivity available with this technique enhances the ability to identify weak transitions often missed with conventional DSC. All features of HyperDSC improve researchers' ability to study material characteristics. Accurate interpretation of results and fast scanning make HyperDSC the preferred tool of the pharmaceutical and polymer industries to reduce time-to-market for new products and increase manufacturing efficiency. Other markets will soon begin to discover the benefits of HyperDSC.

## Acknowledgments

We would like to thank Thijs F.J. Pijpers, Vincent B.F. Mathot and Eric W. van der Vegte of DSM Research, The Netherlands for their valuable work in HyperDSC development.

## References

1. Thijs F.J. Pijpers, Vincent B.F. Mathot, Bart Goderis, Rolf L. Scherrenberg, Eric W. van der Vegte; *Macromolecules* 2002, 35, 3601-3613.
2. James L. Ford, Tim Mann; HyperDSC of Polymorphic Transitions in Nifedipine, Paper at TAC2002, UK.
3. Eder, G.; Janeschitz-Kriegl, H. Crystallization. In *Processing of Polymers*; Meijer, H.E.H., Ed.; Material Science and Technology 18; Cahn, R.W., Haasen, P., Kramer, E.J., Vol. Eds.; VCH Verlagsgesellschaft mbH: Weinheim, Germany, 1997; Chapter 5, pp 296-344.
4. Mathot, V.B.F. In *Calorimetry and Thermal Analysis of Polymers*; Mathot, V.B.F., Ed.; Hanser Publishers: Munich, Germany, Vienna, and New York, 1994; Chapter 9 (The Crystallization and Melting Region), p. 231.
5. Wunderlich, B. *Macromolecular Physics*; Academic Press: New York, 1980; Vol. 3 (Crystal Melting).

## Thermal Analysis

## Authors

Wim M. Groenewoud  
Eerste Hervendreef 32  
5232 JK 'S Hertogenbosh  
The Netherlands

Nik Boer  
PerkinElmer, Groningen  
The Netherlands

Phil Robinson  
Thermal Analysis Consultant  
Ruston Services Limited  
Staffordshire, United Kingdom

## Characterization of Polyketone Copolymer by High Speed DSC

### Introduction

The aliphatic polyketone copolymer (PK copolymer) is a perfectly alternating copolymer of ethylene and carbon monoxide.<sup>1</sup> It exhibits many desirable engineering thermoplastic properties, such as a high tensile yield stress and

an excellent impact performance. Its high degree of chemical resistance and superior barrier properties make this polymer an interesting, new thermoplastic for engineering applications.

After a washing and drying procedure, the reactor product consists of a white, semi-crystalline powder, soluble only in a few exotic solvents, like hexafluoroisopropanol (HFIPA) and meta-cresol. The crystalline phase of this polymer is built of orthorhombic unit cells with a polymer chain at each corner and one in the center. These polymer chains crystallize into two different modifications the alpha and the beta modification. The alpha modification changes into the beta form material at temperatures higher than about 120 °C. The beta form material, which is the dominant unit cell for the (unoriented) PK copolymer, fuses at about 250 °C. Lommerts *et al*,<sup>2</sup> calculated the dimensions of both cell types. Alpha form  $a = 6.91 \text{ \AA}$ ,  $b = 5.12 \text{ \AA}$ ,  $c = 7.60 \text{ \AA}$ ; cryst. density =  $1.382 \text{ g/cm}^3$ . For the beta form,  $a = 7.97 \text{ \AA}$ ,  $b = 4.76 \text{ \AA}$ ,  $c = 7.57 \text{ \AA}$ ; cryst. density =  $1.297 \text{ g/cm}^3$ .

The density increase obtained when the standard beta phase material is converted into the alpha phase material might improve the barrier properties even more (the structure and extent of the crystalline phase are important barrier-properties determining parameters). To see if and how the beta phase material could be changed into the alpha phase material PK copolymer was studied.

Polymerization-solvent induced and pressure/shear forces induced alpha crystallinity effects prove to be (partly) irreversible after heating through the alpha/beta crystal transition, indicated by  $T_m^*$ . A third method found, thermally induced alpha crystallinity, annealing at a temperature just below the melting of the beta crystalline phase, proved to be completely reversible.<sup>3</sup> So, this method was used to make PK copolymer systems with high alpha/beta crystal ratios. A series of three such samples were put aside to measure possible effects of storage time on the alpha/beta ratio.

The conventional DSC analysis of these samples using a PerkinElmer® DSC 7 had many problems. The three main problems were:

- Uncertainty about  $T_{m1}$  (max) value, (cross-linking reactions, possibly already started during the fusion, might influence the measured  $T_{m1}$  values).
- Uncertainty about proper  $T_{m1}$  values in connection with clearly present re-crystallization effects during the main fusion process.
- Investigation of the amorphous phase, i.e. determination of the  $T_g$ -value by conventional DSC was not possible for PK copolymer.

Recent developments in high speed DSC provide many advantages over conventional DSC. HyperDSC® is the premier fast scan DSC technique from PerkinElmer. It requires a DSC instrument with an extremely fast response time and very high resolution. It allows very fast linear heating and cooling scanning (up to 500 °C/min) over a broad temperature range. Not only does HyperDSC provide higher sensitivity, but it can also suppress kinetic events during scanning, thus analyzing the sample as received. During the discussions about the advantages of the HyperDSC, we realized that this improved technique might give the answers we were still looking for.

## Experiment

The samples used for this study and the sample treatment as a function of temperature and time are schematically shown in Appendix I. The following experiment conditions were used to measure these samples in 2005:

Instrument:	PerkinElmer Pyris 1 DSC*
Sample mass:	1 mg (approximately)
Heating/cooling rate:	300 °C/min
Number of scans:	First and second heating scans taken for each sample
Temperature range:	-100 °C to +300 °C

The HyperDSC was calibrated for temperature and enthalpy responses using high purity indium and lead. The systems' base-line was checked before and after the measurements (Figure 1).

In 1993, the data was obtained by using a PerkinElmer DSC 7 with a scanning rate of 20 °C/min.

## Results

### Experiment and calculated values

This study was started with a number of scouting experiments to check our reported  $T_{m1}(\text{max})$  value of 258 °C ±1 °C (20 °C/min).<sup>3</sup> A reactor powder sample measured at a heating rate of 300 °C/min resulted in  $T_{m1}(\text{powder}) = 258.6$  °C and 256.6 °C. Hence, the  $T_{m1}$  value determination proved that it was not hampered, or hardly hampered by possible cross-linking effects.

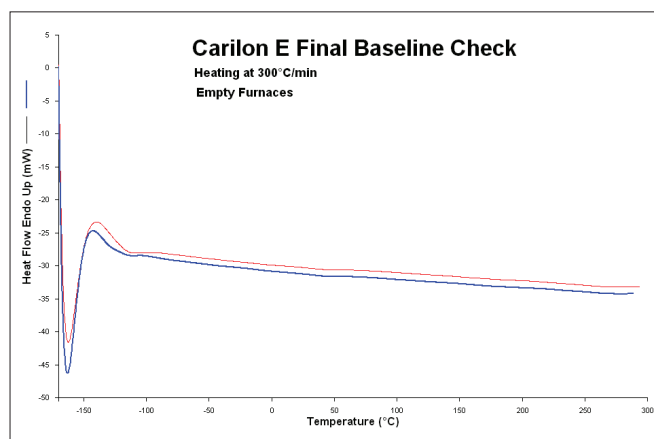


Figure 1. System baseline before and after the experiments (red: before, blue: after).

\*Pyris 1 DSC instrument is superseded. It has been replaced by DSC 8500.

Figure 2 shows the first and second heating scan results measured on sample 1 in 2005. Both curves clearly illustrate that the alpha phase crystallinity present in this sample (see alpha/beta crystal transition between about 100 °C and 150 °C) completely disappeared at the start of the second heating scan. But then, the second scan clearly showed a shifted fusion process of the beta crystalline phase to lower temperatures. This raised the question; might both effects be coupled? We started to summarize both fusion effects in  $T_m$  and  $H_f$  values (results shown in Table 1) and used Figures 3 and 4 to get a better look at the fusion processes. Figure 3A shows the fusion endotherms of the three samples at the standard heating rate in 1993. Figure 3B gives the same results, but measure at 300 °C/min. in 2005. Both figures show that the fusion endotherms of the samples 2 and 3 in 1993 were clearly influenced by recrystallization effects during the fusion process. These effects were (barely) present in the three endotherms measured at a high rate in 2005.

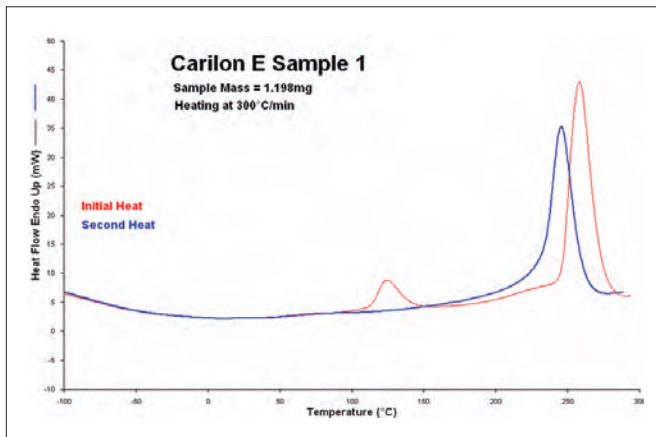


Figure 2. First and second heating scans measured on sample 1. (in 2005). Red curve is initial heating and blue curve is second heating.

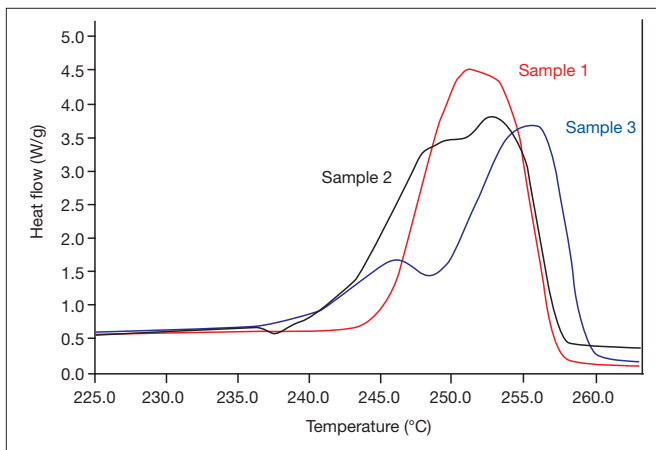


Figure 3A. The beta phase fusion effects of the systems 1, 2, and 3 (in 1993), i.e. heating rate 20 °C/min.

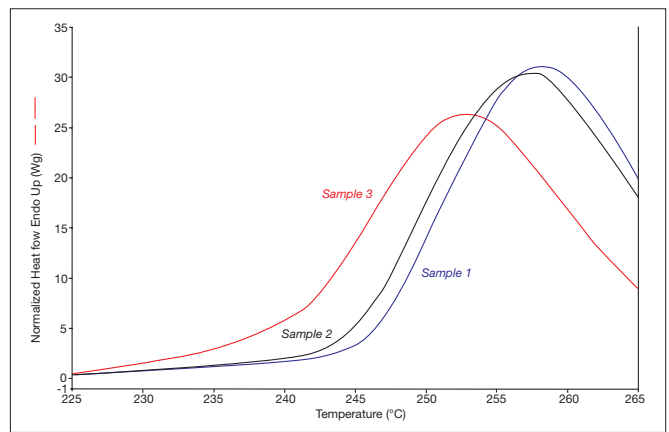


Figure 3B. The beta phase fusion effects of the systems 1, 2 and 3 (in 2005), i.e. heating rate 300 °C/min.

Figures 4A and B show the alpha/beta crystal transitions of these samples. Figure 4A shows the expected result, i.e. no annealing – no alpha crystallinity – no alpha/beta crystal transition in sample 3 (1993), besides, an increasing strength of the alpha/beta crystal transition with increasing annealing times. The alpha/beta crystal transitions measured in 2005 at a high heating rate are shown in Figure 4B. The strength of the crystal transition of the two annealed samples (1 and 2) are not only increased, but that the non-annealed reference sample 3 is also now showing a clear crystal transition. Thus, during the longtime storage at 20 °C of this sample, beta crystallinity has been partly changed into alpha crystallinity due to the release of built-in stress during the compression molding procedure. This important aspect will be discussed later on separately.

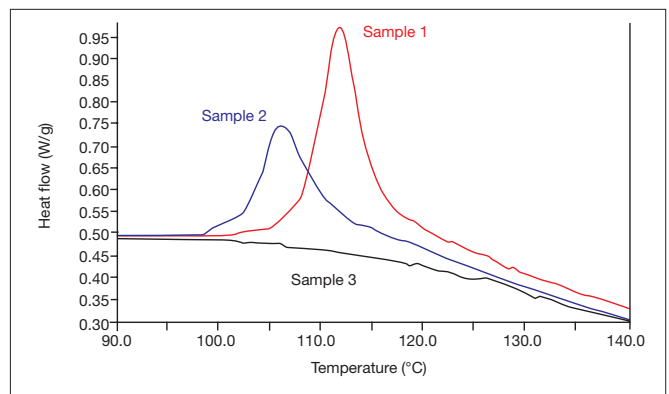


Figure 4A. The alpha phase fusion effects of the systems 1, 2 and 3 (in 1993), i.e. heating rate 20 °C/min.

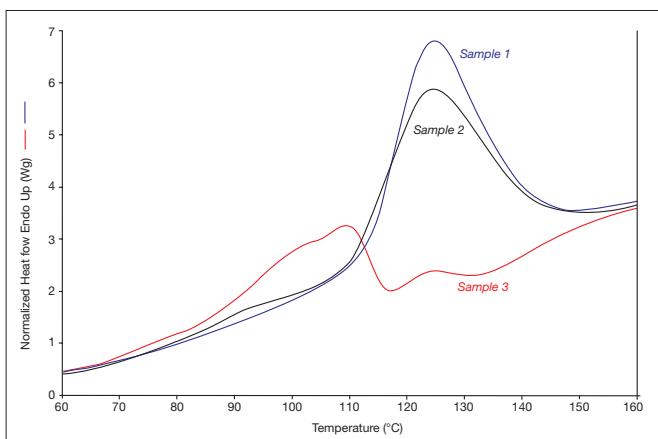


Figure 4B. The alpha phase fusion effects of the systems 1, 2 and 3 (in 2005), i.e. heating rate 300 °C/min.

**Table 1. High and low heating rate results measured on PK copolymers.**

Sample Code	Alpha Cryst. Phase		Beta Cryst. Phase	
	$T_m^*$ °C	$H_f^*$ J/g	$T_{m1}$ C	$H_{f1}$ J/g
1. 1993**	111.8	8.3	252	116.1
1. 2005***	124.4	18.2	258	126.9
2. 1993	106.3	5.1	251.8 *	116.0*
2. 2005	124.2	15.8	257	126.1
3. 1993	-	-	249.4 *	112.0*
3. 2005	109	4.3	252.7	118.2

\* corrected by calculation, see text.

\*\* (1993) low, i.e. 20 °C/minute heating rate experiments.

\*\*\* (2005) high, i.e. 300 °C/minute heating rate experiments.

In order to check the consistency of all fusion effects measured, we first tried to find a manner to correct for the recrystallization effects during the fusion of samples 2 and 3 (1993). It soon became clear that especially strong coupling between the alpha/beta fusion effects offered correction possibilities.

The  $H_{f1}$  values of the four other samples were plotted as a function of  $H_f^*$ . The linear relation fitting these values was extrapolated to  $H_f^* = 0.0$  with a  $H_{f1}$  value of 112.8 J/g. This value of 112.8 was subsequently changed in small steps between 114.0 and 110.0 to find the  $H_{f1}$  value for  $H_f^* = 0.0$ , giving the highest correlation factor value. Using this value as a 'calculated' data point, an 'optimized'  $H_{f1}/H_f^*$  relation was calculated i.e.:

$$H_{f1} = 0.8497 \times (H_f^*) + 111.89 \quad (n = 5, R_{val.} = 0.9537) \quad (1)$$

Substitution of  $H_f^* = 0.0$  for sample 3 (1993) resulted in a corrected  $H_{f1}$  value of  $\leq 111.7$ , i.e. 112 J/g instead of the experimental value 110.6 J/g. Substitution of  $H_f^* = 5.1$  J/g for sample 2 (1993) resulted in a corrected  $H_{f1}$  value of 116 J/g instead of the experimental value of 119.1 J/g.

The linear relation  $T_{m1}/H_f^*$  was used in the same way to calculate the corrected  $T_{m1}$  values for both samples 2 and 3 (1993). The corrected  $T_{m1}$  value of sample 2 (1993) was calculated at 251.8 °C. The corrected  $T_{m1}$  value of sample 3 (1993) was calculated at  $\leq 249.4$  °C.

These four calculated values are also listed in Table 1, with the warning: calculated values.

### Calculation of beta phase $T_{m1}$ and $H_{f1}$ values based on the alpha phase $T_m^*$ value.

The differences in the  $T_{m1}$  and  $H_{f1}$  values listed in Table 1 are not straightforward. Hence, we tried to calculate these values to see if they fit in one model. The used model is simple: assuming that the  $T_m^*$  values are known, it calculates the other three parameters i.e., the  $H_f^*$ ,  $T_{m1}$  and  $H_{f1}$  values with three derived equations:

$$H_f^* = 0.7200 \times (T_m^*) - 72.5678 \quad (2)$$

$$T_{m1} = 0.4668 \times (H_f^*) + 249.4099 \quad (3)$$

$$H_{f1} = 0.8497 \times (H_f^*) + 111.7243 \quad (4)$$

with  $T_{m1}$  and  $T_m^*$  : °C

$H_{f1}$  and  $H_f^*$  : J/g and

$100 \text{ °C} < T_m^* < 125 \text{ °C}$

It is important to realize that these equations only hold for compression molded PK copolymer systems.

Subsequently, the four  $T_m^*$  values listed in Table 1 with corresponding experimental  $T_{m1}$  and  $H_{f1}$  values were used to calculate the fusion values of their beta crystalline phase, see Table 2. The comparison of the calculated values with the reported measured values is satisfactory. It indicates that the measured differences in  $T_{m1}$  and  $H_{f1}$  of both important properties are correct. Continuation of this research is necessary to obtain further/better understanding of this fascinating behavior. But, in fact these results obtained with experimental data:

- differ in time more than twelve years
- are measured at different locations and by different persons
- are performed on different DSC systems

and are, in our eyes the best proof of the excellent quality, high stability and reliability of PerkinElmer's Thermal Analysis Systems.

**Table 2. Testing the consistency of the results of high and low heating rate DSC experiments performed in 1993 and 2005.**

Beta Phase $T_{m1}$ Values			
Sample Code	$T_{m1}$ (calc.) °C	$T_{m1}$ (meas.) °C	$ \Delta T $ °C
1.(1993)	253.1	252	1.1
1.(2005)	257.3	258	0.7
2.(2005)	257.3	257	0.3
3.(2005)	252.2	252.7	0.5
		$ \Delta T $ °C average	0.7
Beta Phase $H_{fi}$ Values			
Sample Code	$H_{fi}$ (calc.) J/g	$H_{fi}$ (meas.) J/g	$ \Delta H_f $ J/g
1.(1993)	118.5	116.1	2.4
1.(2005)	126.2	126.9	0.7
2.(2005)	126	126.1	0.1
3.(2005)	116.8	118.2	1.5
		$ \Delta T $ °C average	1.2

### The glass-rubber transition

The Tg value determination of high crystalline polymers by DSC is, for most systems, not possible, or at least difficult. Earlier, we reported our attempts to determine the Tg values of PK co- and terpolymer by conventional DSC. The conclusion then was the DSC Tg value determination of PK co- and terpolymers is only possible on PK terpolymers after a proper thermal pre-treatment. The DSC Tg (onset) value reported for these systems was  $4\text{ °C} \pm 3\text{ °C}$ .<sup>3</sup>

The heat flow/temperature curves of the present three samples were blown-up to see if any Tg effect was present. A clear Tg effect was measured for the systems 1 and 3 (2005), see Figure 5. For system 2 (2005) only the Tg onset was detected. So we found:

1. (2005) DSC Tg (onset) = 7 °C
2. (2005) DSC Tg (onset) = 2 °C
3. (2005) DSC Tg (onset) = 9 °C

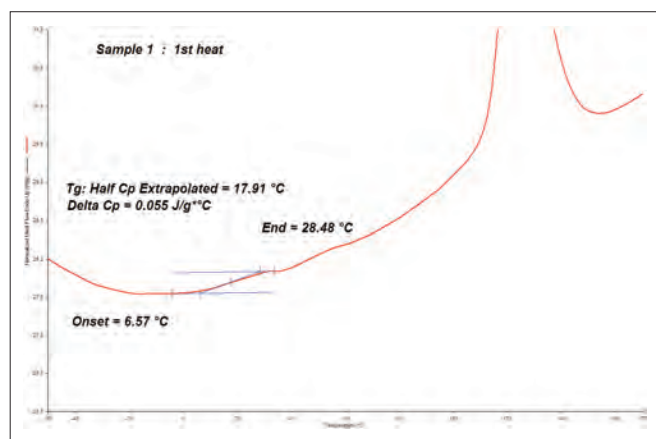


Figure 5. The DSC Tg value determination of sample 1 at 300 °C/min (in 2005).

This result is much better than we ever measured for such semi-crystalline polymers. We do think that a proper optimization in terms of sample mass, sample shape and sample pre-treatment<sup>3</sup> will improve these results even more.

### Summary and conclusions

Two simple HyperDSC heating scans on three PK copolymer samples provided more information about the amorphous and crystalline phases of this high crystalline polymer than a lot of standard DSC heating rate measurements did in the past. The high heating rate measurements (300 °C/min) dismissed the doubts that the reported maximum  $T_{m1}$  value, i.e. 258 °C, and the alpha- and beta-phase fusion effects were measured without any hampering due to recrystallization effects during both processes. The results of both the recent high rate and the old low rate measurements fit perfectly in the proposed alpha/beta fusion model. Besides, Tg effects were clearly detected in these scans without any pre-treatment (this is rare for such high crystalline polymers). The results of these measurements show that the HyperDSC technique is really the most effective and most sensitive DSC technique available at the moment for the characterization of both the crystalline and the amorphous phase of a polymeric system.

## References

1. E. Drent, European Patent 121,96 (Shell), 1984.
2. B.J. Lommerts et al., J. of Pol. Sc. : Part B: Polymer Physics, Vol. 31, p. 1319 – 1330 (1993).
3. W.M. Groenewoud: Characterization of Polymers by Thermal Analysis, Elsevier Science Amsterdam/New York, ISBN:0-444-50604-7 (2001).

## Appendix I: Thermal history of investigated PK copolymer samples

I. Reactor powder PK copolymer (Carilon E) – MDU batch 91.091

$$T_{m1} = 258 \pm 1 \text{ } ^\circ\text{C}^*$$

$$H_{f1} = 152 \pm 6 \text{ J/g}^*$$

II. Sample sheet molding i.e. Compression molded for 2.5 min. at 280 °C

III. Annealing procedure

10 min. at 240 °C  
DSC sample 1. (1993)

6 min. at 240 °C  
DSC sample 2. (1993)

no annealing  
reference DSC sampe 3. (1993)

IV. Storage time 1993-2005 storage in darkness at 20 °C and 50% R.H.

DSC sample 1. (2005)

DSC sample 2. ( 2005)

DSC sample 3. (2005)

\* reported average values; specific batch values 257.0 °C / 151.8 J/g

## Differential Scanning Calorimetry

## Authors

Geert Vanden Poel

DSM Resolve  
The Netherlands

Vincent B.F. Mathot

SciTe B.V.  
The Netherlands

Peng Ye

PerkinElmer, Inc.  
Shelton, CT 06484 USA

## Crystallization Temperature vs. Cooling Rate: the Link with “Real-Life” Polymer Processes

### Introduction

A relatively new technology for calorimetry has recently been discussed for practical use and since then marketed by PerkinElmer under the name HyperDSC®. The detailed characteristics and use of this new mode of measurement, which represents a major step forward in Fast Scanning Calorimetry (FSC) as compared to Standard DSC, have been published.<sup>1-4</sup> Controlled and constant scan rates of hundreds of degrees per minute and combinations thereof, both in the cooling and heating mode, are possible thanks to the small furnace size compared with the bulky furnace of the conventional heat flux DSC (Figure 1). Thanks to the power compensation design which supports accurate heat flow rate measurement, heats of transition, heat capacities, temperature-dependent crystallinities etc. can be established at the extreme rates applied. The short measuring times also provide the high throughput needed in e.g. combinatorial chemistry.

### PerkinElmer Power Compensation vs. Heat Flux

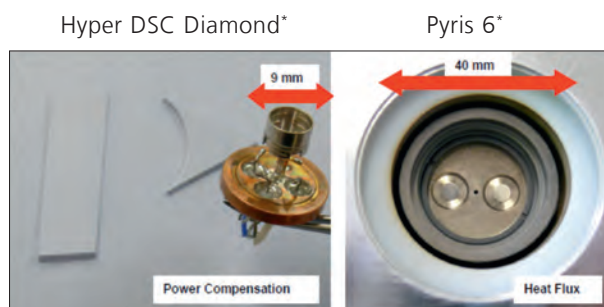


Figure 1. Furnace of HyperDSC versus heat flux DSC furnace.

\*Hyper DSC Diamond instrument is superseded. It has been replaced by DSC 8500.

\*Pyris 6 instrument is superseded. It has been replaced by DSC 4000.

Application fields benefiting from HyperDSC concern study of the kinetics and metastability of macromolecular and pharmaceutical systems, particularly the analysis of rate-dependent phenomena under real temperature-time conditions. Thus, HyperDSC is very much suited to investigate these systems with respect to their kinetics of processes such as crystallization, cold crystallization, recrystallization, annealing, and solid-state transformations.

Milligram and submilligram amounts of material can be investigated at controlled cooling and heating rates as high as hundreds of degrees per minute, which facilitates the analysis of films, expensive and extraordinary products, inhomogeneities in materials etc.

High cooling rates need to be applied to simulate processing conditions such as in film blow molding, injection molding and extrusion. It appears that for some processing techniques the cooling rate can be mimicked by HyperDSC. Measurements concerning metastability and kinetics are also necessary to (re)connect heating behavior with cooling history.

### Experimental

The PET/PBT samples reported have been supplied by DSM. DSC measurements were performed using a Diamond DSC\* (PerkinElmer) with an Intracooler II cooling accessory. Cooling rates of 10 to 250 °C/min have been used to study their effect on the crystallization behavior of the polymers involved. To keep the thermal lag minimal, the sample sizes were reduced with increasing cooling rates.

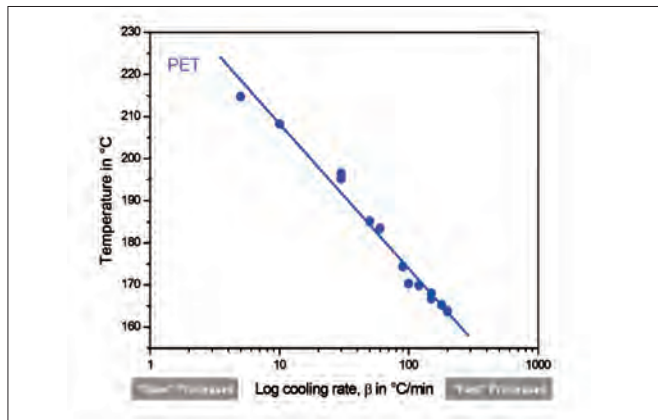


Figure 2. PET crystallization peak temperature as a function of log cooling rate.

### Results and Discussion

In industrial applications the crystallization temperature of a polymer is considered to be the temperature at which the polymer becomes solidified during processing. This temperature is the limiting value for proper injection molding conditions

\*Diamond DSC is superseded. It has been replaced by DSC 8500.

for “real-life” applications. A polymer or compound which crystallizes “too fast” will solidify too soon resulting in a not-completely filled mold. If the polymer or compound crystallizes “too slow”, the release from the mold will be problematic.

Presenting a characteristic crystallization temperature as a function of the (log) cooling rate provides useful insight into the crystallization behavior of the material studied. Figure 2 shows the crystallization peak temperature of PET vs. log cooling rate. With increasing cooling rates, this temperature decreases significantly.

In case of polyethylene terephthalate (PET) and polybutylene terephthalate (PBT), Standard DSC experiments at relatively slow cooling rates suggest that PET will crystallize prior to PBT. However, when measured during fast cooling by means of HyperDSC it is seen that one should expect that PBT crystallizes first, followed by PET (Figure 3). Thus, it is obvious that in many cases fast scanning represents realistic conditions in practice – like extrusion – much better than the often used low scan rates, like 10 °C/min. Consistent with this awareness the window of analysis of the HyperDSC range of PerkinElmer has been enlarged up to cooling rates of 750 °C/min by way of the recently introduced DSC 8500.

Not only is the sequence of crystallization important but also the crystallizability itself matters: PBT crystallizes at 173 °C while the PET studied here does not crystallize anymore at cooling rates of 225 °C/min and higher. One should consider putting such “right” values into computer-aided industrial design software to improve polymer applications for automotive, shipbuilding, and aerospace industries, industrial and architectural design, prosthetics, and many more.

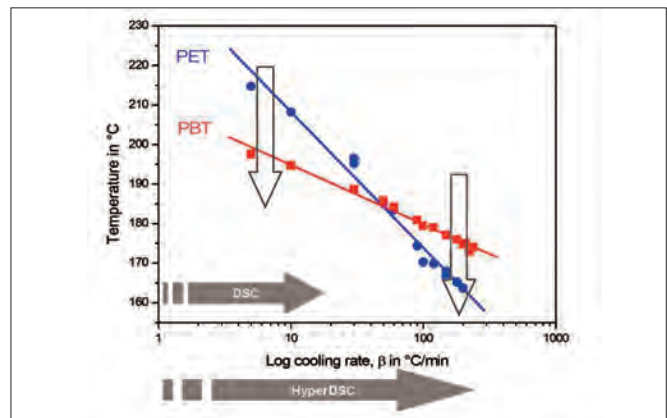


Figure 3. Crystallization temperatures of PET and PBT as a function of log cooling rate.

Thus, HyperDSC should be applied in order to mimic “real-life” processes and industrial processing much better than hitherto has been done. Furthermore, HyperDSC can handle sample masses ranging from approximately 1 µg or less up to more than 10 mg, by which one can choose a representative sample mass.

## Conclusions

Since polymer crystallization is significantly influenced by the actual cooling rate, the measurement of a characteristic crystallization temperature should be carried out at the same cooling rates as realized during polymer processing conditions. The conventional 10 °C/min cooling rate represents the low and small part of processing cooling rates applied in practice. Rates usually are much higher, near hundreds of degrees centigrade per minute. Therefore, results from a conventional cooling experiment using a scan rate of e.g. 10 °C/min can be misleading in practice, as illustrated by the PET and PBT case. Therefore, the fast cooling capability of HyperDSC is crucial for mimicking actual polymer processes – such as extrusion – and provides a realistic insight into polymer crystallization behavior. As such, it is an indispensable analytical tool to link experimental data with real-life polymer processes.

## References

1. Pijpers T.F.J., Mathot V.B.F., Goderis B., Scherrenberg R.L., van der Vegte E. *Macromolecules* 2002; 32:3601
2. Vanden Poel G., Mathot V.B.F. *Thermochim. Acta* 2006; 446:41.
3. Vanden Poel G., Mathot V.B.F. *Thermochim. Acta* 2007; 461:107.
4. V.B.F. Mathot, G. Vanden Poel and T.F.J. Pijpers, *American Laboratory*, 38(14) (2006) 21: downloadable for free from the website of SciTe B.V.: [www.scite.eu](http://www.scite.eu).

A special thanks to DSM Resolve and Science & Technology of the Netherlands for their contributions to this application note.

## Thermal Analysis

## Authors

Beppe Casassa

PerkinElmer, Inc.  
Milan, Italy

Peng Ye

PerkinElmer, Inc.  
Shelton, CT USA

## Double-DSC Isothermal Crystallization Studies for Improved Injection Molding of Polymers

- Melting temperature
- Heat of melting
- Percent crystallinity
- Glass transition (T<sub>g</sub>) or softening
- Crystallization
- Presence of recycled material (regrinds)
- Presence of plasticizers
- Polymer blends (presence, composition and compatibility)

In the characterization of polymer materials, DSC is most commonly used to verify the quality of the resin prior to release for processing. This avoids the potential loss of many thousands of dollars from processing a product that does not meet final quality tests, or a resin that may cause problems during processing, potentially as serious as a close-down of the processing line until the unsuitable material is removed. These routine, goods-in, quality tests are generally performed by heating the sample from ambient conditions to above the melting temperature then observing the position of the melting peak and/or glass transition.

### Introduction

Differential scanning calorimetry (DSC) is widely used to characterize the thermophysical properties of polymers and can be used to measure important thermoplastic properties including:

However, for some thermoplastics, differences in physical properties can be seen during processing, yet the melting points or glass transitions may not show any significant changes. Here, a real world example demonstrates a product quality issue where standard DSC heating and cooling was uninformative but where the use of isothermal crystallization revealed the subtle differences in material properties during processing.

For superior sensitivity, isothermal crystallization demands a fast-scanning DSC such as the PerkinElmer® DSC 8500. In this instance, without the fast-cooling capability of the DSC 8500, the differences between the good and bad batches will have remained a mystery and the customer unable to eradicate the quality issue.



Figure 1. The PerkinElmer DSC 8500.

### Double-DSC Furnace Design: Power Compensation DSC

The DSC 8500 incorporates two independently controlled, low mass sample and reference furnaces. This technique is known as the power compensation approach. The very low mass of the furnaces yields a DSC with low thermal inertia and the fastest response time of any DSC instrument on the market. This double-furnace design approach and the extremely advanced electronics in the DSC 8500 allow samples to be linearly heated and cooled at rates as fast as 750 °C/min. This is extremely important when measuring isothermal crystallization behaviors of polymers.

In contrast, heat-flux DSC instruments employ a single large mass furnace. Some DSC devices use a silver block with a mass of 100 g or more. This provides a much higher thermal inertia and a slower inherent DSC response time. Single-furnace DSC instruments cannot achieve the very fast cooling and heating provided by the double-furnace instruments.

The outstanding rapid response of the double-furnace DSC 8500 may be seen in Figure 3. This plot shows the cooling performance of the DSC 8500 over a typical thermoplastics cooling range.



Figure 2. The double-furnace design pictured on the right allows very fast cooling and heating required for isothermal crystallization studies.

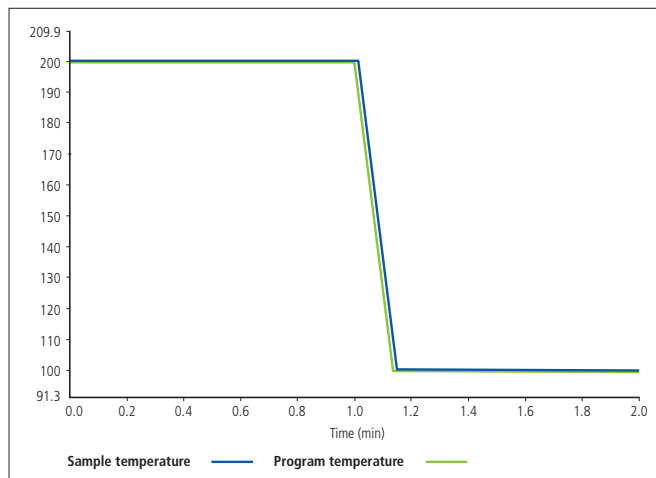


Figure 3. Sample temperature curve from DSC 8500 showing controlled cooling at 750 °C/min.

### Failing thermoplastic resin in an injection molding process

In this study, an injection molder was having problems with a specific batch of polypropylene-polyethylene (PP-PE) resin used in the manufacture of automotive fuel tanks. Compared to “good” batches, the “bad” batches did not yield the desired flow properties and could not be processed into the final form. In order to prevent bad raw materials going into the molding process, the company began screening for materials that failed to have the desired flow qualities.

To the injection molder, DSC seemed an obvious candidate for this screening as it is a very easy to use and accurate tool to measure the melting point of a material. Unfortunately however, the heating curves (Figure 4) of the good and bad batches did not show any significant difference in the melting profile of the PP at 160 °C, and only a minor change in the intensity of the PE melt at 120 °C. This small change would be very difficult to screen for on a routine basis or for a less experienced DSC analyst.

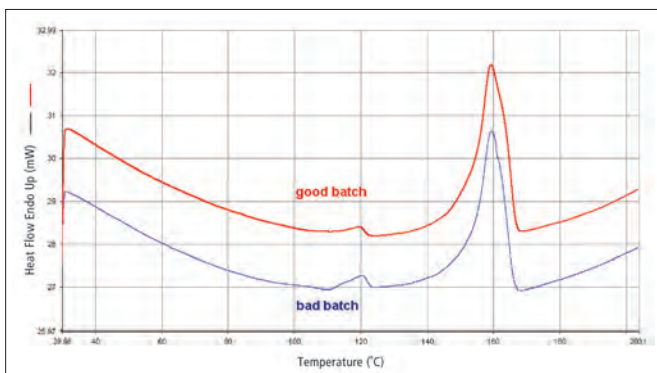


Figure 4. Standard DSC heating curve (10 °C/min) where no distinguishable differences are apparent between good and bad sample batches.

## Isothermal crystallization

It is common that the standard heating curve cannot distinguish between polymer batches that perform differently during processing, yet clearly they are dissimilar because they behave differently during the manufacture of these molded parts.

One property of a plastic that will have large impact on processing or final product performance is the resin's crystallization behavior. A large number of additives are used to control and optimize crystallization behavior for a given end use or processing method. Its importance in injection molding is that if a polymer resin begins to crystallize too quickly then its flow properties are altered. With a higher viscosity, the molten resin does not fill complex molds correctly, injectors are likely to get blocked and the products and the process begin to fail. Understanding crystallization is of paramount importance to anyone involved in the processing of thermoplastics.

The primary method used to understand crystallization behavior is isothermal crystallization. A DSC instrument heats the sample until it is molten, then cools it to a constant temperature (an isotherm). Being exothermic, the crystallization of a material will be evident on a DSC curve. When the DSC is held at a constant temperature, the time of the exothermic event becomes an indicator of how quickly the material crystallizes. The intensity of the curve can be used as an indicator of how much of the material is crystallized.

The successful measurement of the isothermal crystallization of polymers requires a DSC instrument that can cool the sample extremely quickly. This is because many thermoplastics crystallize rapidly when cooling from the melt. The DSC must be able to cool and equilibrate as fast as possible in order to detect the complete crystallization exothermic peak.

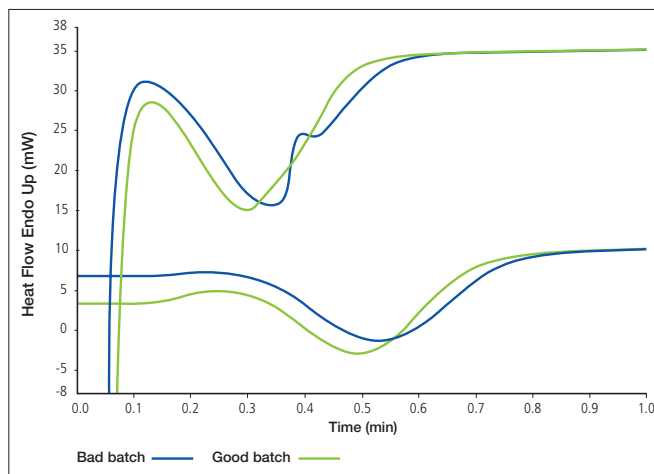


Figure 5. Isothermal crystallization results for the good and bad batches on heat flux DSC (lower curve) and DSC 8500.

In this case, isothermal crystallization behaviors of the good and bad batches were studied using both a single-furnace DSC instrument and the double-furnace DSC 8500. With the single, larger mass furnace and its longer response times, a typical cooling rate for the DSC using an intracooler-type accessory is 50 °C/min whereas the hyper-enabled double-furnace DSC 8500 is capable of reaching cooling rates of 750 °C/min.

While the standard heat-flux DSC was unable to show a clear distinction between the good and bad samples, the hyper-enabled DSC 8500 readily shows a significant difference between the two batches (Figure 5).

## Summary

In this material, the crystallization of the PE-PP resin is clearly rapid. With the slower cooling rates on the heat-flux DSC, crystallization is partly underway by the time the instrument reaches its isothermal temperature. This has prevented the system from capturing the double crystallization behavior in the bad batch samples.

With its fast-cooling rates, the DSC 8500 is able to characterize this behavior and provides a detection technique for the quality testing of all future incoming raw materials.

Further analytical experimentation would be required to understand the chemical and phase changes that underlie this issue. One possibility would be to take a sample from the bad batch and combine this isothermal crystallization experiment with direct Raman spectroscopy, applying the emerging Raman-DSC hyphenated technique. The additional information offered by the Raman-DSC technique would further increase the processor's chances of getting to the root cause of batch variations and so eliminate completely the problem further down the processing line.

PerkinElmer, Inc.  
940 Winter Street  
Waltham, MA 02451 USA  
P: (800) 762-4000 or  
(+1) 203-925-4602  
[www.perkinelmer.com](http://www.perkinelmer.com)



---

For a complete listing of our global offices, visit [www.perkinelmer.com/ContactUs](http://www.perkinelmer.com/ContactUs)

Copyright ©2009-2011, PerkinElmer, Inc. All rights reserved. PerkinElmer® is a registered trademark of PerkinElmer, Inc. All other trademarks are the property of their respective owners.

008499A\_01



## Importance of DSC Rapid Cooling for the Analysis of Plastic Microwave Food Trays



DSC 8000

### Introduction

Differential scanning calorimetry (DSC) is widely used to characterize the thermophysical properties of polymers. DSC can measure important thermoplastic properties including:

- Melting temperature
- Heat of melting
- Percent crystallinity
- Tg or softening
- Crystallization
- Presence of recyclates/regrinds
- Nucleating agents
- Plasticizers
- Polymer blends (presence, composition and compatibility)

Most DSC experiments on polymers are conducted by heating from ambient conditions to above the melting temperature. But, for some thermoplastics, which do exhibit differences during processing, standard heating DSC may not show any significant differences. A more sensitive test, for detecting subtle, but important differences between different batches of a given thermoplastic, is the DSC isothermal crystallization test.

During the manufacture of plastic products, such as bottles, fibers, films, containers, housings, pipes and trays, the thermoplastic is melted, cooled, thermoformed and crystallized. The complete

study of the behavior of plastics, which are melt-processed, requires having a DSC instrument that is capable of rapid cooling to simulate and fully explore the properties of these materials.

To study the melt-crystallization properties of polymers, several informative DSC tests can be conducted:

- Isothermal crystallization (at a single or multiple temperatures)
- Cooling (at different rates from very fast to normal)
- Reheating after cooling (at different rates)

The successful measurement of these particular tests requires a DSC instrument with a very fast response time. This is because many thermoplastics can crystallize rapidly when cooling from the melt. It is important that the DSC be able to cool and equilibrate as fast as possible in order to detect the complete crystallization exothermic peak. The DSC with the fastest response time is the Pyris™ Power Compensated DSC from PerkinElmer.

### Power Compensated DSC

The DSC 8000 from PerkinElmer uses the Power Compensated approach. This DSC uses two independently controlled, low mass (1 g) sample and reference furnaces. The low mass of the Power Compensated furnaces yields a DSC with low thermal inertia and the fastest response time of any DSC instrument available.

The Power Compensated DSC allows samples to be linearly heated and/or cooled at rates as fast as 500 °C/min. This is important when measuring isothermal crystallization times and behaviors of polymers.

In contrast, heat flux DSC instruments employ a large mass furnace. Some DSC devices use a silver block with a mass of 100 g or more. This provides a much higher thermal inertia and a slower inherent DSC response time. The heat flux DSC instruments cannot achieve the very fast cooling and heating provided by the Power Compensated DSC.

### Need for Fast Cooling for Microwave Food Trays

The thermophysical properties of plastic microwave food trays were studied using Power Compensated DSC. The microwave food trays must be capable of withstanding large and rapid extremes in temperatures. The trays are generally thermoformed from polyethylene terephthalate (PET) since this polymer is semicrystalline and exhibits the desired end-use properties such as stability, ease of processing and impact resistance. However, to further enhance the thermal stability of the PET polymer for use as microwave food trays, the crystallinity of the polymer is increased by adding nucleating agents. These agents induce a higher level of crystallization of the PET resin during cooling from the melt. Higher concentrations of a given nucleating agent will result in a higher level of crystallinity of the plastic during processing.

DSC cooling experiments are important for the assessment of the effects of these nucleating agents on the crystallization properties of the PET resin. Standard DSC may not reveal obvious differences between two different nucleated resins, whereas these differences will become evident during DSC cooling experiments. For the highly nucleated and fast crystallizing PET microwave food trays, the Power Compensated DSC is necessary for the best in-depth study of the rapid crystallization of the resin.

### Experimental

The heat flow properties of two different PET microwave food trays (Tray 1 and Tray 2) were studied, along with the non-nucleated PET precursor resin. The experiment conditions presented in the table were used to study the cooling properties of the PET resins.

The outstanding rapid response of the Power Compensated DSC may be seen in Figure 1. This plot shows the heating and cooling performance of the Power Compensated DSC at heating and cooling rates of 400 and 200 °C/min between 200 and 0 °C. The DSC was equipped with the refrigerated cooling system, Intracooler II and a helium purge was applied. The actual sample temperature (red) and program temperature (blue) are displayed as a function of time. The sample temperature tracks the program temperature very well even at the ballistic cooling rate of 400 °C/min and the use of a refrigerated cooling system, rather than liquid nitrogen. No other DSC instrument can match this level of performance.

Experimental Conditions	
Instrument	DSC 8000
Cooling system	Intracooler II
Sample pan	Crimped aluminum standard pan
Sample mass	Approximately 10 mg
Purge gas	Helium
Cooling rate (isothermal crystallization studies)	500 °C/min from 300 °C
Cooling rates for cool-reheat experiments	400, 300, 100 and 50 °C/min between 300 and 0 °C
Heating rate for heating experiments	20 °C/min

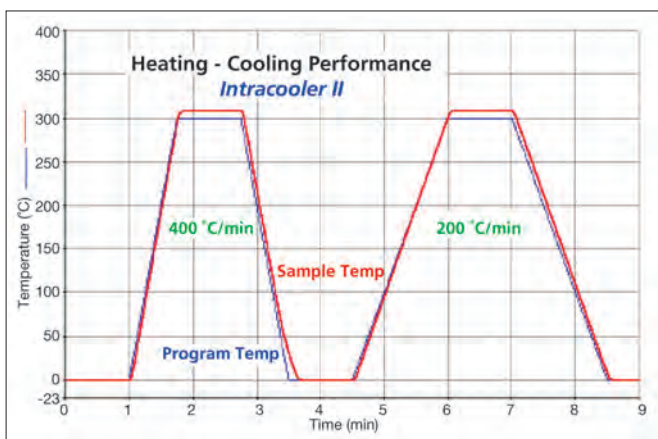


Figure 1. Fast heating and cooling performance of the Power Compensated DSC.

## Results

Displayed in Figure 2 are the DSC results obtained on the PET precursor polymer before the nucleating agents are added. The plot shows the first and second heating results. The PET resin was rapidly cooled at a rate of 200 °C/min between the first and second heats. During the first heating, no crystallization exothermic peak is observed reflecting the fact that the polymer has a high level of crystallinity in its as received state. The resin undergoes melting at 261 °C with a heat of melting of 66.7 J/g.

When the PET sample is rapidly cooled down to room temperature and then reheated, a well-defined cold crystallization peak is obtained at 173 °C, which is typical for this polymer. The heat of crystallization is found to be 30.1 J/g. During the second heating segment, the PET undergoes melting at 257 °C with a heat of melting of 33.0 J/g. The net heat of crystallization (melting – cold crystallization) is 2.9 J/g, which is reflective of a nearly amorphous polymer. This demonstrates the ability of the Power Compensated DSC to yield an amorphous polymer directly in the DSC with the application of a fast cooling rate. In comparison, many heat flux DSC instruments require that the sample be physically removed from the hot cell in order to generate an amorphous state by manual quench cooling.

To make the PET resin suitable for the manufacture of the microwave food trays, nucleating agents are added to the polymer. The presence of these nucleating additives drastically changes the morphology of the polymer allowing it to crystallize much more rapidly. Displayed in Figure 3 are the DSC results obtained from the PET sample extracted from a microwave food tray (Tray 1). The sample was heated through its melt temperature and then cooled at a rate of 200 °C/min back to room temperature.

When the cooled food tray is reheated, the cold crystallization exothermic peak occurs at a much lower temperature (134 °C) and is much smaller than that of the PET chip. These major differences are reflective of the changes caused by the presence of the nucleating agents.

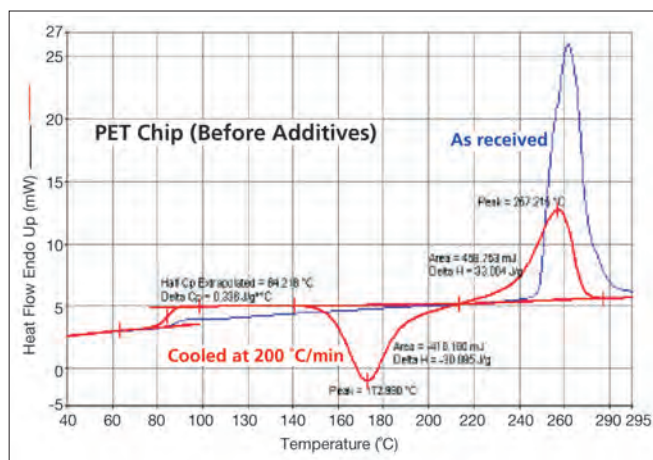


Figure 2. DSC results for PET chip (before additives) showing as received resin and resin after being melted and cooled at 200 °C/min.

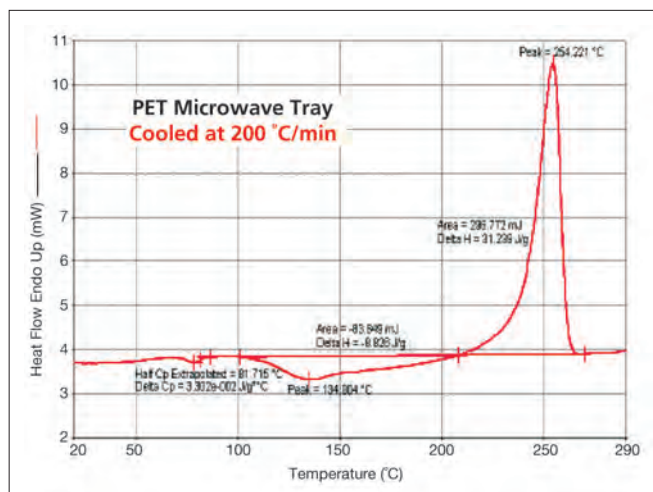


Figure 3. DSC heating results for PET microwave tray resin after cooling from the melt at 200 °C/min.

For quality assurance purposes, the manufacturers of the plastic microwave food trays like to induce a more well-defined cold crystallization peak for the nucleating resin. This provides a sensitive indicator as to the effectiveness of the nucleating agents based on the peak shape, magnitude and temperature. However, this requires ballistically cooling the PET resin from the melt to develop an amorphous material. Displayed in Figure 4 are the DSC results obtained on the food tray PET resin when cooled at the very fast rate of 400 °C/min. It may be seen that a well-defined cold crystallization peak is observed at 131 °C. This is possible only with the cooling capability provided by the Power Compensated DSC for such heavily nucleated polymers.

In contrast, most heat flux DSC units can heat at a maximum rate of only 100 °C/min. This is not fast enough to avoid crystallization for fast crystallizing polymers such as nylon or nucleated PET. Shown in Figure 5 are the DSC results generated for the PET tray resin when cooled from the melt at a rate of 100 °C/min. The cold crystallization peak is just barely observed, as these results demonstrate. Much valuable characterization information on the effects of the nucleating agents is lost when required to use the slower heating rates necessitated with heat flux DSC. The Pyris Power Compensated DSC provides the ability to cool over an extremely wide range of rates for the most comprehensive characterization information.

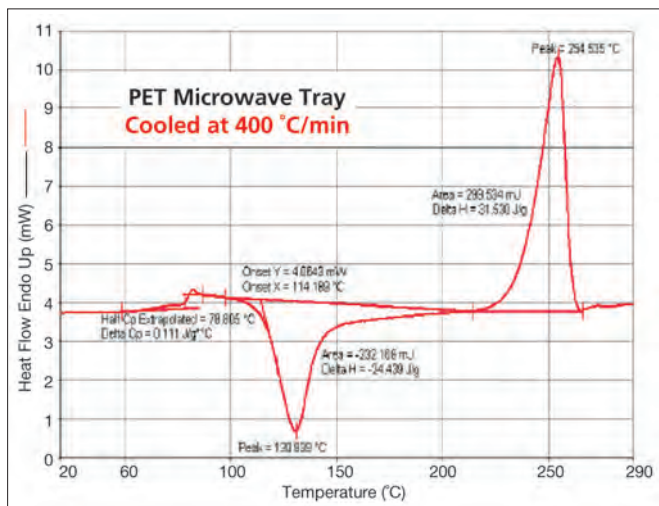


Figure 4. DSC results for PET tray resin after cooling at 400 °C/min.

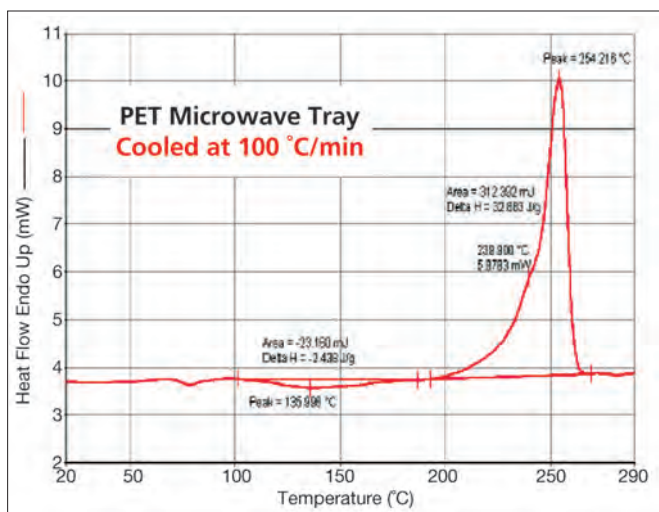


Figure 5. DSC results for PET tray resin after cooling at 100 °C/min.

The effects of the applied cooling rate for the PET tray resins may be seen in Figure 6. This shows a direct overlay of the heating curves obtained after cooling from the melt at 400, 200, 100 and 50 °C/min. Due to the heavy nucleation of the PET resin, there is a major change in the results when the cooling is slowed from the very fast 400 °C/min to 200 °C/min.

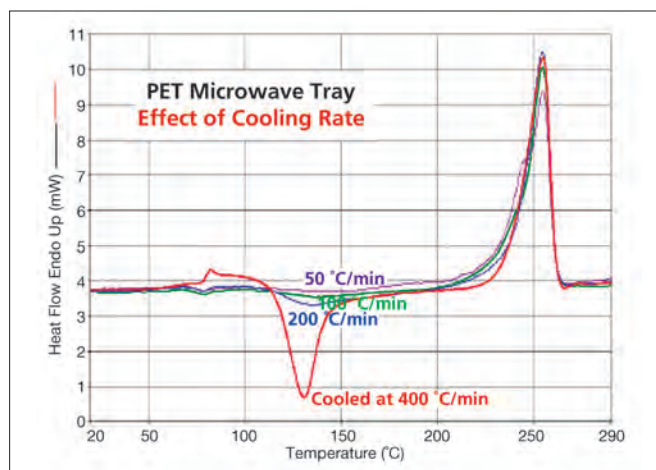


Figure 6. Overlay of DSC results on PET tray after cooling at rates of 400, 200, 100 and 50 °C/min.

This demonstrates the great importance of the need for the very fast cooling to get a complete picture of the crystallizable nature of this PET resin material.

Additional supplementary characterization information can be obtained by performing isothermal crystallization measurements on the nucleated PET resins. With this test, a sample of polymer is heated up through its melt and held under isothermal conditions for several minutes to destroy the existing crystalline structure. The sample is then ballistically cooled to a temperature below the melting temperature to allow the polymer to crystallize under tightly controlled conditions. DSC monitors the resulting crystallization exothermic peak as a function of time.

The isothermal crystallization test provides valuable information on polymers including:

- Average molecular weight
- Molecular weight distribution
- Presence of recyclates/regrinds
- Plasticizers
- Nucleating agents, pigments or other additives
- Copolymers
- Injection molding lubricants or flow enhancers

Because of its very fast response time and ability to cool quickly, the Power Compensated is ideally suited for the measurement of the isothermal crystallization of polymers.

Displayed in Figure 7 are the isothermal crystallization results generated for Tray 1. The sample was cooled from 300 °C to the target isothermal temperatures at a cooling rate of 500 °C/min. The crystallization behavior was monitored at temperatures of 230, 225, 220, 215 and 210 °C. At the temperature of 210 °C, the resin reached its maximum rate of crystallization in about 30 seconds. This demonstrates the ultra fast responsiveness of the Power Compensated DSC.

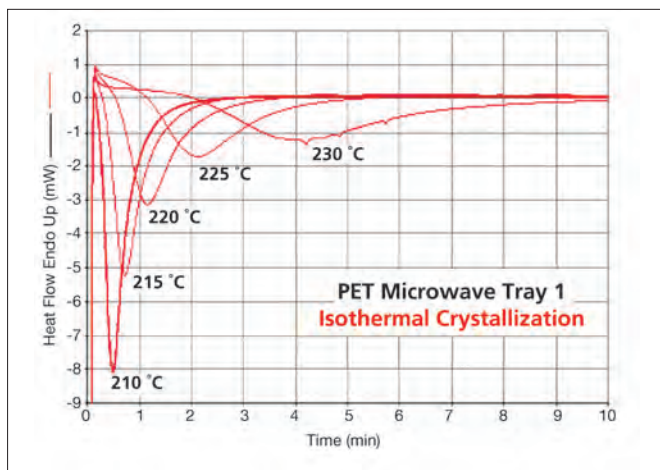


Figure 7. Isothermal crystallization results for PET Tray 1.

Another PET microwave tray (Tray 2) was analyzed using the DSC isothermal crystallization test and these results are displayed in Figure 8. This resin was clearly different in its resulting crystallization behavior as compared to the Tray 1 sample in that it took longer for it to crystallize under identical conditions. This indicates that the Tray 1 resin was more heavily loaded with nucleating agents as compared to Tray 2.

The differences between the crystallization behaviors of the Tray 1 and Tray 2 PET resins is more evident in an overlay (Figure 9) of the isothermal crystallization behaviors at 220 °C. Tray 1 clearly crystallizes more rapidly as compared to Tray 2.

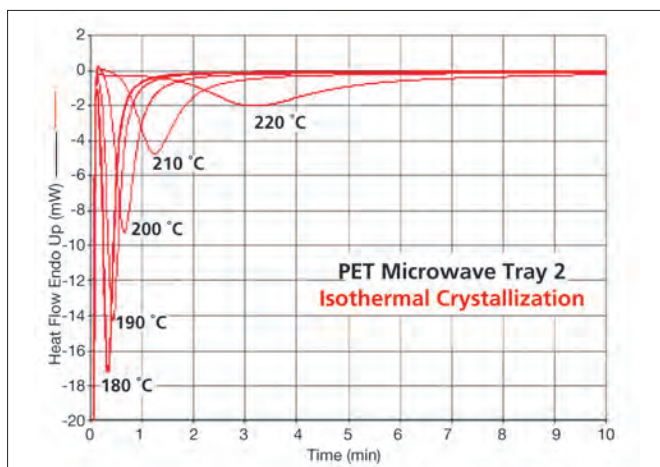


Figure 8. Isothermal crystallization results for PET Tray 2.

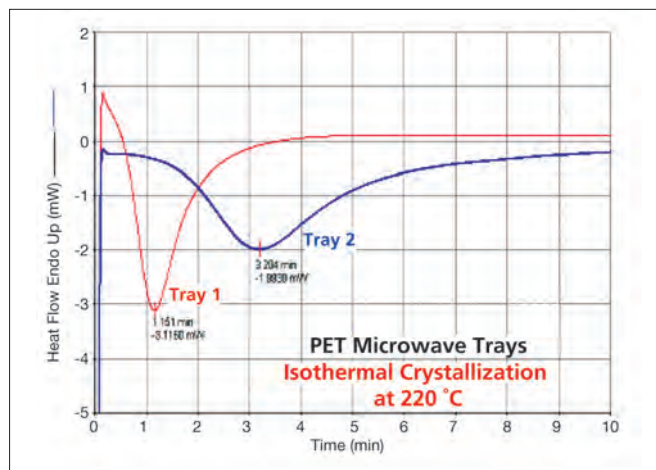


Figure 9. Overlay of DSC isothermal crystallization results at 220 °C for PET microwave trays 1 and 2.

These differences would not be apparent with standard heating DSC, but are very noticeable with the DSC isothermal crystallization measurements. The measurement of the very fast crystallization responses of these nucleated resins requires a DSC with an ultra-fast response time, and this is the Power Compensated DSC.

### Summary

Most plastic processes require that the polymer be melted and cooled during the thermoforming stage. The most comprehensive characterization of plastics undergoing melt processing necessitates that the material be studied under both heating and cooling conditions. The cooling analysis allows the effects of nucleating and plasticizing agents to be more fully quantified. Oftentimes thermoplastics may not exhibit any significant differences by standard heating DSC. However, when cooling studies are performed, significant differences, due to the presence of nucleating agents or flow enhancers, may become apparent. Such DSC data is extremely valuable for quality assurance or for process control purposes. The successful performance of cooling studies requires a DSC with a fast response time so that the sample can be analyzed at ballistic cooling rates. The DSC instrument with the fastest response time and the ability to heat and cool ballistically (up to 500 °C/min) is the power compensated DSC 8000 from PerkinElmer.

**Thermal Analysis****Authors:**

S. R. Woodruff and N. V. Tsarevsky

PerkinElmer, Inc.  
Shelton, CT USA

## Preparation of poly (glycidyl methacrylate) polymers with multiple pendant azide functionalities

Thermal analysis techniques are some of the fundamental techniques used in the characterization of polymers as their physical properties are strongly dependent on heat history. Differential Scanning Calorimetry (DSC) is for this reason the most common technique used. However in the development of novel polymeric materials, other techniques like Thermogravimetric Analysis (TGA) and Dynamic Mechanical Analysis (DMA) are often used. In this application note we look at the application of the TGA 4000 in understanding the changes made to a polymer after polymerization.

Thermogravimetric analysis (TGA) is very useful in determining the efficiency of post-polymerization modifications of polymers by allowing us to observe weight changes as a function of temperature. By analyzing degradation behavior of a specific polymer before and after modifications, the inherited properties can be studied more in-depth to gain a greater understanding into both the success of the modification and how this modification affects the thermal stability of the polymer. In this note, TGA analysis of azide-functionalized polymers derived from poly (glycidyl methacrylate), an epoxide-containing polymer, is performed to better characterize the materials. Epoxide-containing homopolymers and segmented copolymers often serve as a scaffold for the synthesis of a variety of different functional polymers with a range of application including crosslinkable (curable) materials, reactive coatings, surfactants and many others, many of which rely upon the epoxide ring-opening by various nucleophiles. The reaction with azides affords azide-containing polymers. One of the many interests in azide-functionalized polymers is specifically in their behavior during thermal degradation. This degradation is accompanied by a loss of nitrogen and formation of very reactive nitrenes, which in turn can participate in further crosslinking reactions. The analysis of polymeric azides can be carried out using NMR and IR spectroscopic techniques as well as TGA.

## Experimental

In order to synthesize polymers with controlled molecular weights and narrow molecular weight distribution derived from glycidyl methacrylate (GMA), a controlled/living radical polymerization technique was employed, known as *initiators for continuous activator regeneration* atom transfer radical polymerization (ICAR ATRP), which utilizes a fairly low-catalyst concentration (in this case, 200 ppm of Cu with respect to monomer). The reaction was carried out using tris (2-pyridylmethyl) amine as a ligand, azobisisobutyronitrile as the radical reducing agent, and diethyl 2-bromo-2-methylmalonate as the initiator<sup>1,2</sup>. The monomer, GMA, was purified with neutral alumina in order to remove the polymerization inhibitor present in the commercial product. The polymerization was carried out at 65 °C under nitrogen, with kinetics and molecular

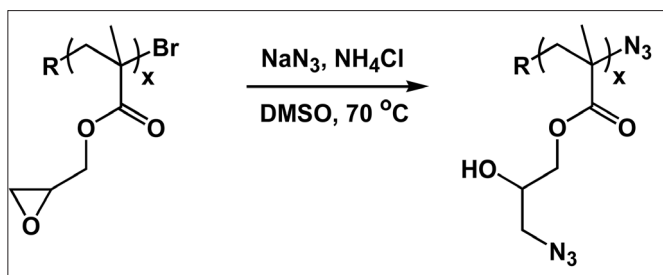


Figure 2. Azidation of PGMA with  $\text{NaN}_3$ <sup>3,4</sup>.

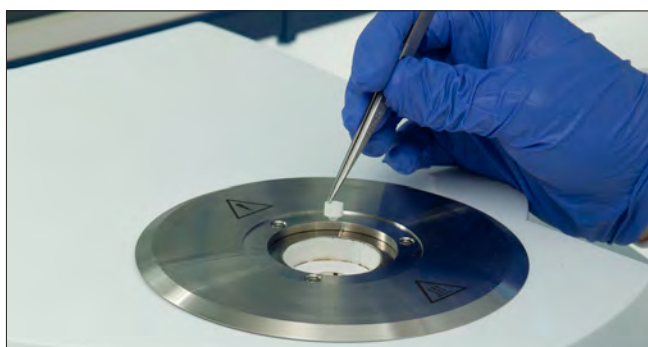


Figure 1. The TGA 4000 is a small rugged Thermogravimetric analyzer, available with and without auto-sampler, suitable for research grade work.

weight evolution monitored by NMR spectroscopy and size exclusion chromatography, respectively. After polymerization was finished (75% conversion), the resulting polymer was precipitated in methanol, filtered, and dried overnight. After drying, polyGMA was reacted with  $\text{NaN}_3$  in the presence of a proton donor ( $\text{NH}_4\text{Cl}$ ) in DMSO at  $70\text{ }^\circ\text{C}$  for 4 h (Figure 2). NMR was used to determine the disappearance of the epoxide peaks, indicating full conversion to azide-containing polymer. The resulting polymer was precipitated in water, filtered, washed several times, and dried thoroughly.

Both polyGMA and the resulting azide-containing polymer were carried out using a PerkinElmer TGA 4000, equipped with a PolyScience Chiller. Two analyses of each polymer were conducted to affirm precision of data. In each analysis, the balance was zeroed and approximately 7 mg of polymer was transferred into the sample tray. For every sample, behavior was studied from  $40.00\text{ }^\circ\text{C}$  to  $600.00\text{ }^\circ\text{C}$ , with a heating rate of  $10.00\text{ }^\circ\text{C}$  per minute and nitrogen flow rate of  $20.0\text{ mL}$  per minute (Table 1). Data traces can be seen in Figure 2.

## Results

The polyGMA (blue line in Figure 3) started to decompose

Sample Size	Heating Rate	Temperature Range in C	Purge Gas	Gas Rate	Cooling System
~ 7 mg	10 C/min	40-600	N2	20 mL/min	PolySci Chiller

Table 1. Experimental Conditions for the TGA 4000 runs.

appreciably at around  $260\text{ }^\circ\text{C}$ : the most likely mechanism being depolymerization via “unzipping”, which is typical for most polymethacrylates. In contrast, the azide-containing polymer (black line) started to decompose earlier at  $215\text{ }^\circ\text{C}$  in a distinct step. In this first step, about 30-35 wt % of the polymer mass was lost. This is most likely due to the evolution of nitrogen ( $\text{N}_2$  represents about 20 wt % of the repeat units), immediately followed by another, yet unidentified reaction. This second step started at about  $400\text{ }^\circ\text{C}$  and appears to be approximately 40% weight loss. This differs

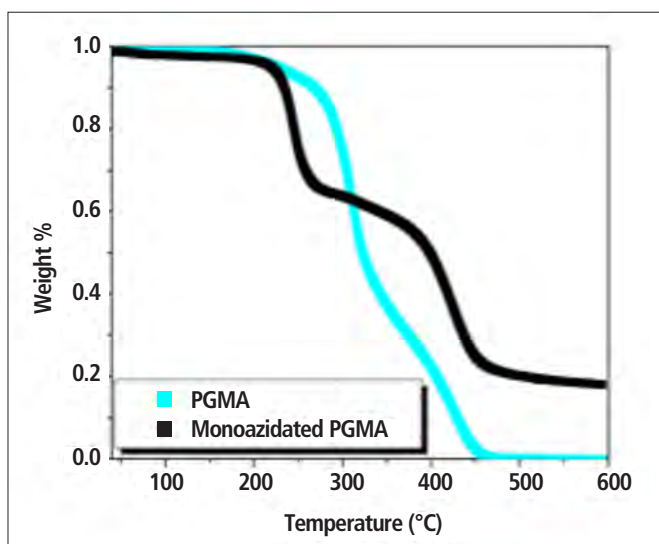


Figure 3. TGA analyses of PGMA and azide-containing polymers.

considerably from the original polymer, which decomposes more rapidly. We believe the formation of nitrenes from first decomposition step leads to efficient crosslinking of the rest of the polymer. The reaction product from this step was “stabilized” through the crosslinking and the stabilization was efficient enough that it did not decompose until a temperature of about 400 °C was reached. After the end of the second decomposition, a carbon-rich residue (about 20 wt % of the original polymer) remained did not decompose further up to 600 °C. This is consistent with the decomposition of the polymer to a coke like material, which burns above 600 in the presence of air or oxygen. In contrast, the initial polymer was totally decomposed by 460 °C.

## Conclusion

TGA represents a powerful way to investigate the structure changes in modified polymers. While polymer modification is often necessary to functionalize polymers for catalytic or medical uses, these modifications can alter the decomposition temperatures of the material greatly. In this case, we saw a 45 °C decrease in the start of decomposition. In addition, the decomposition studies in the TGA 4000 reveal some interesting chemistry occurring after the initial degradation of the polymer.

## References

1. Tsarevsky, N. V.; Jakubowski, W. J. *Polym. Sci. A Polym. Chem.* **2010**, *49*, 918.
2. Woodruff, S. R.; Davis, B. J.; Tsarevsky, N. V. *ACS Symp. Ser.* **2012**, *1100*, 99.
3. Tsarevsky, N. V.; Bencherif, S. A.; Matyjaszewski, K. *Macromolecules* **2007**, *40*, 4439.
4. Woodruff, S. R.; Tsarevsky, N. V. *Polym. Prepr.* **2011**, *52*, 671.

## Differential Scanning Calorimetry

Author

Phil Robinson

Ruston Services Ltd.  
Cheddleton, UK

# Effect of Processing Temperature on the Analysis of PVC Samples for Gelation using the DSC 4000

## Introduction

PVC Gelation Analysis by DSC has been described by a number of workers over the years, and has become an accepted method for analysis of processed PVC. What might not be well known, is the manner in which this analysis is made valid, which is discussed in this work.

Most errors in the analysis results from sample preparation, and some data will need to be discarded. The reproducibility can be significantly improved by observing a few simple points.

## Samples Submitted

Four samples of extruded PVC section were submitted for testing by DSC to determine the degree of gelation. The samples provided were;

1. Sample A63: Extruder Temperature = 198.5 °C
2. Sample A65: Extruder Temperature = 198.5 °C
3. Sample B70: Extruder Temperature = 201 °C
4. Sample B72: Extruder Temperature = 201 °C

## Sample Presentation and Analysis

### Calibration

The DSC was calibrated using the recommended procedure by PerkinElmer, using indium (In melting point = 156.60 °C) and lead (Pb melting point = 327.47 °C). Peak area (energy) was calibrated using the heat of fusion of indium. (28.45 J/g).

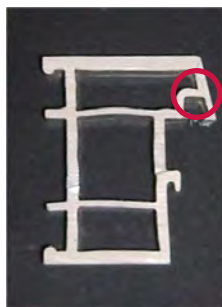
## Sample Preparation

The sample under test was an extruded box section which is shown in the photograph to the right. Very thin flat samples are necessary for this work, because the DSC is measuring heat-flow differences in response to sample shape changes caused by the various relaxations, seen up to 240 °C.

Samples were therefore cut from the sections of PVC extrusion in the area shown for all four samples. The cuts were made using a low-speed diamond saw which does not produce any stresses in the sample during preparation, and produces very smooth samples, which allow good thermal contact with the DSC sample pan.

Using a knife to cut samples produces distortions in the material (curling) during cutting, resulting in poor thermal contact with the sample pan at the start of the test. When such a sample is heated subsequently, these stresses are released and produce distortion of the baseline as the glass transition is passed, causing changes in thermal contact and leading to errors in the determination of gelation.

The following cutting using the diamond saw produced thin sheets sample material about 0.5 mm to 0.7 mm thick and these were cut to size to suit the DSC sample pan using a circular "punch". The flattest side following the "punching" process was laid downwards in the open aluminium sample pan used for the test to ensure the best possible thermal contact. Sample masses of around 20 mg were used for this testing.



Samples taken from circled area of the extrusion.

The sample pan was left open during testing since it is the sample shape changing. Producing the baseline, shifts the measured gelation effect to produce the evaluation. Because each sample changes in a slightly different way, there is some variability in the data from each test, requiring that a number of tests on each sample are made to confirm reproducibility.

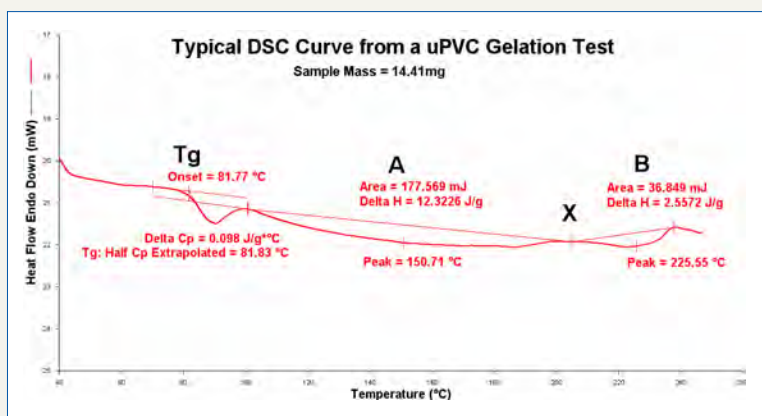
## Method

The method used in the DSC was to heat from ambient to 240 °C at 10 °C/min under a nitrogen atmosphere flowing at 40 mL/min. The sample pans used were PerkinElmer standard aluminium sample pans (0219-0041), which are about 6 mm diameter. The DSC was water cooled, with a water circulator/chiller set at 5 °C.

*NOTE: The sample pan is not crimped, allowing the sample freedom to move and distort in the pan during heating.*

## Background

The background of this method is based on that developed by Dr. M. Gilbert and Dr. J. Vyvoda and published in Polymer, produced August 1981. Other workers include those from Norsk Hydro Polymers, and Becetel.



This curve shows a typical DSC curve for this type of analysis. The features seen are;

- Tg The glass transition of unplasticized PVC, seen at about 82 °C, followed immediately by a small relaxation phenomenon.
- A A broad endotherm with a peak area "A" which it is proposed (Potente and Schultheid, 1987) to be related to the melting of partly gelled PVC.
- X A peak at about 204 °C which is proposed to be the processing temperature.
- B A broad endotherm which is proposed (JWThe, AACooper, ARudin, JHLBatiste – Measurements of the degree of fusion of Rigid PVC, March 1989) to be the melting of the previously non-gelled part of the PVC.

## Calculation of Results

The degree of gelation of the PVC is calculated as the ratio of A to the total area A+B as follows:

$$\% \text{ Gelation} = \frac{\text{Area A}}{(\text{Area A} + \text{Area B})}$$

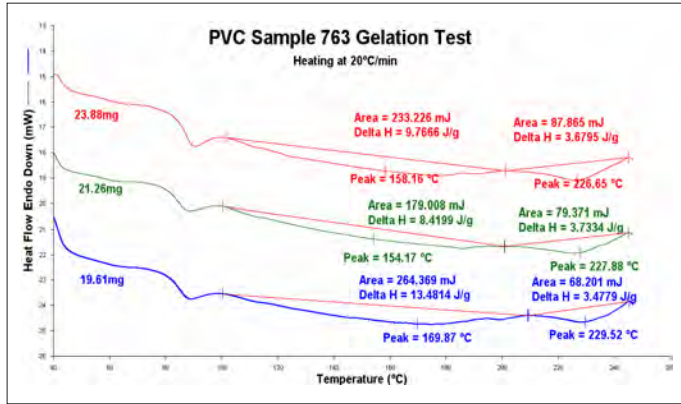
## Results and Discussion

From the data shown in Curves #1 to #4, it can be seen that the processing temperature does influence the degree of gelation determined by this method. The results, based on averaging of the three values obtained, indicates that the lower extrusion temperature (198.5 °C) has resulted in a lower degree of gelation (73.6% – 73.8%) than material extruded at 201 °C. This 201 °C material demonstrated a degree of gelation calculated to be 85.1% - 85.3%.

Single Furnace DSC such as the DSC 4000 allows PVC processors to monitor the degree of gelation of the PVC in their extruders.

Extruded PVC Material in which the gelation is too low has been shown to have poor impact properties, and single furnace DSC can provide a simple method of examining this property of the material. Variation in extruder characteristics can be easily identified, with the result that the PVC sections being produced will be more dimensionally stable and have better impact resistance when given the correct level of gelation. Single Furnace DSC therefore allows PVC processors to have better control of the extrusion process, which will enhance the quality of their products.

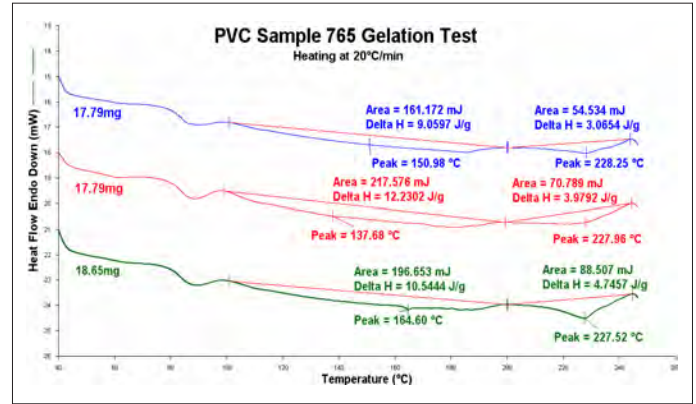
### Curve #1 - PVC Sample A63



The three data sets in Curve #1 above have the following calculated degrees of gelation:

Peak A	Peak B	Gelation	Average
9.7666	3.6795	72.6%	73.8%
8.4199	3.7334	69.3%	
13.4814	3.4779	79.5%	

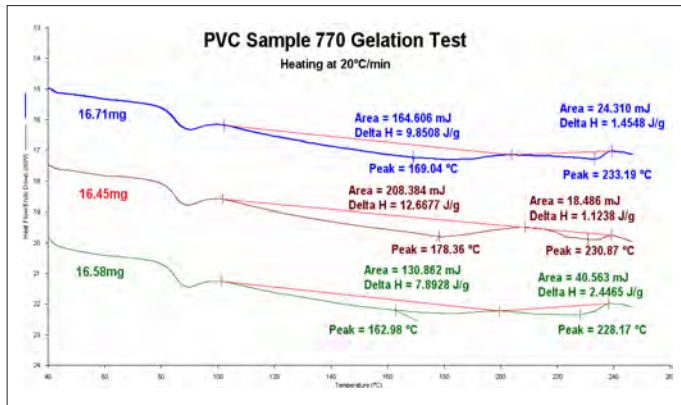
### Curve #2 - PVC Sample A65



The three data sets in Curve #2 above have the following calculated degrees of gelation:

Peak A	Peak B	Gelation	Average
9.9057	3.0654	76.4%	73.6%
12.2302	3.9792	75.5%	
10.5444	4.7457	69.0%	

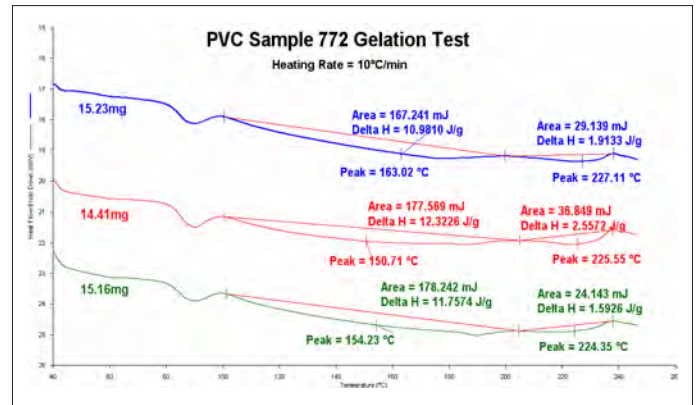
### Curve #3 - PVC Sample B70



The three data sets in Curve #3 above have the following calculated degrees of gelation:

Peak A	Peak B	Gelation	Average
9.8508	1.4548	87.1%	85.1%
12.6677	1.1238	91.9%	
7.8928	2.4465	76.3%	

### Curve #4 - PVC Sample B72



The three data sets in Curve #4 above have the following calculated degrees of gelation:

Peak A	Peak B	Gelation	Average
10.9810	1.9133	85.2%	85.3%
12.3226	2.5572	82.8%	
11.7574	1.5926	88.1%	

PerkinElmer, Inc.  
940 Winter Street  
Waltham, MA 02451 USA  
P: (800) 762-4000 or  
(+1) 203-925-4602  
www.perkinelmer.com



For a complete listing of our global offices, visit [www.perkinelmer.com/ContactUs](http://www.perkinelmer.com/ContactUs)

Copyright ©2014, PerkinElmer, Inc. All rights reserved. PerkinElmer® is a registered trademark of PerkinElmer, Inc. All other trademarks are the property of their respective owners.

## Infrared, IR Microscopy

Author:

Ian Robertson

PerkinElmer, Inc.  
Seer Green, UK

### Rapid Characterization of Multiple Regions of Interest in a Sample Using Automated IR Microscopy

#### Introduction

IR microscopy is a well-established analytical technique for the measurement and identification of small samples down to a few micrometers in size. It is used extensively in the polymer, pharmaceutical, chemical, food, and electronics industries, to name a few, often identifying small contaminations or foreign objects of unknown origin. In forensic applications small particles of materials such as

drugs, paint chips, residues or fibers are often collected as evidence and analyzed by IR microscopy.

The type and size of the material, as well as the matrix in which the sample is contained, will dictate the type of IR microscopy sampling technique to be deployed; transmission, reflectance, or ATR.

The Spotlight™ 200i IR microscope is a fully automated system comprising:

- Automated X, Y, Z stage
- Automatic illumination LEDs
- Autofocus
- Auto correction
- Automated switching between transmission and reflectance
- Automated dropdown ATR crystal

All of these features are controlled using the Spectrum 10 software.

Traditionally, measurement of a sample on an IR microscope involves several manual steps to find and specify the regions of interest for the analysis and manual processing of the collected data. All of which can be very time consuming. These processes have now been fully automated within the Spectrum 10 software, using intelligent detection routines for the typical types of samples measured on an IR microscope: particles, multilayer samples, and sample inclusions.

This Application Note will demonstrate the advantages of such an automated IR microscopy platform for the characterization of particles and/or foreign objects in different types of materials.

### Automated detection and analysis of microplastics extracted from a cosmetic formulation

An example of this automation is the detection and classification of microplastic particles extracted from a cosmetic formulation. Cosmetic exfoliating agents contain small microplastic particles as the abrasive material to scrub the skin. These microplastics make their way into the river systems and ultimately into the marine environment where they are serious pollutants. A commercially available product was mixed with hot water to dissolve the soluble ingredients in the formulation. The resulting solution was filtered using a 50-micrometer mesh, capturing any insoluble components greater than 50 micrometers in size. The filter was allowed to dry before transferring the residual particles onto an IR transmitting window on a microscope holder. A Visible Image Survey was collected over the area containing the majority of the particles. Selecting the "Analyze Image" icon in the Spectrum 10 software calls up the intelligent, automated routine for analyzing the image, as shown in Figure 1.

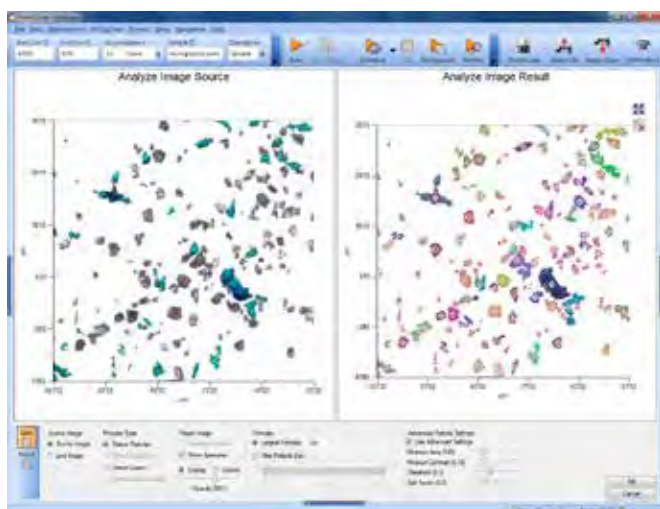


Figure 1: The "Analyze Image" function detected filtered particles deposited on a KBr window.

This routine will detect any particles present in the visible image and mark them as regions of interest. It will then calculate the maximum rectangular aperture size that can fit wholly inside each of the particles, thus minimizing signal-to-noise when the data is scanned. (In the past manual selection of the regions of interest and setting of apertures took a considerable amount of time.) Clicking "Scan Markers" will then initiate collecting transmission spectra (using equivalent apertures for the background) for each sample, displaying ratioed sample spectra in real time as they are collected. Automatic processing of the spectra, such as Search, Compare or Verify, will be performed during data collection. In the case of the analysis of the microplastics a spectral search was performed against a library of polymer spectra to give the identity of each of the particles.

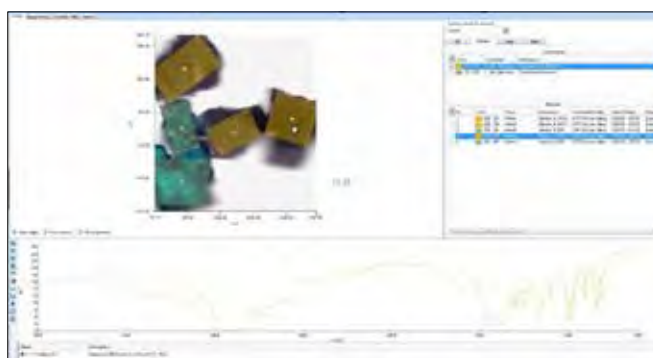


Figure 2: Results screen for detection and identification of particles.

Two different polymer types were detected in this sample, identified as polyethylene and polypropylene. The spectra are shown in Figure 3.

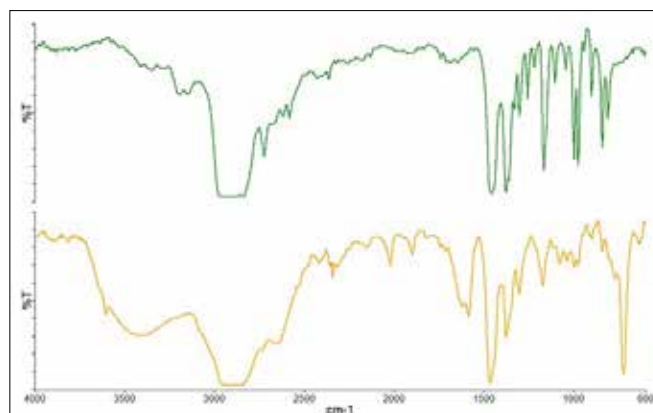


Figure 3: Spectra of the two different polymer types are shown here. Top: polypropylene, Bottom: polyethylene.

## Automated detection and analysis of contaminants on an electronic contact

Electronic contacts need to be clean and free from contamination to avoid problems in operation. A sample was submitted for analysis that had visible contaminants. The sample was placed in the Spotlight 200i and a "Visible Image Survey" collected over the entire contact. The resulting image was then analyzed using the "Detect Particles" function in the Spectrum 10 software in an attempt to find any contamination. The Visible Image Survey and an expanded region showing the particles detected are shown as Figure 4.

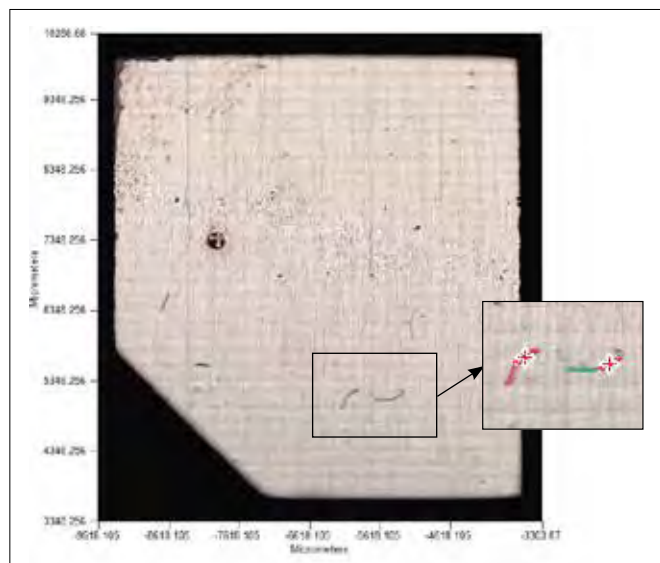


Figure 4: The Visible Image Survey and expanded region show automatic detection of contaminants.

After selecting "Scan Markers", the software automatically collected reflectance backgrounds and spectra for the particles (fibers), their spectra shown as Figure 5.

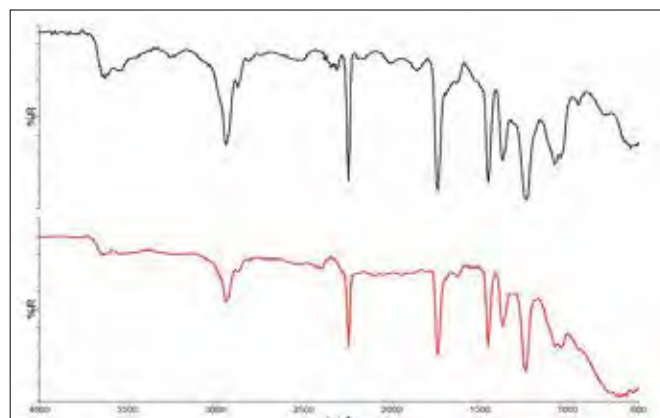


Figure 5: Reflectance spectra of the two contaminant fibers.

The spectra of these two materials are similar with the lower spectrum showing an additional broad peak centred around 700  $\text{cm}^{-1}$ . The top spectrum was identified as an acrylonitrile-butyl methacrylate copolymer by searching the spectrum against a spectral library of polymers and polymer additives. Since the lower spectrum clearly has another component present, it was subjected to a mixture search that also detected the presence of tin oxide in the sample.

## Automated ATR analysis of layers in a polymer laminate

ATR is a convenient sampling technique requiring minimal sample preparation that has been routinely applied within the polymer industry. An automated drop-down ATR crystal on an IR microscope allows for automated measurement of polymer samples, including layers of multilayer laminates. A multilayer polymer card was clamped in a sample holder and placed on the stage of the Spotlight 200i. A "Visible Image Survey" was recorded over a 2 mm x 2 mm area of the sample and the automated "Detect Layers" function in the Spectrum 10 software was applied, as shown in Figure 6.

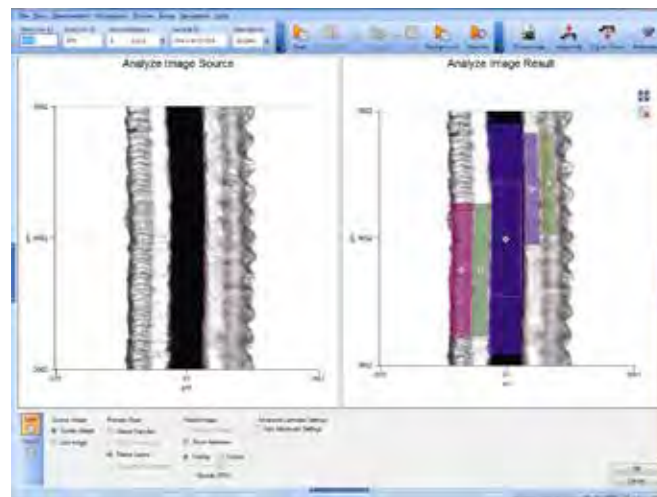


Figure 6: Automated detection feature of the Spotlight 200i show multiple layers in a polymer laminate.

Five different layers were detected in the image and markers placed in the center of each layer. Clicking "Scan Markers" will automatically collect the background scans then move to each of the markers, lower the automated ATR crystal onto the sample (Figure 7), and measure the spectra. The spectra obtained from each of the layers are shown in Figure 8 and were identified by comparison against search libraries.

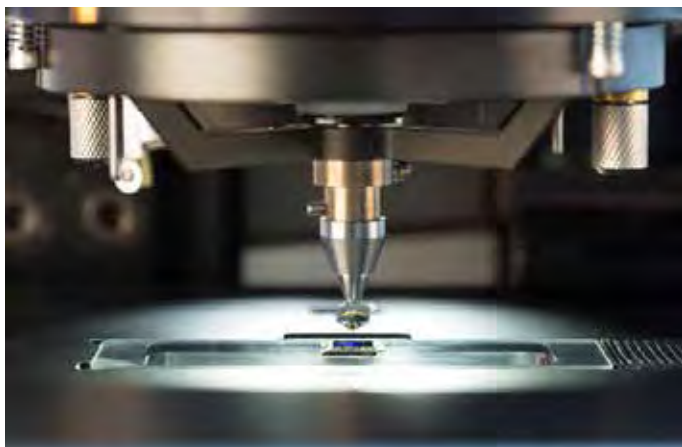


Figure 7: The automated dropdown ATR crystal.

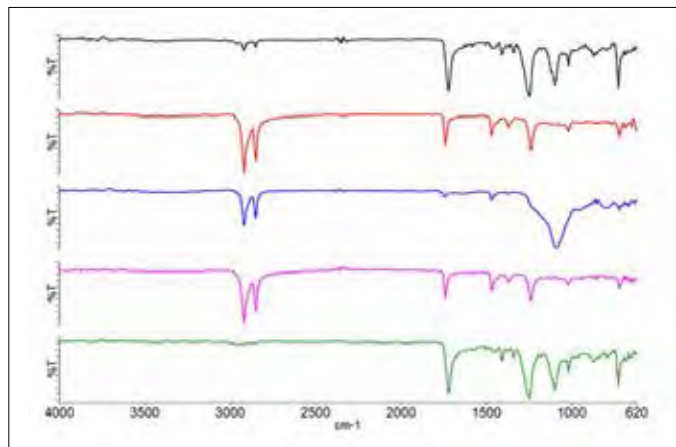


Figure 8: Spectra of the five layers.

The layers were identified from top to bottom as Polyethylene terephthalate (PET), ethylene-vinyl acetate (EVA) co-polymer, silica-loaded polyethylene, another layer of EVA and another layer of PET.

### Summary

The Spotlight 200i, an intelligent automated IR microscope system, is able to simplify and dramatically speed up the process of collecting and analyzing spectra from a variety of sample types. The automation has been applied to all sampling modes: Transmission, Reflectance, and ATR, as well as a variety of different sample types: particles, fibers and multi-layers.

## Thermal Analysis

## Authors

David Norman

Peng Ye

PerkinElmer, Inc.  
Shelton, CT 06484 USA

## Detecting Weak Glass Transition ( $T_g$ ) in Polymers by HyperDSC

### Introduction

Many polymers are semi-crystalline material. The percentage of crystallinity depends on many factors including chemical structure, interaction between polymer chains and processing conditions. When polymers get heated, the amorphous part will change from the glassy state to the rubbery state at the glass transition temperature ( $T_g$ ). Since only the amorphous

part contributes to the glass transition, for highly crystalline polymers, the glass transition ( $T_g$ ) can be very weak. One typical example is High Density Polyethylene (HDPE), a highly crystalline engineering thermoplastic. It is typically used in applications demanding a material that is chemically inert, does not absorb moisture, can be utilized over a wide range of temperature, and exhibits a high tensile modulus.

The amorphous region in HDPE is generally accepted to account for about 5% or less of the sample. Historically, the glass transition for a highly crystalline material like HDPE could not be determined by DSC since the step change in the heat flow signal as the material is heated through its glass transition cannot be observed at traditional scanning rates.

The advance of fast scanning DSC technology offers the opportunity to detect weak T<sub>g</sub> in such cases. The step change in heat flow signal during glass transition is proportional to the heating rate. The sensitivity is increased by a fast scanning rate. HyperDSC<sup>®</sup> can be performed on a double-furnace DSC, such as the PerkinElmer<sup>®</sup> DSC 8500. In contrast to most single-furnace DSCs, the double-furnace DSC uses ultra lightweight furnaces with very low thermal inertia and can achieve the fastest possible DSC response time. It allows very fast controlled linear heating and cooling scanning (up to 750 °C/min). In this study, an HDPE sample is used to demonstrate the increased sensitivity and ability to detect weak glass transitions with HyperDSC.

## Result

The DSC 8500 with liquid nitrogen cooling was used for this study. While the data generated for this work was performed utilizing HyperDSC, the DSC 8000 with scanning

rates up to 300 °C/min can also be used for traditional as well as StepScan DSC studies, which is one of the modulated temperature DSC technologies.

The data in Figure 1 indicates the T<sub>g</sub> of the HDPE sample to be approximately -111 °C. For comparison, the same sample was run under conventional DSC conditions at 10 °C/min. As indicated in Figure 1, there is no detectable transition in this temperature range even when zooming into the curve with conventional 10 °C/min scanning rate. This result clearly demonstrates the increased detection sensitivity with HyperDSC.

Also worth noting is that the experiment started at -150 °C, just 40 °C below the expected glass transition at 100 °C/min. This is only possible with a double-furnace DSC because the ultra light double-furnace enables very fast response times. It takes less than 10 seconds for the DSC curve to stabilize and a valid measurement to be made. Therefore

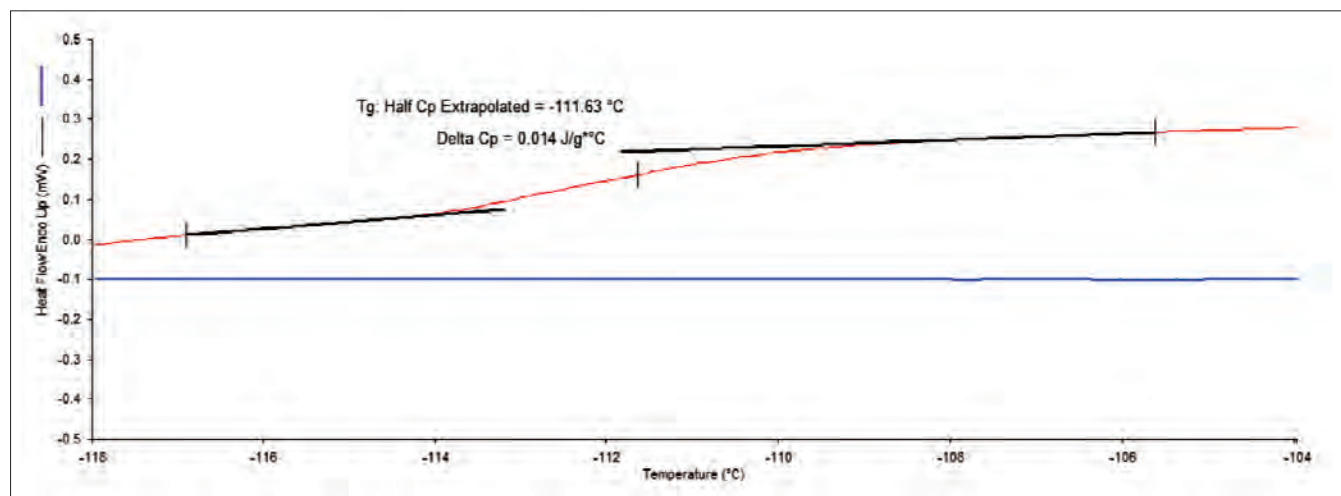


Figure 1. HDPE heating at 100 °C/min (red) and 10 °C/min (blue).

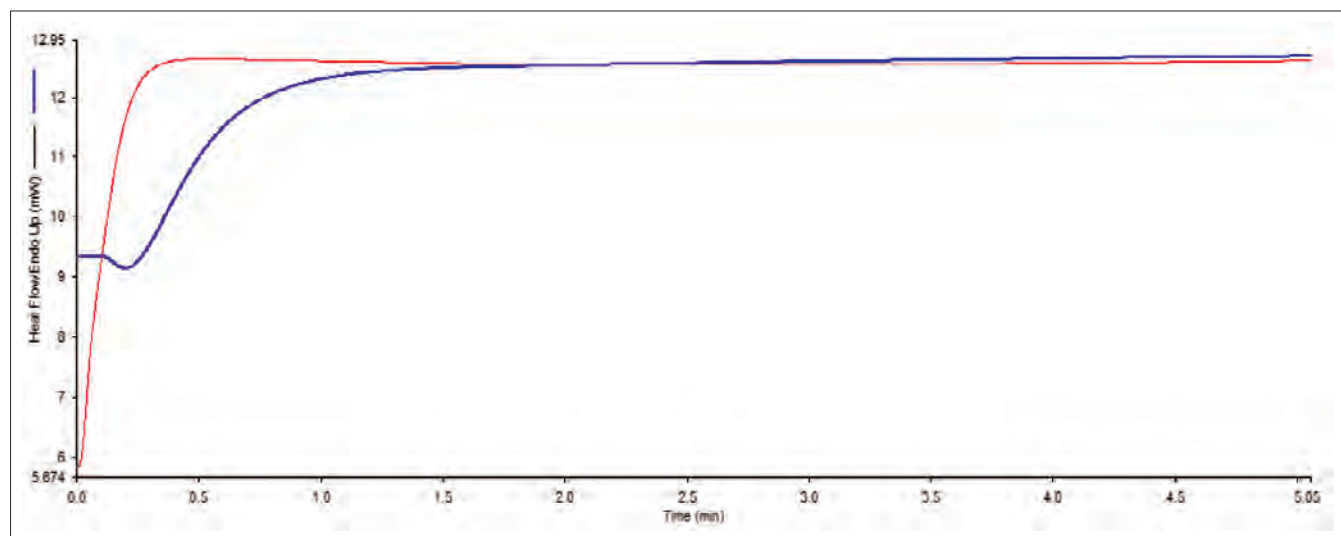


Figure 2. Example of startup transition of double-furnace DSC (red) and single-furnace heat flux DSC (blue) with the same experimental condition.

the startup transition is just 15 °C. So the 40 °C temperature range below the expected transition is already enough for this experiment. This fast response is not achievable with a heat flux DSC because of its bigger, heavier furnace. As illustrated in Figure 2, the single-furnace heat flux DSC has a much longer startup transition than the double-furnace power compensation DSC. In the case of HDPE experiment, if the startup transition for heat flux DSC takes 1 min, then the experiment will have to start at least 100 °C below the expected glass transition at a heating rate of 100 °C/min. That means that the experiment needs to be started at as low as -211 °C which is not achievable on liquid nitrogen cooling accessory.

## Summary

Since the ordinate axis in DSC data is expressed in units of power, or energy per unit time, the fast scanning rate increases the signal and sensitivity of a DSC measurement. HyperDSC, which employs heating rates of approximately an order of magnitude faster than traditional DSC, makes it possible to detect some challenging weak glass transitions, such as that of HDPE. The very quick response of the double-furnace power compensation DSC also makes the measurement feasible with the liquid nitrogen cooling accessory.

## Author

**Christoph Schick**  
University of Rostock  
Inst. of Physics  
Universitätsplatz 3, 18051  
Rostock, Germany

## Study Rigid Amorphous Fraction in Polymer Nano-Composites by StepScan and HyperDSC

### Introduction

It is known that there is a rigid amorphous fraction (RAF) in semicrystalline polymers. The RAF exists at the interface of crystal and amorphous phase as a result of the immobilization of a polymer chain due to the crystal. There is debate on whether the crystal melts first and then RAF devitrifies or the RAF devitrifies before the crystal melts. It can not be answered easily because these two things often happen in the same temperature range. Also, the RAF fraction sometimes exists at the surface of silica nanoparticles in the polymer silica nanocomposites material. However, unlike semi-crystalline polymers, the silica nanoparticle does not undergo any transition at the temperature when RAF devitrifies. So polymer silica nanocomposites offer a good opportunity to study the devitrification of RAF<sup>1</sup>.

Some studies have indicated a second glass transition from RAF in dynamic measurements. To the author's best knowledge, there is no evidence of a second T<sub>g</sub> in polymer nanocomposites from DSC experiments. In order to identify RAF in DSC, absolute heat capacity measurement is very important. A formula has been well established for the determination of RAF in semicrystalline polymers based on accurate heat capacity measurement as described by Wunderlich, see<sup>2</sup> for a review.

Here, heat capacity measurement has been performed in order to detect a possible second T<sub>g</sub> on nanocomposites of polymethyl methacrylate (PMMA) with silicon oxide nanoparticles of different shape. StepScan™ DSC was used for determination of precise heat capacity and HyperDSC® to prevent degradation and identify devitrification of the RAF at elevated temperatures.

## Experimental

Precise heat capacity curves were obtained using a PerkinElmer® Diamond DSC. Heat capacity was determined from StepScan, a special variant of temperature modulated DSC<sup>3</sup>. Measurements were performed using samples of about 20 mg, 3 K steps at heating rate 6 K/min and isotherms of about 1 minute. The temperature range, if not otherwise indicated, was 30 to 170 °C. The instrument was calibrated as recommended by GEFTA using indium and zinc at zero heating rate for temperature and sapphire for heat capacity. Due to the low underlying heating rate, 3 K/min, deviations from the zero rate calibration were less than 0.2 K and not further considered. Uncertainty of heat capacity was about 2%. HyperDSC measurement was performed at 400 K/min in order to prevent the degradation of polymer up to about 360 °C.

## Result

A sketch of the polymer silica nanocomposite material is presented in Figure 1. Three phases are present including silica nanoparticles, mobile amorphous polymer phase and rigid amorphous phase at the particle interface.

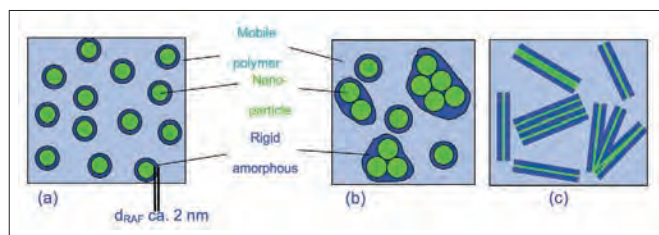


Figure 1. Sketch of spherical (a), (b) and layered (c) nanoparticles covered by a layer of immobilized polymer (RAF). Total degglomeration of the particles is assumed in (a); a more realistic situation is shown in (b) and (c).

For semicrystalline polymers it is well known that the observed step in heat capacity,  $\Delta C_p$ , at the glass transition is often less than expected from crystallinity. Wunderlich et al. therefore introduced the concept of a rigid amorphous fraction (RAF):

$$RAF = 1 - \text{crystallinity} - \Delta C_p / \Delta C_{p \text{ pure}} \quad \text{eq. (1)}$$

where  $\Delta C_p$  and  $\Delta C_{p \text{ pure}}$  are the heat capacity increments at the glass transition for the semicrystalline and the amorphous polymer, respectively. The ratio of both step heights represents the fraction of the polymer contributing to the glass transition, which is called mobile amorphous fraction (MAF).

For polymer nanocomposites sometimes a reduced step height (relaxation strength),  $\Delta C_p$ , at glass transition is observed too. Similarly an immobilized or rigid amorphous fraction can be determined from heat capacity according eq. 1 replacing the crystalline by the nanoparticle fraction.

$$RAF = 1 - \text{filler content} - \Delta C_p / \Delta C_{p \text{ pure}} \quad \text{eq. (2)}$$

In order to apply eq. 2 precise heat capacity data in the temperature range of the glass transition of the polymer nanocomposite are needed. In Figure 2 the measured specific heat capacities for the PMMA based nanocomposites are shown. The curves were calculated in respect to the sample mass (polymer + nano particles). As for semicrystalline polymers a slight increase in glass transition temperature was observed for all nanocomposites after carefully drying at reduced pressure. The glass transition temperature of the nanocomposites was determined as the half step temperature from the StepScan DSC measurements. The values are slightly different compared to scan measurements at 10 K/min because of the different time scale of the experiment.

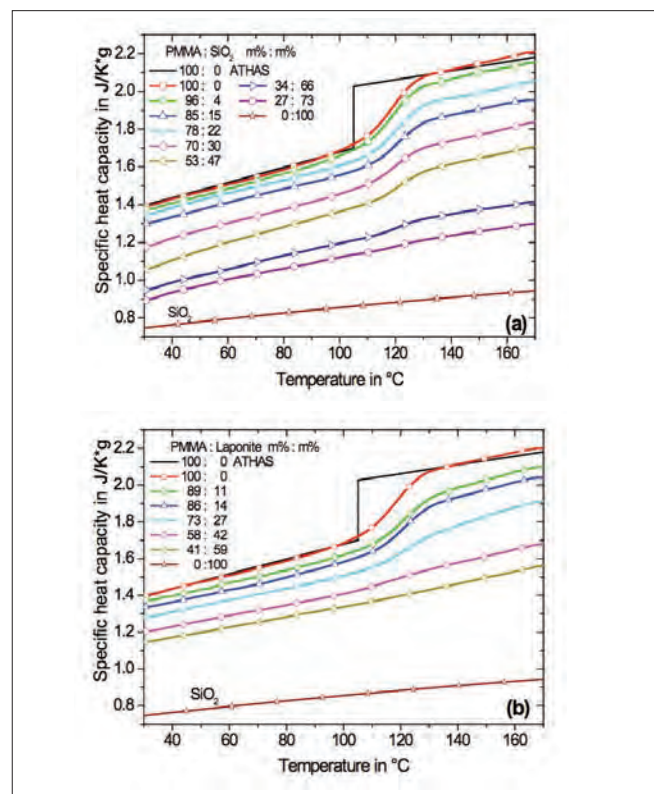


Figure 2. Specific heat capacity of nanocomposites in respect to sample mass. (a) – PMMA with spherical SiO<sub>2</sub> nanoparticles, (b) – PMMA with Laponite RD™. Specific heat capacity for SiO<sub>2</sub> is shown too. The black lines represent reference data for PMMA from ATHAS<sup>4</sup>. Diamond DSC, StepScan mode.

Next, the amount of RAF in the PMMA nanocomposites was quantified applying eq. 2. The step in heat capacity at the glass transition for the different samples was determined as usual at T<sub>g</sub> and normalized by the step in heat capacity for the pure polymer. The results for the PMMA and PS nanocomposites are shown in Figure 3.

According eq. 2 the diagonal in Figure 3 represents the case when no RAF is present. In other words, a two phase system (filler + polymer) which is expected if there is no interfacial immobilization. The data for the PS nanocomposite are close to this line. For the PMMA nanocomposites, the decrease of the

normalized relaxation strength is much steeper than the diagonal. From the normalized relaxation strength the different fractions according eq. 2 can be obtained. The upper arrow at 27 m% filler corresponds to the filler fraction. The lowest indicates the mobile amorphous fraction (MAF) contributing to the calorimetric relaxation strength at glass transition. The difference between the measured values and the diagonal (middle arrow) represents the immobilized (rigid) fraction (RAF) which can be calculated according eq. 2.

Straight lines in Figure 3 correspond to a constant ratio between RAF and filler fraction. In other words, it is assumed in ideal cases that each filler particle is covered by the same amount of RAF (all according mass). This assumption is not well justified by the data of Figure 3. The mass percentage of the RAF normalized by the filler content is shown in the inset as a function of the filler mass fraction. If all nanoparticles were covered by the same immobilized layer one would expect to find a constant ratio between the RAF and the filler content. The slight decrease of the ratio indicates a decrease of the RAF per nanoparticle with increasing filler concentration. This is most probably due to agglomeration of the particles as indicated schematically in the inset. Then the effective surface is no longer proportional to filler content and the points in Figure 3 should follow a line parallel to the diagonal. For the highest filler fractions this seems to be the case.

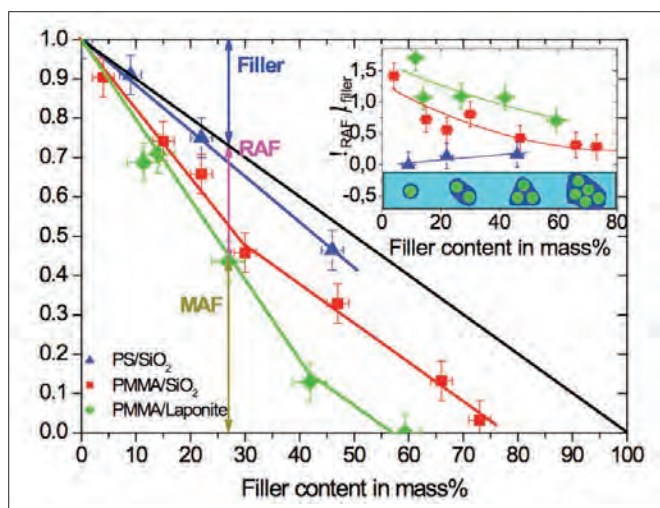


Figure 3. Calorimetric relaxation strength as a function of nanofiller content. The vertical double arrow indicates the amount of RAF for PMMA at 27 m% Laponite RD™ filler. Symbols:  $\Delta$  – PS with spherical SiO<sub>2</sub> nanoparticles;  $\square$  – PMMA with spherical SiO<sub>2</sub> nanoparticles;  $\diamond$  – PMMA with Laponite RD™ clay nanoparticles. The inset shows the percentage of the RAF versus filler content, see text.

In order to check the behavior of the RAF layer and to detect a possible second glass transition we performed heat capacity measurements up to the degradation of the polymer. StepScan DSC was used first to obtain precise heat capacity data up to the beginning of degradation. Measurements were performed up to degradation temperature but because of the

isotherm after each 3 K temperature step, heat capacity could be obtained until the heat flow during the isotherm was not stable anymore. RAF devitrification is expected to appear as a second step in heat capacity towards liquid heat capacity. But there is no step like or gradual transition observed up to 250 °C where the polymer starts to degrade at slow heating.

Influence of degradation on the heat capacity determination can be reduced by using high heating rates. To shift the beginning of degradation to higher temperatures, HyperDSC<sup>5</sup> measurements at 400 K/min heating rate were performed. Also, the fast scanning rate increases the sensitivity of the measurement. So if there was a second glass transition due to the RAF, it would be more easily detected by fast scanning experiments.

At 400 K/min heating rate, the polymer in the nanocomposite does not degrade up to about 360 °C. But there is again no second glass transition visible below 360 °C (Figure 4). This means that the interaction between the polymer matrix and the nanoparticles is so strong that heating even up to such high temperatures is not enough to remove the anchors and to allow relaxation and devitrification of the RAF.

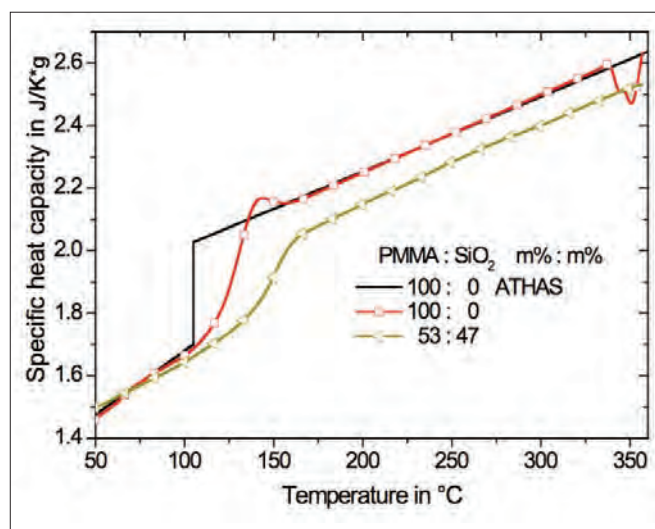


Figure 4. HyperDSC measurements at 400 K/min heating rate for pure PMMA and the nanocomposite filled with 47 m% spherical SiO<sub>2</sub> nanoparticles. Sample mass 0.5 mg. The black lines represent reference data for PMMA from ATHAS<sup>4</sup>.

Interaction between PMMA and SiO<sub>2</sub> at the interface of the nanoparticles is expected to be weaker than a covalent bond, which is present in polymer chains leaving the crystal and proceeding in the amorphous region between the lamellae. If the non covalent bond between the inorganic nanoparticle and the PMMA does not allow devitrification before degradation of the polymer to occur it is very unlikely that in semicrystalline polymers the RAF devitrifies as long as the polymer chains are covalently anchored to the rigid polymer crystals. Most likely, the polymer crystals must melt or gain mobility in another way before the RAF can relax and devitrify.

## Conclusion

StepScan method was used to determine the heat capacity at the glass transition of the polymer accurately. Based on that, the existence of an immobilized fraction in PMMA SiO<sub>2</sub> nanocomposites was demonstrated. It was found that the interaction between the SiO<sub>2</sub> nanoparticles and the PMMA is so strong that no devitrification occurs before degradation of the polymer. The nonexistence of a second glass transition was further confirmed by HyperDSC.

The results obtained for the polymer nanocomposites support the view that the reason for the restricted mobility must disappear before the RAF can devitrify. For semicrystalline polymers this means that rigid crystals must melt before the RAF can relax. Only for semicrystalline polymers with significant chain mobility inside the crystals, may RAF devitrify before melting.

1. A. Sargsyan, A. Tonoyan, S. Davtyan, C. Schick, The amount of immobilized polymer in PMMA SiO<sub>2</sub> nanocomposites determined from calorimetric data, *Eur. Polym. J.* 43 (2007) 3113-3127.
2. B. Wunderlich, Reversible crystallization and the rigid-amorphous phase in semicrystalline macromolecules, *Progr. Polym. Sci.* 28(3) (2003) 383-450.
3. C. Schick, Temperature modulated differential scanning calorimetry (TMDSC) – Basics and applications to polymers, in *Handbook of Thermal Analysis and Calorimetry*, Vol. 3, series editor: P. K. Gallagher, Elsevier, Amsterdam, New York, Tokyo, 2002.
4. B. Wunderlich, The athas database on heat capacities of polymers see on WWW URL: <http://athas.prz.edu.pl>, *Pure Appl. Chem.* 67(6) (1995) 1019-1026.
5. M.F.J. Pijpers, V.B.F. Mathot, B. Goderis, R. Scherrenberg, E. van der Vegte, High-speed calorimetry for the analysis of kinetics of vitrification, crystallization and melting of macromolecule, *Macromolecules* 35(9) (2002) 3601-3613.

Thermogravimetric Analysis – GC  
Mass Spectrometry

## The Analysis of PVC with Different Phthalate Content by TG-MS and TG-GC/MS

### Introduction

The combination of thermogravimetric analyzers (TGA) with mass spectrometers (MS) to analyze the gases evolved during a TGA analysis is a fairly well-known technique. In cases of complex samples, TG-MS often results in data in which it is nearly impossible to differentiate gases that evolve simultaneously.

Combining TGA with gas chromatography mass spectrometry (GC/MS) allows for a more-complete characterization of the material under analysis and precisely determines the products from the TGA. This application will demonstrate the relative advantages of TG-MS and TG-GC/MS – a summary of the strengths of each technique is presented in Table 1 (Page 2).

**Table 1. Relative Advantages of TG-MS and TG-GC/MS.**

TG-MS	TG-GC/MS
Real-time analysis	Sequential analysis
No resolution capabilities	Resolves overlapping events
Limits to library effectiveness	Resolution improves GC libraries effectiveness
Oxygen sensitive	Oxygen sensitive
	Can use alternate/multiple detectors
Simple	More complicated

## Experimental

This analysis was performed on a PerkinElmer® Pyris 1 TGA\* 8000 using alumina pans and the standard furnace. The instrument was calibrated with nickel and iron and all samples were run under helium purge. Heating rates varied from 5 to 40 °C/min, depending on the sample under test. The furnace was burned off between runs in air. Samples were approximately 10-15 mg. Data analysis was performed using Pyris Software.

During the TG-GC/MS analysis, the PerkinElmer Clarus® 680 C GC/MS was used. In the TG-MS work, a 0.1 mm I.D. deactivated fused-silica transfer line was connected directly to the MS. The transfer line was heated to 210 °C. In the TG-GC/MS work, a 0.32 mm I.D. deactivated fused-silica transfer line was plumbed into the GC injector port where it was connected to the Elite™-1ms capillary GC column. In both cases, data analysis was performed using TurboMass™ GC/MS Software.

## Results

In this example, polyvinylchloride (PVC) formulated with two different types of phthalates – disiononyl phthalate (DINP) which is regulated and another formulation of non-regulated phthalates are analyzed to determine if a difference can be seen and correlated to the phthalate type.

Figure 1 is the thermogram from the analysis of the two different PVC samples. The purple line in the thermogram with a weight loss of 50.99% in the first event corresponds to the PVC sample with DINP. The green line with the weight loss of 64.82% corresponds to the PVC with the non-regulated mixture of phthalates.

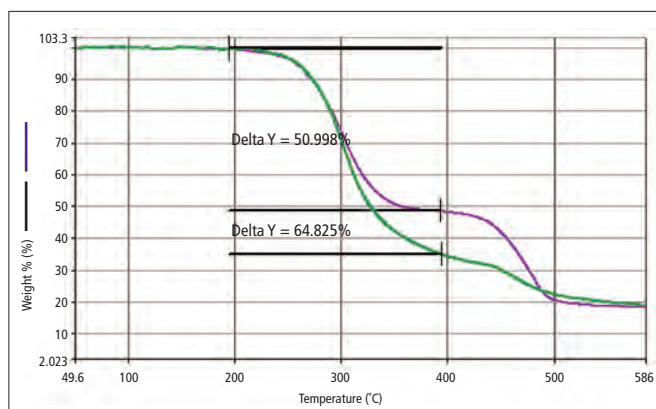


Figure 1. TGA percent-weight-loss curve generated from the analysis of two PVC samples: one with DINP (purple), a regulated phthalate, and a weight loss (delta y) of 50.998%; and a second with a mixture of non-regulated phthalates (green) and a weight loss (delta y) of 64.825%.

The weight-loss curve from TGA shows a clear difference between the two materials. This may be a result of either different additives or the amount of additive needed to achieve specific physical properties in the PVC sheeting.

The evolved gas from each sample was analyzed by both MS and GC/MS to determine if either technique would confirm the presence or absence of regulated vs. non-regulated phthalates. Figure 2 demonstrates the MS data obtained from the analysis of each sample.

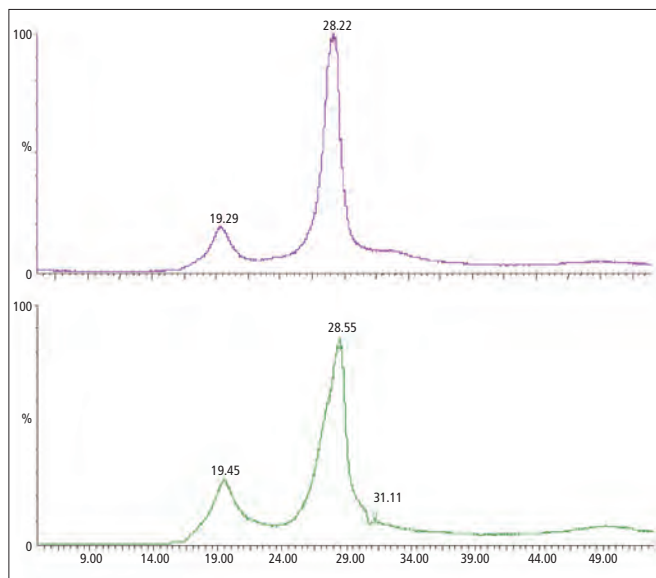


Figure 2. The MS analysis of the evolved gas generated during the TGA analysis of PVC materials with DINP (purple - top) and a mixture of non-regulated phthalates (green - bottom).

\*Pyris 1 TGA instrument is superseded. It has been replaced by TGA 8000

In Figure 2, it is difficult to find a difference between each material. The gas evolved in the TGA showed little difference in the MS. Each of the two major weight-loss events generated a mixture of gases generating many ion fragments simultaneously. TG-MS is very useful when the evolved gases are relatively simple; here resolution of the evolved gas is needed to identify each component.

The TGA analysis was performed again; however, a sample of the first weight loss was collected and introduced into a GC column. This will allow some resolution of evolved gases and better identification of specific components. Figure 3 demonstrates the chromatogram of the analysis of the gas evolved during the first weight loss of the TGA. It can be seen that the gas evolved is indeed very complex with a chromatogram full of different components – many unresolved.

In this case, differences can be noted in the evolved gas of each TGA. Most significant were in the peaks around

30 minutes. These peaks contained a strong response at  $m/z$  149 – an ion associated with many phthalates. Further work would need to be done to determine if qualitative and/or quantitative data is provided by the analytical approach used here, but differences are much more significant when TG-GC/MS is employed over TG-MS.

## Conclusions

TGA analysis allows quantification of the weight loss of a material at specific temperatures. MS increases the power of the technique by providing the ability to identify the species evolved during thermal analysis; however, if a complex gas is evolved during a single event, the MS data is difficult to interpret. The use of TG-GC/MS adds chromatographic separation of co-evolved gases, enabling identification of individual components, making data interpretation easier than TG-MS.

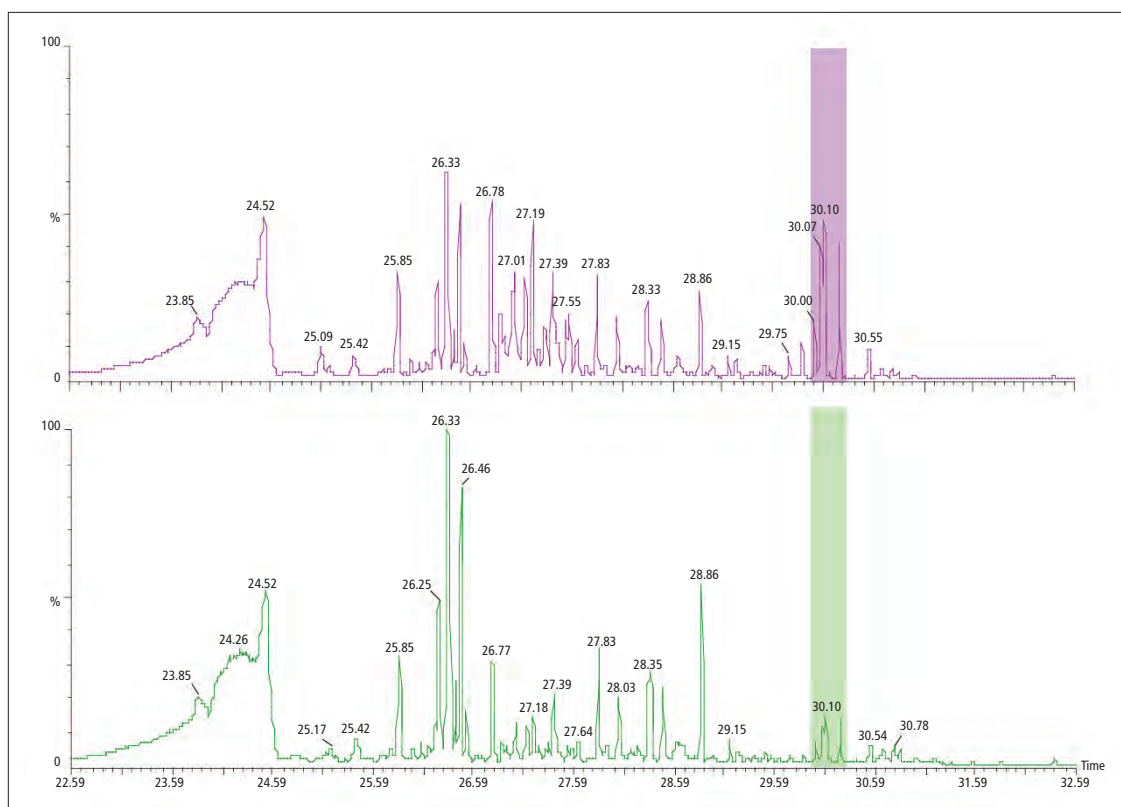


Figure 3. The GC/MS data collected during the TGA analysis of PVC with DINP (purple - top) and with a mixture of non-regulated phthalates (green - bottom). Differences are noted in peaks with tentative identification as phthalates around 30 minutes.



## Better Characterization of Polymer Blends Using StepScan DSC

### Introduction

Polymer blends are widely utilized for a variety of applications as the particular thermo-physical properties of the individual components comprising the blend result in better overall properties. This is particularly the case of polymer blends used in the automotive industry where impact resistance, toughness, stiffness and paintability all become important issues. The blending of polymers yields a better overall product with the desired end use properties and characteristics. Polymer blends are also used for container applications where there is a need for good impact resistance coupled with long term stability, barrier resistance and opacity.

With polymer blends, it can become difficult to characterize their physical properties, especially the glass transition event, as the components can interfere with one another or mask the other's presence. Additionally, the processing of the blends, via extrusion or injection molding, can lead to the occurrence of frozen-in stresses, which can make the interpretation of DSC results difficult. A large enthalpic relaxation peak or other interfering, irreversible thermal event may accompany the Tg's of the different polymer phases. All of these factors can make it difficult to observe the unique glass transition events of the polymer components in a blend.

One means of greatly improving data interpretation from DSC is using StepScan™ DSC from PerkinElmer.

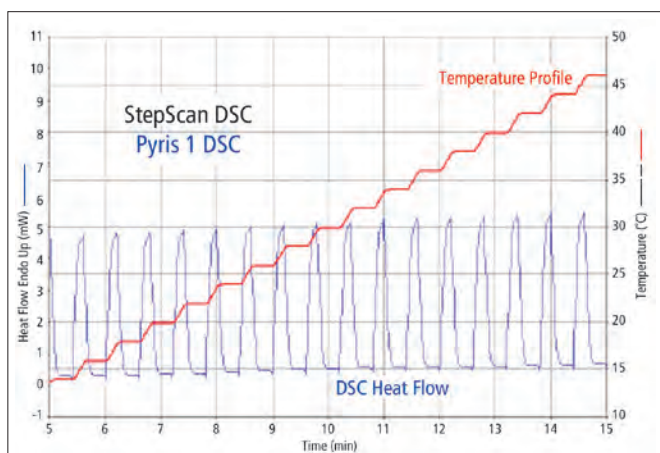


Figure 1. StepScan DSC approach using time-temperature profile.

## StepScan DSC

StepScan DSC is software for the enhanced characterization of the thermal properties of materials. The technique permits the separation of DSC results into thermodynamic (reversible) and kinetic (irreversible) components for better interpretation. The method is straightforward and utilizes the traditional approach for measuring the heat capacity,  $C_p$ , for the highest possible reliability of results without interfering experimental problems. The StepScan DSC approach is only possible with the design of the power compensated Pyris™ 1 DSC, with its very low mass sample and reference furnaces and rapid response time.

Figure 1 shows the StepScan DSC approach with the application of a repetitive sequence of short heating – isothermal hold segments.

With the application of heating (10 °C/min) over small temperature increments (1.5 or 2 °C), and by holding for a short time interval (e.g., 30 seconds), the heat capacity that is yielded reflects the reversible aspects of the sample. Kinetic or irreversible effects (on the time scale of the experiment) are eliminated in the **Thermodynamic  $C_p$**  data set, which reflects ‘fast’ or reversible phenomenon, such as the sample’s heat capacity (molecular vibrations) or  $T_g$  (molecular rotations). For example, if a sample has a  $T_g$ , with an overlapping enthalpic relaxation, moisture loss or crystallization event, the Thermodynamic  $C_p$  signal will show the classic, stepwise change in the heat capacity. This then makes it simple and straightforward to analyze and interpret. The StepScan DSC approach also provides the kinetic or **IsoK Baseline** data set, which is reflective of the irreversible or ‘slow’ processes taking place during the experiment. The enthalpic relaxation event, which can occur on physically aged samples at  $T_g$ , will show up in the IsoK Baseline data set.

Because the StepScan DSC approach requires rapid DSC response times, the technique is only feasible with the power compensated DSC, which allows for fast heating and thermal equilibration. The application of the StepScan approach to a large mass furnace, heat flux DSC instrument would be difficult or technically unfeasible due to the inability to rapidly respond and equilibrate. In addition, the StepScan DSC experiments are generally faster (by a three-fold improvement) as compared to equivalent TMDSC results generated on a slower responding, heat flux DSC device.

## Polymer Blend Results by Standard DSC

Displayed in Figure 2 are the standard DSC results generated on a polymer tri-blend sample consisting of ABS, polycarbonate and amorphous PET. The sample was heated at a temperature rate of 10 °C/min.

From these results, the blend yields two  $T_g$ ’s: one at 80 °C for the amorphous PET component and one at 115 °C for the SAN (styreneacrylonitrile) component of the ABS polymer. The amorphous PET also yields a cold crystallization transition at 140 °C and the melting event at 255 °C. However, the  $T_g$  of the polycarbonate component, which should be around 155 °C, is not observed. The crystallization peak of the PET obscures the  $T_g$  of the polycarbonate component.

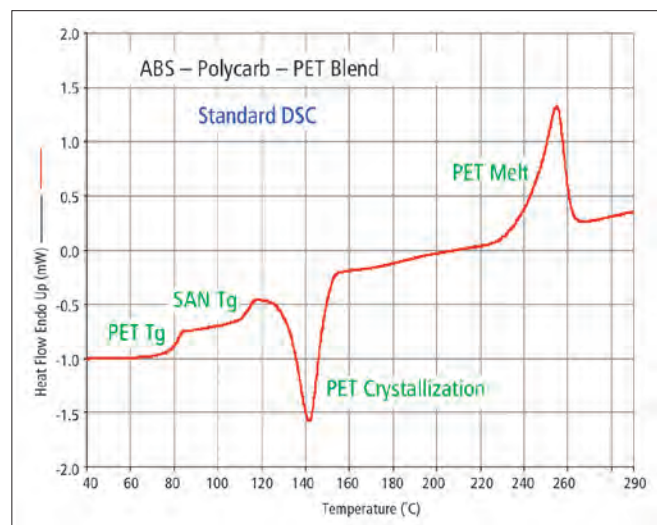


Figure 2. Standard DSC results obtained on polymer tri-blend of ABS, polycarbonate and amorphous PET.

## StepScan DSC Results on Polymer Blend

The polymer tri-blend was analyzed using the StepScan DSC technique. The experimental conditions used are given in the following table.

### Experimental Conditions

Instrument	Pyris 1 DSC with StepScan DSC
Heating rate between steps	10 °C/min
Step isothermal hold time	20 seconds
Temperature increment between steps	2 °C
Initial temperature	0 °C
Final temperature	280 °C
Sample mass	20 mg in standard crimped Al pan
Cooling system	Cryofill liquid nitrogen
Purge gas	Helium

Displayed in Figure 3 are the StepScan DSC results obtained for the polymer blend sample.

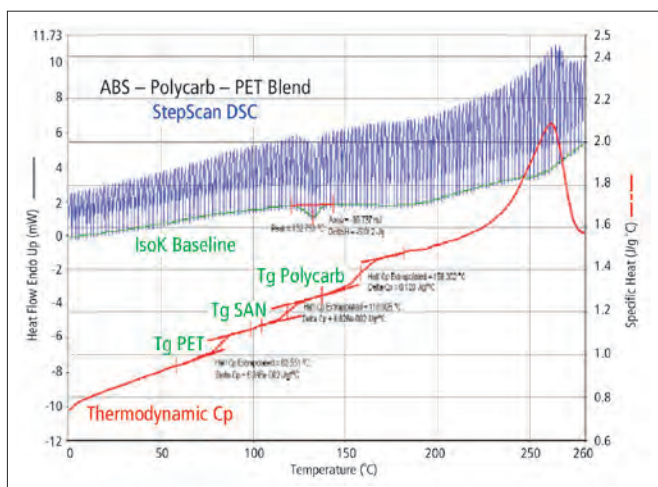


Figure 3. StepScan DSC results on polymer tri-blend.

From the StepScan DSC Thermodynamic Cp results, the polymer blend shows three distinct glass transition events – Tg for the amorphous PET at 82 °C, Tg for the styrene-acrylonitrile (SAN) of ABS at 115 °C, and the Tg of the polycarbonate component at 158 °C. With StepScan DSC, the polycarbonate Tg is separated out from the interfering and irreversible crystallization of the amorphous PET component. The use of the StepScan DSC technique allows for the detection and analysis of the hidden polycarbonate Tg, which provides valuable characterization information on the polymer tri-blend.

### Summary

The high performance Pyris 1 DSC provides outstanding results on materials, such as polymer blends. The use of the StepScan DSC technique yields enhanced characterization information by separating out the reversible and irreversible thermal events. The StepScan DSC approach allows for the observation and quantitative analysis of transitions that might be hidden or obscured. The polycarbonate Tg, masked by the crystallization of the amorphous PET component, was clearly identified and analyzed with the StepScan DSC technique. The high resolution of the Pyris 1 DSC coupled with the StepScan DSC technique yielded all three Tg's of each of the polymer tri-blend components.

## Differential Scanning Calorimetry

**Authors**Bruce Cassel<sup>1</sup>Andrew Salamon<sup>1</sup>E. Sahle-Demessie<sup>2</sup>Amy Zhao<sup>2</sup>Nicholas Gagliardi<sup>3</sup><sup>1</sup> PerkinElmer, Inc.  
Shelton, CT, USA<sup>2</sup> U.S. Environmental Protection Agency  
Cincinnati, OH, USA<sup>3</sup> University of Dayton Research Institute  
Dayton, OH, USA

## Improved HyperDSC Method to Determine Specific Heat Capacity of Nanocomposites and Probe for High-Temperature Devitrification

**Introduction**

There has been tremendous interest in recent years in nanocomposites – using small scale particulate fillers – to improve the properties of thermoplastics and thermosets. For example, the effect of using such small scale filler particles is such as to toughen the plastics, reduce vapor transfer, and improve transparency. One rapid way to quantify the effect of a particular filler formulation is to measure its effect on the change in specific heat ( $C_p$ ) that occurs at the

glass transition ( $T_g$ ). In this analysis, discussed by Christophe Schick,<sup>1</sup> the  $C_p$  of an amorphous nanocomposite can be usefully partitioned between three entities: (1) unaffected amorphous polymer whose properties are the same as that in the pure amorphous polymer, called the mobile amorphous fraction; (2) the  $C_p$  of the filler itself; and (3) the  $C_p$  of the polymer which is immobilized by its attachment to the nanoparticle, the rigid amorphous fraction (RAF). The properties of the composite can be related to the extent of these fractions. The chemical bonding – weak or strong – of the RAF to the nanomaterial filler may be an indicator of the performance of the nanocomposite, and it may be an indicator of how readily it will decompose in the environment. A second  $T_g$  – devitrification of the RAF – would indicate a relatively weak bond of the RAF to the nanomaterial filler.

## Background

Christophe Schick demonstrated the use of the HyperDSC® technique to measure RAF and to look for evidence of devitrification of the RAF in the temperature region between the glass transition temperature ( $T_g$ ) and the rate-suppressed onset of decomposition. He demonstrated how this  $C_p$  data, made accurate by corroborative use of StepScan™ methods, could be compared to the  $C_p$  function of neat polymer to further evaluate the degree of agglomeration of filler in a nanocomposite.<sup>1</sup>

The key relationship in his paper for quantifying the RAF in a composite is:

$$RAF = 1 - \text{Filler Content} - \frac{\Delta C_p}{\Delta C_p \text{ pure}}$$

Where  $\Delta C_p$  and  $\Delta C_p \text{ pure}$  are the changes in specific heat at the glass transition temperature,  $T_g$ , for the composite, and for the unfilled polymer, respectively.

This work suggests an alternative method for determining  $C_p$  that takes advantage of fast heating and cooling rates to obtain quantitative  $C_p$  in the upper temperature region without having to dwell in that high temperature region to establish an upper isothermal.

In the conventional method to measure  $C_p$  (ASTM® E1269), a sample is equilibrated at a low temperature and then heated at some rate to an upper temperature where the temperature is again held constant until there is full equilibration. The problem with the conventional  $C_p$  method – and with modulated temperature methods – is that the sample is likely to degrade when held at high temperatures, and this degradation compromises the accuracy of measurement.

In the method suggested here, the temperature program for the sample (and baseline) is that of heating at a very rapid rate (here 400 °C/min) to the upper temperature, then immediately cooling at the same rapid rate to a temperature sufficiently low with little or no sample decomposition. Figure 1 shows the raw data, including sensor temperature and heat flow.

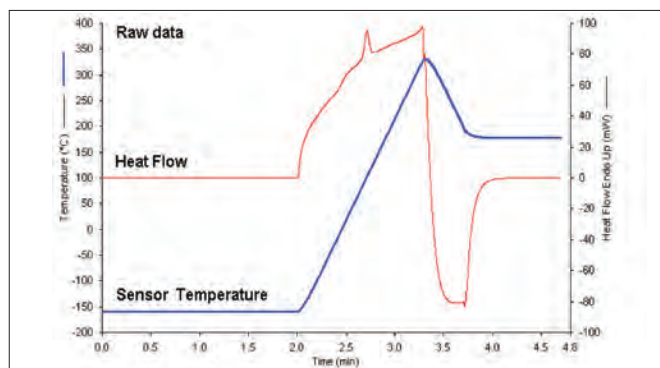


Figure 1. Raw data for thermoplastic polyurethane nanocomposite using the 400 °C/min heat-cool  $C_p$  method – analysis time: 5 minutes.

## Experimental and Data Handling

The instrument employed for this analysis was the PerkinElmer® DSC 8500, a power-controlled, dual-furnace differential scanning calorimeter (DSC) with the ability to scan at rates up to 750 °C/min and achieve rapid equilibration, a requirement when using rapid scan rates. The purge gas was helium. The block heat sink temperature selected was -180 °C, with the cooling provided by the CLN<sub>2</sub> liquid nitrogen cooling accessory. Calibration used the two melting standards indium and lead. Encapsulation was with aluminum HyperDSC pans, which are low mass and provide optimum thermal coupling (Part No. N5203115).

When PerkinElmer Pyris™ software's AutoSlope function is selected in Preferences, all runs are automatically shifted and sloped to zero heat flow using the final heat flow points of the highest and lowest temperature isotherms. To convert to  $C_p$  units, one subtracts the iso-aligned baseline data and then selects Single Curve  $C_p$  from the Calculate/Specific Heat menu. The result is a specific heat data curve as a function of temperature tested that can be plotted, further analyzed, and saved (Figure 2).

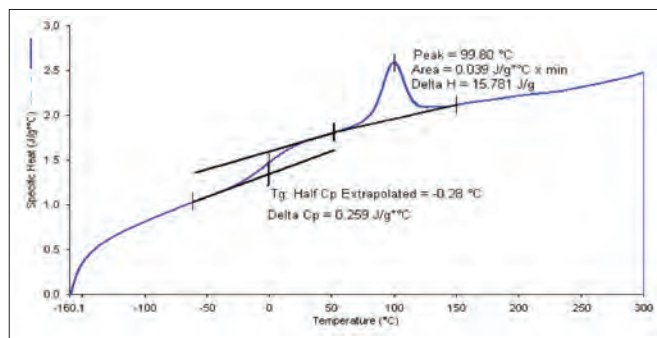


Figure 2. Specific heat capacity data for thermoplastic polyurethane composite using the 400 °C/min heat-cool  $C_p$  method, with  $T_g$  and peak calculations applied.

This method enabled the specific heat to be obtained up to 300 °C without appreciable error from decomposition. The data was delivered to the supplier of the nanocomposites in the form of tables created in Pyris and transferred into a spreadsheet (Figure 3).

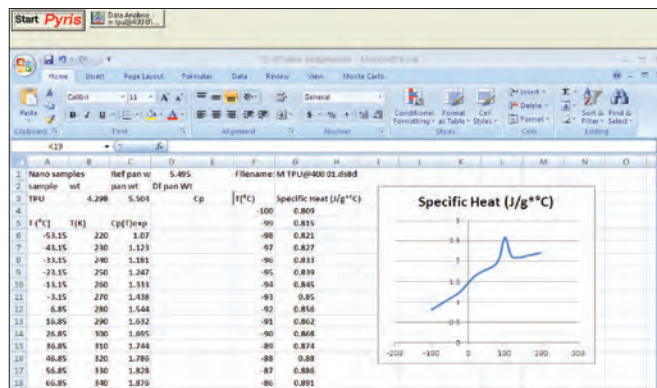


Figure 3. Microsoft® Excel® spreadsheet, for further analysis of  $C_p$  data, after transferring a table from Pyris software.

## Assessing Method Accuracy

The goal of this project was to show generation of sufficiently accurate specific heat capacity data from HyperDSC – that the more time consuming StepScan analysis would not be required. To demonstrate accuracy, the same method that produced the above data was also used to analyze the smaller of the two sizes of sapphire specific heat standard in the PerkinElmer Specific Heat Kit (Part No. 02190136). The  $C_p$  results were then compared with those in the table that was provided with the kit. The 400 °C/min data were in agreement with literature values within 1% from -50 °C to 200 °C, and within 1.5% up to 320 °C. While this accuracy may be somewhat less when running plastics samples because of extraneous effects (e.g., sample inhomogeneity, moisture loss, sample movement, less than optimal thermal coupling), the sapphire test has proven that the new method can be highly accurate with proper sample preparation.

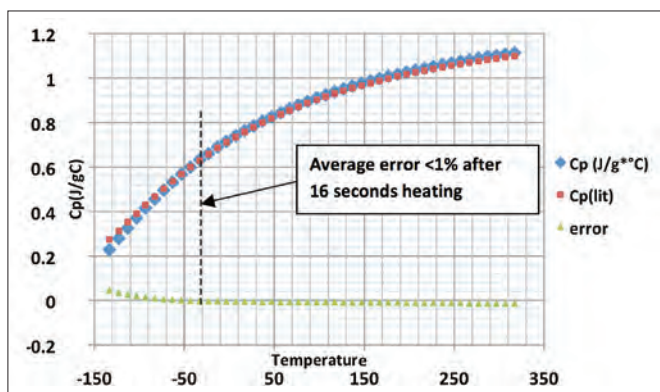


Figure 4. Specific heat capacity of sapphire using the 400 °C/min heat-cool method, showing Pyris data, literature data and error.

## Looking for Evidence of Devitrification

The Schick et al. (2007) investigation was looking for evidence that, at higher temperatures, kinetic energy might free up the rigidly held polymer and reveal a second, but higher and weaker, glass transition attributed to devitrification of the RAF phase. This was the reason for using the HyperDSC technique to obtain access to the high-temperature region as well as specific heat data, while kinetically delaying the onset of decomposition. He did not report any evidence

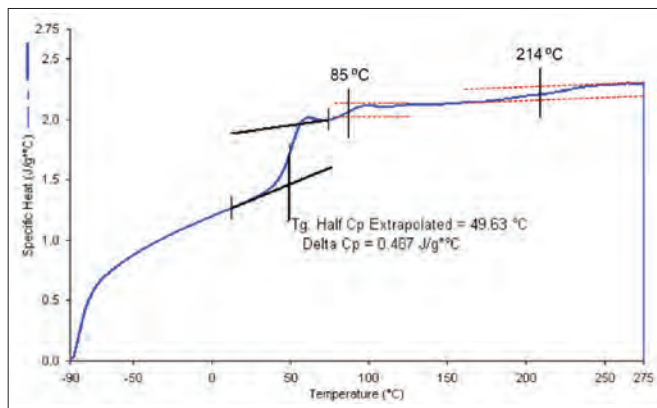


Figure 5. Specific heat capacity of uncured epoxy nanocomposite using the 400 °C/minute heat-cool method, showing possible second  $T_g$ s. One interpretation of this data is that the multiple  $T_g$ s are due to devitrification of RAF. Not all portions of this sample showed this effect. The sample for analysis was visibly inhomogeneous. **Note:** at normal DSC scan rates, or when using a modulated technique, decomposition would show additional thermal effects above 200 °C, which would mask evidence of devitrification.

of this devitrification effect in the formulation (PMMA and  $\text{SiO}_2$ ) he investigated, but we wanted to provide a rapid method of assessing other formulations for this effect. In the (proprietary) nanocomposite samples we evaluated, we observed some evidence of increased  $C_p$  at higher temperatures, but further work would be required – including analyzing the unfilled plastics – to make any definitive statement about devitrification.

## Conclusions

HyperDSC shows promise for elucidating nanocomposites. The use of a rapid heat-cool method, such as demonstrated here, extends the upper temperature range for which accurate specific heat capacity measurements are practical. This should help identify devitrification – loss of nanocomposite bonding – in the amorphous polymer system. This method further extends the utility of power-controlled DSC to investigate metastable states of polymer systems.

## References

1. Sargsyan, A. Tonoyan, S. Davtyan, C. Schick, The amount of immobilized polymer in PMMA  $\text{SiO}_2$  nanocomposites determined from calorimetric data, Eur. Polym. J. 43 (2007) 3113-3127.



## UV/Vis Spectroscopy

**Authors**

Frank Padera

PerkinElmer, Inc.  
Shelton, CT USA

## Measuring Absorptance ( $k$ ) and Refractive Index ( $n$ ) of Thin Films with the PerkinElmer LAMBDA 950/1050 High Performance UV/Vis/NIR Spectrometers

**Introduction**

An optical coating consists of a combination of thin film layers that create interference effects used to enhance transmission or reflection properties for an optical system. How well an optical coating performs is dependent upon the number of factors, including the number of layers, the thickness of each layer and the differences in refractive index at the layer

interfaces. The transmission properties of light are predicted by wave theory. One outcome of the wave properties of light is that waves exhibit interference effects. Light waves that are in phase with each other undergo constructive interference, and their amplitudes are additive. Light waves exactly out of phase with each other (by  $180^\circ$ ) undergo destructive interference, and their amplitudes cancel. It is through the principle of optical interference that thin film coatings control the reflection and transmission of light.

When designing a thin film, though the wavelength of light and angle of incidence are usually specified, the index of refraction and thickness of layers can be varied to optimize performance. As refraction and thickness are adjusted these will have an effect on the path length of the light rays within the coating which, in turn, will alter the phase values of the propagated light. As light travels through an optical component, reflections will occur at the two interfaces of index change on either side of the coating. In order to minimize reflection, ideally there should be a 180° phase shift between these two reflected portions when they recombine at the first interface. This phase difference correlates to a  $\lambda/2$  shift of the sinusoid wave, which is best achieved by adjusting the optical thickness of the layer to  $\lambda/4$ . Figure 1 shows an illustration of this concept.

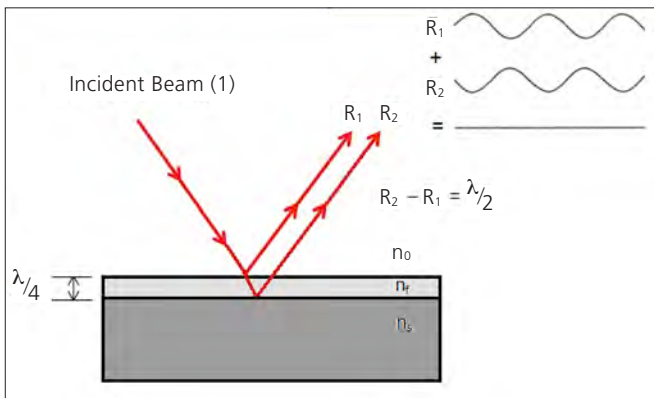


Figure 1. For an air ( $n_0$ ) / film ( $n_f$ ) interface, illustrated is the 180° phase shift between the two reflected beams ( $R_1$ ,  $R_2$ ), resulting in destructive interference of the reflected beams.

Index of refraction influences both optical path length (and phase), but also the reflection properties at each interface. The reflection is defined through Fresnel's Equation<sup>2</sup>, which provides the amount of reflection that will occur from the refractive index change at an interface at normal incidence:

$$R = \left( \frac{n_p - n_m}{n_p + n_m} \right)^2$$

The intensity of reflected light is not only a function of the ratio of the refractive index of the two materials, but also the angle of incidence and polarization of the incident light. If the incident angle of the light is altered, the internal angles and optical path lengths within each layer will be affected, which also will influence the amount of phase change in the reflected beams. It is convenient to describe incident radiation as the superposition of two plane-polarized beams, one with its electric field parallel to the plane of incidence (p-polarized) and the other with its electric field perpendicular to the plane of incidence (s-polarized). When a non-normal incidence is used, s-polarized and p-polarized light will reflect differently

at each interface which will cause different optical performances at the two polarizations.

Determining the refractive index,  $n$ , and the absorptance (absorption coefficient),  $k$ , of a coating are two important parameters in thin film research. In real materials, the polarization does not respond instantaneously to an applied field. This causes dielectric loss, which can be expressed by the complex index of refraction that can be defined<sup>2</sup>:

$$\mathbf{n} = n + ik$$

where:

$n$  = the complex refractive index

$i$  = the square root of -1

$n$  = the refractive index

$k$  = the absorption index

Here,  $k$  indicates the amount of absorption loss when the electromagnetic wave propagates through the material. The term  $k$  is often called the extinction coefficient in physics. Both  $n$  and  $k$  are dependent on the wavelength. In most circumstances  $k > 0$  (light is absorbed).

In this paper we will show how the absorptance, refractive index, and film thickness of thin films can be calculated from the spectral data.

## Experimental

To determine  $n$  and  $k$  a number of optical measurements are needed which require accessories to be added to the UV/Vis spectrometer. To calculate the absorption coefficient (re: absorptance, extinction) of a thin film the transmission and absolute reflectance spectra of the material needs to be acquired (it follows that the material cannot be opaque). Using a high performance LAMBDA spectrometer (LAMBDA 650/750/850/950/1050) an integrating sphere accessory, ideally the PE-Labsphere 150 mm Spectralon coated sphere, or the Universal Reflectance Accessory (URA) are ideal accessories for this determination. Though a smaller sphere may be used for these measurements, the accuracy level will decrease as the size of the sphere gets smaller. When the absorption gets low, smaller spheres may not have the inherent accuracy to be used. A number of other accessories can be used where absolute specular reflectance can be measured, accompanied by the transmission, such as the VN 8 degree absolute specular reflectance accessory.

Discussed in the next section are the procedures and some example results for calculating absorptance using a LAMBDA 1050 UV/Vis/NIR spectrometer fitted with a Labsphere Spectralon 150 mm InGaAs integrating sphere. Absorptance is light that is not transmitted or reflected by a material, but is absorbed. The equation  $T + R + A = 1$  describes the theory, where  $T$ =transmittance,  $R$ =reflectance, and  $A$ =absorptance.

## Measuring the Absorptance (k) of Materials

The procedure presented here will describe the accurate measurement of absorptance using the 150 mm Integrating Sphere accessory. A picture of the 150 mm integrating sphere (L6020204) installed in a LAMBDA 950 is shown in Figure 2, with a top down view of the schematic of the sphere beneath the picture. This accessory occupies the second sample compartment area (right side in picture) of the instrument, leaving the primary sample compartment free to accept liquid samples and other accessories.

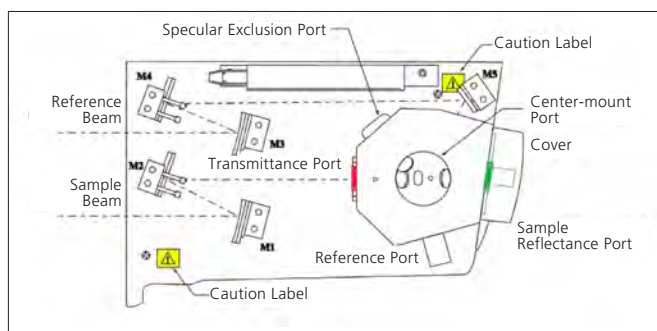


Figure 2. Picture of the 150 mm integrating sphere installed in a LAMBDA 950 with a top down view of the diagram of the sphere below. The red marked area is where transmission of the material is done, and the green area the reflectance of the material.

In addition to the integrating sphere accessory, this procedure requires a calibrated standard, either a calibrated Spectralon white reference plate, or a calibrated mirror. When measuring absorptance using the integrating sphere it needs to be noted that samples need to be clear (haze will cause problems with the calculation) and the coatings need to be applied to fairly thin substrates (i.e., glass slides are ideal). Coatings applied to thick substrates run the risk of some of the reflected light being clipped on the port on the return of the reflected light into the sphere.

### A. Measuring Transmission using the Integrating Sphere

The %T measurements have little considerations as long as the sample is large enough to cover the transmittance port of the sphere, and sample and reference beams are aligned properly. The sphere should be set for Total %R (Specular Exclusion Port plug in place). For sample sizes that are smaller than the instrument beam the Small Spot Kit Accessory (L6020211) might be necessary. In transmission the Correction settings in the method should be the same as shown in Figure 3, making sure the 0%T baseline option is checked.

### B. Measuring Reflectance with the Integrating Sphere

Reflectance measurements have a number of considerations. The reflectance needs to be measured in Absolute %R, which means the spectra are corrected for the reflectance of the reference material (**Light Spectral Reference**), as well as the dark level (0%R) of the sphere (**Dark Spectral Reference**). Though correction of spectra with calibration reference data can be done off-line in Microsoft® Excel®, UVWinLab™ V6 has the capability to define the calibration file in the method so that the reflectance spectral correction is performed automatically as data is being acquired in real-time (note: no calibration file is required for transmission data collection).

There are two common approaches for generating Absolute %R with an integrating sphere.

1. Use a **calibrated mirror**, either a primary (i.e., NIST, OMT) or secondary standard (PE # N1010504). The latter

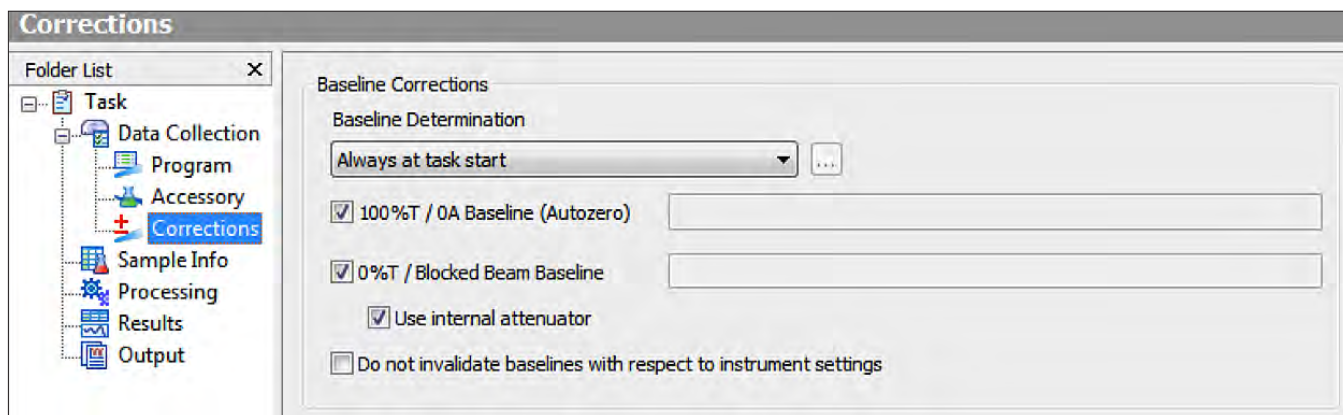


Figure 3. Corrections settings for a transmission scan with the sphere accessory.

is calibrated against a primary NIST traceable mirror, however the error tolerances are larger than with a primary mirror.

2. Use a **Labsphere Calibrated Spectralon Standard** (i.e., PELA 9058) having a specific calibration sheet for that standard.

Either which standard is used, the reflectance calibration data that comes with the standard needs to be converted to an UVWinlab V6 compatible file so it can be used in the method to automatically correct the spectral data. The procedure to do this is outlined in the application note **“Procedure for Creating %RC Correction Files in UVWinlab V6.docx”** (to obtain this paper contact your local PerkinElmer UV/Vis Product Specialist). Once the calibration data has been entered into an ASC file, this file can be copied to any location on the hard drive on to the computer operating the LAMBDA spectrometer, or alternatively it can be placed into the folder *“C:\Program Files\PerkinElmer\UVWinlab\6.0\Data\Corrections Data”* where the file will be registered automatically for method access.

When measuring reflectance for absorption determination, because the samples on the reflectance port also transmit light, it is important to correct for the dark level of the sphere. Without a sample in place on the reflectance port, due to minute scatter of the light beam traversing the length of the sphere and the inherent back scatter of light off the sphere cover, it is normal to see a sphere dark level in the range of a few tenths of a percent to nearly a percent above zero.

There are two ways of correcting for the sphere dark level for reflection of transmitting samples:

1. Acquire a new dark reference correction every time the method is run (the correction settings for this option are shown in Figure 4).
2. Perform dark reference beam correction from a stored file. The dark reference is measured and saved as a file so it can be assigned as the **Dark Spectral Reference** under the Correction menu (the correction settings for this option are shown in Figure 5).

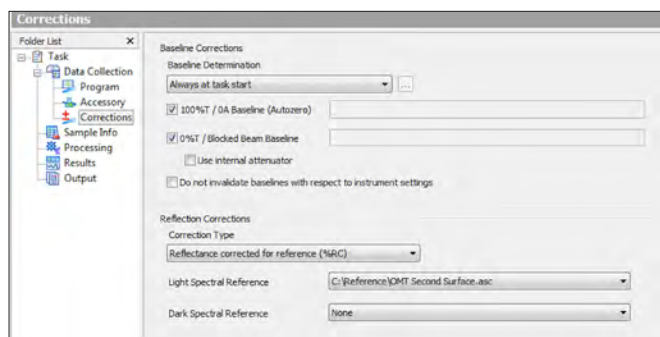


Figure 4. Reflectance corrections settings with the integrating sphere, where a dark reference correction is acquired before sample analysis. In this example, the “Light Spectral Reference” has been defined with an OMT primary

The setup for the option (1) requires that in the Corrections menu of the method, the options for both the **100%T/0A Baseline and the 0%T/Blocked Beam Baseline** are checked, but the option **Use internal attenuator** is left unchecked, as shown in Figure 4. Using this setup, when the correction prompt is given **“Block the beam and press OK to perform a 0%T/Blocked Beam correction”** the user will not actually block the beam, but rather will remove the Spectralon white plate from the reflectance port and replace the sphere cover.

Though it is fine to acquire the dark reference of the sphere in this manner each time 100% and 0% corrections are taken, it may be more convenient to acquire the dark current scan only once and then save this file so it can be assigned as the Dark Spectral Reference file in the Corrections menu. To acquire this file, make sure the white sample reflectance reference plate is removed, there is no sample in the beam, and replace the sphere cover. Start a scan over the widest wavelength range that will be used (i.e., 2500 to 250 nm is typical). When completed, right-click on the filename and select Save as ASC to any location on the computer, or save to *“C:\Program Files\PerkinElmer\UVWinlab\6.0\Data\Corrections Data”*, to add this correction file to the list of files in the method view.

To assign the calibrated mirror or calibrated Spectralon ASC files, and the dark current sphere file, to the UVWinlab method, select an ordinate mode of %R, click on the Corrections menu, under the Reflection Corrections section, select the Correction Type **“Reflectance corrected for reference (%RC)”**. Under the **“Light Spectral Reference”** setting, click the down arrow and then **“Select – Import”**. Browse to the location of the calibrated mirror or calibrated Spectralon ASC file, and assign this file to the field. Repeat this for the **“Dark Spectral Reference”** field. Note that when using a Dark Reference File correction, the option for **“Use internal attenuator”** is checked. Saving the method will store these correction file assignments.



Figure 5. Reflectance correction settings where the dark reference correction is being applied from a stored spectral file.

Note that if using a calibrated Spectralon white reference, this plate is used in place of the sample regular Spectralon plate that is included with the sphere, and the regular reference plate is used on the reference port of the sphere.

### C. Example of Determining the Absorptance (k) of a Sample

When both the %T and the %R files have been acquired, the Processing section of the method can be used to calculate the absorptance of the sample. A single equation is required.

$$(100 - \text{Transmittance} - \text{Reflectance}) / 100$$

Shown in Figure 6, are the %T and %R scans of a sample transmission and reflectance spectra of thin film crystalline silicon deposited on a glass slide, for characterization of its semiconductor properties, acquired with a LAMBDA 1050 with 150 mm InGaAs Integrating sphere accessory.

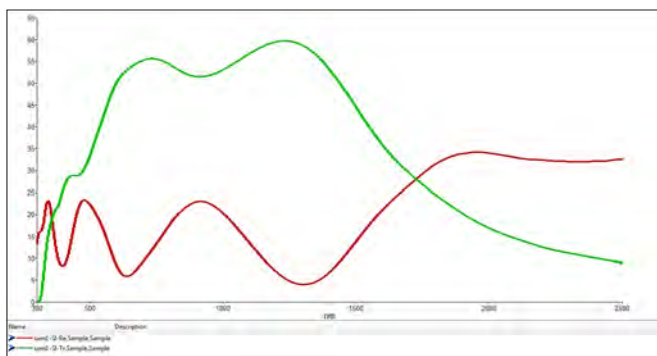


Figure 6. Transmission (green) and reflectance (red) spectra of thin film crystalline silicon acquired for absorptance determination.

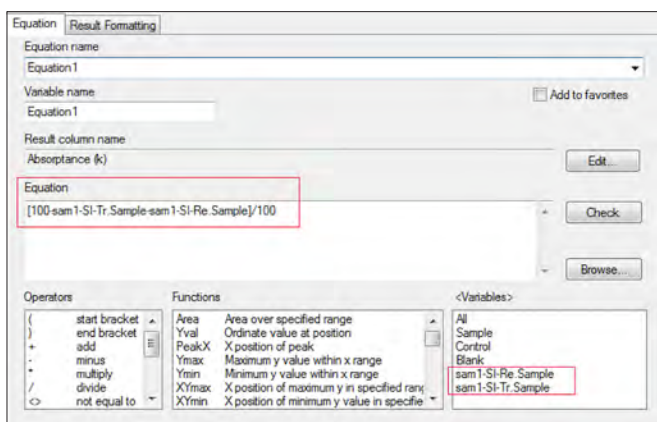


Figure 7. Equation (boxed) programmed into the Processing section of UVWinLab to calculate absorptance (k). The filenames assigned for the %T and %R measurements are variables.

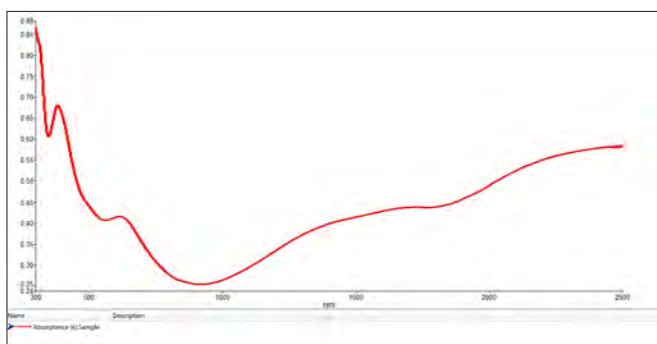


Figure 8. Equation calculated absorptance (k) from the %T and %R spectra shown in Figure 6.

Under the Processing section of the method a single equation can be entered to calculate the extinction as shown Figure 7. The result is shown in Figure 8.

### Measuring the Refractive Index (n) of Materials

Numerous mathematical approaches exist to calculate the refractive index and film thickness from transmittance and reflectance spectra of thin films. Three approaches will be discussed here, all within the capabilities of the high performance LAMBDA spectrometers and UVWinlab software.

1. Using the **Ri** and **Tcalc** equation functions under the Processing editor of UVWinlab V6
2. Calculating refractive index from transmission or reflectance spectra acquired at two different angles of incidence
3. Calculating refractive index and thin film thickness using formulas from either the reflectance or transmittance spectra where no interference fringe pattern is available

Each of these approaches will be discussed in detail below.

#### 1. Calculating Refractive Index and Film thickness using the built-in Ri and Tcalc Equation Functions

Thin films in the thickness range of about 0.1 to 10 microns can exhibit a constructive-destructive interference pattern as a function of wavelength. If the film thickness is known, the refractive index can be calculated using the built-in **Ri** equation function under the Processing section of the software. Conversely, if the refractive index is known, the film thickness can be calculated using the **Tcalc** function. The equations programmed into these functions are shown in Figure 9<sup>2</sup>.

$$t = \frac{N(\lambda_1 \times \lambda_2) c}{2((\lambda_1 - \lambda_2) ((n^2 - \sin^2 a)^{1/2}))}$$

$$n = \left[ \left( \frac{N(\lambda_1 \times \lambda_2) c}{2(\lambda_1 - \lambda_2) t} \right)^2 + \sin^2 a \right]^{1/2}$$

where:

- $\lambda_1$  = maximum wavelength
- $\lambda_2$  = minimum wavelength
- $N$  = number of fringes
- $n$  = refractive index
- $a$  = angle of incidence
- $c$  = conversion factor to angstroms

Figure 9. Film thickness and refractive index equations programmed into the **Tcalc** and **Ri** equation functions of UVWinlab.

To calculate film thickness and refractive index the user enters the required data, including the wavelength range, the refractive index (or film thickness), the number of fringes, and angle of incidence in the equation formats for Tcalc and Ri shown below.

Film thickness (**Tcalc**) and refractive index (**Ri**) preprogrammed equations:

<b>Tcalc</b> Tcalc[<spectrum>, range start x, range end x, Refractive Index, Number of Fringes(-1=Auto), Angle of Incidence, result unit 1=Å/2=µm, Peak Threshold (optional)]
<b>Ri</b> Ri[<spectrum>, range start x, range end x, Sample Thickness, Number of Fringes (-1=Auto), Angle of Incidence, Thickness Unit 1=Å/2=µm, Peak Threshold (optional)]

In the example shown in Figure 10, a polycarbonate protection lens having a thin film anti-abrasion coating with a nominal film thickness of 6 microns is shown.

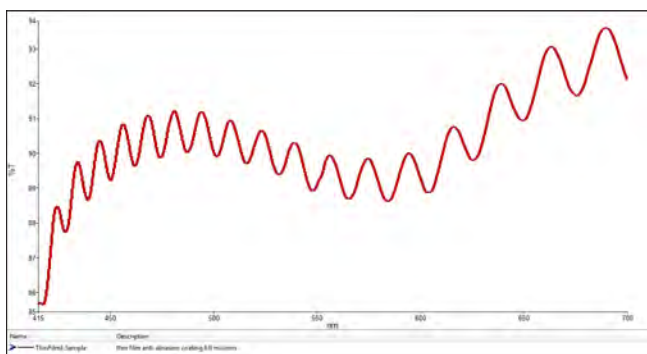


Figure 10. Spectra acquired from a lens having a thin film anti-abrasion coating, showing a characteristic constructive-destructive interference pattern.

In this example a film thickness of 6.00 microns was entered in the Ri function under the Processing section of the method, and a refractive index of 1.467 was calculated between 675 and 548 nm (6 fringe peaks. Conversely, the film thickness was calculated by entering a refractive index of 1.467. The results from these calculations are put into the Results table, as shown in Figure 11.

Sample ID	Description	Thickness (microns)	Refractive index (n)
1	ThinFilm1.Sample thin film anti-abrasion coating 6.0 microns	5.973	1.467

Figure 11. Film thickness and refractive index calculated by the Ri and the Tcalc functions of UVWinlab for the lens sample in Figure 10.

## 2. Calculating Refractive Index from Spectra Measured at Two Different Angles of Incidence

For samples that exhibit an optical thin film interference pattern it is possible to calculate the refractive index by acquiring the transmittance or reflectance spectra at two different angles of incidence, and entering the shift observed in the interference pattern into an equation (Figure 12). For this measurement a variable angle transmission or a variable angle specular reflectance accessory is required. This can be a relative (i.e., B0137314) or absolute variable angle (i.e., Universal Reflectance Accessory – URA L6020202) reflectance accessory. Additionally, because light impinging on the sample at oblique angles will be transmitted or reflected in two orthogonal planes, s-polarized or p-polarized, either a Common Beam Depolarizer (CBD) is recommended, or a polarizer drive unit fitted with a polarizer crystal allowing measurement at a known angle of polarization.

Procedure:

1. Using a variable angle transmittance or variable angle specular reflectance accessory measure at two different angles of incidence.
2. Obtain the fringe pattern at each angle.
3. For each angle of incidence, measure the spacing between adjacent fringes.
4. Use the following formula to calculate the refractive index (ref. 4):

$$n = ((\sin^2\theta_1\Delta v_1^2 - \sin^2\theta_2\Delta v_2^2) / (\Delta v_1^2 - \Delta v_2^2))^{1/2}$$

where  $\theta_1$  and  $\theta_2$  are the two different angles of incidence, and  $\Delta v_1$  and  $\Delta v_2$  are the fringe spacing for adjacent fringes measured at angles  $\theta_1$  and  $\theta_2$  respectively (note: if entering wavelength values the result is multiplied by  $10e^7$ ).

Figure 12. Formula to calculate refractive index from thin film spectra at two different angles of incidence.

The Universal Reflectance Accessory (URA) was used to acquire the absolute reflectance data at two different angles of incidence of a silicon nitride coated semiconductor wafer. Like the 150 mm integrating sphere accessory, the URA fits into the second sample compartment area of the High Performance LAMBDA spectrometer (Figure 13). A close-up of the URA is shown below. Samples are laid horizontal over the beam port for measurements, and the motorized accessory will drive to the angles programmed.



Figure 13. The Universal Reflectance Accessory (URA) fitted into a LAMBDA 950. The URA is a programmable motorized absolute reflectance with an angle range of 8-68 degrees.

The parameter setup screen and the sample table entries for the measurements are shown in Figure 14. Once the angles are programmed, all angle changes and corrections proceed automatically without operator intervention.

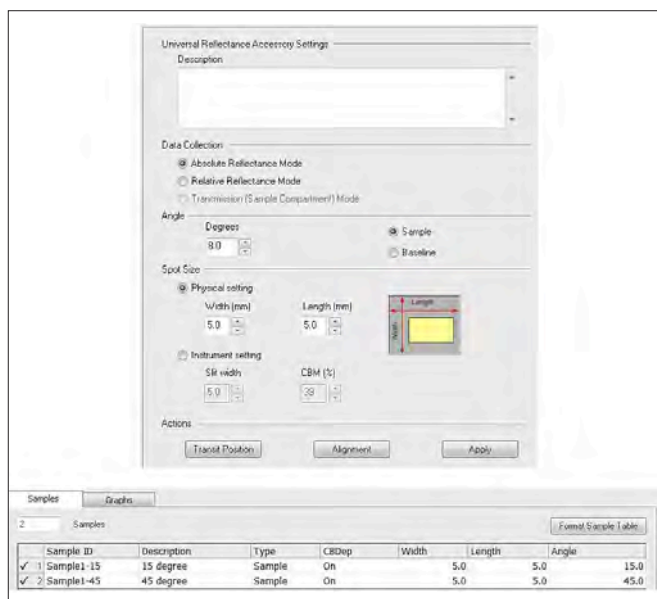


Figure 14. Universal Reflectance Accessory parameter page and associated sample table to acquire absolute reflectance data at 15 and 45 degrees angle of incidence, using a beam size of 5x5 mm (length x width). When the run is started all angle changes and corrections are done automatically.

In the example shown in Figure 15 is a silicon nitride coated semiconductor wafer on silicon which was scanned in reflectance at a 15 and a 45 degree angle of incidence. The interference patterns are clearly observed, and the adjacent peak wavelength separation can be measured easily.

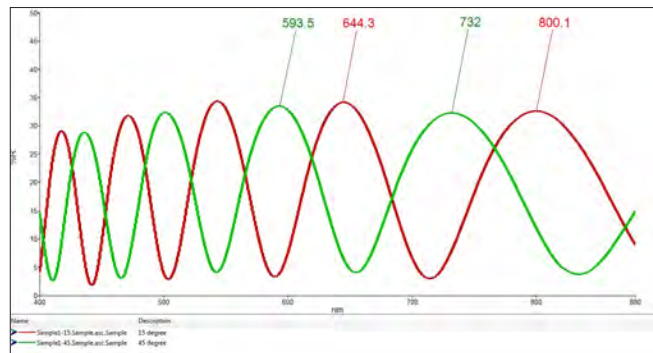


Figure 15. Silicon nitride thin film coating on a silicon substrate semiconductor wafer scanned in absolute reflectance at two different angles of incidence (red = 15°, green = 45°) using the URA accessory.

Using the peaks at 800.1 and 644.3 for 15°, and 732.0 and 595.5 for 45°, deltas of 155.8 nm and 138.5 nm were calculated respectively. After entering the equation in Figure 12 into the Processing section of UVWinLab a refractive index of 2.22 was calculated for this sample. The equation output is shown below:

1	Equation1	24273.64
2	Equation2	0.1971
3	Equation3	19182.25
4	Equation4	0.954981
5	Equation5	0.954981
6	Equation7	-0.757836
7	Refractive Index (n)	2.22

### 3. Calculating Refractive Index Using Formulas From Either the Reflectance or Transmittance Spectra

Besides providing information on the absorption of a sample, transmission and reflectance spectra can be used to calculate the refraction indices of a sample. If the absorption is high with no or minimal interferences the sample refractive index  $n_f$  can be calculated using the equations below<sup>1</sup>:

$$n_s = \frac{\sqrt{M + \sqrt{M^2 - n_s^2}}}{T_{max}} \quad 1$$

where  $M = \frac{2n_s^2}{T_{min}} - \frac{n_s^2 + 1}{2}$

If interferences are determined, from the maxima in the transmission spectra the refractive index of the substrate can be derived by the following equation. Note this formula only applies to cases where absorption of the substrate is negligible:

$$T_{max} = \frac{2n_s}{n_s^2 + 1} \quad 2$$

where  $n_s = \frac{1 + \sqrt{1 - T_{max}^2}}{T_{max}}$

If the absorption is low and there are no or minimal interferences the sample refractive index can be calculated from the transmission minima by using the following formula:

$$R = \left( \frac{n_f - 1}{n_f + 1} \right)^2 \quad 3$$

where  $n_f = \frac{1 + R + \sqrt{R}}{1 - R}$

Since the absorption of thin film coatings is usually not uniform as a function of wavelength, ranging from low to high absorption, the formulas above can be applied to the appropriate sections of the spectra for a valid calculation of refractive index.

Shown in Figure 16 are the transmission and reflectance spectra of thin film crystalline silicon deposited on a glass slide, for characterization of its semiconductor properties. Shown in Figure 17 is the absorptance spectrum. In the area between 1800 and 2500 nm the absorption was significant, so the first equation above (1) above was used to calculate

the refractive index over that part of the spectrum. Again, the equation was entered into the Processing section of UVWinlab.

Shown in Figure 18 are the calculated refractive indices at a select number of wavelengths, with a mean refractive index of 4.87 calculated from 2500 to 1800 nm.

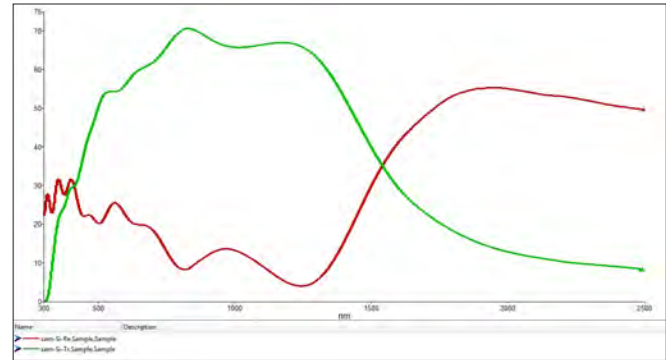


Figure 16. Transmission (green) and reflectance (red) spectra of thin film crystalline silicon deposited on a glass slide.

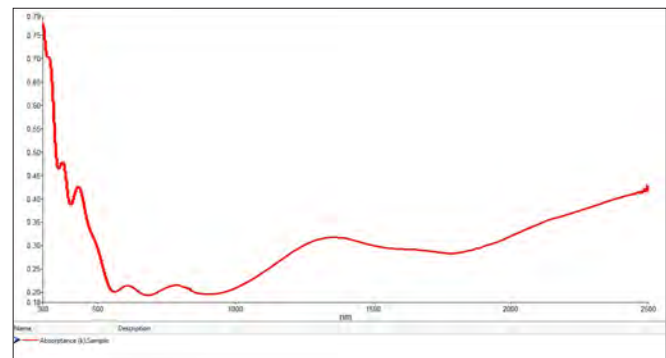


Figure 17. Absorptance spectrum calculated from the spectra in Figure 16.

Sample ID	Description	Ri (2500) nm	Ri (2300) nm	Ri (2000) nm	Ri (1800) nm	Mean (Ri) 2500-1800 nm
✓ 1	cam-Si-Pie Sample crystalline silicon on glass	4.95	5.10	5.08	4.36	4.87

Figure 18. Refractive index calculated over the range of 2500-1800 nm using the first equation (1) above from the reflectance spectrum (Figure 15) of thin film crystalline silicon deposited on a glass slide. The equation was programmed into the Processing section of UVWinlab and a mean refractive index of 4.87 was determined.

### Conclusion

The reference grade high performance LAMBDA 1050 when fitted with the proper accessories becomes an ideal tool for the determination of optical thin film constants. In this paper procedures were described for the determination of refractive index ( $n$ ), absorptance ( $k$ ), and film thickness for thin films. The 150 mm InGaAs integrating sphere and the Universal Reflectance Accessory proved to be ideal accessories for acquiring the data for the examples presented in this paper.

## References

1. M. Born and E. Wolf, Principles of Optics, 7th Edition, Cambridge University Press, 2005
2. M. Rand, Spectrophotometric Thickness Measurement for Very Thin SiO<sub>2</sub> Films on Si, Journal of Applied Physics, Volume 41, Number 2, 1970
3. J. Rancourt, Optical Thin Films User's Handbook, McGraw-Hill Publishing Company, 1987
4. PerkinElmer Publication 0993-8288, Applications of Variable Angle Specular Reflectance, 1988

PerkinElmer, Inc.  
940 Winter Street  
Waltham, MA 02451 USA  
P: (800) 762-4000 or  
(+1) 203-925-4602  
[www.perkinelmer.com](http://www.perkinelmer.com)



---

For a complete listing of our global offices, visit [www.perkinelmer.com/ContactUs](http://www.perkinelmer.com/ContactUs)

Copyright ©2013-2016, PerkinElmer, Inc. All rights reserved. PerkinElmer® is a registered trademark of PerkinElmer, Inc. All other trademarks are the property of their respective owners.

Gas Chromatography/  
Mass Spectrometry

Author

Ulrich Meier

PerkinElmer, Inc.  
Ferdinand-Porsche-Ring 17  
D-63110 Rodgau, Germany

## Determination of Monomers in Polymers by Multiple Headspace Extraction – GC/MS

### Abstract

Polymer production and quality control (QC) requires a variety of analytical testing – one common QC test is the analysis of residual monomers in the final polymer material. This analysis is well suited for headspace sampling because headspace eliminates the sample preparation. The sample is analyzed directly with no need to dissolve the polymer.

The analysis of solid samples with headspace does require compensation for the sample matrix, as calibration standards cannot be created with the same matrix interactions. Multiple headspace extraction (MHE) is a technique to exhaustively extract a sample and calculate the amount of analyte by comparison to an external standard.

This application note will discuss the testing of polymers for residual monomers by MHE-GC/MS. The polymers tested in this application are used for the manufacturing of corrective eyeglass lenses. This material is monitored for acrylic acids, such as methylmethacrylic acid methyl ester (MMA).

## Introduction

Multiple headspace extraction is used because it is a technique to quantify samples in a solid or difficult matrix without matrix matching the calibration standards. The standard is analyzed, without matrix, in a total evaporation headspace with MHE, determining a response factor (Figure 1, Page 3). MHE is an option the user selects in the method which initiates a specific extraction process in the instrument.

In MHE, the HS method follows the standard extraction steps in the first round of extraction. The vial is equilibrated, pressurized, an injection is made, and the vial is vented. Following the first round of extraction, the MHE method differs from a standard HS method – rather than ejecting the vial after venting, the vial remains into the headspace oven, it is re-equilibrated, and the injection process repeated. The instrument can run this process unattended for the number of times, up to nine, that the operator selects in the method.

With this technique, the sample is extracted until nothing remains – this data is used to determine the total amount of analyte within the sample and the rate of extraction specific to the sample matrix. This data is input into a report template (Figure 2, Page 3) and used to calculate the amount of analyte in each sample of similar matrix.

## Experimental

Headspace sample preparation is simple. A sample of known weight is placed into a headspace vial, then the vial is crimped and placed into the PerkinElmer® TurboMatrix™ HS-40 Headspace Sampler (HS). The headspace method was created with the parameters listed in Table 1. The conditions used for the PerkinElmer Clarus® 600 GC/MS system are presented in Tables 2 and 3. A PerkinElmer Elite™-5MS column achieved the necessary separation, while the Clarus 600 MS operated in full-scan mode, providing both qualitative and quantitative data.

**Table 1. Headspace Conditions Used in Analysis of Monomers in Polymers.**

Headspace Unit:	PerkinElmer TurboMatrix HS-40
Headspace Mode:	MHE
Oven Temperature:	180 °C
Needle Temperature:	185 °C
Transfer Line Temperature:	190 °C
Thermostat Time:	30 min
Vial Pressurization Time:	2 min
Withdraw Time:	0.2 min
Injection Time:	0.03 min
Column Pressure:	120 kPa
Injection Pressure:	160 kPa
Vial Pressure:	160 kPa
Vial Vent:	On
Transfer Line:	Fused Silica (0.32 mm)

**Table 2. GC Conditions Used in Analysis of Monomers in Polymers.**

Gas Chromatograph:	PerkinElmer Clarus 600 GC												
Analytical Column:	PerkinElmer Elite-5MS (30 m x 0.25 mm x 0.25 µm)												
Injection Port Type:	Programmable Split/Splitless												
Injector Temperature:	200 °C												
Injection Type:	HS-Control												
Carrier Gas Type:	Helium												
Carrier Gas Program:	80 kPa Constant												
Oven Program:	<table><thead><tr><th>Temp.</th><th>Hold Time</th><th>Rate</th></tr></thead><tbody><tr><td>40 °C</td><td>4 min</td><td>5 °C/min</td></tr><tr><td>160 °C</td><td>5 min</td><td>20 °C/min</td></tr><tr><td>260 °C</td><td>2 min</td><td>End</td></tr></tbody></table>	Temp.	Hold Time	Rate	40 °C	4 min	5 °C/min	160 °C	5 min	20 °C/min	260 °C	2 min	End
Temp.	Hold Time	Rate											
40 °C	4 min	5 °C/min											
160 °C	5 min	20 °C/min											
260 °C	2 min	End											

**Table 3. MS Conditions Used in Analysis of Monomers in Polymers.**

Mass Spectrometer:	PerkinElmer Clarus 600 T MS
GC Inlet Line Temperature:	180 °C
Ion Source Temperature:	200 °C
Function Type:	Full Scan
Full-Scan Range:	<i>m/z</i> 45-350
Full-Scan Time:	0.35 sec
InterScan Delay:	0.05 sec
Solvent Delay:	0 min

## Results

MHE is used because it is a technique to quantify samples in a solid or difficult matrix without matrix matching the calibration standards. The standard is analyzed, without matrix, in a total evaporation headspace with MHE, determining a response factor (Figure 1).

In this case, 1 µL of MMA was vaporized in the vial; the amount of 935 µg was calculated with the known density. The sample was exhaustively extracted over several MHE steps, in this case 5.

A sample, 0.688 g, of polymethyl methacrylate (PMMA) was placed into a headspace vial and analyzed by MHE. The total peak area of the analyte was calculated and the concentration of analyte in the sample determined by comparison to this response factor. The necessary calculations for MHE are completed using an Excel® macro available from PerkinElmer and pictured in Figure 2. The sample was determined to have 1726 µg/kg of MMA.

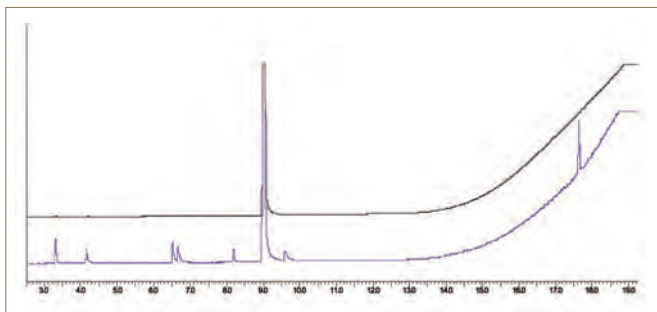


Figure 1. Chromatogram of a MMA calibration standard by total vaporization (top); and chromatogram of the MMA in a PMMA sample (bottom).

In this application, two samples of polycarbonate lenses were analyzed, both demonstrating MMA peaks. In routine analysis of the same polymer, in this case polycarbonate, the number of extraction steps can be reduced and the formula from a previous sample used. This is an acceptable practice, because the matrix will behave in a predictable fashion under specified experimental conditions. Reducing the number of extraction steps speeds up the analytical cycle time and continues to provide the accurate calibration of exhaustive extraction. Two samples of eye-glass lenses were analyzed (Figures 3 and 4) both containing MMA.

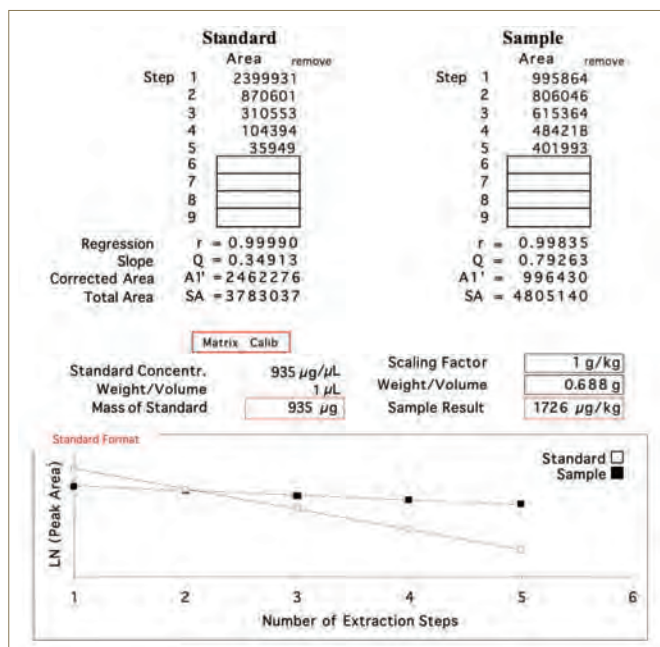


Figure 2. Example of the Excel®-based macro used to calculate concentration of MMA in MHE.

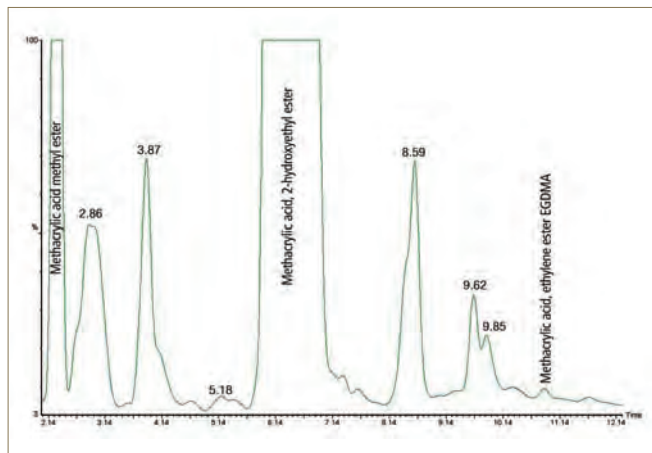


Figure 3. Chromatogram of Sample 1, demonstrating methacrylic acid methyl ester, methacrylic acid-2-hydroxyethyl ester, and methacrylic acid ethylene ester.

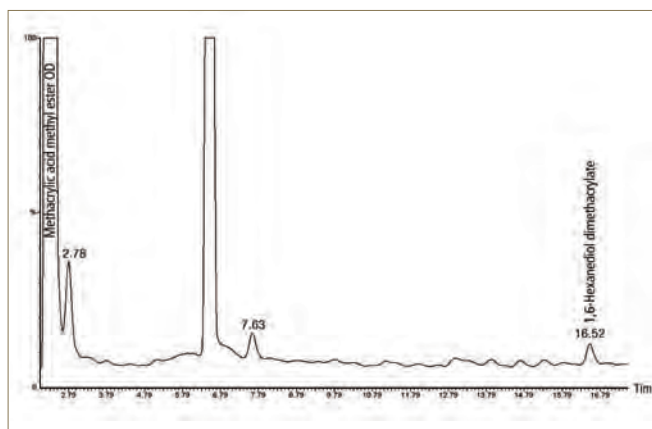


Figure 4. Chromatogram of Sample 2, demonstrating methacrylic acid methyl ester and 1,6-hexanediol dimethacrylate.

## Conclusion

This paper has shown that multiple headspace extraction is a suitable and effective technique for the analysis of polymeric materials for residual monomers. The headspace sample introduction reduces sample preparation to an absolute minimum and solvent use is eliminated. Complicated matrix matching of calibration standards was replaced with an automated multiple headspace extraction technique. Additionally, mass spectral characteristics allowed for the identification of each analyte. Several samples were analyzed qualitatively and quantitatively here with a simple and effective headspace-GC/MS technique.

## Infrared, IR Microscopy

Author:

Ian Robertson

PerkinElmer, Inc.

Seer Green, UK

## Detection and Identification of Contaminations in the Manufacturing Process Using an IR Microscope

### Introduction

Manufacturing processes are designed to create products that contain only the required components. Occasionally, foreign objects can appear within the final product as unexpected contaminations effecting product quality or even causing product failure. Investigation is required to determine what the contamination is and where it has originated. Infrared spectroscopy is one of the

primary analytical techniques for the identification of materials. If the contaminant is large enough that it is visible to the naked eye then a simple (macro) IR measurement can usually be performed on the sample. In many industries, such as electronics and polymers, even micro-contaminants can cause product problems. IR microscopy allows samples as small as a few micrometers in size to be analyzed and identified and is the ideal solution for these types of problems. A range of IR microscope sampling modes (transmission, specular reflectance, and Attenuated Total Reflectance) allow spectra to be measured for contaminants in a variety of sample matrices.

This Application Note describes the use of the Spotlight™ 200i system, an automated IR microscope for the detection and measurement of different types of contaminants in a range of manufactured samples.

## Automated Detection and Analysis of Contaminants on an Electronic Contact

Electronic contacts need to be clean and free from contamination to avoid problems in operation. A sample was submitted for analysis that had visible contaminants. The sample was placed in the Spotlight 200i and a "Visible Image Survey" collected over the entire contact, as shown in Figure 1. The "Detect Particles" function in the Spectrum 10 software found some contaminant particles as shown in the enlarged box of Figure 1.

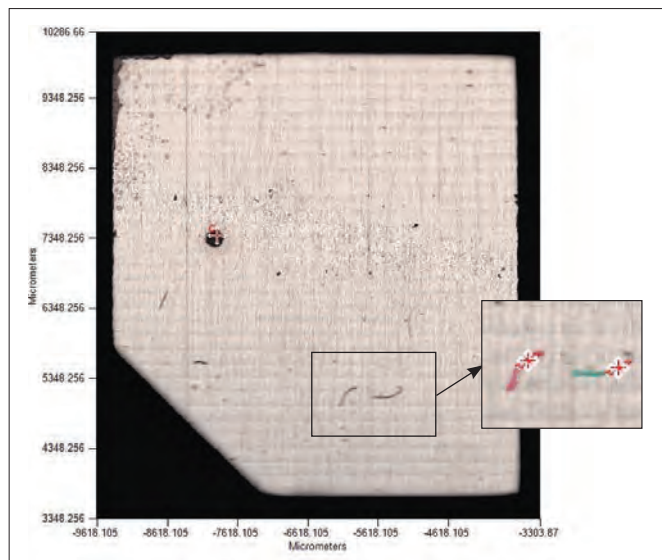


Figure 1: The Visible Image Survey and expanded region, Figure 1b, showing automatic detection of contaminants.

The software then automatically collected reflectance backgrounds and spectra for the particles (fibers), with their spectra shown as Figure 2.

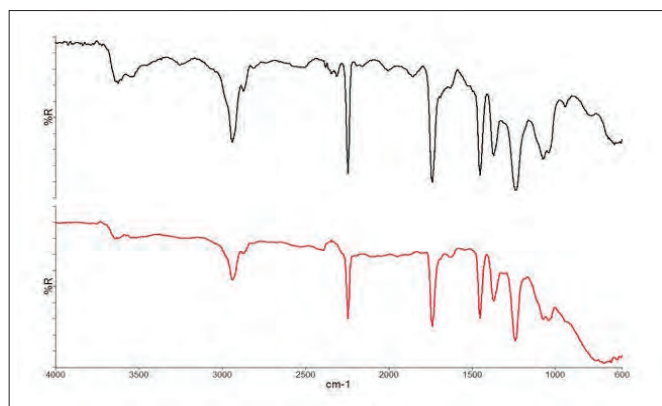


Figure 2: Reflectance spectra of two contaminant fibers.

The spectra of these two materials are similar with the lower spectrum showing an additional broad peak centered around  $700\text{ cm}^{-1}$ . The top spectrum was identified by spectral comparison against a library of polymer and polymer additives spectra as an acrylonitrile-butyl methacrylate copolymer. Since the lower spectrum clearly has another component present it was subjected to a mixture search, which also detected the presence of tin oxide in the sample.

## Fiber Contamination on a Pharmaceutical Tablet

A pharmaceutical tablet was observed to have visible contaminants present, appearing to be on the surface. It was unclear as to whether this contamination occurred during manufacturing or at a later stage from external contamination. The sample was observed using the visible image in reflectance on the Spotlight 200i, as shown in Figure 3 and is seen to be a fiber. The image shows that a large proportion of the fiber is embedded under the surface of the tablet and hence could not have simply fallen onto the surface post-manufacturing.

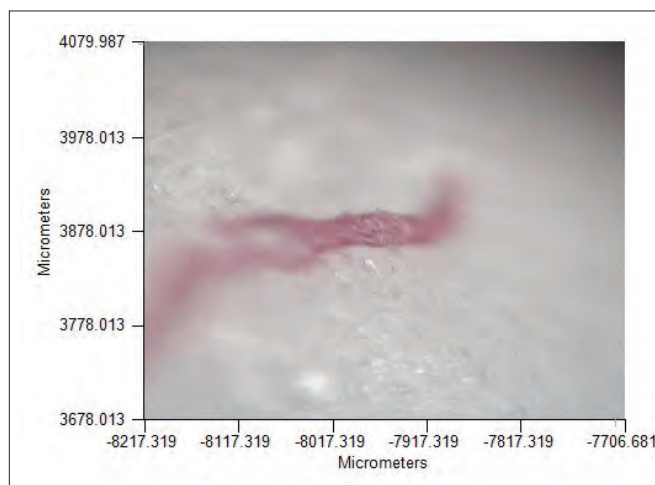


Figure 3: The visible image of a fiber embedded in pharmaceutical tablet.

Due to the fiber being embedded in the sample and covered in excipients, it was not possible to perform a direct ATR measurement. In such cases it is necessary to physically remove the fiber from the sample matrix. The sample was then placed on a KBr window, Figure 4, and the sample spectrum measured in transmission, the spectrum is shown in Figure 5.

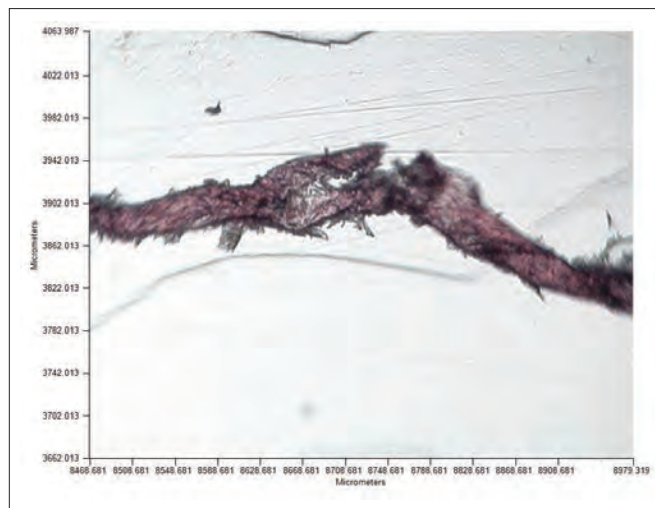


Figure 4: The visible image of the extracted fiber on KBr window.

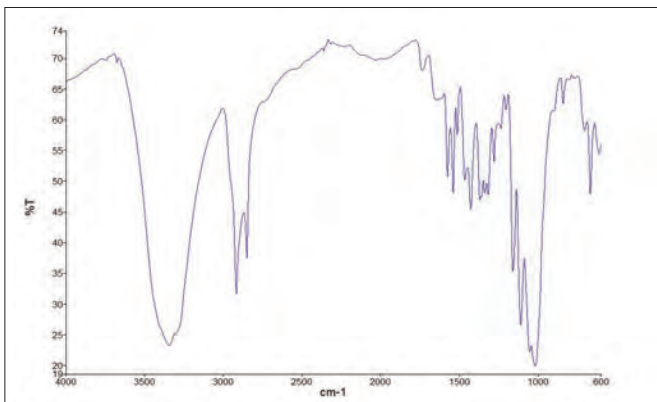


Figure 5: Transmission spectrum of fiber extracted from pharmaceutical tablet.

The spectrum obtained still contains spectral features (broad –OH in the region  $3400\text{ cm}^{-1}$  and C-O band at  $\sim 1020\text{ cm}^{-1}$ ) due to the microcrystalline cellulose, one of the excipients. However, performing mixture search allowed the fiber material to be identified as a chlorinated polyethylene as shown in Figure 6.

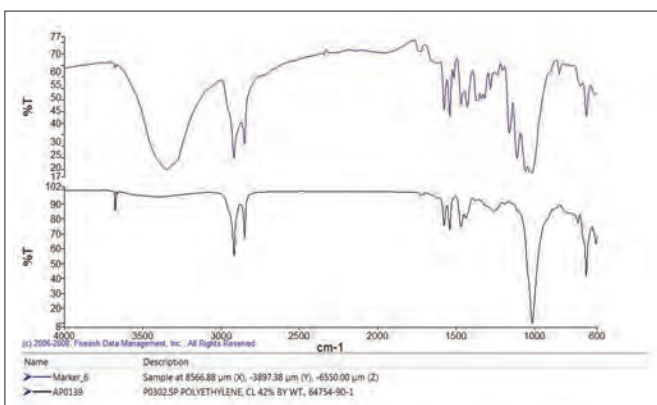


Figure 6: Transmission spectrum of fiber extracted from pharmaceutical tablet.

## Summary

IR microscopy is an invaluable technique for identifying small contaminations in the manufacturing process, and we have demonstrated how an automated IR microscope is suitable for their rapid detection and measurement. Contaminants can often be automatically detected, scanned and identified by the software. The range of IR microscopy sampling modes means that samples can often be measured in-situ, speeding up the process of identification. However, there are cases where the contaminant may need to be physically removed from the sample matrix in order to provide higher quality spectra free from matrix interference.

## Infrared, IR Microscopy

Author:

Ian Robertson

PerkinElmer, Inc.

Seer Green, UK



## Detection and Identification of Microplastic Particles in Cosmetic Formulations Using IR Microscopy

### Introduction

It is estimated that there is in excess of 150 million tons of plastic materials in the world's oceans<sup>1</sup>. Much of this pollution consists of large items such as discarded drink bottles and plastic bags. However, there is increasing research into the amount of much smaller materials, termed microplastics, in the river and ocean systems which present a different type of problem for marine life.

Many cosmetic products, such as facial scrubs, toothpastes, and shower gels, currently contain microplastic beads as abrasive materials. These microplastics, which are typically sub-millimetre in size, get washed down the sink and are too small to be filtered by sewage treatment plants consequently ending up in the river systems and ultimately in the oceans. These microplastics can be ingested by marine organisms and fish and end up in the human food chain.

In 2014 a number of U.S. states banned the use of microplastics in cosmetic formulations and most cosmetic companies are voluntarily phasing out their use.

Infrared (IR) spectroscopy is the established technique for identifying polymer materials and has been used extensively for identifying large (over 100 micrometer) polymer materials. The Spectrum Two™ is a portable FT-IR spectrometer that can operate from a battery pack and has been used on boats for immediate identification of these polymers.<sup>1</sup> For microplastics, down to a few micrometers in size, an IR microscope can be used for the detection and identification of these materials.

Two commercially available products were tested using the Spotlight™ 200i IR microscope system in order to determine whether microplastics were present as the exfoliant and to identify the types of plastics used.

Product 1 is a commercially available facial scrub. Product 2 is a commercially available body scrub. Each of these products was mixed with hot water in order to dissolve the soluble ingredients in the formulation. The resulting solution was filtered through a 50 micrometer mesh, capturing any insoluble components greater than 50 micrometers in size. The filter was then allowed to dry in air prior to IR microscopy measurements. The samples were measured both directly on the mesh and also after transferring the residual particles onto an IR transmitting window on a microscope holder. Visible images of the collected microplastics are shown as Figures 1a and 1b.

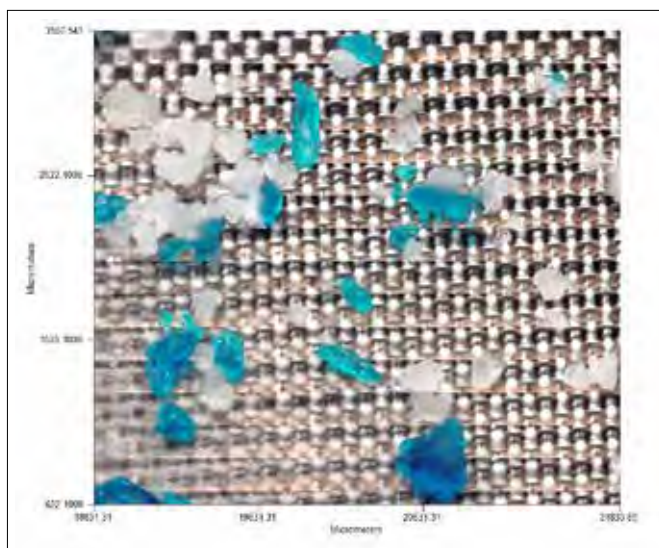


Figure 1a: Microplastics in Product 1 (facial scrub) collected on mesh.

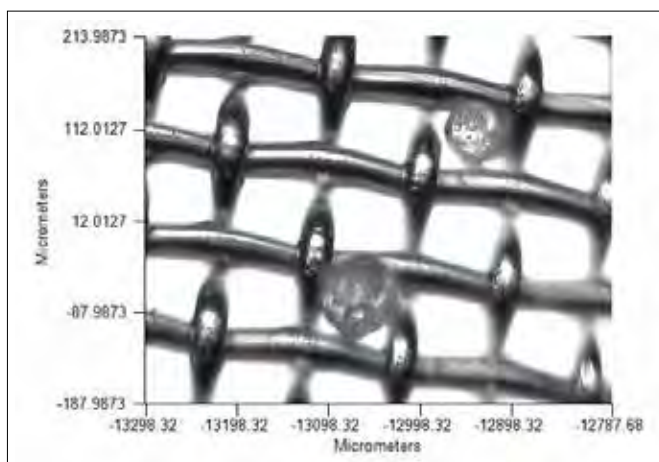


Figure 1b: Magnified view of microplastics collected from Product 2 (body scrub).

It is clear from these images that Product 1 has irregular-shaped microplastics with particles of two different colors. The particles from Product 2 are regular spheres with those visible in Figure 1b being approximately 50 and 80 micrometers in diameter. Infrared spectra of these materials can be measured in either transmission or reflectance on the IR microscope. Spectra measured on one of the particles in Figure 1a, in-situ on the mesh, are shown as Figure 2.

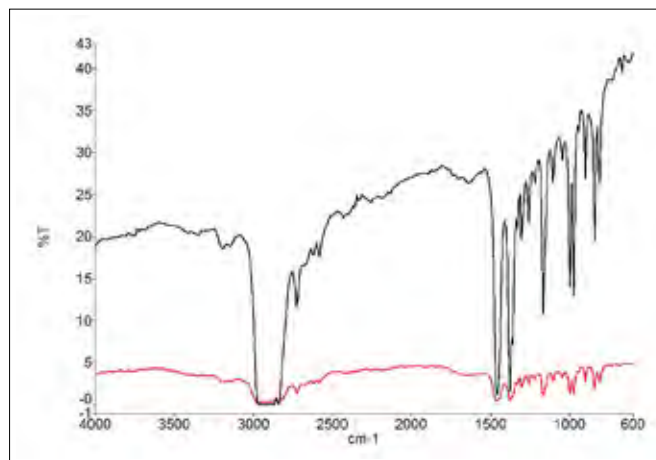


Figure 2: Spectra from a microplastic particle in Product 1. Transmission spectrum (black) and reflectance spectrum (red).

The transmission spectrum has a much higher signal than the reflectance spectrum and gives better sensitivity for this measurement. In addition, the bands in the reflectance spectrum are more intense due to the fact that the IR beam is effectively passing twice through the sample, known as transmittance. For smaller particles this does not cause any problems; but for larger particles the path length may be too large leading to totally absorbing bands, thus making identification more difficult. However, in this case, it would be possible to identify the material from either the transmission or reflectance spectrum. The mesh may interfere with the transmission measurement, slightly decreasing the amount of energy reaching the detector. This explains the baseline slope observed in the spectrum, but it does not significantly impact the overall measurement. To obtain the best quality spectrum of the material, the sample can be transferred onto an IR-transmitting window material, such as potassium bromide (KBr). A KBr window was placed onto the mesh containing the sample and the mesh inverted thereby transferring the microplastic particles directly onto the KBr window.

A “Visible Image Survey” was collected over the area containing the majority of the particles in Product 1. Selecting the “Analyze Image” function in the Spectrum 10 software invokes the intelligent automated routine for detecting particles within this Visible Image Survey, which is displayed as “analyze image result” shown in Figure 3.

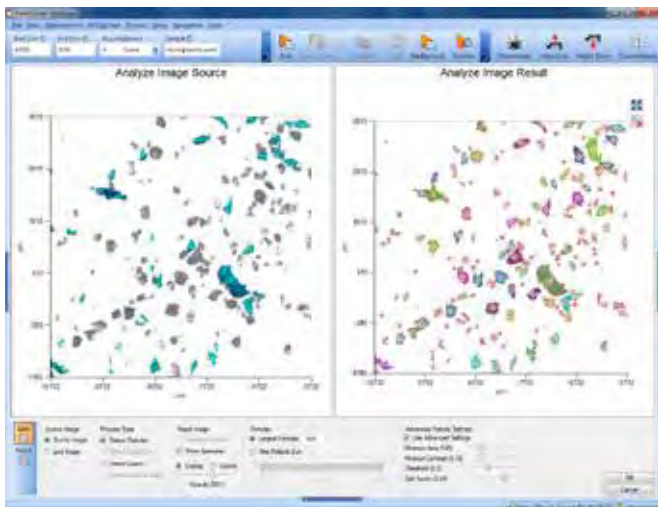


Figure 3: The Analyze Image software routine detects the particles in Product 1.

This routine will automatically detect any particles present in the visible image and mark them as regions of interest. It will then calculate the maximum rectangular aperture size that can fit wholly inside each of the particles, thus maximizing signal-to-noise when the data is scanned. In the past, manual selection of the regions of interest and setting of apertures took a considerable amount of time. Clicking “Scan Markers” initiates the collection of transmission spectra (using equivalent apertures for the background) for each particle, displaying ratioed sample spectra in real time as they are collected. Automatic processing of the spectra, using software routines such as Search, Compare, or Verify, can be performed during data collection. In this case, the analysis of the microplastics, a spectral search was performed against a library of polymer spectra to give the identity of each of the particles as shown in the results screen in Figure 4.

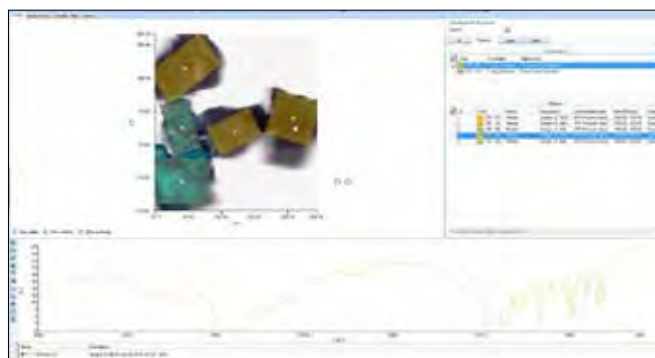


Figure 4. Results screen for the detection and identification of particles.

The results show that Product 1 has two different types of polymers present, polypropylene and polyethylene. Product 2 contains only particles of polyethylene. Representative spectra are shown in Figure 5. Small differences are observable in the spectra of the polyethylene between the two different products, most likely due to additives present.

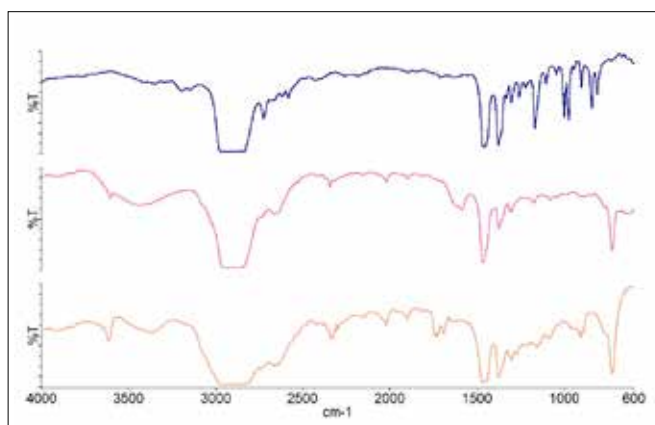


Figure 5: Top – spectrum of polypropylene in Product 1. Middle – spectrum of polyethylene in Product 1. Bottom – spectrum of polyethylene in Product 2.

## Summary

Microplastics are a major concern regarding their impact on the environment and as such their use in consumer products is increasingly being prohibited. An automated IR microscopy system has been shown to be an invaluable method for the detection and identification of a source of microplastics in cosmetic formulations. The work presented here will be extended to analyze samples of microplastics collected from European river systems to illustrate how widespread this pollution problem is within marine environments.

## References

1. Labo magazine – Oktober 2010 Wasserverschmutzung durch Mikroplastikpartikel, [www.labo.de](http://www.labo.de)

PerkinElmer, Inc.  
940 Winter Street  
Waltham, MA 02451 USA  
P: (800) 762-4000 or  
(+1) 203-925-4602  
[www.perkinelmer.com](http://www.perkinelmer.com)



---

For a complete listing of our global offices, visit [www.perkinelmer.com/ContactUs](http://www.perkinelmer.com/ContactUs)

Copyright ©2015, PerkinElmer, Inc. All rights reserved. PerkinElmer® is a registered trademark of PerkinElmer, Inc. All other trademarks are the property of their respective owners.

## Authors

Zoe Grosser, Ph.D.  
Laura Thompson  
Lee Davidowski, Ph.D.  
PerkinElmer Inc.  
Shelton, CT

Suzanne Moller  
Innov-X Systems  
Woburn, MA

## Lead and Other Toxic Metals in Toys Using XRF Screening and ICP-OES Quantitative Analysis

### Introduction

From 2007 to 2008, the number of recalls for toys exceeding the U.S. limits set for lead dropped 43%. This represents however, more than 300,000 individual products posing potential hazardous exposure for children. The Consumer Product Safety Improvement Act of 2008 (CPSIA 2008) defines a children's product as a product primarily used by a child under the age of 12 and defines new levels of lead allowed in those products<sup>1</sup>. Allowable lead in painted surfaces will be reduced from 600 mg/kg to 90 mg/kg one year from enactment of the legislation (enactment date:

August 14, 2008). Allowable total lead content (surface and substrate) is reduced from 600 mg/kg to 100 mg/kg, incrementally over the course of three years. The American Academy of Pediatrics suggests that a level close to the background level in soil of 40 mg/kg would be most protective of children's health<sup>2</sup>.

Currently, EN-71, Part 3 and ASTM 963 specify evaluation of the toy by soaking in a mild hydrochloric acid solution at body temperature and measuring the accessible metal extracted into the solution. If a coating can be separated, a total analysis of the coating to comply with lead content requirements can be done. CPSIA 2008 provides no exemption for electroplated substrates, so that a total analysis on both coating and substrate must be done, though little other measurement guidance is currently available. EN-71 may also be revised in the near future to add other hazardous elements, such as aluminum, cobalt, copper, nickel, and others. The evolving need to measure lead and other metals at increasingly lower levels makes information on analysis technologies and performance valuable in making knowledgeable decisions.

A variety of techniques can be used to meet the regulations, including atomic absorption (both flame FLAA and graphite furnace GFAA), inductively coupled plasma optical emission spectroscopy (ICP-OES) and inductively coupled plasma mass spectrometry (ICP-MS). Hand-held energy dispersive XRF, requiring minimal or no sample preparation can provide a way to screen products on-site as to determine whether further quantitative analysis is required.

The techniques are compared for several parameters in Table 1.

Since the techniques in Table 1 have different characteristics, which would be the most suitable for the variety

of children’s products, including toys that may require analysis? This question is addressed in this work using ICP-OES and hand-held XRF to examine a variety of toy materials. Ease of use and agreement between techniques at the current level for lead were evaluated.

### Experimental

A variety of children’s toys were obtained randomly from a church nursery room and other sources. One known recalled item, Boy Scout totem badges of differing ages were also obtained. Figure 1 shows the variety of toys, including fabric, soft and hard toys and some with painted surfaces.

**Table 1. Comparison of Several Analysis Techniques for Lead Determination (mg/kg).**

	GFAA	ICP-OES	ICP-MS	Hand-held XRF
Estimated detection limit for lead*	0.025	0.5	0.025	NA**
Sample prep required	Yes	Yes	Yes	No
Simultaneous multielement	No	Yes	Yes	Yes

\* Includes a 500x dilution to account for sample preparation for GFAA, ICP-OES, and ICP-MS. Detection limits can be further improved if a smaller dilution is used.  
 \*\*NA: screening tool, detection limits matrix driven.



Figure 1. Variety of toys measured.

**Table 2. Microwave Digestion Program.**

Power (W)	Ramp (min)	Hold (min)	Fan
500	5:00	15:00	1
900	10:00	15:00	1
0		20:00	2

**Table 3. ICP-OES Instrumental Conditions.**

Instrument	Optima 7300 DV ICP-OES
RF Power	1450 W
Nebulizer Flow	0.55 L/min
Auxiliary Flow	0.2 L/min
Plasma Flow	15.0 L/min
Sample Pump Flow	1.2 mL/min
Plasma Viewing	Axial
Processing Mode	Area
Auto Integration	5 sec min-20 sec max
Read Delay	30 sec
Rinse	30 sec
Replicates	3
Background Correction	one or two points
Spray Chamber	Cyclonic
Nebulizer	SeaSpray (Glass Expansion®, Pocasset, MA)

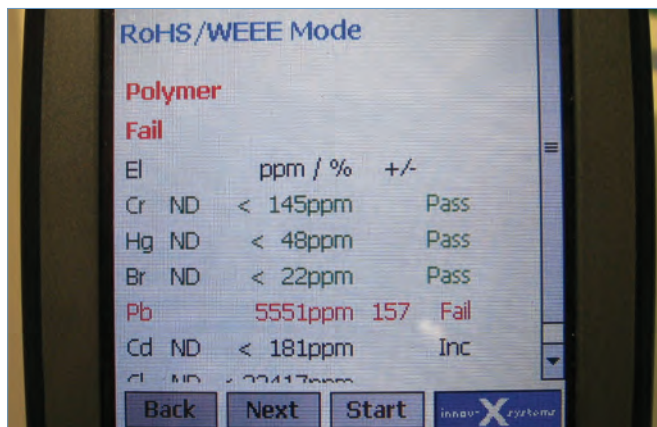


Figure 2. XRF result screen.

Samples were prepared for ICP-OES analysis by scraping off the paint or cutting the substrate into small pieces. Approximately 0.01-0.1 g was weighed into a PTFE microwave digestion vessel and 6 mL of concentrated nitric acid (GFS Chemical®, Columbus, Ohio) and 1 mL of concentrated hydrochloric acid (GFS Chemical®, Columbus, Ohio) were added. The samples were placed in the Multiwave™ 3000 microwave digestion system (PerkinElmer, Shelton, Connecticut) and digested according to the program shown in Table 2.

The Optima™ 7300 DV was used for analysis of the full suite of elements currently regulated in EN-71, Part 3<sup>3</sup> and referenced in ASTM D963<sup>4</sup>, and CPSIA, including lead. The conditions are as shown in Table 3.

The Innov-X® Import Guard model was used for all hand-held XRF measurements, and a general calibration was performed. For analysis of the same samples with XRF, no sample preparation was required. The system uses energy dispersive X-ray fluorescence and easily identifies

elements over a wide dynamic concentration range, from ppm levels up to virtually 100% by weight. An example of the result obtained on the screen is shown in Figure 2.

## Results and Discussion

The analysis of the toys by hand-held XRF and ICP-OES are shown in Table 4. The check mark in the XRF column indicates the XRF analysis displayed a lead value higher than the limit of 600 mg/kg in the screened toy indicating further quantitative analysis is recommended. The value determined by ICP-OES confirms that the value was higher than the regulatory limit in the coating or for a total analysis of the substrate material. In this case, the value measured with XRF is not reported although the value would give further refinement of the concentration for the elements measured.

Detection limits for the ICP-OES are shown in Table 5 for both the digested solution and the amount in the original material. Since the amount taken for digestion may vary and the dilution can be changed, a 500x dilution was assumed for the calculation. This represents a typical 0.1 g of material diluted to a final volume of 50 mL.

Duplicate sample preparation and analysis of several samples can indicate the reproducibility of the method, provided the samples are homogeneous. Table 6 shows the results for duplicate sample preparation and analysis of three different types of samples. The fabric and the uniformly-colored plastic show good agreement between the duplicate analyses (less than 20% relative percent difference). The puzzle board required scraping paint from the surface for analysis and it was difficult to uniformly remove only the paint without taking some of the substrate, as shown in Figure 3. This may contribute to the very different values obtained for the duplicate analysis.



Figure 3. Puzzle board and scrapings.

**Table 4. Results for Toys Measured with XRF and ICP-OES (mg/kg).**

	XRF	Antimony	Arsenic	Barium	Cadmium	Chromium	Lead	Mercury	Selenium
Toy Stove Knob	✓	32	<DL	2	4	773	3950	<DL	13
Yellow Mega Block	✓	12	<DL	56	3	774	3690	<DL	27
Badge-1 New (Yellow Paint)	✓	<DL	<DL	16900	14	7340	34500	<DL	85
Badge-2 Older (Yellow Paint)	✓	<DL	<DL	21200	2	8870	42100	<DL	20
Yellow Baby Rattle	✓	<DL	<DL	70	<DL	544	2970	<DL	8
Yellow Crib Toy Holder Strap	✓	15	<DL	146	<DL	377	1900	<DL	<DL
Green Cup		<DL	<DL	3220	2260	4	17	<DL	6
Red Ring		<DL	<DL	91	4	3	15	<DL	8

**Table 5. Estimated Detection Limits.**

Element	Detection Limit in Solution (mg/L)	Detection Limit in Solid (mg/kg)
Antimony (271 nm)	0.008	3.8
Arsenic (189 nm)	0.002	1.2
Barium (233 nm)	0.004	1.9
Cadmium (228 nm)	0.002	1.1
Chromium (267 nm)	0.003	1.6
Lead (220 nm)	0.010	6.4
Mercury (254 nm)	0.005	2.2
Selenium (196 nm)	0.011	5.7



Figure 4. Yellow ball measured in replicate.

**Table 6. Duplicate Sample Preparation and Analysis (mg/kg).**

	Antimony	Arsenic	Barium	Cadmium	Chromium	Lead	Mercury	Selenium
Green Fabric	15	<DL	302	<DL	332	1780	<DL	<DL
Green Fabric - Duplicate	13	<DL	329	<DL	362	1940	<DL	<DL
Puzzle Board	919	<DL	14	4	21,200	121,000	<DL	49
Puzzle Board - Duplicate	2187	<DL	5	5	14,600	82,600	<DL	15
Yellow Handle	<DL	<DL	360	<DL	1310	4990	<DL	<DL
Yellow Handle - Duplicate	<DL	<DL	336	<DL	1200	4620	<DL	12

A more extensive analysis of reproducibility is shown in Table 7. The standard deviation of five separate digestions and analyses for a yellow ball (Figure 4) show excellent precision.

It is interesting to note the lead level is high, in agreement with the XRF analysis. Several other elements, such as chromium, are also high. The XRF value reported for lead in the ball was 3940 mg/kg.

Regulations are continually changing and may require different elements to be monitored in the future, at different concentration levels. One way to help in preparing for that eventuality is the use of the universal data acquisition (UDA) feature, exclusive to the Optima ICP-OES software. In this case the Optima ICP-OES collects data for all of the wavelengths all of the time. If a standard is run at the time of the original data acquisition that includes more elements than the elements of interest at that moment, other elements can be measured with good quantitative accuracy by reprocessing at a later date. If an elemental concentration is of interest for an element that was not included in any of the usual multi-element standards, reprocessing can provide a semiquantitative result, usually within  $\pm 30\%$  of the true value.

Table 8 shows an example for a hydrochloric acid extract from a toy, extracted and measured using procedures specified in EN-71, Part 3. Both the original set of elements reported and the elements determined later (in blue) by reprocessing the data to examine the information previously stored for those elements are listed. This can be useful in assessing samples that may have been disposed or in better understanding the scope of samples in preparing for future analyses.

**Table 7. Analysis of Five Replicate Samples of a Yellow Ball.**

Element	Average (mg/kg)	SD
Antimony (271 nm)	10.6	0.49
Arsenic (189 nm)	12.4	1.8
Barium (233 nm)	707	3.1
Cadmium (228 nm)	78.3	0.73
Chromium (267 nm)	414	2.3
Lead (220 nm)	1980	9.7
Selenium (196 nm)	16.3	1.3
Mercury (254 nm)	<DL	-

## Conclusion

The regulatory landscape of toy measurements for hazardous metals is changing and will continue to change as elements, concentrations, and sample preparation procedures are refined and harmonized between the U.S. and Europe. Indeed, the lowest limits of 90 and 100 ppm are designated as what the CPSC deems to be feasible at the time and lower limits may be regulated in the future.

ICP-OES is the accepted certifying tool in determining a wide variety of metals that may contaminate toys, either in the substrate or a paint coating. Lead can be determined at the current 600 mg/kg concentration level permitted and the ICP-OES has sufficient detection capability that the new limits of 90 mg/kg can be reliably detected.

**Table 8. Universal Data Acquisition for Additional Elemental Data.**

Element	mg/kg extracted from solid
Antimony (271 nm)	6.7
Arsenic (189 nm)	1.5
Barium (233 nm)	1850
Cadmium (228 nm)	< DL
Chromium (267 nm)	655
Lead (220 nm)	2900
Selenium (196 nm)	< DL
Aluminum (396 nm)	438
Cobalt (228 nm)	< DL
Copper (327 nm)	< DL
Manganese (257 nm)	< DL
Nickel (231 nm)	< DL
Tin (189 nm)	< DL
Zinc (206 nm)	1230

ICP-OES and XRF are complementary techniques that work well together at the current regulatory level of 600 mg/kg. XRF provides rapid screening with a high degree of confidence when the sample is contaminated with lead. Highly accurate ICP analyses can be efficiently directed to the samples most likely contaminated using hand-held XRF's quick screening and no-sample prep characteristics. Samples identified as contaminated can be prepared and analyzed by ICP with less wasted time on uncontaminated samples, because of the positive screening result. As the limits are lowered, XRF will continue to perform as a screening technique, with ICP-OES providing confirmation with regulatory requirements.

## References

1. Consumer Product Safety Improvement Act, <http://www.cpsc.gov/ABOUT/Cpsia/legislation.html>
2. Testimony of Dana Best, MD, MPH, FAAP on behalf of the American Academy of Pediatrics, [http://www.aap.org/visit/coeh/COEH\\_Ltr\\_2007-09-20\\_Lead\\_Testimony.pdf](http://www.aap.org/visit/coeh/COEH_Ltr_2007-09-20_Lead_Testimony.pdf)
3. EN-71, Part 3 The Safety of Toys, Migration of Certain Elements, may be purchased from [http://www.standardsuk.com/shop/products\\_view.php?prod=26164](http://www.standardsuk.com/shop/products_view.php?prod=26164)
4. ASTM D-963-07, Standard Consumer Safety Specification for Toy Safety, may be purchased from <http://www.astm.org>

## UV/Vis Spectroscopy

## Author

Christopher Lynch

PerkinElmer, Inc.  
Shelton, CT 06484 USA

## Determination of Formaldehyde Content in Toys and Fabrics Using UV/Vis Spectrometry



Figure 1. LAMBDA XLS+ UV/Vis spectrometer.  
Wavelength: 540 nm; Measurement Mode:  
Absorbance; Cell 10 mm.

### Introduction

As product safety regulations for industry are becoming stricter, more testing at lower levels is required for toxic elements or hazardous organic chemicals such as formaldehyde in children's toys/clothing. Formaldehyde resins are used in fabrics to bind pigments to the cloth, as a fire retardant and to provide stiffness. In cotton and cottonblend fabrics they are used to enhance wrinkle resistance and water repellency. They can often be noted by the odor of treated fabric. The types of resins used include urea-formaldehyde, melamine-formaldehyde and phenolformaldehyde. Resins without formaldehyde are typically much costlier. Increases in temperature (hot days) and increased humidity both increase the release of formaldehyde from coated textiles.

Long term chronic exposure or short-term exposure to high concentrations of formaldehyde can lead to cancer. In animal studies, rats exposed

to high level of formaldehyde in air developed nose cancer. The European standard EN 71 specifies safety requirements for toys. EN 71, Part 9 contains requirements for organic chemical compounds in toys and specifies the limit for accessible textile components of toys intended for children under 3 years of age. The limit specified for formaldehyde content is not more than 30 mg/kg or 2.5 mg/L in the aqueous migrate prepared following EN 71, Part 10. EN 71, Part 11, section 5.5.3 specifies a method of analysis.

## Experimental

The analysis was carried out using a PerkinElmer LAMBDA™ XLS+ UV/Vis Spectrometer.

## Apparatus and Reagents

Table 1. List of apparatus and reagents used.\*

Volumetric flasks, volume 50 mL
Volumetric flasks, volume 100 mL
Hot plate for distillation
Boiling chips
Erlenmeyer flasks, volume 100 mL
Eppendorf® micropipettes
Ammonium acetate, anhydrous
Acetic acid, glacial
Pentane-2,4-dione
Hydrochloric acid, 1 mol/L
Sodium Hydroxide solution 1 mol/L
Starch solution freshly prepared, 2 g/L
Formaldehyde solution, 370 g/L to 400 g/L
Standard iodine solution, 0.05 mol/L
Standard sodium thiosulfate solution, 0.1 mol/L
Water, deionized
Stainless steel tweezers
250 mL glass bottle with flat base, screw neck and PTFE lined rubber septum (Make: Schott Duran)
Magnetic stirrer

\*The reagents, chemicals, standards used were of ACS grade.

**Pentane-2,4-dione reagent:** Dissolved 15 gm of anhydrous ammonium acetate, 0.3 mL glacial acetic acid and 0.2 mL pentane-2,4-dione reagent in 25 mL water and diluted up to the mark in 100-mL volumetric flask with water.

**Reagent without pentane-2,4-dione:** Dissolve 15 gm of anhydrous ammonium acetate and 0.3 mL glacial acetic acid in 25 mL water and diluted up to the mark in 100-mL volumetric flask with water.

**Formaldehyde stock solution:** Transferred 5.0 mL of formaldehyde solution into a 1000-mL volumetric flask and made up to the mark with water.

### Standardization of formaldehyde stock solution:

10.0 mL of freshly prepared formaldehyde stock solution was transferred into a conical flask, added 25.0 mL of a standard iodine solution and 10.0 mL of sodium hydroxide solution. The solution was allowed to stand for five minutes. Then the solution was acidified with 11.0 mL of hydrochloric acid and titrated for excess iodine by standard sodium thiosulfate solution. 0.1 mL of starch solution was added when color of the solution became pale straw. After addition of starch solution, immediately the color was changed to deep blue-black. The titration was continued until the color changes from deep blue-black to colorless. Similarly, the blank titration was performed. The difference between titration values of blank and sample was used for calculation of formaldehyde contents in stock solution.

The concentration of formaldehyde was found to be 1.99 mg/L.

### Formaldehyde dilute standard solution (0.001 mg/mL):

2.5 mL of formaldehyde stock solution was transferred to 50-mL volumetric flask; mixed well and diluted up to the mark with water. 1 mL of this solution was further diluted to 100 mL with water and mixed well.

A series of reference solutions were prepared by pipetting suitable volumes of above formaldehyde dilute standard solution into a 50-mL conical flask as follows

Table 2. Calibration solutions.

	Amounts (mL) Formaldehyde dilute standard solution in 50-mL conical flask	Amount of pentane-2,4-dione reagent (mL)	Concentration (mg/L) of Formaldehyde after making volume to 30 mL with water
Blank	–	5.0	0.0
Reference 1	5.0	5.0	0.167
Reference 2	10.0	5.0	0.333
Reference 3	15.0	5.0	0.499
Reference 4	20.0	5.0	0.667
Reference 5	25.0	5.0	0.833

### Absorbance measurement of calibration solutions:

Absorbance measurements of calibration reference solutions and blank were done by using water as reference. The calibration curve was constructed by subtracting absorbance value of the blank solution (A<sub>2</sub>) from each of absorbances obtained from the calibration solutions. Figure 2 shows calibration graph.

**Sample preparation:** Three different toy samples made up with fabrics were selected for analysis. Sample with surface area of 10 cm<sup>2</sup> was taken and transferred to 250 mL extraction bottle with the help of tweezers. 100 mL of simulant (water, deionized) was added to the sample at 20 °C ± 2 °C and the extraction bottle closed. The extraction bottle was kept on a magnetic stirrer for uniform stirring of the solution over the period of 60 minutes. Aqueous migrate was then filtered through a plug of glass wool. 5.0 mL of aqueous migrate was transferred into a 50-mL conical flask followed by addition of 5.0 mL of pentane-2,4-dione reagent and 20.0 mL of water.

**Sample reference solution:** 5.0 mL of aqueous migrate was transferred into a 50-mL conical flask followed by addition of 5.0 mL of reagent without pentane-2,4-dione and 20.0 mL of water.

These solutions were shaken for about 15 seconds and immersed in a thermostatic water bath at 60 °C ± 2 °C for ten minutes followed by cooling for about two minutes in a bath of iced water.

Absorbance measurements were done between 35 minutes and 60 minutes from the time when the conical flasks were placed in a water-bath at 60 °C.

Absorbance measurements of sample solutions were done by using the reference solution as reference (A<sub>1</sub>).

**Calculation of analyte concentration:** Calibration curve was prepared manually by taking the absorbance values obtained for calibration reference solutions. To determine the analyte concentration, absorbance value of blank solution (A2) was subtracted from absorbance value of sample solution (A1). The subtracted absorbance value was then read off from the manual calibration curve.

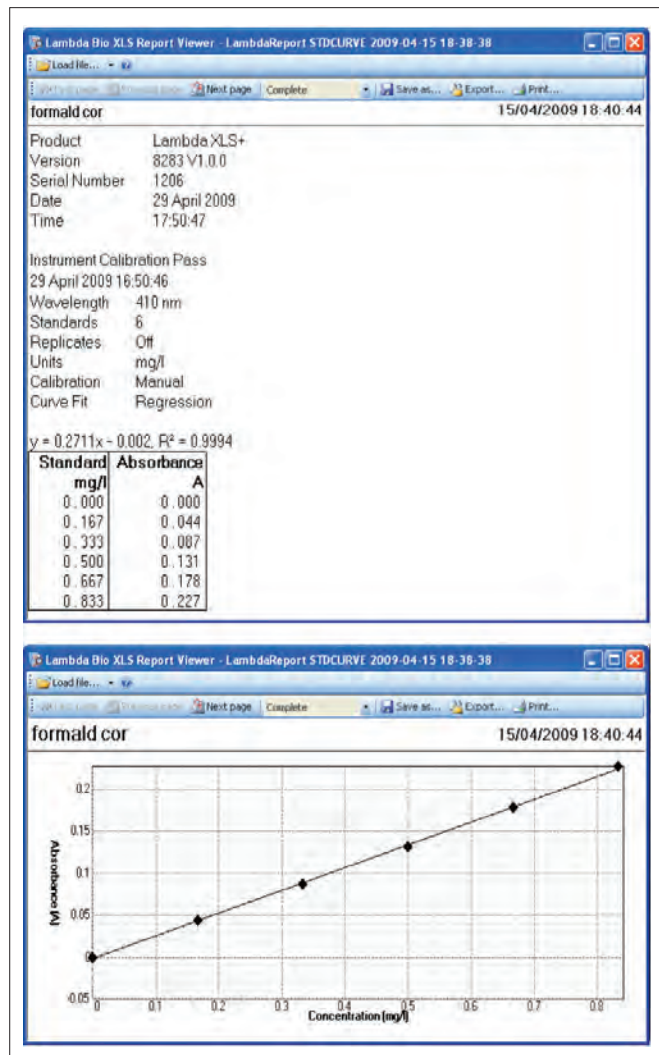


Figure 2. Calibration graph.

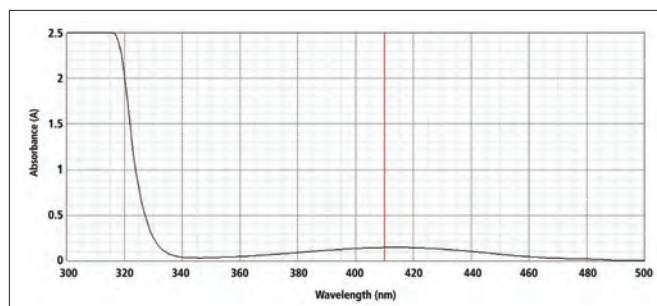


Figure 3. Spectrum of color formed for the determination of 'Formaldehyde' contents.

The formaldehyde content in aqueous migrate was calculated by using following equation,

$$C_s(\text{mg/L}) = C \times 5 \text{ where,}$$

$C_s$  = concentration of formaldehyde in the sample solution (mg/L)

5 = dilution factor of the sample solution.

## Results and discussion

### Calibration – linearity:

The six different levels of calibration standards were prepared in the range from 0.167 mg/L to 0.833 mg/L with the reagent blank as first level. Results showed linearity with a good correlation co-efficient of 0.9994. The calibration curve is shown in Figure 2. Figure 3 shows the spectrum of the developed color, confirming the peak maximum at 410 nm.

**Method detection limit:** 10 replicate reagent blank solutions were prepared to make an estimate of method detection limit. To determine method detection limit, seven replicate aliquots of fortified reagent water (0.1 mg/L) were prepared and processed through entire analytical method. The method detection limit was calculated as follows,

$$\text{MDL} = (t) \times (s) \text{ where,}$$

$t$  = student's t value for a 99% confidence level and a standard deviation estimate with n-1 degrees of freedom. [t = 3.143 for seven replicates].

$s$  = standard deviation of replicate analyses.

The method detection limit was found to be 0.0178 mg/L.

**Sample analysis:** Three different toy samples, as shown in Figure 4, made up of polyester, rayon and synthetic fibers were analyzed as per the procedure given under 'Experimental'. Results obtained in duplicate were averaged and are shown in Table 3. These measurements are below the action level of 2.5 mg/L in the aqueous migrate.

Table 3. Sample analysis results.

Sample	Concentration (mg/L)
Toy 1 (polyester fiber)	0.18
Toy 2 (rayon fiber)	0.25
Toy 3 (synthetic fiber)	Not Detected

**Spike recovery studies:** A recovery study was performed by spiking 0.5 mg/L concentration in three replicates of the synthetic fiber sample aqueous migrate. The results are summarized in Table 4. As seen in Table 4 the recoveries are good, falling within the usual acceptance range of 80-120% recovery.

Table 4. Replicate spike recoveries.

Sample	% Recovery
Sample 1	113
Sample 2	107
Sample 3	105



Figure 4. Toy samples.

## Conclusion

The LAMBDA XLS+ UV/Vis spectrometer can be used to measure formaldehyde contents in fabric toys. The detection limit is sufficient to determine formaldehyde at the level of 30 mg/kg in the original material or 2.5 mg/L in the aqueous migrate solution as specified in the current version of EN-71. Linearity and spike recoveries further validate the performance of this methodology.

## References

1. EN 71 Safety of Toys – Part 9, 10, 11 – organic chemical compounds in toys – requirements, limits and sample extraction procedure.
2. 40 CFR, Part 136 Appendix B – Definition and Procedure for the Determination of the Method Detection Limit.

FT-IR Spectroscopy and  
Thermogravimetric Analysis

## Authors

Dale C. Mann, BS

Keith G. Cline, PE

MDE, Inc  
700 S. Industrial Way  
Seattle, WA 98108

## Confirmation of the Presence of Styrene Butadiene Resin (SBR) Polymer in Drywall Primer Applications.

A combination of Fourier Transform Infrared (FT-IR) Spectrometry and Thermogravimetric Analysis (TGA) was used to distinguish and identify styrene butadiene from polyvinyl acrylic resin-based interior latex primers and paints. A wide range of standard mixtures of the two resins were analyzed and the relative percentages of the two accurately estimated using the two methods. The isolation techniques and analytical methods of analysis were developed to verify the composition of primer/texture/paint applications used on interior condominium walls.

### Introduction

Over the past several years, architects and developers of condominium housing projects in western Washington have begun to utilize the Washington State's Energy Code<sup>1</sup> allowing a rated vapor barrier primer/paint to replace the traditional polyethylene plastic sheeting or Kraft-backed insulation bats historically used in the construction to achieve the required water vapor perm rating of 1.0 or less. Building specifications for the interior wall finish called for the application of a vapor barrier rated primer followed by the normal decorative paint/top coat.

A literature review of many major paint distributors of interior vapor barrier primers shows the resin in the vapor barrier primers is a styrene butadiene rubber (SBR) formulation. This formulation is quite different from the normal drywall primer, polyvinyl acrylic (PVA). Litigation involving the perceived lack of a SBR primer on interior drywall surfaces soon led MDE Forensic Laboratories to develop methods to positively identify the presence/absence of an SBR primer after a PVA top coat had been applied to the walls.

## Laboratory Methods

Cross sections of the texture, primer and paint applied to the interior of the drywall were prepared by mounting specimens in acrylic and polishing. Examination of these samples showed the presence of a primer layer applied to the drywall, followed by a texture and finally the decorative top coat paint. The primer layer exhibited an average dry film thickness that met all manufacturers' specifications, regardless of the potential resin formulation of the primer.

### Fourier Transform Infrared Spectrometry

The decorative top coat and texture were physically separated from the primer layer. The primer layer and uppermost layer of drywall paper were peeled off and ultrasonically extracted using a 50/50 mixture of tetrahydrofuran/methylene chloride solvent. The solvent was evaporated to dryness and the isolated primer resin analyzed using FT-IR<sup>2,3</sup>.

FT-IR results for pure SBR and PVA resins are shown in Figure 1. The predominant absorbances for an SBR resin, resulting from the styrene content, are at 700 and 730  $\text{cm}^{-1}$ . Figure 2 illustrates some typical results from the extracted condominium primer layers. Many of these did not yield pure SBR spectra, however absorbances typically due to styrene were readily detected in all extractions. The primary absorbances in these spectra appeared to be due to the co-extracted presence of a quantity of PVA resin. Note that a PVA resin decorative top coat was originally present on each sample.

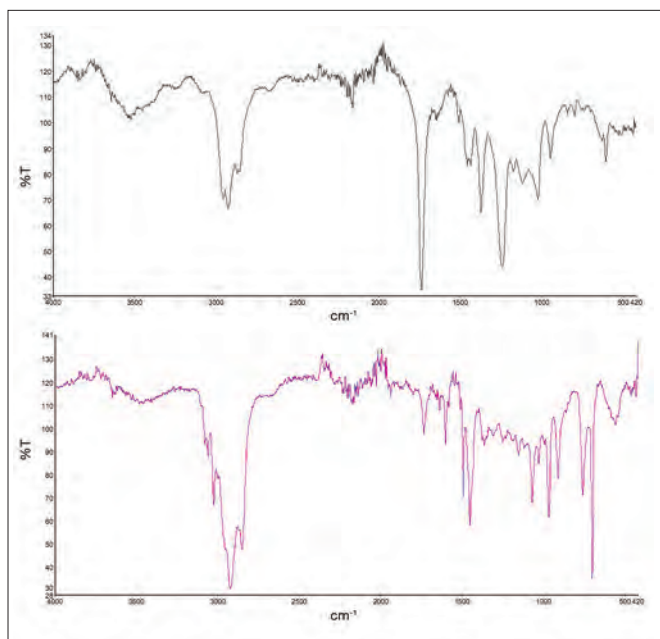


Figure 1. FT-IR comparison of a pure PVA resin (top) and a pure SBR resin (bottom).

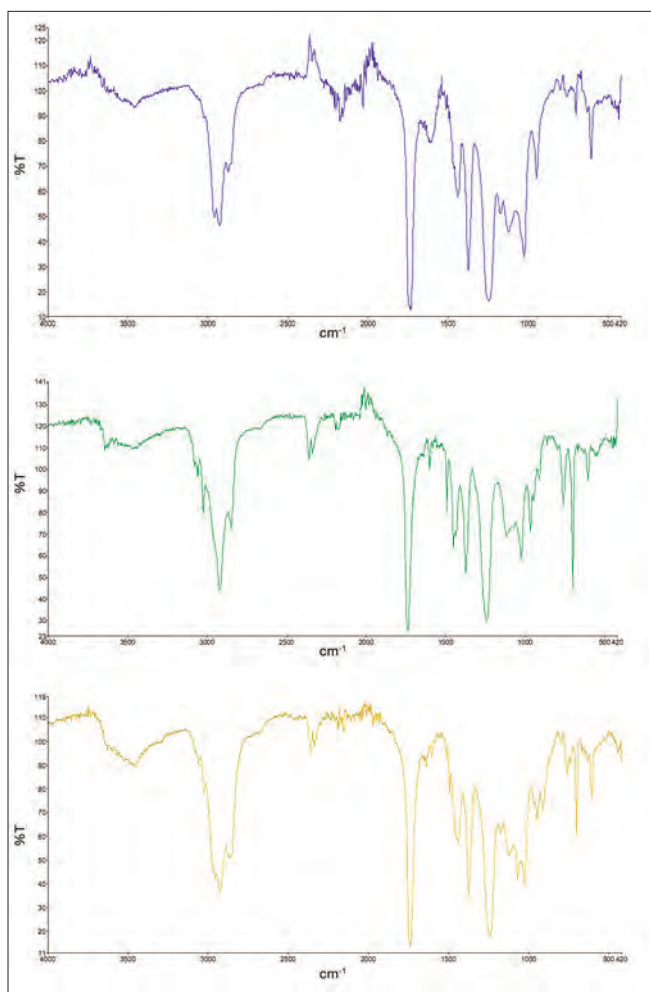


Figure 2. Examples of three "typical" FT-IR results from the solvent extraction of isolated primer layers from three separate condominium units. Note the lack of a definitive SBR spectra but the presence of a styrene absorption at 700  $\text{cm}^{-1}$ .

### Thermogravimetric Analysis

Resins extracted from both PVA and SBR formulated paints were analyzed using TGA<sup>4,5,6</sup>. The samples were analyzed using nitrogen gas and a temperature program of 25-600  $^{\circ}\text{C}$  with a 20  $^{\circ}\text{C}/\text{min}$  ramp. This temperature program caused the complete pyrolysis of the paint resin samples. Evaluation of the data showed distinctly different slopes in the weight loss versus temperature curves. The first derivative of these curves was used to identify the inflection points. The temperatures of these inflection points were found to be 350  $^{\circ}\text{C}$  for the PVA resin and 425  $^{\circ}\text{C}$  for the SBR resin. Figure 3 illustrates the first order weight loss curve and the first derivative of that curve for both pure SBR and PVA resins.

### Pyrolysis Gas Chromatography/Mass Spectrometry

Pyrolysis GC/MS methodology was also investigated as a means of verifying the presence of SBR by using the presence of styrene. However, it was found that small amounts of styrene were produced during the pyrolysis of PVA resin. This artifact and the desire to use available instrumentation led us to not pursue this methodology.

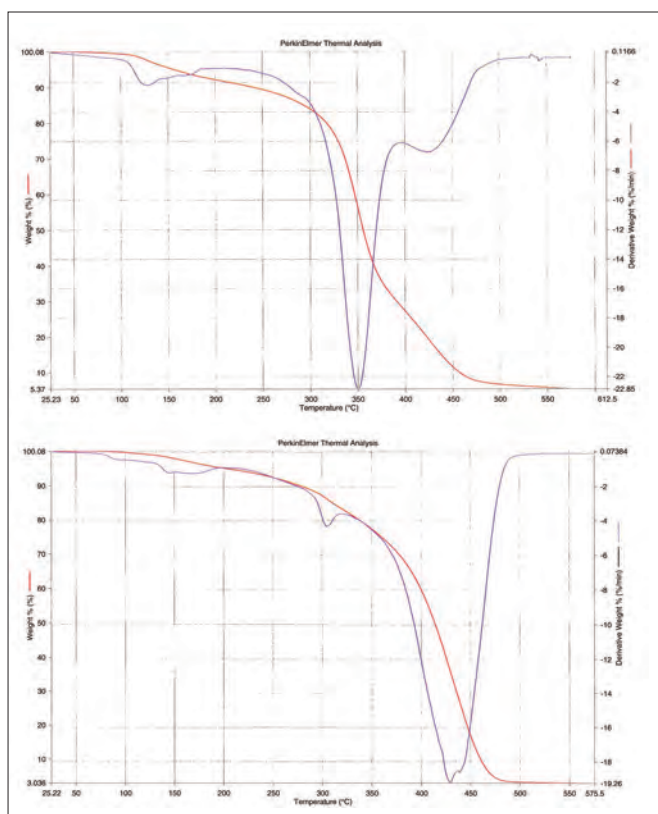


Figure 3. TGA comparison of a pure PVA resin (top) and a pure SBR resin (bottom). The weight loss vs. temperature is shown in blue and the 1st derivative of that curve is shown in red.

### Analysis of Standard Mixtures

Pure SBR and PVA resins were extracted from exemplar primer and paint products. The purity of the resulting evaporated extracts was evaluated using FT-IR and TGA. Mixtures of the two were made by adding a weighed amount of each resin, dissolving in solvent to homogenize and drying for analysis.

The standard mixtures were 0%, 10%, 30%, 50%, 70%, 90% and 100% of SBR resin in PVA. These mixtures were analyzed using both FT-IR and TGA. The ratio of the peak height at  $700\text{ cm}^{-1}$  (the styrene absorption for the SBR) to the  $1740\text{ cm}^{-1}$  (the carbonyl adsorption for the PVA) was used to estimate the relative amounts of the two resins. Figure 4 illustrates typical FT-IR results and Figure 5 depicts the resulting calibration curve.

The standard mixtures were likewise analyzed using TGA. The ratio of the peak heights of the second derivative plots at  $425\text{ }^{\circ}\text{C}$  (for the SBR) to the  $350\text{ }^{\circ}\text{C}$  (for the PVA) was used to estimate the relative amounts of the two resins in the mixture. Figure 6 illustrates typical TGA 1st derivative plots and Figure 7 depicts the resulting calibration curve using the log of the ratio of the peak heights of these curves.

### Subject Samples

Samples isolated for the several condominium projects evaluated during the course of the investigations yielded a wide range of FT-IR and TGA results. In some instances, a SBR was easily and cleanly confirmed by both analytical methods. In other condominium projects evidence of SBR was much less pronounced. Figures 2 and 8 depict the range of FT-IR and TGA results for some of these investigations.

Some “contamination” of the physically isolated primer layer by the overlying PVA paint was expected due to the difficulty of mechanically separating the coating layers during sample preparation. This was particularly true when the primer and paint had been applied without an intervening layer of texture. For some projects only low relative concentrations of SBR were calculated, even when it was thought a “clean” isolation of the primer layer was performed.

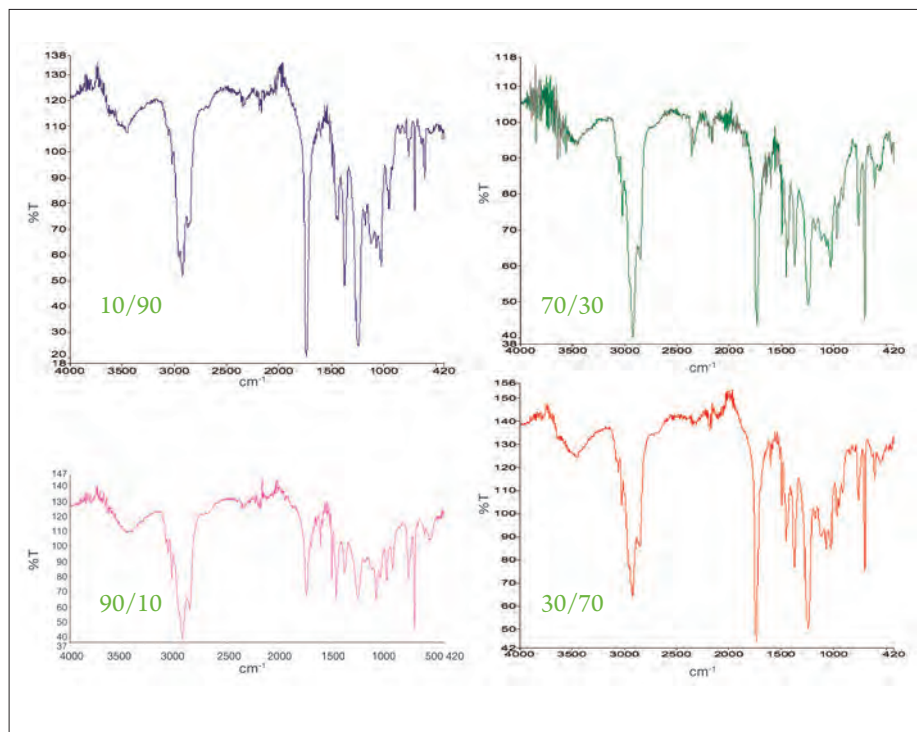


Figure 4. FT-IR comparison of standard mixtures of SBR and PVA resins. The SBR/PVA ratios are 10/90 (blue), 90/10 (red), 70/30 (green), and 30/70 (brown).

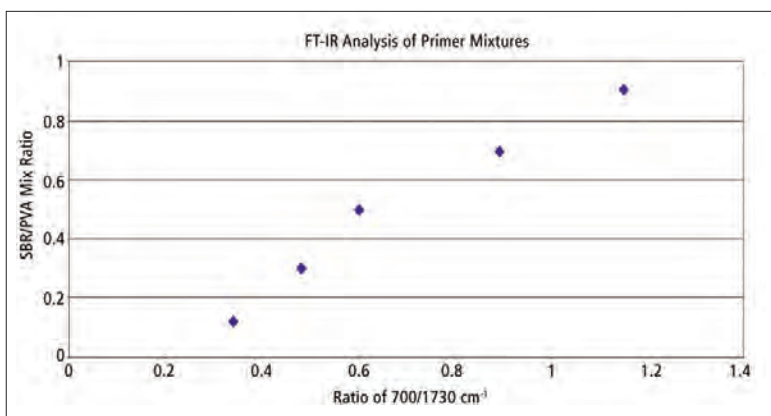


Figure 5. Calibration curve for the FT-IR analysis of standard mixtures of SBR and PVA. Peak height ratios are the SBR/styrene absorbance at 700 cm<sup>-1</sup> divided by the PVA/carbonyl absorbance at 1732 cm<sup>-1</sup>.

As laboratory work progressed during these investigations, many of the locally available drywall primers (both vapor barrier products and traditional drywall primers) were analyzed. Though not clearly specified on product labels or in the product technical data sheets, it became apparent during the laboratory analysis that many primers labeled as vapor barrier products were actually a blend of SBR and PVA resins. At least one manufacturer alluded to this in their product information. Figures 9 and 10 depict the FT-IR and TGA results for a variety of exemplar vapor barrier primers.

Calculation of the relative amount of SBR to PVA in the analyzed exemplar primers showed a range from 100% SBR to 20% SBR. In one condominium project, the calculated SBR in the isolated primer layer never exceeded 20%. The primer that was later confirmed to have been used as the vapor barrier was a blended resin containing only 20% SBR. This information was only confirmed after the laboratory results were used as motivation to persuade the manufacturer to release their formulation.

## Summary

The combination of FT-IR and TGA analysis of vapor barrier primers is a powerful analytical method useful for confirming the presence/absence of a styrene butadiene resin in the primer. A semi-quantitative estimate of the relative amount of the SBR compared to the more traditionally used PVA resin is possible.

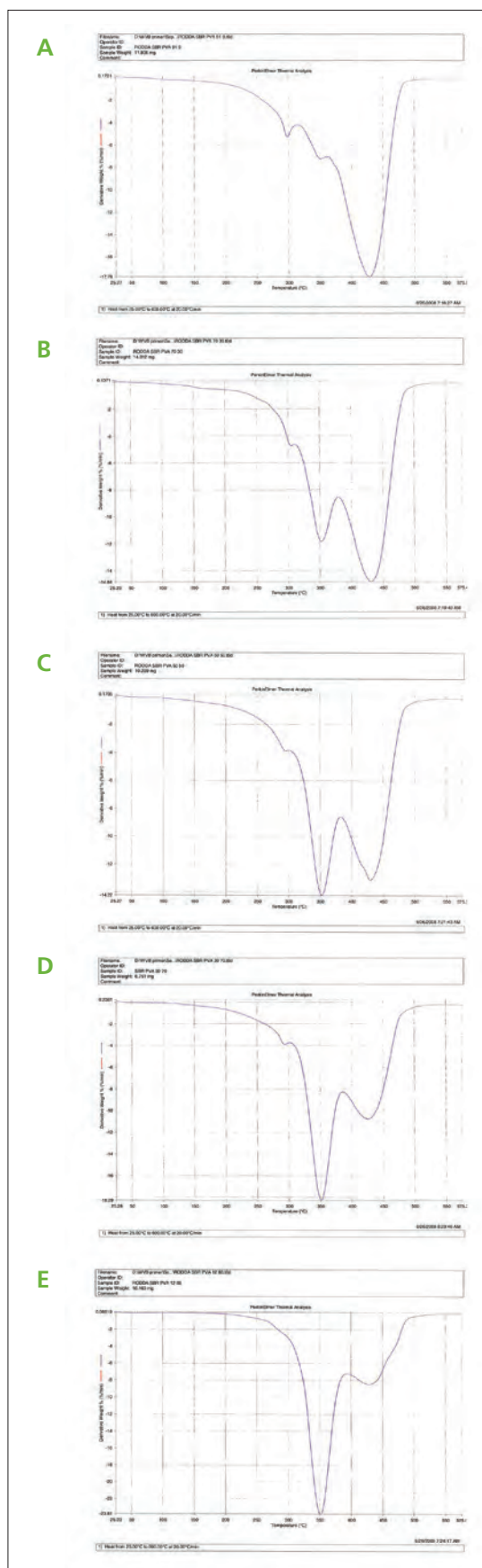


Figure 6. TGA comparison (using 1st derivative of weight loss curve) of standard mixtures of SBR and PVA resins. From top to bottom, the SBR/PVA ratios are 90/10 (A), 70/30 (B), 50/50 (C), 30/70 (D) and 10/90 (E).

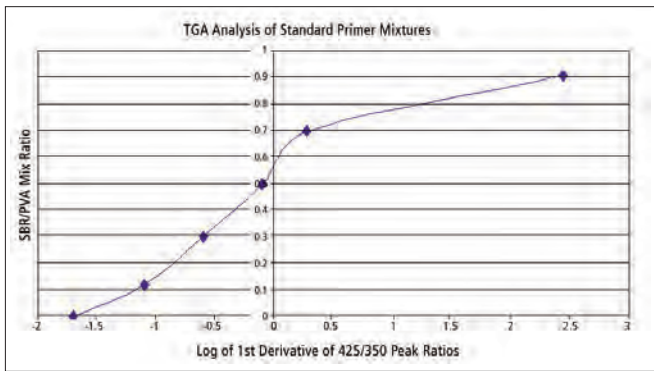


Figure 7. Calibration curve for the TGA analysis of standard mixtures of SBR and PVA. Calculated ratios are the SBR/1st derivative peak height at 425 °C divided by the PVA/1st derivative peak height at 350 °C.

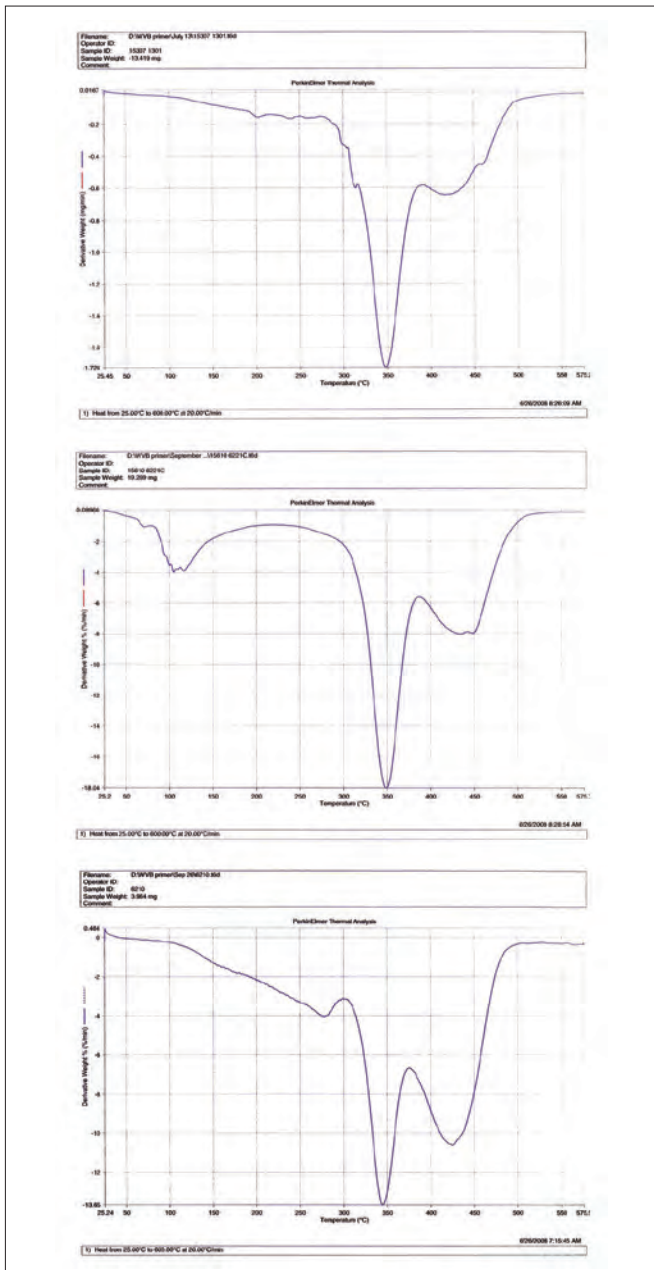


Figure 8. Examples of three “typical” TGA 1st derivative results from the solvent extraction of isolated primer layers from three separate condominium units.

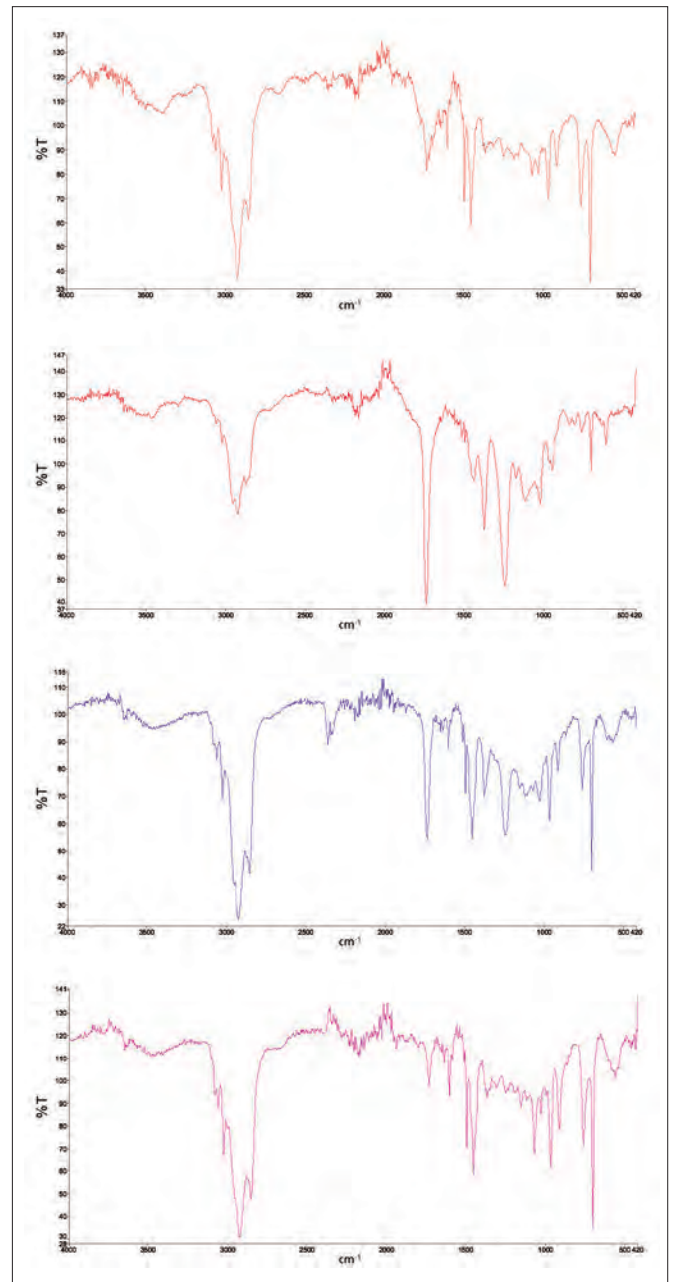


Figure 9. FT-IR spectra of four different brands of vapor barrier primer. Each is a mixture of SBR and PVA resins.

## References

1. Washington State Energy Code, 502.1.6.1-4, 1994.
2. ASTM® D3168-85 (2005) Standard Practice for Qualitative Identification of Polymers in Emulsion Paints, 2005.
3. Kolske, Joseph V. Paint and Coating Testing Manual, Chapter 75:850-852, 1995.
4. Earnst, C.M, Ed. The Compositional Analysis by Thermogravimetry, STP 977, ASTM®, 1988.
5. ASTM® E1131-03 Standard Test Method for Compositional Analysis by Thermogravimetry, 2003.
6. ASTM® E2008-06 Standard Test Method for Volatility Rate by Thermogravimetry, 2006.

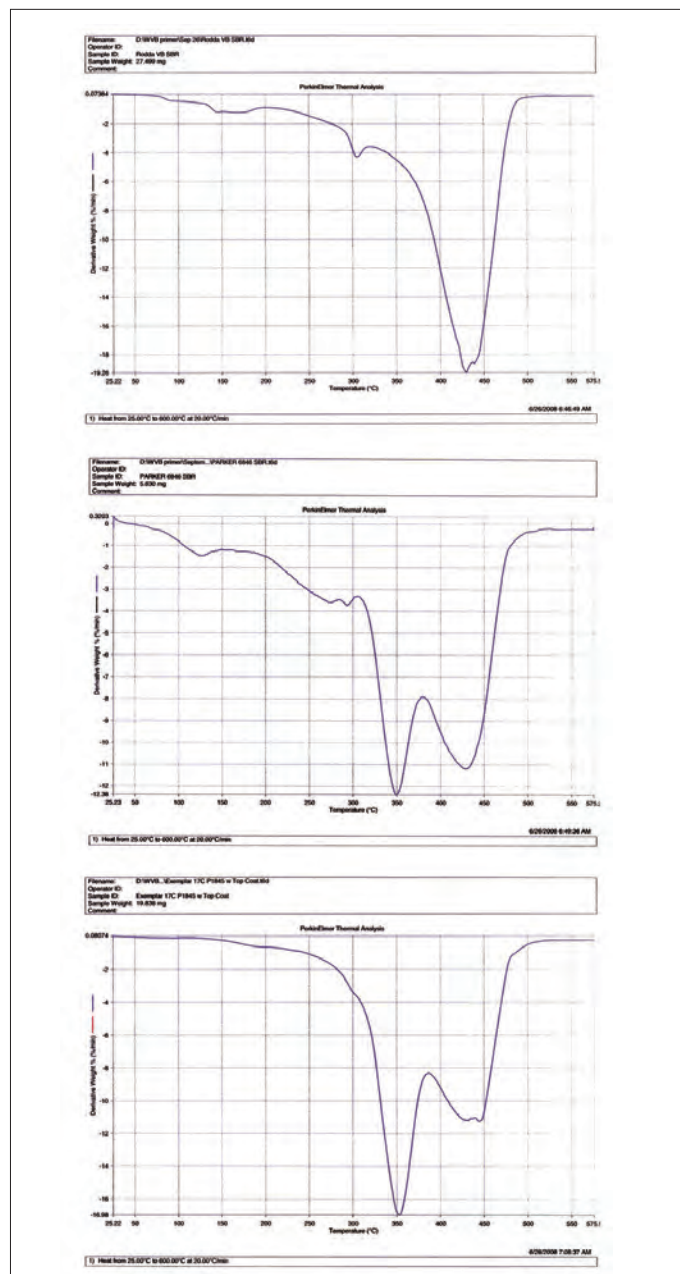


Figure 10. TGA 1st derivative curves of three different brands of vapor barrier primer. Each is a mixture of SBR and PVA resins.

Gas Chromatography/  
Mass Spectrometry**Author****Meng Yuan****PerkinElmer, Inc.  
Shelton, CT 06484 USA**

## Increasing Sensitivity in the Determination of Volatile Organics in Toys with Headspace Trap-GC/MS

### Introduction

The safety of toys has gained publicity on a global scale, with numerous recalls and new regulations. One aspect of toys which needs to be considered under European Union regulations (EN-71) is the content of volatile organic compounds (VOCs). These compounds, such as benzene and toluene, are residual after the manufacture of various types of polymers, additives and coatings. VOCs are potentially hazardous to the health of children if present at high levels in toys. As a result, it is necessary to accurately determine the level of VOCs in toys to ensure safety.

This application note will present an approach developed to measure VOCs at low levels using headspace trap (HS Trap) sample introduction with gas chromatography/mass spectrometry (GC/MS). This technique is based on European standard method EN-71 Part 11,<sup>1</sup> which specifies details for the analysis of toy and toy-material extracts – included in this method are headspace-GC/MS parameters for VOC analysis. In this application note, the sensitivity of the method presented in EN-71 is improved with the use of headspace-trap instrumentation.

In addition to method optimization and calibration, a variety of toys are analyzed and the level of VOCs determined.

## Experimental

VOCs in toys are identified and the amount is determined by HS Trap-GC/MS. Samples are heated in a sealed vial to 80 °C, allowing the volatile organics to migrate from the toy material into the headspace of the vial. The sample is equilibrated at this temperature for 40 minutes while this process occurs. Using the automated headspace trap technology of the PerkinElmer® TurboMatrix™ HS Trap, the headspace gas is extracted from the vial, concentrated on an adsorbent trap, and injected into a GC/MS system. In this application, a PerkinElmer Air Toxics trap was used.

The technique is very sensitive because the trap provides focusing before instrument introduction and remains clean because of limited sample contact. Table 1 shows the instrumental setup parameters for the HS Trap-GC/MS system.<sup>2</sup>

The headspace transfer line was passed through the GC injector port and connected to the GC column using a universal capillary-column connector.

### Calibration-Standards Preparation

A 20 ng/μL standard stock solution was prepared by diluting 0.200 mL of a 1000 μg/mL VOC standard to 10.0 mL with methanol. From this, a working solution of 1 ng/μL was prepared by diluting 0.50 mL of the 20 ng/μL standard stock solution to 10 mL with methanol. Working calibration standards at 5, 10, 20, 50, and 100 ng/μL were prepared fresh each day.

An internal standard solution of toluene-d8 at 20 ng/μL was prepared by diluting 0.2 mL of a 1000 μg/mL toluene-d8 solution to 10 mL with methanol.

The working curve was prepared by injecting 5 μL and 10 μL of each working calibration standard and 1 μL, 2.5 μL and 5 μL of each standard-stock solution into headspace vials. Additionally, 5 μL of the 20 ng/μL internal standard solution was injected into each headspace vial. All headspace vials were sealed immediately and transferred to the headspace-trap vial tray.

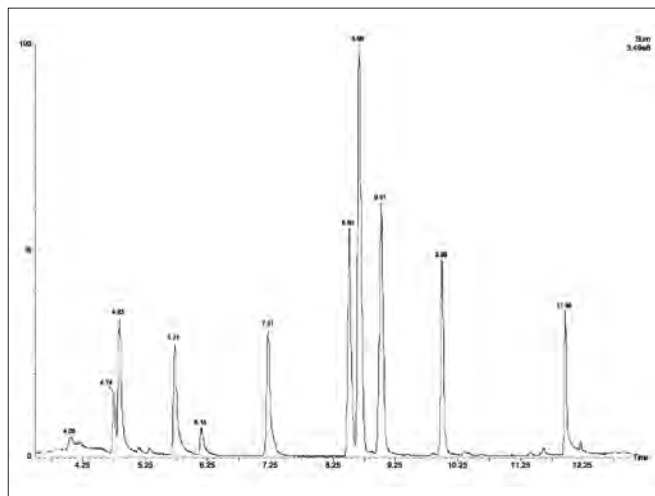


Figure 1. 50 ng injection of a reference standard for volatiles analysis by EN-71 with HS Trap.

Table 1. Instrument Parameters.

Sample Introduction	PerkinElmer TurboMatrix HS-40 Trap
Needle Temp	90 °C
Transfer Line Temp	120 °C
Oven Temp	80 °C
Trap Low Temp	45 °C
Trap High Temp	280 °C
Dry Purge (Helium)	5 min
Trap Hold Time	6 min
Desorb Time	0.5 min
Thermostating Time	40 min
Pressurization Time	1 min
Decay Time	2 min
Column Pressure	15 psi
Vial Pressure	35 psi
Desorb Pressure	10 psi
Transfer Line	Fused Silica 2 m x 320 μm (Part No. N9301357)

Gas Chromatograph	PerkinElmer Clarus® 600 GC
Headspace Connector	Universal Connector (Part No. N9302149)
Oven Program Initial Temp	50 °C
Hold Time 1	1 min
Ramp 1	15 °C/min to 210 °C
Hold Time 2	5.33 min
Vacuum Compensation	On
Column	Elite™ Volatiles 30 m x 0.25 mm x 1.4 μm (Part No. N9316388)
Carrier Gas	Helium
Mass Spectrometer	PerkinElmer Clarus 600 MS
Mass Range	45-220 u
Solvent Delay Time	0.1 min
Scan Time	0.20 sec
InterScan Delay Time	0.05 sec
Transfer Line Temp	200 °C
Source Temp	200 °C
Multiplier	400 V

## Results

Five calibration levels are recommended for method EN-71 Part 11. The standard deviation of response should be below 15 %RSD (relative standard deviation). Table 2 shows %RSD data of a 50 ng standard. All compounds meet the specified criteria of RSD less than 15%. Figure 1 is an example chromatogram of a 50 ng standard injection.

Toluene-d8 was used as an internal standard. Peak-area ratio was used to calculate amounts of VOC.

The peak-area ratio for the component in the sample was calculated by dividing the peak area of the component (target ion) by the peak area (target ion) of the internal standard toluene-d8 (IS):

$$\text{peak-area ratio} = \frac{\text{peak area of the component ion}}{\text{peak area of the IS ion}}$$

Amounts of VOC (concentration in ng) were calculated by plotting the peak area ratio in the following calibration functions:

$$\text{conc}(x)\text{in ng} = \frac{y(\text{peak-area ratio}) - b}{a} = y^{ax+b}$$

Method detection limits (MDL) were calculated to give an indication of the measurement capability. The quantification limit is generally 10x above the MDL. The method detection limits were calculated using the following equation:

$$\text{MDL} = t_{(n-1, a = .99)} \times s$$

An empty vial was analyzed to determine the baseline and seven samples were prepared at 5 ng. Each individual MDL was obtained by multiplying the standard deviation by the 99% t-statistic. Table 2 also shows the list of calculated MDLs.

Following the calibration of the system, 4 toy samples (toy ball, noise putty, modeling compound, crab) obtained from the local market were analyzed. The resultant chromatogram for the analysis of the toy-ball sample is pictured in Figure 2. The sample preparation with headspace analysis is very simple.

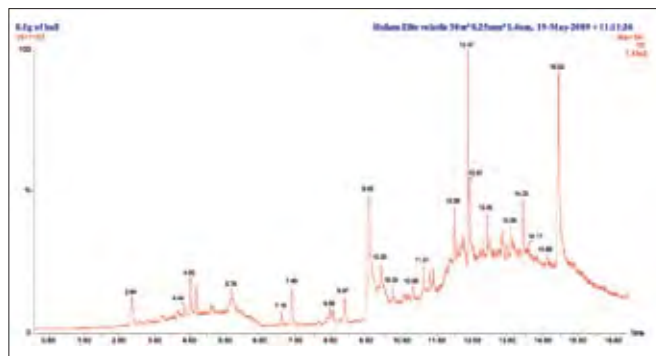


Figure 2. Total ion chromatogram of 0.1 g of toy-ball sample.

**Table 2. Calibration Table for 12 Volatiles.**

Name	Retention Time	Quantifier Ion	Qualifier Ion 1	Qualifier Ion 2	%RSD	r <sup>2</sup>	MDL (µg/g)
Dichloromethane	4.041	49	86	84	9.51	0.9962	0.002
Benzene	5.703	78	77	52	4.41	0.9939	0.002
Trichloroethylene	6.128	130	132	95	4.31	0.9970	0.003
Toluene-d8	7.134	98	100	–	Internal Standard		–
Toluene	7.192	91	92	65	2.62	0.9995	0.002
Ethylbenzene	8.487	91	106	51	5.45	0.9993	0.002
m,p-Xylene	8.649	91	106	105	6.42	0.9992	0.002
Cyclohexanone	8.972	55	98	–	6.76	0.9979	0.003
o-Xylene	8.997	91	106	105	5.94	0.9979	0.002
1,3,5-Trimethylbenzene	9.973	105	120	119	4.82	0.9983	0.002
Nitrobenzene	11.595	77	123	51	4.91	0.9956	0.010
Isophorone	11.958	82	138	54	8.42	0.9959	0.009

**Table 3. VOC Content ( $\mu\text{g/g}$ ) for Four Toy Samples.**

	Sample	( $\mu\text{g/g}$ )
<b>Ball</b>	Dichloromethane	68.0
	Benzene	11.1
	Toluene	26.5
	Ethylbenzene	10.5
	m,p-Xylene	10.4
	Cyclohexanone	94.3
	o-Xylene	13.2
	1,3,5-Trimethylbenzene	15.4
	Isophorone	15.1
<b>Noise Putty</b>	Benzene	26.1
	Toluene	19.4
	Cyclohexanone	84.5
	Nitrobenzene	9.5
	<b>Modeling Compound</b>	Benzene
Ethylbenzene		71.6
m,p-Xylene		20.3
o-Xylene		16.0
<b>Crab</b>		Benzene
	Toluene	62.8
	Ethylbenzene	16.4
	m,p-Xylene	11.9
	Cyclohexanone	303.0
	Isophorone	67.7

A known amount of the toy was cut into small (1 mm x 1 mm) pieces with a razor blade and placed into the headspace vial, internal standard was added and the vial was capped. Detectable solvents were seen in each sample (Table 3) – however, the levels determined in this application were below regulatory limits.

## Discussion

Headspace trap is an additional sample-handling technology to improve upon the sensitivity of static headspace. In this article, HS Trap demonstrated high sensitivity and linearity across the range of 25–500 ng.

The HS Trap uses heat to extract compounds out of the toys into the headspace, offering three advantages: easy sample preparation, high sensitivity, and no cross-contamination of samples. After the analytes are extracted, the trap is dry-purged to eliminate the moisture. Then the trap is heated and carrier gas transfers a narrow band of the desorbed analytes into the GC/MS system.

Table 4 compares the guideline of EN-71 for selected compounds with the MDL achieved using this method. The method developed provides sufficient capability to measure with confidence at the concentrations lower than regulatory level.

**Table 4. MDL Guideline of EN-71 and MDL in this Method.**

	MDL in EN-71 (ng)	MDL in this Method (ng)
Dichloromethane	10	2.2
Benzene	30	1.7
Trichloroethylene	20	3.1
Toluene	20	2.2
Ethylbenzene	40	1.5
m,p-Xylene	30	1.8
Cyclohexanone	30	2.8
o-Xylene	20	1.9
1,3,5-Trimethylbenzene	10	2.0
Nitrobenzene	60	10.2
Isophorone	40	9.6

## Conclusion

This application note shows that the Clarus 600 GC/MS system with TurboMatrix HS Trap meets and exceeds the requirements for method EN-71 Part 11, including minimum detection limits and calibration requirements. The calibration of the system was demonstrated across the range of 25–500 ng, with a linear response. Toy samples were analyzed and the VOC content was determined. Advantages of the headspace-trap technology for this application include ease of use, high sensitivity, ease of disposable sample vials, and no cross-contamination of samples. Plus, the novel GC oven design of the Clarus 600 GC improves separation and decreases run time.

## References

1. EN-71 Part 11 "Safety of toys - Part 11: Organic chemical compounds – Methods of analysis" 2004-07-01
2. Yuan, Meng "Measuring Volatile Organic Compounds by Headspace Trap GC-MS in the Beijing Food Laboratory", American Laboratory, On-Line Edition, April 2009
3. Yuan, Meng "Reliably Detect 86 of Pesticides in a Single Run Down to 10pg with GC/MS in the Beijing Food Lab", PerkinElmer Field Application Report, available from [www.perkinelmer.com](http://www.perkinelmer.com)

PerkinElmer, Inc.  
940 Winter Street  
Waltham, MA 02451 USA  
P: (800) 762-4000 or  
(+1) 203-925-4602  
[www.perkinelmer.com](http://www.perkinelmer.com)



---

For a complete listing of our global offices, visit [www.perkinelmer.com/ContactUs](http://www.perkinelmer.com/ContactUs)

Copyright ©2009, PerkinElmer, Inc. All rights reserved. PerkinElmer® is a registered trademark of PerkinElmer, Inc. All other trademarks are the property of their respective owners.

008957\_01



## Gas Chromatography / Mass Spectrometry

### Authors

Meng Yuan

PerkinElmer, Inc.  
Shelton, CT 06484 USA

Jie Jiang  
Ting Mao  
Liping Feng

The Beijing Municipal Center for Food Safety  
Beijing, China

## Measuring Alkylphenols in Textiles with Gas Chromatography / Mass Spectrometry

### Introduction

Alkylphenols are nonionic surfactants widely used in detergent formulations both for industrial and household use. Additional industrial uses include manufacture of plastics, paper and textiles. Nonylphenol, a specific alkylphenol, is classified as an endocrine disruptor.

It is known to bioaccumulate, especially in aquatic animals. Nonylphenol is classified as a 'priority hazardous substance' in Directive 2000/60/EC and 2003/53/EC of the European Parliament.<sup>1</sup> The maximum concentration has been limited to 0.1% in many materials, including textiles – as a result of this regulation, it is necessary to accurately determine the level of nonylphenol in textiles.

This application note will present a method to measure octyl- and nonylphenols at low levels using gas chromatography/mass spectrometry (GC/MS). It will also describe a simple and reliable procedure for extraction and purification of octyl- and nonylphenols from textile samples.

In addition to method optimization and calibration, a variety of textiles are analyzed and the level of alkylphenols determined.

## Experimental

### Sample Preparation

0.5 g of the textile was cut into small (10 mm x 2 mm) pieces with a razor blade and placed into the glass centrifuge vial. Then it was extracted supersonically for 30 minutes with 10 mL of toluene. 1 mL of the extract was placed into a 2-mL plastic centrifuge tube with a purification matrix. This mixture was vortexed for 2 minutes. Five combinations of purification materials, including MgSO<sub>4</sub> combined with one of the following were tested: silica gel, aluminium oxide, polyamide, florisil, and primary secondary amine (PSA). Following cleanup, the extract was centrifuged for 2 minutes at 5000 rpm.

The evaluation of a cleanup procedure was performed on a brown leather sample. It was found that PSA, aluminium oxide, and florisil absorbed alkylphenols and achieved low recoveries of the matrix spike (Table 1). The cleanup with silica gel and anhydrous MgSO<sub>4</sub> removed the dye completely from the sample and had better than 75% recovery of both octyl- and nonylphenol (Table 1). This combination of 50 mg silica gel and 100 mg MgSO<sub>4</sub> was used for the remaining experiments.

### Instrument Conditions

The alkylphenols in the extracted textile samples were identified and amount determined by GC/MS. The system used was a PerkinElmer® Clarus® 680 T GC/MS. Table 2 shows the complete instrumental-setup parameters for the GC/MS system.

**Table 1. Matrix-Spike Recovery Using Different Purification Chemicals.**

Sample	Purification Chemicals	Color of the Extract	Compounds	Matrix-Spike Recovery (%)
Brown Leather	50 mg of silica gel and 100 mg of anhydrous MgSO <sub>4</sub>	No color	4-tert-octylphenols Nonylphenols	78 92
	50 mg of aluminium oxide and 100 mg of anhydrous MgSO <sub>4</sub>	No color	4-tert-octylphenols Nonylphenols	1 20
	50 mg of polyamide and 100 mg of anhydrous MgSO <sub>4</sub>	Pale	4-tert-octylphenols Nonylphenols	75 92
	50 mg of florisil and 100 mg of anhydrous MgSO <sub>4</sub>	Pale	4-tert-octylphenols Nonylphenols	0 15
	50 mg of PSA and 100 mg of anhydrous MgSO <sub>4</sub>	Brown	4-tert-octylphenols Nonylphenols	44 51

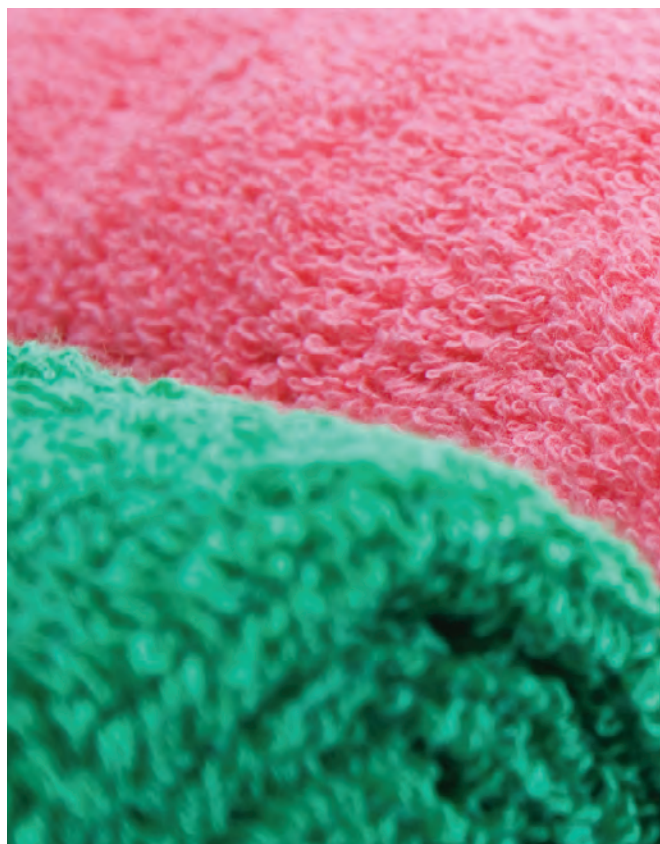


**Table 2. Instrumental Parameters.**

Gas Chromatograph	PerkinElmer Clarus 680 GC
Inlet type	PSSI
Inlet temperature	280 °C
Oven program initial temperature	50 °C
Hold time 1	2 min
Ramp 1	25 °C/min to 300 °C
Hold time 2	3 min
Vacuum compensation	On
Column	PerkinElmer – Elite™-5ms 30 m x 0.25 mm x 0.25 µm
Carrier gas	Helium
Carrier flow	1 mL/min (Splitless 1.5 min)
Mass Spectrometer	PerkinElmer Clarus 600 T MS
Mass range	<i>m/z</i> 50-300
Solvent delay time	6 min
Scan time	0.20 sec
InterScan delay time	0.05 sec
Transfer-line temperature	280 °C
Source temperature	240 °C
Multiplier	400 V

## SIM Mode

To increase the sensitivity of this analysis, a selected ion monitoring (SIM) method was created. Each compound had one quantifier ion and two qualifier ions, with a dwell time of 0.04 seconds each – the ions monitored for each compound are listed in Table 3. Nonylphenol is a multi-component mix that elutes as an unresolved group of peaks – as a result, the area of all isomers was integrated as a single compound.

## Calibration Standards Preparation

A 10 µg/mL standard stock solution was prepared by diluting 0.1 mL of a 1000 µg/mL standard to 10 mL with toluene. From this stock solution, a working calibration standard set at 0.1, 0.2, 0.5, 1, 2, 4, 6 µg/mL was prepared. The calibration range extends well below the EU regulatory limit of 50 µg/mL (0.5 g sample to 10 mL solvent extraction), allowing laboratories to collect useful information about nonylphenol in samples, even if this amount is well below the regulatory limit.

## Results

The calibration of the GC/MS system included seven standard levels. The response of the calibration was linear for both octylphenol and nonylphenol (Table 4 – Page 4). The precision of the GC/MS system was tested with five injections of a 0.2 ppm standard – for both analytes, the relative standard deviation of this analysis was less than 3%.

Following the calibration of the system, four textile samples were analyzed: dark cloth, red cloth, green towel and brown leather. The alkylphenol concentration was quantified in each (Table 4). Table 4 also shows that 1 µg/mL of alkylphenols was spiked into the samples and their matrix spike and matrix-spike duplicate recoveries were calculated. An example chromatogram from the analysis of the green towel sample is pictured in Figure 1.

**Table 3. Calibration Table for Alkylphenols.**

Name	Retention Time	Quantifier Ion	Qualifier Ion 1	Qualifier Ion 2	%RSD	r <sup>2</sup>	MDL (µg/mL)
4-tert-octylphenols	7.63	135	136	107	2.8	0.9981	0.023
Nonylphenols	9.26 to 9.55	135	121	107	1.7	0.9994	0.015

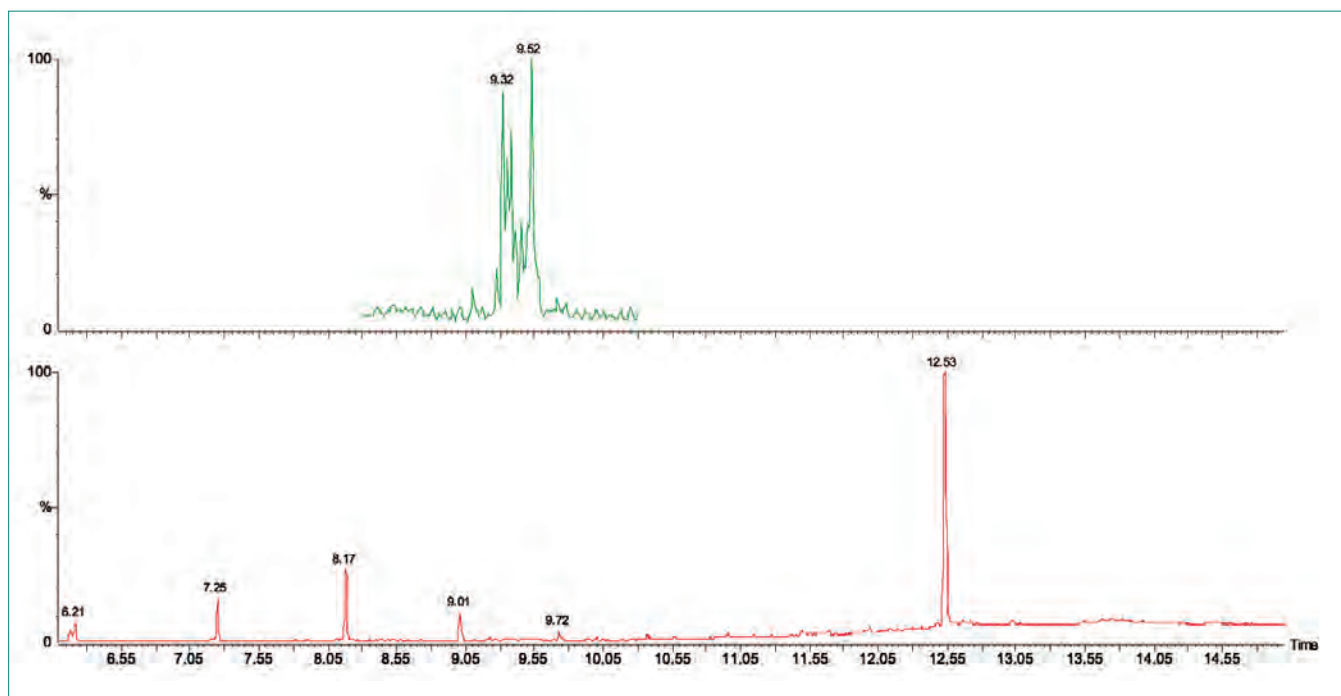


Figure 1. Total ion chromatogram (TIC – bottom) and selected ion monitoring chromatogram (SIM – top) of 0.05 g of green-towel sample.

**Table 4. Sample Analysis and Matrix-Spike Recovery.**

Sample	Compounds	Concentration (µg/mL)	Matrix-Spike Recovery (%)	Matrix-Spike Duplicate Recovery (%)
Dark Cloth	4-tert-octylphenols	0	105	107
	Nonylphenols	0.11	99	107
Red Cloth	4-tert-octylphenols	0	115	101
	Nonylphenols	0.16	106	92
Green Towel	4-tert-octylphenols	0	98	105
	Nonylphenols	1.44	96	93
Brown Leather	4-tert-octylphenols	0	86	87
	Nonylphenols	0.18	80	81

## Discussion

The European guidelines limit the concentration of nonylphenols in textiles to 0.1%. This method is able to quantitate nonylphenols down to a level 100 times lower than the regulatory limit. This will provide laboratories sufficient capability to measure with confidence the amount of nonylphenols in a sample that meets the regulatory guidance. This is very useful because it will allow the manufacturers of textiles to monitor their process and have advanced notice of changes in the levels of nonylphenols that may eventually exceed the regulations. If the sensitivity requirements of this analysis are at the regulatory limit – 50 µg/mL – rather than 10 times lower, 1 mL of sample extract can be diluted to 10 mL. This will make the effective regulatory limit – 5 µg/mL – within the calibration range presented here. This dilution approach will further reduce co-extracted material introduced by each injection, keeping the system cleaner over the long term.

## Conclusion

This application note demonstrates a precise and accurate method to quantitate the amount of alkylphenols in textile samples. The Clarus 680 GC/MS system has demonstrated to be linear across the calibration range of 0.1 to 6 ppm, meeting and exceeding the analytical requirements for Directive 2003/53/EC of the European Parliament and of the Council of 18 June 2003.

In addition to calibration, a fast and reliable extraction technique with sample cleanup was developed and applied to textile samples. The precision of the extraction was verified by the analysis of textile samples spiked with known levels of nonylphenols.

## Acknowledgements

This method was developed in collaboration with the Beijing Municipal Center for Food Safety Monitoring (China). This organization was set up by the Beijing Safety Administration in 2004 and assigned to provide technical support for food safety management for the Beijing municipal government and the Beijing 2008 Olympic Games. The Beijing Food Laboratory has developed methodology using a variety of analytical technologies in preparing for routine and emergency monitoring for both food and merchandise.

## References

1. Directive 2003/53/EC of the European Parliament and of the Council of 18 June 2003.

Thermographic Analysis –  
Mass Spectrometry

## The Analysis of Ethylene Vinyl Acetate by TG-MS

### Introduction

The combination of thermogravimetric analyzers (TGA) with mass spectrometers (MS) to analyze the gases evolved during a TGA analysis is a fairly well-known technique. In this application, TG-MS technology is used to determine the components of an evolved gas from the TGA of ethylene vinyl acetate (EVA). EVA is a polymer used in many industries – two common applications are in solar panels and foam for footwear.

### Experimental

This analysis was performed on a PerkinElmer® Pyris 1 TGA\* using alumina pans and the standard furnace. The instrument was calibrated with nickel and iron and all samples were run under helium purge. Heating rates varied from 5 to 40 °C/min, depending on the sample under test. The furnace was burned off between runs in air. Samples were approximately 10-15 mg. Data analysis was performed using Pyris 9.0 Software.

During the TG-MS analysis, the PerkinElmer Clarus 600 GCMS\* was used. In the TG-MS work, a 0.1 mm i.d. deactivated fused-silica transfer line was connected directly to the MS. The transfer line was heated to 210 °C. The data analysis was performed using TurboMass™ GC/MS Software.

### Results

In this example, ethylene vinyl acetate (EVA) and the components of the evolved gas are analyzed to confirm their identity. Figure 1 (Page 2) shows the thermogram from the TGA of EVA.

\*Pyris 1 TGA instrument is superseded. It has been replaced by TGA 8000.

\*Clarus 600 GCMS instrument is superseded. It has been replaced by SQ8.

The thermogram demonstrates two weight losses, the first corresponding to acetic acid and the second corresponding to fragments from the polymer backbone. The MS analysis (Figure 2) of the evolved gas confirms the identity of acetic acid with spectral data included in Figure 3.

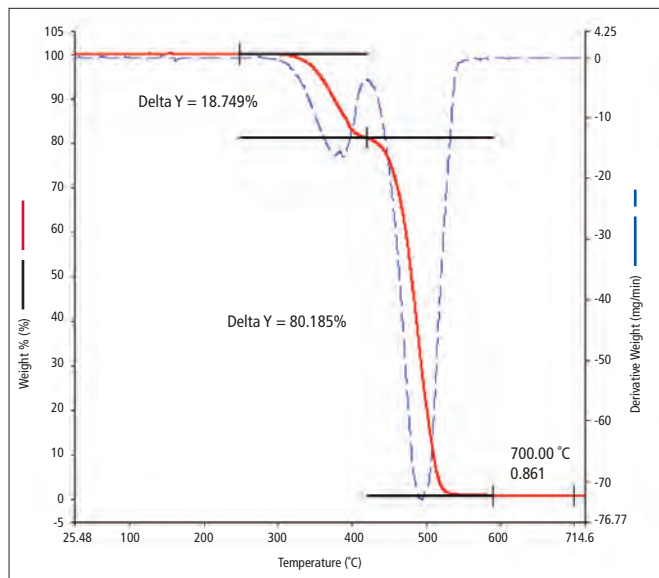


Figure 1. TGA curve generated from the analysis of EVA samples.

## Conclusions

TGA analysis allows quantification of the weight loss of a material at specific temperatures. The coupling of the TGA with the MS increases the power of the technique by providing the ability to identify the species evolved during thermal analysis.

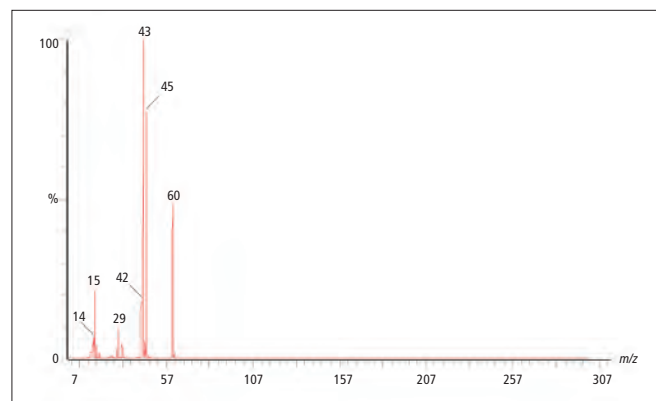


Figure 3. Spectral data verifying the identity of the evolved gas from the first transition of the TGA as acetic acid.

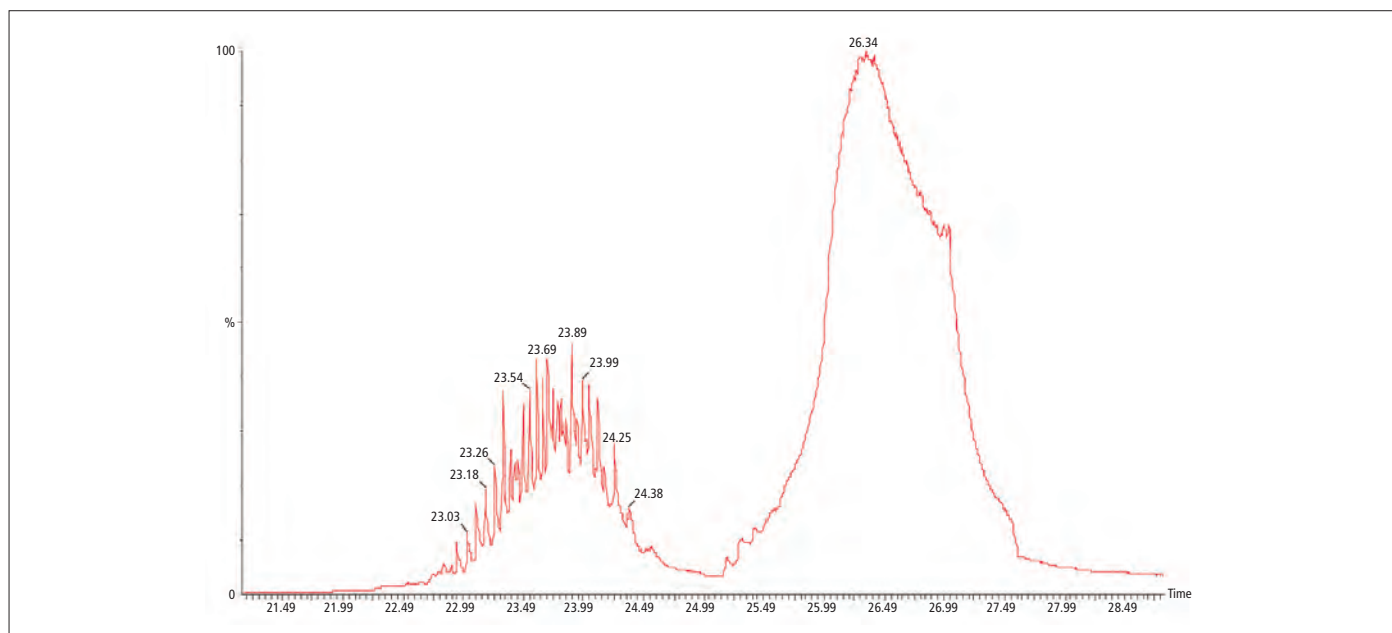


Figure 2. The MS analysis of the evolved gas generated during the TGA of EVA.

## Thermal Analysis FT-IR Spectrometry



The Spectrum Two FT-IR DSC 4000 and TGA 4000 Thermogravimetric Analyzer work together to allow improved polymer identification for recycling.

## Polymer Recycling Pack

Polymer recycling is a growing industry, as many bottles and containers that were once destined for landfills are now being recycled into new products. Because polymers tend to be mutually immiscible, it is important that something identified as polyethylene terephthalate (PET) or polyethylene (PE) really be that polymer and not polycarbonate (PC) or polystyrene (PS). The chemical identification of the polymer can be done easily using the Spectrum Two™ Fourier Transform Infrared (FT-IR) and Universal Attenuated Total Reflectance (UATR) accessory as shown in Figure 1.

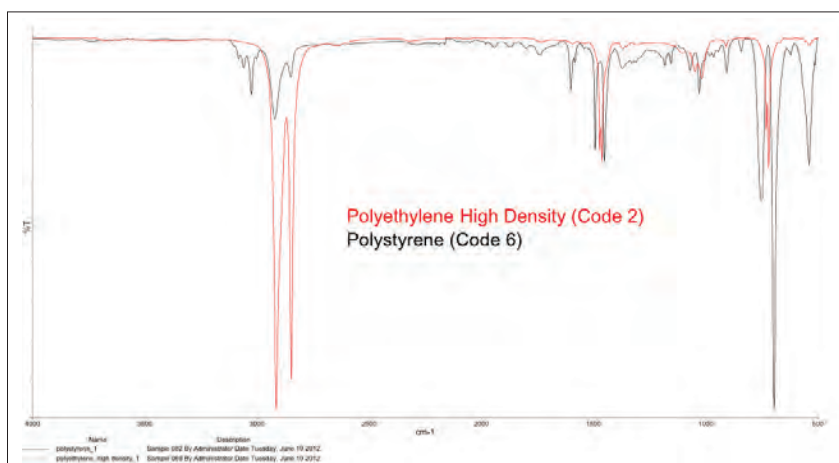


Figure 1. Overlay of PE and PS spectra in the FT-IR. FT-IR is a fast and accurate way to detect chemical differences in polymers.

Spectroscopic chemical identification alone is not always adequate to determine the classification of a polymer sample. Grades 2 and 4 are chemically the same polymer, polyethylene. As a result they have similar FT-IR spectra. As Figure 2 shows, the spectra of Grade 2 High Density Polyethylene (HDPE) and Grade 4 Low Density Polyethylene (LDPE) are similar. Differential Scanning Calorimetry (DSC) measurements of low density and high density polyethylene. Figure 3, clearly demonstrate the differences between the polyolefin grades. DSC can identify not only the correct form of polymer, but it can also determine when a finished product contains a physical mixture of polymers. An example of such is provided with multilayer thin films. When measured with a DSC, it is easy to determine the identity of the constituents and, in some cases, their concentrations (Figure 4). In this example, it was determined that the weight percent of HDPE in the thin film was between 12-14%.

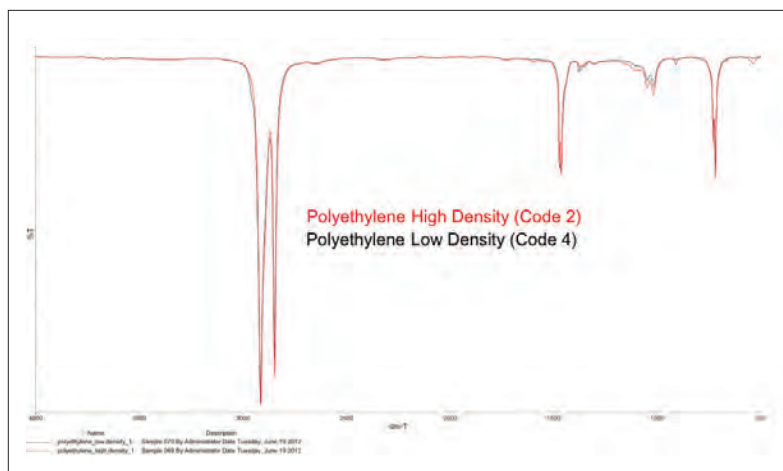


Figure 2. Overlying Code 2 and 4, both polyethylenes, show the identical spectrum in the FT-IR. Other methods are needed to see the differences.

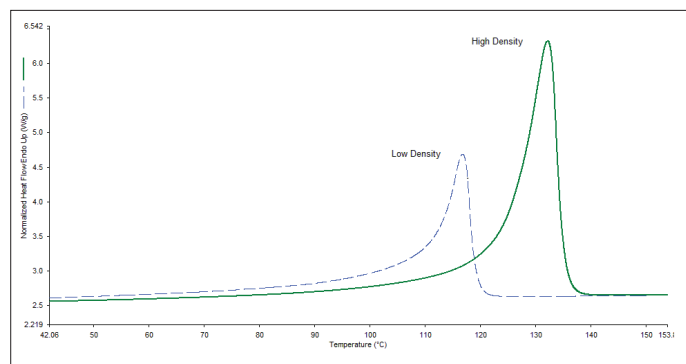


Figure 3. Grades 2 and 4 in the DSC show strong differences.

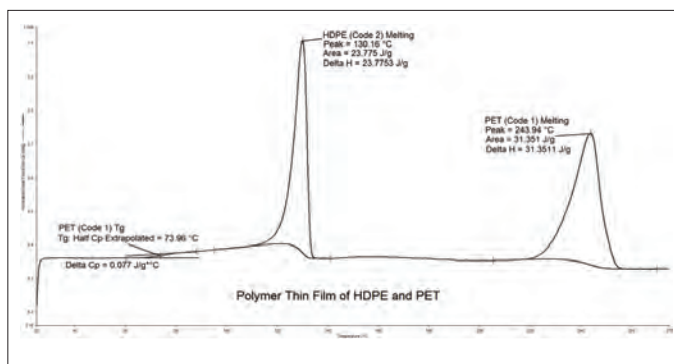


Figure 4. Thin film analysis by DSC, detecting the presence of two polymers within the sample.

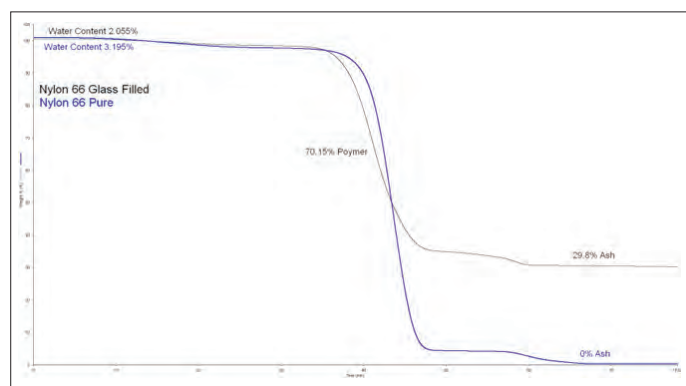


Figure 5. Detecting a filler in nylon

In addition to these concerns, the amount of fillers used in materials, such as glass fibers, calcium carbonate, talc, etc., can be detected using Thermogravimetric Analysis (TGA). Within the compendium library, files are provided to demonstrate how one can use TGA to determine the amount of filler in a polymer (Figure 5).

The Polymer Recycling Resource Pack consists of a polymer compendium that addresses how to identify the various grades or codes used in recycling as well as common problems encountered, and three libraries of data files. One library for each of the techniques discussed above is supplied: FT-IR, DSC, and TGA. Working from the compendium, one can first chemically identify the material and then get more precise information on the quality or state of the material. In addition, the compendium also addresses common problems and difficulties with the interpretation of data relevant to the recycling industry.

PerkinElmer, Inc.  
940 Winter Street  
Waltham, MA 02451 USA  
P: (800) 762-4000 or  
(+1) 203-925-4602  
[www.perkinelmer.com](http://www.perkinelmer.com)



For a complete listing of our global offices, visit [www.perkinelmer.com/ContactUs](http://www.perkinelmer.com/ContactUs)

Copyright ©2014, PerkinElmer, Inc. All rights reserved. PerkinElmer® is a registered trademark of PerkinElmer, Inc. All other trademarks are the property of their respective owners.

**Authors:****Chunhong Xiao****PerkinElmer, Inc.  
Shelton, CT****Chris Ernst****Advanced Blending Technologies  
Tiffin, OH**

## Analyzing Recycled Polyethylene Resin for Polypropylene Contamination Using FT-IR

### Introduction

The use of post-consumer recycled, high-density polyethylene (HDPE) has been steadily growing over recent years. For example, approximately 974,000,000 pounds of HDPE were recycled in 2011, according to a recent Association of Post-Consumer Plastic Recyclers report (1). Thus, recycled HDPE, a Green, cost-effective alternative to virgin HDPE, has become an important raw material for many HDPE-based products, such as sheet, pipe, decking material, electrical conduit, bottles, etc. Most recycled HDPE is from bottles, many of which have caps and pour spouts made of polypropylene (PP), a material that has similar physical properties to HDPE. Consequently, PP is a common contaminate in post-consumer recycled HDPE resin and can adversely affect end-product performance (e.g., products can be more brittle and susceptible to stress cracking). In order to maintain high quality, it is imperative that processors monitor and control the amount of PP contained in recycled resin. For this purpose, a reliable tool is Fourier Transform Infrared Spectroscopy (FT-IR), and, to that end, the PerkinElmer Spectrum Two™ FT-IR is the easy-to-use, accurate system for measuring the amount of PP in recycled HDPE resin. This Application Report presents the methodology for employing the PerkinElmer Spectrum Two for this analysis.

## Experimental

Standards were prepared by Advanced Blending Technologies (Table 1). Samples of virgin HDPE pellets were first dry-blended with virgin homopolymer PP pellets at the percentages shown in Table 1 (covers a range, 3-12%, typically observed for levels of PP in recycled HDPE resin), then hot melt compounded through a ¾-inch single screw laboratory extruder. In order to ensure a homogenous mix, the samples were (i) dry blended and then (ii) re-extruded two additional times for a total of three passes through the extruder.

Table 1. Standards at Four Different Blends of Polyethylene (PE) and Polypropylene

Name	Polypropylene (%)	Polyethylene (%)
12% PP 4	12	88
9% PP 4	9	91
6% PP 4	6	94
3% PP 4	3	97

A PerkinElmer Spectrum Two, fitted with a diamond single-bounce ATR, was used to collect spectra of the standards at 4 cm<sup>-1</sup> spectral resolution with four co-adds. The PP/HDPE resin pellets were placed/pressed on the diamond crystal and measured directly without any further sample preparation. Each standard was tested 5-6 times using different pellets. PerkinElmer Spectrum Quant software was used to build a calibration method with the standards data. (Spectrum Quant is a powerful software package that includes the linear regression-based Beer's Law, which allows the use of area, peak or maximum peak, or peak ratio with baseline options. The software also has options for quadratic and cubic curve fitting, which were not required for this analysis.)

For this analysis, the PE peak (in black) centered at 719 cm<sup>-1</sup> (attributed to methylene group rocking) was ratioed against the PP peak (in green) centered at 1,376 cm<sup>-1</sup> (attributed to methyl group symmetrical bending). Representative spectra (overlaid) are presented in Figure 1. The peak ratios were then used for developing the calibration curve, presented in the next section in Figure 2.

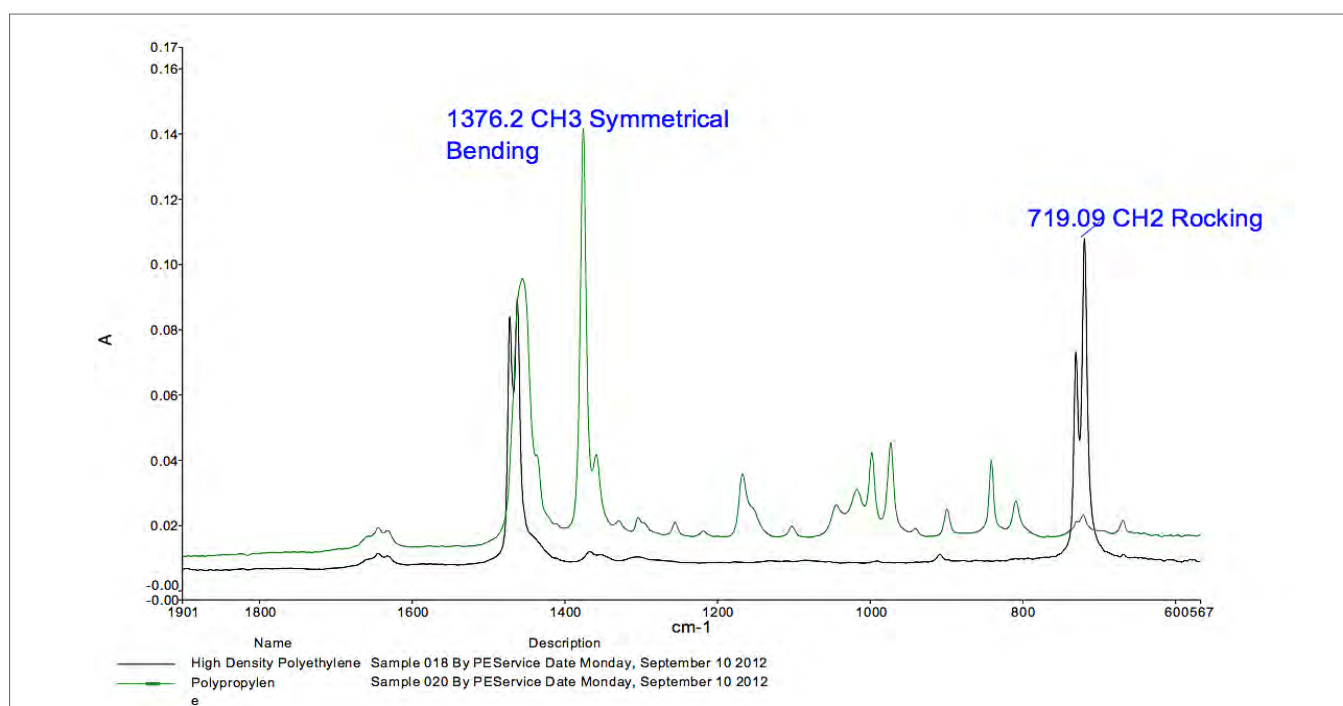


Figure 1. Spectral Comparison of High Density Polyethylene and Polypropylene

## Results

Inspection of Figure 2 reveals a good linear fit for calculated PP (based on the peak ratio) and the specified values, yielding a regression correlation of nearly 0.999. The standard error of prediction (SEP) is low, with a value of approximately 0.19%, indicating that the model is robust.

In any quantitative analysis, an important step is validation of the model. Independent validation was done within the Spectrum Quant software. Table 2 presents the validation results for PP. Consistent with the good linear fit in the calibration curve, the residual values are generally low.

Table 2. Validation Results for PP

Validation Samples Specified		Calculated	Residual
12% PP validation	12	11.7817	0.218282
9% PP validation	9	9.30215	-0.302153
6% PP validation 1	6	5.60739	0.392614
6% PP validation 2	6	5.70573	0.294273
3% PP validation	3	3.17936	-0.179363

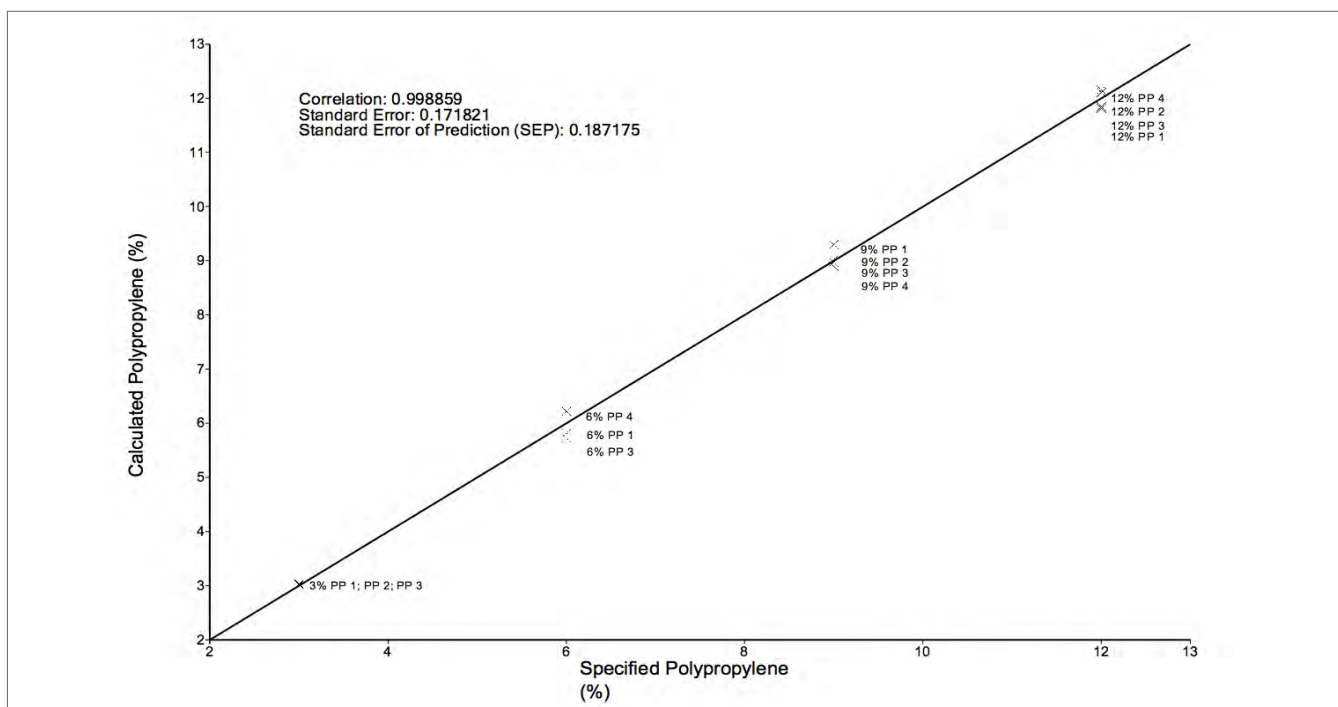


Figure 2. Calibration Model for PP

## Conclusion

A feature of the PerkinElmer Spectrum Two with a single-bounce ATR accessory is that high quality spectra can be collected in seconds, without sample preparation, owing to the advanced design and built-in algorithms, which facilitate ease-of-use. These results were quickly generated, in a matter of minutes; the most time-consuming part of the analysis was preparation of the "contaminated" resin standards. In conclusion, the calibration curve showed excellent linearity and robustness, indicating that, for the

levels of PP in recycled HDPE measured here, the Spectrum Two is an excellent tool for quick screening analysis. It is noted that, for higher concentrations, a second calibration might be required, bracketing the higher concentrations of PP in recycled HDPE resin.

## Reference

1. American Chemistry Council, "2012 United States National Post-Consumer Plastics Bottle Recycling Report", 2013, 14 p.

## FT-IR and NIR Spectroscopy

Author:

Ian Robertson

PerkinElmer, Inc.  
Shelton, CT

## The Advantages of Mid-IR Spectroscopy for Polymer Recycling

### Introduction

Plastics are becoming increasingly utilized in consumer and industrial products. Over five million tons of plastics are used each year. In the UK in 2010 approximately 38% of the

plastics consumption was used in packaging materials, with a quarter of this in production of plastic bottles. In the automotive industry an increasing number of large parts are being made from plastics due to the demand for lighter materials to reduce the overall weight of the vehicle and reduce fuel consumption. Tons of plastics are discarded every year, often ending up in landfill sites. Across the world there are initiatives for consumers to increase the amounts of materials they recycle, rather than discard them to these landfill sites. The waste plastics will then go to plastics recycling plants where they can be identified and reused. Japan is one of the most successful countries in the world for recycling plastics. In 2010, 77% of plastic waste was recycled, over double the rate of the UK, with the US currently achieving about 20%.

The Society of the Plastics Industry introduced the Plastics Identification Code (PIC), to provide a system for categorizing polymer types and to help recycling companies separate various plastics for reprocessing.

Table 1. Polymer Identification Codes (PIC)

	Acronym	Full Name	Example of Uses
	PET	Polyethylene Terephthalate	Fizzy drink bottles and frozen ready meal packages.
	HDPE	High-Density Polyethylene	Milk and washing-up liquid bottles.
	PVC	Polyvinyl Chloride	Food trays, cling film, bottles for squash, mineral water and shampoo.
	LDPE	Low Density Polyethylene	Carrier bags and bin liners.
	PP	Polypropylene	Margarine tubs, microwavable meal trays.
	PS	Polystyrene	Yogurt pots, foam meat or fish trays, hamburger boxes and egg cartons, vending cups, plastic cutlery, protective packaging for electronic goods and toys.
	Other	Any other plastics that do not fall into any of the above categories.	Melamine, often used in plastic plates and cups.

However, the PIC system is not mandatory worldwide and often plastic samples do not have the code on them, especially older materials.

In order to be successfully recycled, the plastics need to be accurately identified and sorted. Many recycling plants rely on the "experienced recycler" to identify the plastics. This can involve traditional tests such as "float test" or "burn and sniff test". The "float" test can supposedly differentiate polyolefins from other types of plastics based on whether the plastic floats on a water-detergent solution. The "burn and sniff" test involves the operator setting fire to a small amount of the plastic and sniffing the evolved fumes. Not only can this lead to misidentification of the plastic, but is extremely dangerous as the fumes from burning polymers can be extremely toxic.

Optical spectroscopic techniques offer an accurate and scientific method of identifying plastic materials. The near-infrared (NIR) region of the electromagnetic spectrum, from 12000 - 4000 cm<sup>-1</sup>, can be used for fast screening of plastic types. However, mid-infrared (MIR) spectroscopy, from 4000 - 450 cm<sup>-1</sup>, offers significant advantages for positive identification of the plastic and any other components in the plastic, such as fillers, plasticizers, surfactants, coatings, or release agents. In addition, NIR instrumentation cannot be used for identification of plastics containing even low amounts (above 2% or 3%) of carbon black. This represents a reasonable proportion of recycled plastics.

Mid-infrared spectra were collected on a Spectrum Two™ FT-IR using the Attenuated Total Reflectance (ATR) sampling technique. Measuring samples is achieved by placing the plastic on top of the sampling accessory and applying pressure to the sample in order to make contact with the diamond crystal. Measurement time is in the region of 10 seconds.



Figure 1. The PerkinElmer Spectrum Two and diamond ATR.

Figure 2 is representative mid-infrared spectra of plastics for the different PICs. Spectra 1 to 6 are spectra for PIC 1 to 6, Spectra 7 and 8 are two different materials representing PIC 7 (OTHER). These materials are polyamide (PA) and polycarbonate (PC).

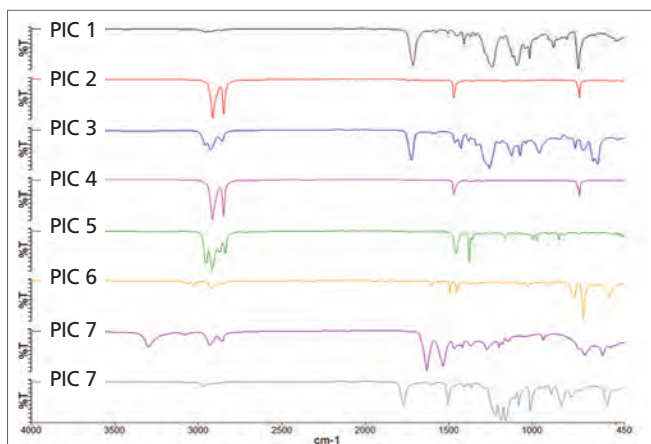


Figure 2. Mid-infrared spectra from the different PIC categories.

The spectra for each of the categories are visibly different. However, the software has the capability of identifying the plastic by comparing the unknown spectrum against a library of standard polymers. The whole routine can be deployed in a simple user interface with on-screen instructions for the plastics recycler rather than requiring expertise to analyse samples. Figure 3 shows a representative result from a library search using a standard polymer library.

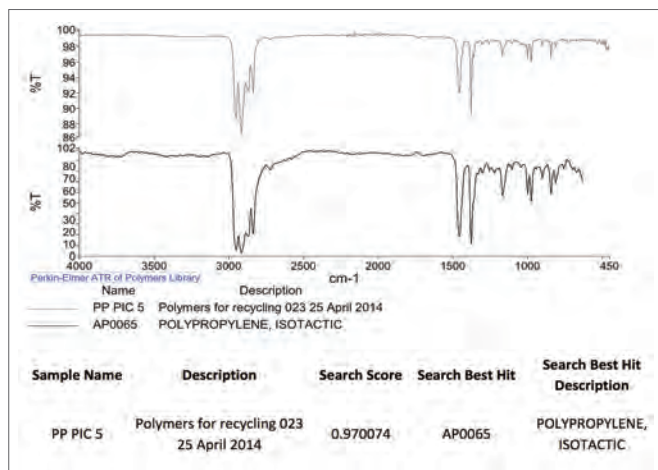


Figure 3. Search result identifying the sample as Polypropylene.

### Measurement of Darkly Colored Samples

Plastics sent for sorting and recycling come in an extremely wide range of colors, with the colors due to pigments or other fillers present in the material. Many of the fillers and pigments will introduce spectral features due to the chemical composition, which is mainly inorganic. A frequently used filler in plastics is carbon black. This material shows no spectral bands in the mid- or near-IR regions of the spectrum. However, in the near-IR region it leads to very intense absorption, masking any other spectral features. The mid-IR region of the spectrum does not suffer as badly from this problem. Rigid plastics will generally only contain carbon levels from a few per cent up to 25 - 30%. Mid-IR diamond ATR measurements are possible with these samples.

Figure 4 shows the mid-IR diamond ATR spectra of two samples of the same plastic type, polystyrene, with one of the samples being a clear plastic, the other is extremely black due to being carbon-filled.

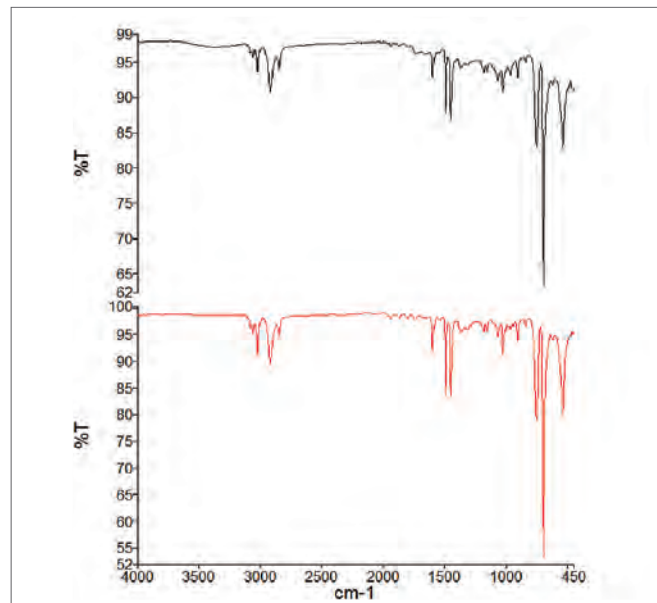


Figure 4. Diamond ATR spectra of black polystyrene (top) and clear polystyrene (bottom).

The spectra are virtually identical showing that the presence of carbon black is not having an effect on the infrared spectrum or the identification of the material. This is not the case with near-IR spectra.

Near-IR spectra of a variety of samples were measured on a PerkinElmer Frontier™ IR/NIR spectrometer configured for operation in the near-IR region. Sampling was performed in reflectance mode using the Near-IR Sampling Accessory (NIRA) over the spectral range 10,000 - 4000 cm<sup>-1</sup> at 16 cm<sup>-1</sup> resolution. Near-IR reflectance is the technique utilized by handheld Near-IR analysers. Figure 6 shows the Near-IR spectra of two different samples of Low Density Polyethylene (LDPE). The upper spectrum was measured on a white sample, whereas the lower spectrum was measured on a black sample.

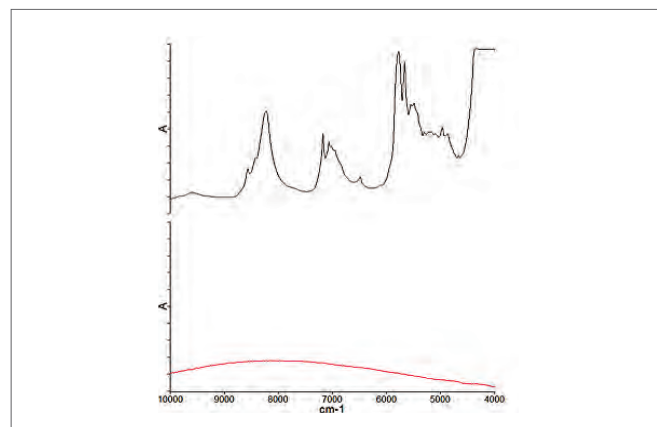


Figure 5. Near-IR spectra of white (top) and black (bottom) samples of LDPE,

The spectra here are completely different. The white LDPE sample generates a good quality spectrum that would allow for identification of the material against a library of spectra. The black LDPE sample generates a broad spectral curve with no discernable spectral features. This appearance is typical for black polymer samples measured in the near-IR spectral region, as seen in Figure 6.

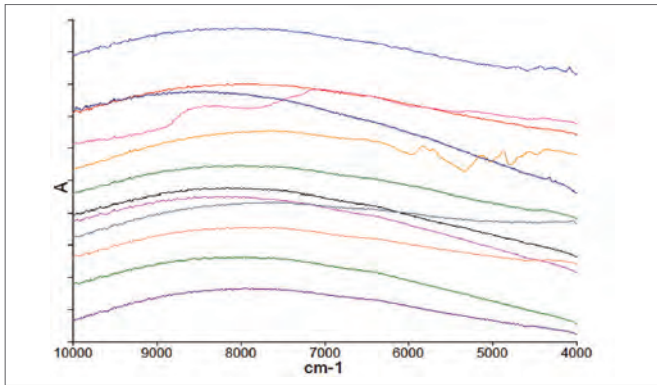


Figure 6. Near-IR reflectance spectra of black plastics.

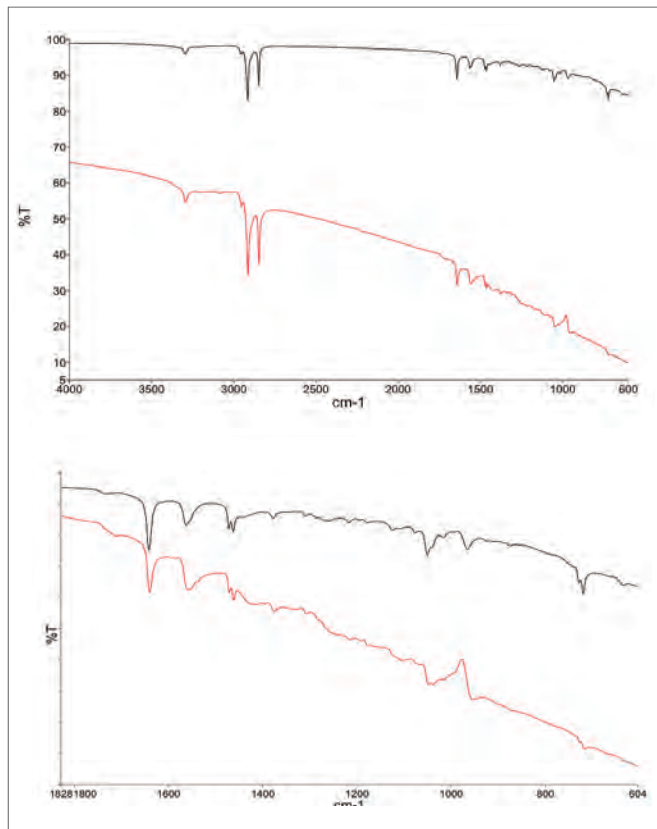


Figure 7. Spectra of carbon-filled o-ring on germanium crystal (upper) and diamond crystal (lower).

Only a couple of the samples measured showed any spectral features in this region of the spectrum. It would be impossible to identify any of the other samples using this near-IR data.

Softer rubber-like materials with high carbon content can be measured by ATR in the mid-IR region of the spectrum, but it requires the use of germanium as the crystal type rather than diamond. The higher refractive index of germanium means the IR beam will have a lower penetration depth into the sample, preventing high absorption due to the carbon.

Figure 7 displays a sample of a carbon-filled rubber o-ring. The spectra were collected on the same sample, using both germanium and diamond as the crystal material. Both of the spectra exhibit a baseline slope, with the slope on the spectrum collected from the diamond crystal being considerably worse. Expanding the spectra to look only at the spectral region from 1800 - 650  $\text{cm}^{-1}$  shows that there are also severe distortions in the spectrum collected using the diamond crystal, especially in the region around 1000  $\text{cm}^{-1}$ . This leads to significant loss of information.

For the spectrum collected on the germanium crystal it is possible to apply simple, automated baseline correction to generate the best quality spectrum, as shown in Figure 8. This would not be possible for the spectrum collected on the diamond crystal due to the spectral distortions.

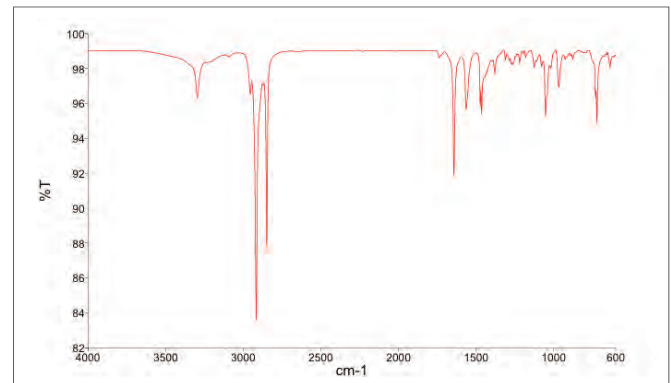


Figure 8. Baseline corrected spectrum of o-ring collected using the germanium crystal.

## Identification of Additives

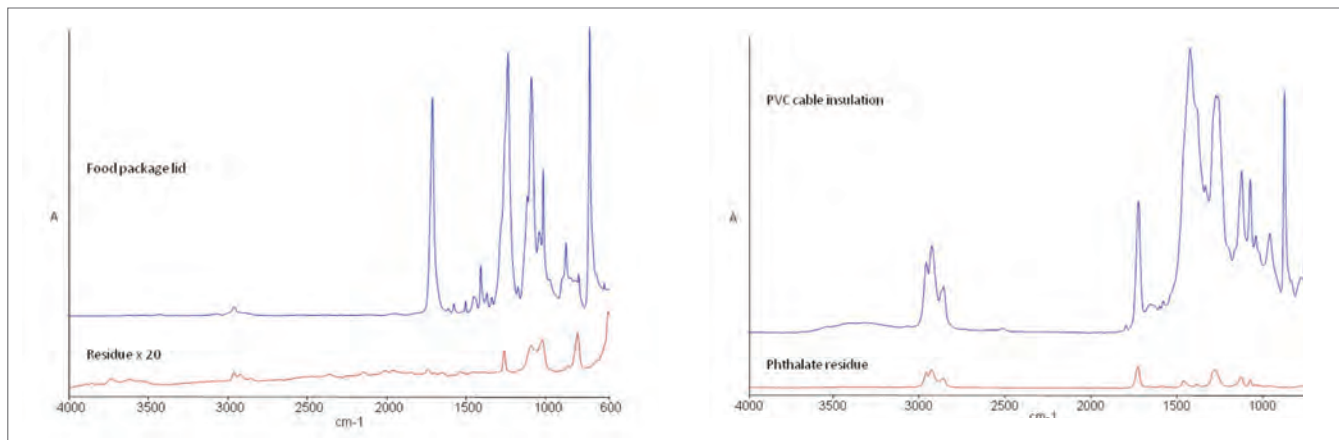


Figure 9. Examples of spectra of bulk material and additives from plastic samples.

The process of running a sample on the ATR accessory involves applying pressure onto the sample in order to get contact between the sample and the ATR crystal. This process can often squeeze out additives that remain as a residue when the sample is removed. This requires a quick clean of the crystal between samples. However, this also allows for the possibility of identifying the additive(s) by means of scanning the residue spectrum. Figure 9 shows two such examples where the plastic sample spectrum is obtained and the material can be identified, but also the residuals can be identified. In the case of the food packaging lid, the additive has been identified as a silicone, often used as releasing agents. In the case of the PVC insulation cable the additive has been identified as a common PVC additive, a phthalate plasticiser.

## Summary

Molecular spectroscopic techniques offer fast and easy measurement and identification of plastic types. Both mid- and near-IR instrumentation can be deployed for this task for a wide range of sizes and shapes of samples. However, if the samples are carbon-filled then near-IR technology, both handheld and laboratory instruments, it is unlikely to yield useable spectra.

In addition, with the use of a germanium crystal in the ATR instead of a diamond, very heavily carbon loaded rubber materials can be identified in the mid-IR region. An instrument with an ATR that is capable of using multiple crystal types for different sample types would be recommended.

Mid-IR instrumentation using ATR will also be capable of identifying a range of additive materials based on the infrared spectrum of the residual left on the crystal after measurement of the bulk material.

	Near-IR	Mid-IR
Identification of common plastics (non-black)	✓	✓
Identification of common plastics (black)	X	✓
Identification of carbon-filled rubber materials	X	✓*
Identification of common additives	X	✓

\*Using Ge crystal

## Infrared Spectroscopy

Authors:

Sushant Jadav

Dr. Manohar Rao

PerkinElmer, Inc.

India

## Rapid and Reliable PVC Screening in Packaging Material

PVC in different packaging materials can be achieved by a simple Beilstein Test followed by FT-IR measurement. The method involves spotting characteristic absorption bands of PVC in the sample by comparing it with standard PVC spectra.

Poly Vinyl Chloride (PVC) is one of the most important and widely used thermoplastics due to good processability, chemical resistance, and low flammability. The physical property of PVC can be controlled by varying the plasticizer content. PVCs are usually used as packaging materials, wires, films and sheet, floor tiles, and a variety of soft children's products. Due to the persistent, bio-accumulative nature of many of the chemicals released by PVC production, their effects are irreversible and pose a huge environmental risk. Textile industry compliance requires that materials, chemicals, parts, and other goods, used or supplied in the manufacture of textile products, comply with the applicable chemical content and chemical exposure laws of every governmental jurisdiction in which those products are manufactured or distributed to protect the health and safety of consumers and others handling finished products. The RSL (Restricted Substance List) of finished products, including apparel, non-apparel, footwear, accessories, and other products requires that parts, other goods, and finished products provided by suppliers and sources comply with the "Limit Value Final Product" (LVFP) levels. The use of PVC in the packaging material in the textile Industry comes under RSL and there is a complete ban on the usage of PVC. The mandatory requirement for screening this material has to be tested using the Beilstein test and FT-IR for confirmation.

### Introduction

A qualitative rapid and reliable method for detection of Polyvinyl Chloride

## Experimental

In this application note we show that Beilstein and FT-IR testing can be used to confirm the presence of PVC in packaging materials. Here we have used various packaging plastics as test samples. The presence of halogens using the Beilstein test in any material containing bound or ionic halogens (chlorine, bromine, iodine) such as salt or polyvinyl chloride (PVC) will react with a copper wire when heated in a flame and produce a brilliant, long-lasting green flame indicating the presence of halogens. The presence of a greenish flame indicates the presence of halides. The flame will burn green for a long period of time if PVCs are present. For PVC confirmatory presence, FT-IR measurement was carried out on a Spectrum Two™ FT-IR using a Diamond ATR. Experimental parameters used for measurement were scanning range of 4000 – 400 cm<sup>-1</sup>, resolution of 4 cm<sup>-1</sup> and 16 scans.

Table 1. Characteristic IR spectra absorption bands for PVC.

Spectral Range (cm <sup>-1</sup> )	Functional Assignment
2900 to 3000	Aliphatic C-H Stretching
1725 to 1740	Ester Peak for Phthalates plasticizers
Peak Around 1426	Bending of aliphatic C-H Bonds
Peak around 1240 to 1260	Bending of C-H bonds near Cl
Peak around 1000	Stretch of C-C bonds
Doublet at 610 and 630 and peak at 695	C-Cl gauche bond



Figure 1. Spectrum Two with Diamond ATR.

## Data Analysis

The following samples were tested by PerkinElmer Spectrum Two instrument with Diamond ATR for PVC qualification. Samples spectra listed in Figure 2 were monitored for PVC characteristic absorption bands. Given in Figure 2 are the spectra of each sample with observations.

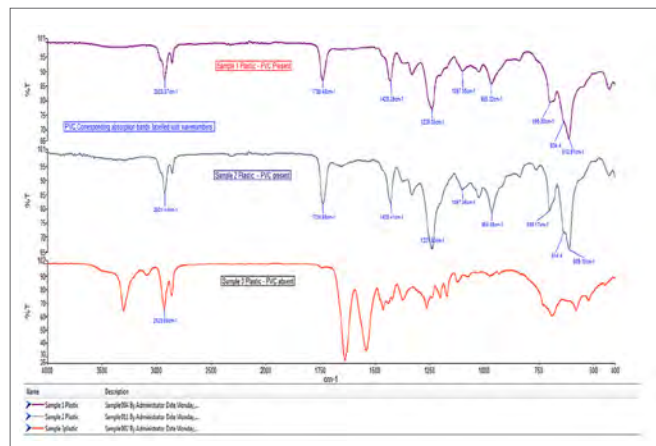


Figure 2. The IR absorption spectra show the confirmation of PVC in Sample 1 and Sample 2, while the absence of PVC in Sample 3.

## Conclusion

In order to characterize and identify the presence of PVC in plastics, a Beilstein test followed by FT-IR analysis was carried out. For PVC which is banned in packaging material in the textile industry, FT-IR with ATR technique can be used as a verification test which is a very fast, reliable, cost effective method for PVC qualification with a good detection limit. The methodology provides the ability to screen PVC qualification of different samples with little or no sample preparation. The portability of the PerkinElmer FT-IR system enables these measurements to be made in the field and help to ensure that plastic parts and objects do not enter the commercial marketplace.

PerkinElmer, Inc.  
940 Winter Street  
Waltham, MA 02451 USA  
P: (800) 762-4000 or  
(+1) 203-925-4602  
[www.perkinelmer.com](http://www.perkinelmer.com)

PerkinElmer India Pvt Ltd  
G-Corp Tech Park 8th Floor  
Ghodbunder Road, Kasarvadavali  
Thane (W) - 400 615 | India  
For Products: [marketing.india@perkinelmer.com](mailto:marketing.india@perkinelmer.com)  
For Services: [las-india.servicerequest@perkinelmer.com](mailto:las-india.servicerequest@perkinelmer.com)  
India Toll free Number# 1800 266 1660 / 1800 200 1660  
[www.perkinelmer.com](http://www.perkinelmer.com)



For a complete listing of our global offices, visit [www.perkinelmer.com/ContactUs](http://www.perkinelmer.com/ContactUs)

Copyright © 2016, PerkinElmer, Inc. All rights reserved. PerkinElmer® is a registered trademark of PerkinElmer, Inc. All other trademarks are the property of their respective owners.

PerkinElmer, Inc.  
940 Winter Street  
Waltham, MA 02451 USA  
P: (800) 762-4000 or  
(+1) 203-925-4602  
[www.perkinelmer.com](http://www.perkinelmer.com)



---

For a complete listing of our global offices, visit [www.perkinelmer.com/ContactUs](http://www.perkinelmer.com/ContactUs)

Copyright ©2016, PerkinElmer, Inc. All rights reserved. PerkinElmer® is a registered trademark of PerkinElmer, Inc. All other trademarks are the property of their respective owners.